DEVELOPING SUSTAINABLE AND ENVIRONMENTALLY FRIENDLY BUILDING MATERIALS IN RAMMED EARTH CONSTRUCTION

By

Chijioke David OKORONKWO

April 2015

DEVELOPING SUSTAINABLE AND ENVIRONMENTALLY FRIENDLY BUILDING MATERIALS IN RAMMED EARTH CONSTRUCTION

By

Chijioke David OKORONKWO

April 2015

A thesis submitted in partial fulfilment of the University's requirements for the award of the degree of Doctor of Philosophy

Civil Engineering
School of Architecture and Built Environment
Faculty of Science and Engineering
University Of Wolverhampton

This work or any part thereof has not previously been presented in any form to the University or to any other body whether for the purposes of assessment, publication or for any other purpose (unless otherwise indicated). Save for any express acknowledgments, references and/or bibliographies cited in the work, I confirm that the intellectual content of the work is the result of my own efforts and of no other person.

Signature……..

Date……..

Abstract

Building rammed earth structures provides a sustainable alternative to concrete. As a building material, rammed earth exhibits very varied physical and material properties depending on the proportion of constituting soil types. When very sandy soil is used in rammed earth production, the properties are different from when a clayey soil is used. This variability can be seen as a very great advantage in the use of rammed earth as a building material. Builders are able to adjust specific properties by changing mix proportions to obtain a desirable balance in the characteristics of the resulting rammed earth structure.

This research work looks at selected mechanical and physical properties of different mixes of rammed earth. It describes typical range of values in density, thermal conductivity, ultrasonic pulse velocity, water ingress and compressive strength. It examines how these factors interrelate in the same soil mixes. Samples were prepared by blending various soil types in specific proportions to ensure that each definition of soil grade is as specific as possible. Unstabilised rammed earth was tested as was cement stabilised rammed earth. Rammed earth was tested at various levels of stabilisation and it was discovered that higher rates of stabilisation was not always beneficial to every material property.

The research also looked into the potential disposal of waste materials in rammed earth. As rammed earth is a monolithic material that largely remains undisturbed throughout its life span, it was suggested that waste materials could be stored in an inert form inside of rammed earth rather than dumping it in otherwise agricultural landmass. Pulverised Fuel Ash and Palm Kernel Shells were identified as wastes to be disposed in rammed earth. Pulverised Fuel Ash, a by-product of industrial furnace is found in abundance in developed countries that burn carbonaceous materials in power plants. Disposals have been seen as a problem as only a small proportion of high loss on ignition (LOI) Pulverised Fuel Ash has found application. Palm Kernel Shell is a by-product of the oil palm industry and is currently a menace in many developing countries that need to dispose large quantities of the shell in landfills.

At an early stage of the research, experimental trial runs quickly showed that these supposedly waste materials had a positive effect on some of the material properties of the rammed earth walls they were made into. This research effort evolved to look into exploiting these materials to improve the physical and material property of rammed earth and to suggest their effect on stabilised and unstabilised rammed earth. The extent to which these materials could be useful and the level at which diminishing returns set in was also investigated.

It was discovered that soil mixes that would otherwise not be considered suitable for use in rammed earth wall production can now be utilised as their characteristics can be improved on simply by adding Pulverised Fuel Ash or Palm Kernel shell in the right proportion. Incorporating Pulverised Fuel Ash in rammed earth resulted in increased compressive strength. Palm Kernel shell improved thermal properties without compromising compressive strength.

Now, to Him who is able to do exceedingly abundantly above all that we ask or imagine, according to the power that is at work within us, to Him be glory by Christ Jesus to all generations, forever and ever. Amen.

Acknowledgement

I would like to express my appreciation to my director of studies, Professor Jamal Khatib for his unbiased encouragement, guidance, support and help throughout the course of my PhD studies. It is no doubt that it is his solicitude and professional experience that has inspired me to get to the end of my PhD with confidence.

I also would like to give thanks to my supervisor Dr. Nwabueze Emekwuru. You saw the potential in me long before I did and knew at the start that I had it in me to go all the way.

Special thanks also extend to our technician Ray Bradley for his help during my experiments.

I am grateful to my colleague Mis Michal who went out of his way to deepen my understanding of the Marc Mentat software

My gratitude goes to all my friends and colleagues for providing friendship, encouragement and support during my PhD study.

I would like to give my profound appreciation to my parents and siblings. A family like ours is hard to come by. Your support, visitations and prayers held me steady through stormy periods.

And to my fiancée Tochi Ononiwu, your prodding, pushing and words of warmth gave me cause to go the whole nine yards. Thank you for coming into my life and bringing your family with you. I felt their prayers every step of the way.

To God almighty, who starts a good thing and brings it to completion, Thank you!!

Table of Contents

List of Figures

List of Tables

List of symbols

λ	surface tension
λ_T	Thermal conductivity
C	Water concentration
C(T)	temperature-dependent heat capacity
C_0	invariance of water concentration
C_c	coefficient of curvature
C_p	specific heat,
C_T	Specific heat capacity
C_u	coefficient of uniformity
D	Diffusion coefficient
D(θ)	hydraulic diffusivity.
D_h	Vapour diffusion
H	film coefficient
h	height of liquid front
h_r	Pore humidity
i	volume of absorbed liquid per unit cross-section
k	capillary coefficient
k	thermal conductivity
K(T)	thermal conductivity matrix
N	Constant related to the distance from the concrete surface over which capillary pores control the initial sorption
ŋ	dynamic viscosity
q	heat flux,
q	low velocity
q	rate of energy transfer,
q	heat flux

r	capillary radius
s	Sorptivity
S	Sorptivity coefficient
T	temperature
t	time
T_∞	ambient temperature respectively
$t_{contact}$	Duration of contact with water
T_s	surface temperature
w	Moisture Content
ε	emissivity
θ	normalised water content.
ϑ	contact angle
P	Density of water
σ	Stefan-Boltzmann coefficient,
Ψ	capillary potential

Chapter One

Introduction

1.1 Earth Building

From disrupting natural habitats to utilising soil, timber and water, building activities have significant impact on the environment and on natural resources. Buildings account for 45% of worldwide energy use and 80% of potable water use (Zhai & Previtali 2010).

The growth in world population as seen from the census figures of most countries has placed a great demand on housing. The cost of building houses, both to the economy and to the environment is also on the increase. Emerging world energy and environment challenges demand a substantial revolution of building design philosophies, strategies, technologies and construction methods (Zhai and Previtali, 2010). Given the environmental destruction and global warming caused by the excessive use of industrial materials, a good number of individuals and researchers have been re-considering the use of non-industrial materials. The notion of non-industrial materials in building is linked to local materials and is becoming worthy of interest again (Kouakou and Morel, 2009). The concept of non-industrial building materials means materials manufactured using a simple, quick process with low embodied energy, using raw materials from the site or nearby (Kouakou and Morel, 2009). These are usually incorporated by local builders whose ingenuity is inspired by traditions in their cultures and enhanced through a long period of trial and error.

Various building techniques far removed from conventional building techniques have been developed. Building with natural materials such as cordwood building, cob buildings, sandbag buildings, rammed earth buildings etc. have all been investigated. However, it is rammed earth that has provided an all-encompassing solution to environmentally friendly buildings. The term earth refers to the more or less argillaceous soil found between the rock substratum and the topsoil layer.

It has been estimated that up to 30 per cent of the total world's population live in houses constructed from unfired earth (Keefe 2012). Earth buildings can be found in every habitable continent but are much more prevalent in arid regions having low rainfall and hot climate.

1.2 Performance of Earth Based Materials

Earth based materials are considered to be more energy efficient than walls made with lightweight materials mainly due to their high thermal capacity. The thermal capacity of an earth wall is the measure of its ability to store heat and then to release it slowly when the source of heat has been taken away. Laurence Keefe (2012) compares the thermal characteristics of earth builds to those of fired bricks.

1.3 Recent Trends in Rammed Earth.

Building with earth has been practiced from time immemorial. However at a certain point, it was abandoned or substituted for such materials as concrete, brick or steel (Niroumand et al. 2012). Earth construction, though undervalued nowadays (Stratton 1997), has however stirred a growing interest from conservation desires or for being considered a good material in Eco building. Such considerations include the manufacture energy savings compared to clay bricks, the less cement used compared to concrete blocks, the transport savings if soil comes from the construction site or vicinity, and the natural appearance and colours that help buildings integrate into the landscape.

1.4 The Problem.

High Loss on Ignition (LOI) Pulverised Fuel Ash continues to be dumped in landfills. Unlike low LOI Pulverised Fuel Ash that is finding application in construction, highway construction and cement production, there is very little use for High LOI Pulverised Fuel Ash. Palm Kernel Shells (PKS) also has very little application. Large quantities of PKS and High LOI Pulverised Fuel Ash continue to find their way to landfill sites (Park & Heo 2002; Ecke 2003; Swanepoel & Strydom 2002; Cheerarot & Jaturapitakkul 2004; Prasertsan & Prasertsan 1996; Wan Ab Karim Ghani et al. 2009).

1.5 Aims:

The focus of this research is:

1. To investigate the suitability of incorporating high LOI Pulverised Fuel Ash and palm kernel shell in rammed earth.
2. To determine how rammed earth performs when various proportions of the waste materials are mixed in.

1.6 Objectives:

The study seeks to meet the above stated aims through the following objectives.

- To produce rammed earth blocks containing Pulverised Fuel Ash and PKS
- To determine the effect of both Pulverised Fuel Ash and PKS on the physical and mechanical properties of rammed earth. These properties include Density, Compressive strength, Ultrasonic Pulse Velocity (UPV), Thermal conductivity and Sorptivity.
- To determine the effect of soil grading on physical and mechanical properties of Rammed earth
- To compare the studied properties of rammed earth mixes in determining the mix that provides optimal material properties when mixed with PKS and Pulverised Fuel Ash.
- To predict the thermal behaviour of rammed earth using finite element method.
- To determine the suitability of cement stabilisation when waste materials (Pulverised Fuel Ash and PKS) are added to rammed earth.

Chapter Two

Literature Review

2.1 Classes of Rammed Earth Walls

Mud rammed earth: Made with very high water content giving the earth high plastic consistency. Fibres can be added for avoiding cracks.

Strengthened rammed earth: Soil grading can be improved, but has to be suitable. Low but optimum water content, 10–14% in proctor test. Ball drop test can be used for checking water content during construction.

Stabilised rammed-earth: Stabilisers such as bitumen, lime or cement are added to improve particular properties.

Calicostrado rammed-earth: Lime plaster is poured in the forms before a new earth layer is added (Delgado and Guerrero, 2006).

2.2 Materials in Rammed Earth Construction

Based on the use intended, soils may be classified in various ways. In Britain and most other countries, there are presently no formally adopted standards for the testing and analysis of soils to be used in constructing load-bearing walls. Important information required in a soil selection procedure would include soil type, physical and chemical properties of mixtures and visual impacts.

2.3 Soil Type and Classification

This refers to obtaining details of the parent material – in relation to source, mineralogy, colour, and its stratigraphy.

2.3.1 Particle Size Distribution

BS 1377 (1990), part 2, classifies soil particle based on their diameter. Particles greater than 2.0mm are classed as stones and gravel. 0.063mm to 2.0mm is termed sand and any particle below 0.063mm is classed fines. Fines usually consist of silts and clay.

2.3.2 Soil Density:

The density of a soil gives an indication of its porosity. This is vital in predicting the level of migration of moisture in the structure. The dry density of soil in rammed earth applications is dependent on soil type, the moisture content during compaction and compactive effort. Knowledge of the dry density of rammed earth is important during design to calculate loads on structural elements. A broad range of dry density values are quoted for rammed earth, varying from 1700 kg/m3 to 2200 kg/m3 (Adam and Jones, 1995; Standards Australia, 2002; Houben & Guillaud. 1994).

2.3.3 Plasticity

Soil plasticity, the ability of a soil to undergo irreversible deformation while still resisting an increase in loading, is indicated by the plasticity index. The plasticity index is the water content increase (% of dry weight) required for a soil to pass from a plastic to a liquid state. Experimentally the plasticity index can be found by estimating the plastic and liquid limits (Maniatidis and Walker, 2003).

A standard method for measuring plastic limit is described in BS 1377-2, (1990). Soil is screened through a 425μm sieve and dried. On re-wetting soil is rolled out by hand on a flat surface, usually glass. The plastic limit is defined as the moisture content at which the soil can no longer be rolled to 3mm diameter thread without breaking.

According to Houben & Guillaud (1994) liquid limit for unstabilised soils should be between 25% and 50% (30%-35% preferred) and the plastic limit between 10% and 25% (12%-22% preferred). Plasticity index is the numerical difference between liquid and plastic limits. The plasticity index is an indication of the clay content and characteristics of the soil. The higher plasticity index is indicative of higher clay content and/or active clay mineral and that higher shrinkage will occur when the earth dries. For rammed earth, Alley (1998) proposed a Plasticity Index as low as 6%, however more recent research allows for higher values.

2.3.4 Durability

Durability in the context of earth construction means the ability of the structure and all its elements to withstand the destructive action of weathering and other actions without degradation to the expected service life. Rain and frost are the most destructive natural actions causing erosion and deterioration of the earthen elements. Accidental abrasion is also a significant agent of deterioration. Some previous studies have noted relationship between compressive strength or durability and accelerated durability test performance (Walker, 2000; Shihata & Baghdadi, 2001; Keable 1996).

2.3.5 Shrinkage

Rammed earth, as all earth building materials containing clay, swell on contact with water and shrink on drying. In both cases failure might occur and hence swelling/shrinkage control is vital. The extent of these phenomena is very much dependent on clay present (type, amount), soil grading and moisture content changes. Only experimental data can confidently predict the percentage of shrinkage expected for a particular soil.

2.3.6 Hygrothermal Properties.

Since earth is a porous, hygroscopic material that contains active clay minerals, it is expected that the walls absorb water vapour from the air when relative humidity increases and release this moisture when the humidity falls. As it is usual practice to leave earth walls exposed to the interior of the building, the availability of combined thermal and hygric buffering (i.e. passive air conditioning) will be maximised when compared with other materials such as brick, timber or concrete that are often covered over with more insulating and less permeable coverings, e.g. varnish and paints (Hall and Allinson, 2009). Rammed earth structures possessing higher bulk porosity results in a reduced volumetric heat capacity, but also produces increased sorptivity and vapour permeance. The hygrothermal properties of Rammed earth can be adjusted to reflect desired conditions by optimising the response rate to match any anticipated fluctuations in vapour pressure gradient.

2.3.7 Anisotropy

Since rammed earth is made by stacking compacted materials in layers, it can be expected that rammed earth walls would show a measure of anisotropy. However, Bui, *et al* (2009) initiated and justified a hypothesis that rammed earth is an isotropic material of the first order if the layers remain adherent to each other. This provides assurance that testing rammed earth samples on a microscopic scale presents a representative result equivalent to that obtained from testing a macroscopic sample.

2.4 Compressive Strength

This property gives an indication of the load bearing capacity of the soil. Higher values are usually welcome. The mechanical strength of a soil is very much dependent on the voids ratio of the soil after ramming, cohesive strength of fines content, aggregate strength and moisture condition during testing. Density of the soil is a very important factor for the strength of the soil. Therefore, in the same way that it is difficult to give a specific value for the density, it is impossible to predict an exact value for the mechanical strength of a soil based on any kind of description with no prior testing.

(a) Field Tests

A simple field test to evaluate the compressive capacity of a soil is the so called thread test. A lump of earth about the size of an olive, wet enough to be easily rolled, is placed onto a clean flat surface. Using the palm and finger, pressure is exerted on the soil to roll it into a thread of equal diameter. If the thread breaks before the diameter is reduced to about 3mm then more water is required. When a 3mm thread is achieved the sample is rolled until it starts crumbling. Then a ball is formed and squeezed between the fingers. If the thread is tough and requires a lot of effort to squeeze, the soil has a lot of clay and should not be used due to potential shrinkage problems. A medium strength thread indicates adequate amount of clay and the soil may be suitable for natural rammed earth while a very weak thread is an indication of a lot of sand and silt and very little clay, soils unsuitable for natural rammed earth construction.

(b) Laboratory Tests

The laboratory tests used for determining the compressive strength of rammed earth are similar to the ones used for concrete, bricks and blocks.

2.5 Thermal Properties

The thermal performance of rammed earth is measured in a number of different ways. The most commonly used properties are:

a. Thermal Storage - This is a measure of the specific heat capacity expressed in volume terms and has units of $J/m^{3o}C$. Houben & Guillaud (1994) claims that for rammed earth the thermal storage is around 1830 $J/m^{3o}C$.

b. Thermal Resistance (R-value) - This is a measure of the opposition to heat transfer offered by a building element of specified thickness and is measured in m^2K/W. According to Standards Australia (2002), a 300mm thick rammed earth wall has an R-value between 0.35-0.70 m^2K/W.

c. Thermal Transmittance (U-values) - This is a measure of the overall rate of heat transfer, by all mechanisms under standard conditions, through a particular section of construction and is measured in W/m^2K. Minke (2000) claims that the U-values for a 300mm thick rammed earth can be as much as 1.9-2.0 W/m^2K. Rammed earth, as a dense material, has poor insulating properties.

To optimise the benefits of stabilisation then soils should meet a number of requirements. Soil should be free of humus and plant matter, though under certain conditions, plant matter like straw can be added, provided it is dry, with no danger of later deterioration (Minke, 2000). In addition soil should mainly consist of sand and fine gravel, with only sufficient clay for any required cohesive strength and a proportion of silt to act as void filler.

The main categories of binders used for earth construction are Portland cement, lime, bitumen, natural fibre and chemical solutions such as silicates.

d. Thermal Conductivity -

As rammed earth continues to gain acceptance, its worth as a building material of choice would come largely by its inherent ability in reducing the heat loss in winter. Finding a combination of earth constituents that achieves this by increasing its thermal insulation properties is important, as it would enable energy efficient buildings and improve environmental sustainability.

The thermal conductivity of a material is the quantity of heat transmitted through a unit thickness in a direction perpendicular to a surface of unit area, due to a unit temperature gradient under given conditions. This means that energy flows from high energy molecules to low energy ones between the boundaries of a body or between bodies in contact.

Two main methods are used to determine the thermal conductivity of materials. They are the steady state method and the transient method. Steady state methods are adopted for homogeneous materials. In this method, the flux is proportional to the temperature gradient along the direction of flow. The experimental procedures are time consuming however, the thermal conductivity values obtained by this method are accurate. The methods of steady state thermal conductivity analysis include, guarded hot plate method, unguarded hot plate method and cylindrical probe method to name a few. The transient analyses are the non-steady methods adopted for heterogeneous materials with moisture. Though the test procedures are relatively fast, the accuracy of the k value is less. The common methods adopted for transient analysis are laser flash method, step method, transient line, transient strip and transient plane method

When thermal energy arrives at the surface of rammed earth (conduction, convection and radiation), the method of propagation into the solid material is

primarily by conduction. This results in a rise in temperature in the structural member. The equation below governs the conduction of heat through rammed earth

$$\vec{q} = k\frac{\overrightarrow{\delta T}}{\delta t} \quad (2.1)$$

where,

q = rate of energy transfer,

k = thermal conductivity

T = temperature

The variation in time of temperature in a region of given geometry is obtained by finding a solution to the heat conduction equation where appropriate boundary conditions are defined.

$$\rho C_p \frac{\delta T}{\delta t} = \nabla.(k\nabla T) \quad (2.2)$$

Where ρ is the density of the sample,

C_p is the specific heat,

k is the Thermal Conductivity and

t is time.

This leads to an FEM-Discretized matrix equation

$$[k]\left[\vec{T}\right] = [Q] + [Q_T] \quad (2.3)$$

The transmission of heat in rammed earth is dependent on the combined physical properties of the constituent material, the degree of compaction and the moisture content. In practice, fine grained soils have been shown to have higher thermal resistivity than coarse soils. For thermal conductivity, the reverse is the case. At very low water contents, water is held with extreme

tenacity on the surface of the soil particles and within the lattice of crystalline clay minerals. More water begins to collect around the points of contact between the particles (Bodman & Edlefsen 1934). This bridge increases the heat transfer from one grain to the other (Lee et al. 1999). It has been observed that the thermal conductivity of soils vary markedly between dry soils and wet soils (Pan & Mahrt 1987; Orchard & Cook 1983; Dickinson 1984; Hall & Allinson 2009)

2.6 Ultrasonic Pulse Velocity

Non-destructive testing of construction materials is currently of growing interest (Khatib 2005; Komlos et al. 1996; Kewalramani & Gupta 2006). Ultrasonic pulse velocity is only one out of many such non-destructive methods. Others include impact-echo, pulse-echo, wave reflection, resonant frequency, acoustic emission and microwave adsorption methods.

The pulse velocity method has been shown, for some time, to provide a reliable means of estimating properties and offers a unique opportunity for direct, reliable, quick, safe, inexpensive and non-invasive quality control of buildings and other construction materials (Komlos et al. 1996). The velocity of ultrasonic pulses traveling in a solid depends on the dynamic Young's modulus, dynamic Poisson's ratio, density and elastic properties of the material. It is thought that ultrasonic pulse velocity can often be used to assess the overall quality of a material (Khatib et al. 2010). Pulses of longitudinal, elastic stress waves are generated by an electro-acoustical transducer that is held in direct contact with the surface of the material being tested.

The equipment measures the speed at which the pulse travels through the length of the material to be received by a second transducer (Popovics 2001). Sometimes, the ultrasonic pulse velocity equipment measures the transit time of a pulse between transducers placed on the surface of the. The pulse velocity is then calculated using the measured path length through the material (Trtnik et al. 2009). According to the BS 1881-201(1986), the

principal advantage of ultrasonic pulse velocity measurement is that it reflects the properties of the interior of the material being tested (Khatib 2008; Keating et al. 1989).

2.7 Soil Selection Criteria for Natural Rammed Earth

A wide variety of sub-soils have been used for natural rammed earth buildings, with the exception of uniform coarse sands and gravels with no fines or cementing agents (Hughes, 1983). For earth wall construction, the soil should contain all four elements (McHenry, 1984). Ideally the soil should have a high sand/gravel content, with some silt and just enough clay to act as a binder and assist soil compaction (Keable, 1996).

According to Norton (1997) any material coarser than 5-10mm should be sieved out. Previous experimental work indicates that increasing gravel size reduces the compressive strength of rammed earth cylinders. However more research is warranted to define grading for rammed earth, especially maximum gravel size and proportions. Proposals tend to converge towards a 30%-70% balance between clay/silt and sand proportions (Easton, 1996).

2.8 Stabilisation

Soil needs to be stabilised because the material, as found in its natural state, is susceptible to damage by water and is not durable for long-term use in buildings. This weakness can be corrected using suitable soil stabilisers. The objective of soil stabilisation is to increase the resistance of a soil to the naturally occurring destructive elements that reduce its structural integrity (Vilane, 2010). Stabilisers are widely used even though their stabilising effects have not been established (Vilane, 2010). Various stabilisers exist. Among the well-known stabilisers are molasses, cow dung, Pulverised Fuel Ash, lime, sawdust, and ordinary Portland cement.

2.8.1 Cement Stabilisation

The use of cement in construction has been seen to be a major concern as it is believed to be a major source of pollution. Over the last decade growing concern about global environmental impact is forcing the Civil Engineering and construction industry to review its conventional cement and concrete production methods with a view to replace them with sustainable alternatives (Nwaubani 2013).

There are however, various advantages in using cement as a stabiliser. Soil samples gain strength from both the formation of a cement gel matrix that binds together the soil particles and the bonding of the surface-active particles, like clay, within the soil (Montgomery, 1998). High levels of cement stabilisation improve the surface coating and reduce erosion (Walker, 2000) while increasing the cement has a considerable influence in improving the resistance of soils vulnerable to frost attack

However there are notable disadvantages in using cement. The permeability of most soils is reduced (ACI Materials Journal Committee, 1990) and hence the natural ability of earth to allow passage of moisture throughout the soil mass is also significantly impaired. Environmental impact of cement production and reduced ability for recycling of rammed earth are also significant arguments against widespread use of cement in rammed earth construction. Less significantly, thermal conductivity, compared to lime stabilized blocks, is reportedly increased (Adam and Jones, 1995).

2.8.1.1 Soil Selection Criteria for Cement Stabilized Rammed Earth

Soils for cement stabilized rammed earth tend to have proportionally higher sand and gravel content and correspondingly lower fines content. A soil suitable for cement stabilisation should have a significant sand content, at least greater than 50% and preferably closer to 75%, and at the same time low clay content, typically less than 25% (Delgado and Guerrero, 2007). As in the case of unstabilised rammed earth, these criteria are intended as a broad initial guide for soil selection and include recommendations for soil blocks as well as rammed earth.

2.8.2 Fibre Stabilisation

Fibres are used to improve the thermal performance and bending and tensile strength of soil. Natural fibres used include straw, sisal fibres and timber. According to Standards Australia (2002), the ideal soil for fibre stabilisation should have a plasticity index between 15% and 35% with the liquid limit from 30% to 50%. One disadvantage of fibre stabilisation is that the compressive strength of soils decreases as the straw content increases (Minke, 2000).

2.8.3 Sodium Silicate Stabilisation

Sodium silicate is used at quantities of around 5% to act as a binding agent to increase compressive strength in sandy and silty soils. According to Houben & Guillaud (1994), a curing period of about 7 days is advisable.

2.8.4 Lime Stabilisation

Lime has been used in building techniques for over 5,000 years. Archaeological evidence shows it to have been in existence for this time frame due to its resilience, durability, and water resistant qualities.

Lime is one of the older materials produced by man and remains a most useful material, e.g., for some chemical, metallurgical and building industries (Ochoa *et al* 2010). Surprisingly enough, the published knowledge on such an old and widespread industry is not as large as could be expected, and some process relations are not well documented (Ochoa *et al*, 2010). This fact stresses the necessity to analyse some empirical knowledge established almost as ‘universal truth’ at basic level.

The Romans used lime extensively in their building programme in Britain, and refined its application into mortars and plasters, which remained the principal surface finish for buildings until the nineteenth century, when cements took over this function (Heathcote KA. 1995). For this reason, many historic buildings in the UK contain large amounts of lime within their fabric, and an understanding of its merits and application is crucial for the care of such

property - important if you are considering an ecologically-minded renovation of an old property (National Lime Association, 2010).

Also, lime as a building material is undergoing a revival of interest and application amongst those who favour a more natural solution to building needs. Lime, gypsum and clay are particularly suited to the construction of straw bale houses or earth ships, where these natural materials seal the straw or rubber creating a strong and solid, yet breathable wall (National Lime Association, 2010).

Soil stabilisation occurs when lime is added to a reactive soil to generate long-term strength gain through a pozzolanic reaction. This reaction produces stable calcium silicate hydrates and calcium aluminate hydrates as the calcium from the lime reacts with the aluminates and silicates solubilised from the clay. The full-term pozzolanic reaction can continue for a very long period of time, even decades -- as long as enough lime is present and the pH remain high (above 10). As a result, lime treatment can produce high and long-lasting strength gains. The key to pozzolanic reactivity and stabilisation is a reactive soil, a good mix design protocol, and reliable construction practices.

In order to produce lime, limestone is calcinated by supplying heat. The dissociation reaction of the carbonates contained in limestone is promoted by the heat absorbed by the limestone in a kiln, which implies three aspects: chemical, energetic and process control. Dissociation begins when limestone reaches the calcination temperature at the limestone surface, with a well-defined reaction interface moving to the centre of the limestone stone, forming a growing shell of quick lime around the unreacted core. To increase the reaction velocity, in order to reach a sufficient rate of production, it is necessary to increase the surface temperature of the stone over the calcinations temperature (Ochoa George *et al*, 2010).This process is carried out in kilns.

Some decades ago the use of lime mortars fell into disuse and the traditional craftsman experience was almost lost, especially in developed countries. This

situation was mainly due to changes in construction technology and the generalized use of cement as binder (Faria *et al*, 2008).

In cement mortars and gypsum plasters, calcium hydroxide is often added to improve plasticity and water retention. However, the carbonation capability of calcium hydroxide allows for its use as the main binder in lime–sand mortars and plasters, since the precipitation of carbonate crystals results in hardening and strength development. High-Ca lime mortar is mainly applied in the conservation of historic buildings, as its properties are more compatible with those of old materials. Among these properties, the higher permeability of lime-bonded in relation to cement ones not only suits historical applications, but can also provide a “breathable” inorganic coating for indoor rendering, thereby reducing moisture and fungus problems (Cardoso *et al*, 2009).

The material is utilized either in the form of “dry” hydrated lime (industrialized powder) or as lime putty (slaked with excess of water). The properties and performance of mortars and plasters differ significantly depending largely on the physical features of the calcium hydroxide used. Particle's characteristics as size distribution, shape and surface area have major influence on rheological properties, water retention and carbonation kinetics. Aged putties, for instance, are known to possess small particle size, a predominant plate-like portlandite morphology and large surface area. Consequently, these present high plasticity and water retention values undergo fast carbonation and provide early strength development (Cardoso *et al*, 2009).

Different deterioration factors can affect the durability of any earthen structure. Some of the most important ones could be included in the following main groups:

i) Wet and dry cycles;
ii) Rain exposure and related leaching;
iii) Freezing and thawing cycles;
iv) Exposure to pollutants (such as SO2); and
v) Sun's rays.

The extent to which rammed earth is affected by these deterioration factors is a function of its properties, which depend, in turn, on several issues, such as the kind and characteristics of the binder and the aggregate, the binder/ aggregate ratio, the amount of mixing water, the mortar's permeability, the water absorption capacity through capillarity, water intake, the presence of admixtures and the curing conditions (Izaguirre *et al*, 2010).

When calcium oxide from lime or cement is added to a soft soil, hydration reactions occur, immediately forming calcium hydroxide. Immediately, Ca^{2+} ions preferentially displace monovalent cat-ions at the negatively charged sites on the clay mineral. These cat-ion exchange processes displace Na^{+} and K^{+} ions into the pore water. The replacement of the monovalent ions by Ca^{2+} ions induces changes in the soil system and soil properties on a timescale of minutes to hours. The increased concentration of Ca^{2+} ions coagulates the clay particles and transforms the plastic soil to a more granular soil character (Lagaly, 2006). The rapid ion exchange is known as soil improvement or modification (Holt and Freer-Hewish, 1998; Rogers and Glendinning, 1996; Boardman *et al*., 2001)

Lime, in one form or another, has been used to modify the properties of fine grained deposits (Broms and Boman, 1975; Okumura and Terashi, 1975; Locat *et al*., 1990, 1996). Treatment of soils with lime has brought many beneficial effects, such as improvements in the plasticity characteristics and strength behaviour with time (Kamon, 1992; Narasimha Rao and Rajasekaran, 1996). It is well established that the use of lime in fine-grained soils makes the system less sensitive to changes in stress and other environmental factors (Kamon and Nontananandh, 1991; Sivapullaiah *et al*., 1998). Many engineers have realized this advantage all over the world and hence, in many situations, lime is used to improve soil characteristics in civil engineering applications. Recently, an attempt was made to improve the engineering characteristics of soft soils by using deep mixing techniques (Okumura and Terashi, 1975; Terashi and Tanaka, 1980; Mitchell, 1981; Rajasekaran, 1998). Lin and Wong (1999) have highlighted the application of

the deep cement-mixing technique for improving the shear strength of soft marine clay.

The deep lime-mixing technique has proved to be a successful method of strengthening or stiffening soft, fine-grained soils, and also of minimizing ground settlement. However, further study is required to determine the effectiveness of the lime stabilisation technique in marine environments, which have high sodium concentrations in the pore water. In view of the above, the compressibility behaviour of lime-stabilized soil systems has to be determined before this technique is attempted (Rajasekaran and Narasimha, 2002). The lime-induced variation in compressibility characteristics of soil systems with time was investigated by using standard oedometer tests as per the procedure given in ASTM D 2435-80 (1989).

In addition to stabilisation of new materials, lime is an excellent choice for the reclamation of road bases. As more and more governmental entities are choosing to reclaim existing road bases rather than replace them, this use of lime will become even more important over time (Morel JC, *et al* 2001).

Lime stabilisation is not difficult to carry out. After proper mix design and testing is performed, in-place mixing is usually used to add the appropriate amount of lime to soil, mixed to an appropriate depth. Pulverization and mixing is used to thoroughly combine the lime and soil. For heavy clays, preliminary mixing may be followed by 24 to 48 hours (or more) of moist curing, followed by final mixing (NLA, 2001). For maximum development of strength and durability, proper compaction is necessary. Proper curing is also important. If sulphates are present at levels greater than 0.3 percent, special procedures are required.

“However, hydraulic lime mortar is not just a building conservation material. It is an excellent all-round performer with a place in general modern construction. Hydraulic lime mortar shares the practical benefits of modern cement based mortars but has none of the disadvantages.

2.8.5 Benefits of Stabilisation

The benefits of soil stabilisation are numerous some of them include:

- Very substantial increases in resilient modulus values (by a factor of 10 or more in many cases)
- Very substantial improvements in shear strength (by a factor of 20 or more in some cases)
- Continued strength gain with time, even after periods of environmental or load damage (autogenous healing)
- Long-term durability over decades of service even under severe environmental conditions.

These performance benefits translate into short- and long-term economic benefits.

- In the short-term, considering the structural contribution of lime-stabilized layers in pavement design can create more cost-effective design alternatives due to the increased strength of the lime stabilized sub base.
- In the longer term, lime stabilisation provides performance benefits that reduce maintenance costs.

2.9 Palm Kernel Shell (PKS)

Palm Kernel Shell (PKS) is a hard, carbonaceous, organic material and is one of the by-products of the process of extracting palm oil from the palm oil fruit. The production of palm oil has increased almost threefold over the past three decades in the world. The total production of palm oil was estimated at 45.1 million tons for the year 2009–2010. After processing and extraction of oil, solid residues and liquid wastes which have been generated from the fresh fruit bunches, result in varying by-product including empty fruit bunches fibre, shell, and effluent. These are usually dumped in the open (Osei & Jackson 2012) or buried in landfills thereby impacting the environment negatively without any economic benefits. As a result, air, river, sea and groundwater pollution have increased due to the large amount of waste produced

(Muntohar & Rahman 2014). The shells have no commercial value, but create disposal and waste management problems (Osei & Jackson 2012). Mahmud *et al* (2009) reports that nearly 4 million tonnes of PKS is produced annually in Malaysia alone and this has been predicted to increase significantly as increased palm oil processing is likely to take place in the near future

The fruit from which both product and waste is obtained from is known as the Oil Palm Fruit which is also known botanically as *Elaeis guineensis*. It is usually reddish in colour. The fleshy pericarp, rich in palm oil gives it this colour. The oil is held together by thick fibres that grow around the kernel's shell. The kernel is housed in a shell known as the Palm Kernel Shell. The kernel is edible or can be processed further to produce oil. While palm oil is used for food, Palm Kernel Oil is used as food and in soap making.

Oil Palm Fruit is commonly found in the tropics. They were originally found in West Africa but can now be found wherever rainfall is abundant and the temperature sufficiently high for most of the year. The fruits found in various countries differ slightly. For instance, the palm varieties, growth conditions and plantation management in Thailand are reportedly different from those in Malaysia and results in a different quantity of solid wastes (Prasertsan & Prasertsan 1996).

2.9.1 Physical and Mechanical Properties of Palm Kernel Shell

In palm oil mills, the hard shells are directly attained by breaking the palm kernel shells with machinery. Normally, OPS aggregates are composed of different shapes (Mannan & Ganapathy 2004) which are flaky, parabolic, angular, and possess smooth concave and convex surfaces (U. Johnson Alengaram, Hilmi Mahmud, Mohd Zamin Jumaat 2010) with 60-90 % of the particles in the range of 5-12.7 mm in size having thickness ranging between 1.7mm to 4mm (U Johnson Alengaram et al. 2008).

Muntohar and Rahman (2014) reports that the Los Angeles abrasion value of PKS was about 4.8%. The aggregate impact value and aggregate crushing

value of PKS aggregates discovered to be much less than traditional crushed stone aggregate. Olanipekun et al (2006) reports that the moisture content of PKS is about 4.35%, but was reported as 9% by Ndoke (2006).

The hard shells do not easily suffer deterioration. The hardness of PKS, when measured by the durability test using Los Angeles abrasion method showed a value of 96.4% (Olanipekun et al. 2006). The water absorption capacity of the shell is also high and ranges from 14% to 33% when subjected to a 24 hour submersion test. This value implies that PKS absorbs more water than conventional gravel aggregates (Muntohar & Rahman 2014).

The unit weight and the specific gravity of the shell ranges between 1462kg/m^3 and 2050kg/m^3 and 1.17 and 1.46 respectively which is lower than the 2.5-3.0 range of specific gravity for normal weight aggregates (Olanipekun et al. 2006). The bulk density was found to be 740kg/m^3 (Olutoge 2010; Ndoke 2006). Other properties are: Void ratio - 0.4, Porosity – 28%, Impact Value – 4.5% (Ndoke 2006), Fines Modulus – 6.24, Flakiness Index 65.17%, Elongation Index 12.36% (Alengaram et al. 2013), Thermal conductivity 0.19W/mK (Alengaram et al. 2013) . Porosity was observed to be in the same range as granite, quartzite and far above limestone (Ndoke 2006). The existence of numerous pores in the OPKS is responsible for high water absorption in the range of 14–33%. The free surface moisture content is reported to be in the range of 8–15% (Alengaram et al. 2013). Dry density values place the palm kernel shells in the same category as lightweight aggregate especially pumice, scoria or vermiculate for natural and Pulverised Fuel Ash and clinker for processed aggregates (Ndoke 2006).

2.9.2 Present Application of PKS

Palm kernel shell has previously been used as partial replacement of coarse aggregate in asphalt (Olutoge 2010; Ndoke 2006), reinforced concrete slabs

(Olutoge 2010), as alternate fuel for firing bricks (Obeng et al. 1997; Jaafar & Ahmad 2011) and the production of light weight concrete (Olanipekun et al. 2006; Mahmud et al. 2009; U J Alengaram et al. 2008) and as replacement of coarse aggregate in Rammed Earth (Okoronkwo, Emekwuru, et al. 2014).

2.9.2.1 Use of Palm Kernel Shell as Coarse Aggregate Replacement

Several research efforts has been carried out into the use of PKS as replacement of coarse aggregate in different materials and as partial replacement of coarse aggregate in asphalt,

U.Johnson Alengaram *et al.* (2008) looked into the use of PKS as light weight aggregate in producing grade 35 lightweight concrete. It was discovered that failure of tested concrete was largely due to breaking of PKS and thus concluded that failure of PKS governed the strength. However, strengths reached 36MPa so it was concluded that PKS was suitable for use in grade 35 concrete.

It was also discovered in the course of research that concrete made from PKS had low workability, had water absorption of more than 10% with higher initial surface absorption than ordinary concrete, showed higher ductile behaviour, higher shear strength, had 8 times the normal amount of creep and reached compressive strength values of 48MPa. PKS concrete had thermal conductivity of 0.43W/mK, lower than 0.76-3.68W/mK usually observed for normal weight concrete (Alengaram et al. 2013).

2.9.2.2 Use of Palm Kernel Shell as Fuel Mass

Palm Kernel Shell has found application as a bio fuel. PKS has been found to have high calorific value (Shuit et al. 2009; Sumathi et al. 2008; Kim et al. 2010). Moisture content in kernel shells is low as compared to most other biomass materials. Different sources have suggested values between 11% and 13%(Olanipekun et al. 2006; Okafor 1988; Mannan & Ganapathy 2004). Palm kernel shells contain residues of Palm Oil, which accounts for its slightly higher heating value than average lignocellulosic biomass. Compared to other

residues from the industry, it is a good quality biomass fuel with uniform size distribution, easy handling, easy crushing, and limited biological activity due to low moisture content.

The problems associated with the burning of these solid fuels are the emissions of dark smoke and the carry-over of partially carbonized fibrous particulates due to incomplete combustion of the fuels

2.10 Pulverised Fuel Ash

Pulverised Fuel Ash is a particulate substance containing metal oxides, carbon and other microelements. It is usually generated during the combustion of coal and other carbonaceous matter for energy production and collected by the cleaning equipment of flue emissions, commonly filters or electrostatic precipitators. It is an industrial by-product which is recognised as an environmental pollutant. Pulverised Fuel Ash particles are considered to be highly contaminating, due to their enrichment in potentially toxic trace elements which condense from flue gas (Ahmaruzzaman, 2009). This should not be confused for bottom ash which is also a product of an incineration process(Siddique et al. 2008; Khatib et al. 2013).

Due to its properties, coal combustion Pulverised Fuel Ash is a commercially valuable additive for the production of blended cements and concrete mixtures. It is an abundant mineral resource with high production rate and its utilization is an attractive alternative to costly disposal. Recycling of the Pulverised Fuel Ash as partial replacement of cement is the key factor of reducing the production costs of concrete (Ctvrtnickova et al, 2009).

Because Pulverised Fuel Ash contains a range of heavy metals of different mobility in its structure and because it is usually disposed of in the form of slurry close to the power plant where it is produced, Pulverised Fuel Ash possesses high environmental risk due to the possibility of leaching of these metals into environment (Khatib 2008; Khatib 2009; Khatib et al. 2009; Khatib

et al. 2011; Jamal M Khatib et al. 2014; Khatib et al. 2008; J M Khatib, Onaidhe, et al. 2014; J M Khatib, Halliday, et al. 2014).

A very high percentage of Pulverised Fuel Ash produced is disposed of as landfill. Disposal of Pulverised Fuel Ash will soon be too costly – if not forbidden. Considerable research is being conducted worldwide on the use of waste materials in order to avert an increasing toxic threat to the environment, or to streamline present waste disposal techniques by making them more affordable. It follows that an economically viable solution to this problem should include utilization of waste materials for new products rather than land disposal (Ahmaruzzaman, 2009).

Pulverised Fuel Ash is generally grey in colour, abrasive, mostly alkaline, and refractory in nature. Pozzolans, which are siliceous or siliceous and aluminous materials that together with water and calcium hydroxide form cementitious products at ambient temperatures, are also admixtures. Pulverised Fuel Ash from pulverized coal combustion is categorized as such a pozzolan. Pulverised Fuel Ash also contains different essential elements, including both macronutrients P, K, Ca, Mg and micronutrients Zn, Fe, Cu, Mn, B, and Mo for plant growth. The geotechnical properties of Pulverised Fuel Ash (e.g., specific gravity, permeability, internal angular friction, and consolidation characteristics) make it suitable for use in construction of roads and embankments, structural fill etc. The pozzolanic properties of the ash, including its lime binding capacity makes it useful for the manufacture of cement, building materials concrete and concrete-admixed products. The chemical composition of Pulverised Fuel Ash like high percentage of silica (60– 65%), alumina (25–30%), magnetite, Fe2O3 (6–15%) enables its use for the synthesis of zeolite, alum, and precipitated silica. The other important physicochemical characteristics of Pulverised Fuel Ash, such as bulk density, particle size, porosity, water holding capacity, and surface area makes it suitable for use as an adsorbent (Ahmaruzzaman, 2009).

From the perspective of power generation, Pulverised Fuel Ash is a waste material, while from a coal utilization perspective, Pulverised Fuel Ash is a resource yet to be fully utilized; producers of thermal electricity are thus looking for ways to exploit Pulverised Fuel Ash. The cement industry might use it as a raw material for the production of concrete. Coal Pulverised Fuel Ash discharged from power plants can also be utilized as a by-product, and its use in recycling materials for agriculture and engineering is also being studied. The conversion of Pulverised Fuel Ash into zeolite has also been widely examined (Ahmaruzzaman, 2009).

2.10.1 Properties of Pulverised Fuel Ash

Characterisation of Pulverised Fuel Ash in terms of composition, mineralogy, surface chemistry and reactivity is of fundamental importance in the development of various applications of Pulverised Fuel Ash.

Pulverised Fuel Ash consists of fine, powdery particles predominantly spherical in shape, either solid or hollow, and mostly glassy, (amorphous) in nature. The carbonaceous material in the Pulverised Fuel Ash is composed of angular particles. The particle size distribution of most bituminous coal Pulverised Fuel Ash is generally similar to that of silt (less than a 0.075 mm or No. 200 sieve). The specific gravity of Pulverised Fuel Ash usually ranges from 2.1 to 3.0, while its specific surface area may vary from 170 to 1000 m2/kg. The colour of Pulverised Fuel Ash can vary from tan to grey to black, depending on the amount of unburned carbon in the ash (Ahmaruzzaman, 2009).

The chemical properties of Pulverised Fuel Ash are influenced to a great extent by the properties of the coal being burned and the techniques used for handling and storage. There are basically four types, or ranks, of coal, each vary in heating value, chemical composition, ash content, and geological origin. The four types (ranks) of coal are anthracite, bituminous, sub-bituminous, and lignite. In addition to being handled in a dry, conditioned, or

wet form, Pulverised Fuel Ash is also sometimes classified according to the type of coal from which the ash was derived.

The several distinct end uses of Pulverised Fuel Ash differ considerably among themselves in the stringency of the properties required in the Pulverised Fuel Ash for its successful utilization. The success of Pulverised Fuel Ash in structural fill applications rests primarily on the ability of the material to be compacted to a reasonably strong layer of low unit weight. This is primarily a function of particle size distribution, and to some extent of the content of spherical particles. The chemical characteristics of Pulverised Fuel Ash are secondary, although the post compaction cementation provided by some high-calcium Pulverised Fuel Ash is likely to prove beneficial. With highway bases chemical considerations come into play, although not in an important way. Stabilization of some base courses (and stabilized sub grades) may rest on lime Pulverised Fuel Ash chemical reactions, i.e. the classical ‘‘pozzolanic’’ reaction, with lime. Low-calcium Pulverised Fuel Ash may be entirely satisfactory or even preferred, especially where sufficient time is available for these slow reactions to take place. The only real chemical requirement is that Pulverised Fuel Ash has a sufficient content of glass that eventually will react with added lime. Some road base applications of Pulverised Fuel Ash depend on the physical effects of Pulverised Fuel Ash incorporation rather than its reaction with lime (Ahmaruzzaman, 2009).

The cement and concrete end-use areas are by far the most demanding of the Pulverised Fuel Ash in terms of adherence to strict criteria and requirements. However, the requirements differ considerably depending on the specific end use involved. Pulverised Fuel Ash for use as a raw material in cement manufacture is sold and used primarily on the basis of its chemical composition, as expressed in the usual oxide convention. Such factors as glass content, the type of crystalline matter present, size distribution, etc., are relatively immaterial. Even high carbon content, which may be limiting in most other end uses, may actually be beneficial in cement raw material use, since it provides a definite (although modest) proportion of the fuel needed. Uniformity

and chemical consistency from day to day and week to week is the prime necessity (Ahmaruzzaman, 2009).

2.10.2 Utilization of Pulverised Fuel Ash

Presently, Pulverised Fuel Ash has found quite a number of applications and every day, new reasons to use Pulverised Fuel Ash emerge. There is still a need to develop new uses for fly as:

- Disposal costs are reduced,
- Reduced need for disposal means that less area of land is needed and thus freeing up land for other uses.
- By-products replace existing natural resources that are either very expensive or do not occur in abundance
- Income is derived from sale of Pulverised Fuel Ash.

Utilization is usually in the form of replacement of a whole or parts of industrial resource. These may include such processes and applications as addition to cement and concrete products, structural fill and cover material, roadway and pavement utilization, addition to construction materials as a light weight aggregate, infiltration barrier and underground void filling, and soil, water and environmental improvement.

Care has to be taken when using Pulverised Fuel Ash as utilization of Pulverised Fuel Ash in water involves the potential leaching of some elements into water. This creates a problem of secondary environmental pollution. The surface layer of Pulverised Fuel Ash particles, probably of microns in thickness, contains a significant amount of readily leachable material deposited during cooling after combustion. Therefore, the charge on the surface of Pulverised Fuel Ash particle and formation of diffuse double layer plays a significant role in leaching. The elements present were divided into two groups based on their concentration dependence of particle size. The elements Mn, Ba, V, Co, Cr, Ni, Ln, Ga, Nd, As, Sb, Sn, Br, Zn, Se, Pb, Hg and S are usually volatile to a significant extent in combustion process. The volatility for these elements is inversely proportional to particle size. Elements,

such as, Mg, Na, K, Mo, Ce, Rb, Cs and Nb possess a smaller volatilized fraction during coal combustion. The volatility is directly proportional to particle size. The elements Si, As, Fe, Ca, Sr, La, Sm, Eu, Tb, Py, Yb, Y, Se, Zr, Ta, Na, Th, Ag and Zn are either not volatilized or may show minor trends related to geochemistry of mineral matter. The volatility of trace elements increased from larger to smaller particle size and establishes an inverse relationship of volatility and particle size (Ahmaruzzaman, 2009).

The use of mineral additions for the manufacture of mortar and concrete normally includes natural pozzolans and by-products such as Pulverised Fuel Ash and silica fume. Several studies have reported that the addition of Pulverised Fuel Ashes improves the mechanical characteristics of mortars and concretes as a consequence of their pozzolanic activity and the spherical form of their particles. The addition of silica fume to mortar or concrete enhances the final resistances since it acts both as a chemically inert filler, improving the physical structure, and as a pozzolan, reacting chemically with the CH formed during the hydration of cement. However, the demand for silica fume is much greater than its supply, and its price is consequently also high. Pulverised Fuel Ash, on the other hand, is a by-product with a low price and whose chemical composition suggests that, with the appropriate treatment, its effect could be similar to that of silica fume (Blanco et al, 2006).

2.10.3 Barriers to Utilization

There are a number of technical, economic, institutional, and legal barriers to the use of large quantities of coal Pulverised Fuel Ash. Technical and economic barriers are not mutually exclusive in that technological advancements usually result in economic feasibility. Principal technical barriers include issues related to coal Pulverised Fuel Ash production, specifications and standards, materials characterization, product demonstration and commercialization, and user related factors. Economic barriers to increased use of coal Pulverised Fuel Ash can be key among all factors affecting by-product use. With proper economic incentives, other barriers to increased use of coal Pulverised Fuel Ash can be overcome. For

coal-burning electric utilities, the revenues from the sale of coal Pulverised Fuel Ash are often insignificant. The high cost of transportation of low unit-value coal Pulverised Fuel Ash and competition from locally available natural materials pose two of the most important economic barriers.

Table 2.1 Summary of requirements for Pulverised Fuel Ash LOI in different Major Coal-Using countries (Dong 2010).

Countries	**LOI limits, %, maximum**
Australia	3-6
Canada	3-10
China	5-15
EU	Type A: 5 Type B: 2-7 Type C: 4-9
India	5
Japan	3-8
Russia	Basic ash: 3-5 Acid ash: 2-25
South Africa	5
USA	Class F: 6 Class C:6

The type of Pulverised Fuel Ash also dictates what it can be used for. In all national standards for Pulverised Fuel Ash use in cement/concrete, the permitted concentration range of unburnt carbon in Pulverised Fuel Ash is indicated by the loss on ignition (LOI) parameter. This mass-based parameter can be measured quickly and serves practically as the first step in Pulverised Fuel Ash quality control (Dong 2010). LOI is calculated by

$$LOI\ (\%) = 100X\ \frac{(\text{as received weight} - \text{ignited weight})}{ignited\ weight} \qquad (2.4)$$

Apart from China and Russia which allow for relatively high LOI values for certain ashes, other major coal consuming countries stipulate very low LOI limits for Pulverised Fuel Ash for use in concrete production (Dong 2010) (see Table 2.1 and 2.2).

Table 2.2. Recommended properties of Pulverised Fuel Ash in brick manufacturing (Bijen 2005).

Chemical composition	*Mass percentage*
LOI	*6*
SO3	*2.5*
MgO	*2*
SiO2	*40*
Fineness	
Residue on sieve: 200μm	*<10*
90μm	*<20*
60μm	*<30*

Other institutional and legal barriers are the lack of knowledge of potential ash uses, sporadic data on environmental and health effects, compositional inconsistencies in the products, belief that other raw materials are readily available, lack of State guidelines, and viewpoint of the industry that Environmental protection agency (EPA) regulations and procurement guidelines are too complicated and rigid rather than being general guidelines for use. An American Society for Testing and Materials subcommittee under the Committee E-50 on Environmental Assessment, on which the U.S. Geological Survey (USGS) is represented, was recently formed to address the question of standards and definitions of coal and coal combustion products (CCP)-related terms. Subcommittee members evaluated the latest draft of the definitions document. Recommendations were submitted to the committee for action in 2001. This draft calls for the change of coal

combustion products (CCPs) to coal combustion by-products (CCBs) to iterate the ideal definition of a product, which is the principal reason for a process. It is argued that coal is burned to produce energy, not ash. Therefore, energy is the product of coal-burning processes; anything else is a by-product. Concerned industry and government representatives, scientists, and engineers have formed a number of national and international organizations to address the removal of barriers to use of coal Pulverised Fuel Ash (Ahmaruzzaman, 2009).

Generally speaking, the utilization of Pulverised Fuel Ash in concrete and mortar production brings economic benefits because it is usually a low-cost material and it can be used to replace higher-cost materials. Additionally, in some cases, the use of Pulverised Fuel Ash in concrete and mortar mixes represents technological advantages, due to pozzolanic activity, workability of mixes and regularity of production and composition. Finally, environmental aspects should be taken into account when Pulverised Fuel Ash is used: for example, energy saving, reduction of carbon dioxide emission, and lessened disposal problems. More questions and factors arise when trying to make these materials applicable to reinforced concrete structures because the protection of rebars from corrosion is essential (Garcés et al, 2009).

2.11 Flow Theory

Fluid molecules exert forces of attraction on each other. Flow of fluids through a porous or semi porous media can be predicted and the methods depend on whether the material is saturated or unsaturated. Rammed earth does not readily exist in a saturated state so this section will look at the methods for the unsaturated flow of water through rammed earth.

Moisture is one of the major factors that contribute to deterioration in Rammed Earth. Transportation of liquid takes place in open pores mainly due to diffusion, suction and capillary absorption. Capillary absorption is driven by surface tension

According to moisture content theory, water transport in porous materials can be classified into two types; Permeability and Sorptivity

Permeability is the passage of fluid through a saturated material under the action of a pressure differential. Permeability capacity is influenced by total porosity. The driving force is concentration and pressure gradient.

Sorptivity is the unsaturated material's ability to absorb and transmit water through it by capillary action. The rate of transport is influenced by pore size distribution. The driving force is surface tension. Capillary absorption takes place in fine pores (10nm - 10µm) and it occurs when forces arising from surface tension are in the same range as gravity forces present in the liquid. It is the prime mechanism when a material is only partially wetted. Rammed earth is rarely saturated while in use so Sorptivity will be examined in greater detail.

Capillary activity is described with reference to

Temperature T,

Moisture Content w,

Pore humidity h_r

Duration of contact with water ($t_{contact}$)

Thermal conductivity λ_T

Specific heat capacity C_T

Vapour diffusion D_h

$$\frac{\partial T}{\partial t} = div\left(\frac{\lambda_T(T,w)}{C_T(w)} . \overrightarrow{grad}\,(T)\right) \quad (2.5)$$

$$\frac{\partial h_r}{\partial t} = div\left(D_h(T,h_r) . \overrightarrow{grad\,(h_r)}\right) - \overrightarrow{D_{cap}}\left(t_{contact,}h_r, E/C\,, T\right)°grad\,(h_r) \quad (2.6)$$

Equation 2.6 obeys the Arrhenius law and shows that water transport is a function of Temperature, moisture content and pore humidity.

The Lucas –Washburn equation also applies defining h as.

$$h = k\sqrt{t} \qquad (2.7)$$

h = height of liquid front

t = wetting time

k = capillary coefficient

but k is also defined as,

$$k = \sqrt{\frac{\gamma_r \cdot \cos\vartheta}{2\eta}} \qquad (2.8)$$

λ = surface tension

r = capillary radius

ϑ = contact angle

ŋ = dynamic viscosity

where these parameters are difficult to obtain, we use:

$$i = s\sqrt{t} \qquad (2.9)$$

but

$$i = \frac{M}{A} \qquad (2.10)$$

i = volume of absorbed liquid per unit cross-section

s = Sorptivity and can be measured in $kg/m^2.h^{1/2}$, easily determined from the slope of the linear part of the curve M/A vs $t^{0.5}$.

The equation for unsaturated flow also applies. This is the extended Darcy's equation

$$\vec{q} = -k(\theta)\nabla\Psi \quad (2.11)$$

q = flow velocity

Ψ = capillary potential

K = hydraulic conductivity function

θ = normalised water content.

Combining this with the mass-conservation equation,

$$D(\theta) = k(\theta)\left(\frac{d\Psi}{d\theta}\right) \quad (2.12)$$

We get

$$\frac{\partial\theta}{\partial t} = \nabla.(D(\theta)\nabla\theta) \quad (2.13)$$

D(θ) is a material property known as hydraulic diffusivity.

For a rammed earth sample which is a one dimensional, semi-infinite system subject to boundary conditions ϑ =1 at x= 0 and an initial condition ϑ = 0, x > 0, t = 0 (describing a condition of uniform initial water content within the sample) the equation may then be described by

$$\frac{\partial\theta}{\partial t} = \frac{\partial}{\partial x}\left(D(\theta)\frac{\partial\theta}{\partial x}\right) 0 < x < \infty \quad (2.14)$$

Bolzmann transformation

$$\emptyset = x/\sqrt{t} \quad (2.15)$$

Reduces the equation to

$$-\frac{1}{2}\emptyset\left(\frac{d\theta}{d\emptyset}\right)=\frac{d}{d\theta}\left(D(\theta)\frac{d\theta}{d\emptyset}\right) \quad (2.16)$$

But because the functional relationship between D and θ is strongly non-linear and is not always feasible to be determined, for the purpose of predicting the water content profile by absorption, it is commonly approximated by the exponential-law

$$D(\theta) = D_o e^{n\theta} \quad (2.17)$$

Where D_o and n are empirically fitted constants.

$\frac{\partial C}{\partial n}$ is the moisture gradient at the drying surface identified by a unit n, C_e is the equilibrium moisture content that an element would reach given particular environmental conditions C_s the moisture content of the drying surface and f the convective moisture transfer coefficient.

In order to solve the boundary problem, the Fourier method can be applied.

$$c(x,t)=C_0\left(1-\frac{4}{\pi}\sum_{n=0}^{\infty}\frac{1}{2n+1}exp\left(-\frac{(2n+1)^2\pi^2Dt}{4L^2}\sin\frac{(2n+1)\pi x}{2L}\right)\right) \quad (2.18)$$

This formula expresses the water concentration profiles according to the (x) coordinate and the (t) time in all the section of the sample.

The volume of water absorbed through the permeable surface

$$M=\iiint_V C(x,t)dxdydz \quad (2.19)$$

Where A is the area (Villar-Cocina et al. 2002),

$$M=AC_0L\left\{1-\frac{8}{\pi^2}\sum_{n=0}^{\infty}\frac{1}{(2n+1)^2}exp\left(-\frac{(2n+1)^2\pi^2Dt}{4L^2}\right)\right\} \quad (2.20)$$

The amount per unit area becomes

$$\frac{M}{A}=N\rho\left(1-exp\left(\frac{-St^{\frac{1}{2}}}{N\rho}\right)\right)+C_0L\left(1-\frac{8}{\pi^2}\sum_{n=0}^{\infty}\frac{1}{(2n+1)^2}exp\left(-\frac{(2n+1)^2\pi^2Dt}{4L^2}\right)\right) \quad (2.21)$$

Where

N = Constant related to the distance from the concrete surface over which capillary pores control the initial sorption

P = Density of water

D= Diffusion coefficient

C = Water concentration

t = Time.

C_0 = invariance of water concentration

When taken in isolation, the first part of equation 2.21 relates to the sorptivity of the material and is the prevailing force at the initial stages of moisture ingress. The second part is dominated by the diffusivity of the material and has influence in water absorption over much longer exposure to moisture.

Using the above model to produce predictive data and comparing this to experimental data yields the results shown in chapter eight. This is also compared to results obtained from recent articles (Villar-Cocina et al. 2002).

2.12 Rammed Earth Building processes

A growing interest has now been focused on earth construction. However several problems have been identified. There is a general lack of resistance to water, uncontrolled shrinkage and low inherent strength. There is also a loss of strength when saturated with water, erosion due to wind or driving rain and poor dimensional stability

These problems over time have been addressed by mechanical compaction, stabilisation with chemical binders like cement and stabilisation with natural fibres. Dynamic compaction close to the Proctor optimum moisture content

increases the inter-particle friction/interlock whilst reducing the bulk porosity. The addition of hydraulic binders (commonly 10% Portland cement) increases the internal cohesion of the material and enhances durability and toughness. Since hardened cement paste bonds particles together by surface adhesion between the paste and particle surfaces (interfacial transition zone), cement stabilisation is most effective on granular soils (Hall and Allinson, 2009).

2.13 Summary

Rammed earth has shown to be very versatile in application. Rammed earth has started to gain acceptance in so many countries and therefore there is a need to better understand the characteristics. Also the possibility of disposing waste products in rammed earth needs to be investigated in detail.

Chapter Three

Methodology

The determination of physical and mechanical properties of rammed earth depended heavily on experimental tests. This chapter describes the techniques used for soil selection, grading, mixing, and blending. Also described in this section is the production of rammed earth cubes and the test methodologies for measuring their engineering properties.

3.1 Materials

Materials used for the procedure include the various components that form the Earth that was rammed to produce cubes and other materials that was either added as additional materials or used in the replacement of earth constituents and they include, Palm Kernel Shells, Cement and Pulverised Fuel Ash. All experiments were carried out in the University of Wolverhampton laboratory using standard laboratory materials.

The earth material compressed to produce rammed earth for this research has been put together by blending three component sub-soils of known origin and properties. The components of rammed earth materials are comparable to those of concrete. The inert aggregate fraction is represented by granular soils (sand and gravel), the binder fraction is represented by cohesive soil (clay) and water is used in activating the lot. Both sand and gravel was sourced from local supplier ‘Carvers’. The sand used had a majority of particles ranging from 2mm to 0.25mm. The gravel was pea shaped and was passed through a 7mm gauge. It was however retained by the 5mm sieve. The clay was sourced from a private firm ‘Valentine Clays Ltd.’. The physical appearance, texture and characteristics of these individual sub soil components can be seen from the picture in the Figure 3.1 below. The Atterberg Limits of the clay was determined. The clay had a plastic limit value of 18.09, and a liquid limit of 37.5. The Plasticity Index was determined to be 19.41. The Pulverised Fuel Ash had properties consistent with that expected from a high LOI grade. The grading of these commercially available soils was found to be highly reliable in terms of consistency and minimal variation, making them suitable as a constant supply of materials.

The process of incorporating these ingredients to form a sub-soil is simple and consists of basic steps. The particle-size distribution of each component soil was determined in accordance with British Standard 1377:1990 Soils for Civil Engineering – Part 2: Classification (BSI, 1990[2]) and reported in table form as permitted in the above standard.

3.2 Sample Preparation:

After the sample selection process, two of the soil components (Sand and gravel) were oven-dried at a temperature of 105°C. The clay was cut into short pieces and air dried until completely dried. The clay was then pulverised into a coarse powder using direct mechanical energy. The sub-soils (Figure 3.1) were then mixed together using an electronic paddle mixer. This ensured even mix of the sand, gravel and clay. The soil was mixed in batches of 10kg (dry mass) such that a 523 mix recipe required 5kg sand, 2kg clay and 3kg gravel.

Clay gritty sand and gravel Pulverised Fuel Ash

Figure 3.1 Specimens of clay, grit sand, gravel and Pulverised Fuel Ash.

3.3 Schedule of Mixes

Cube samples were produced in batches, each containing fifteen cubes. Five extra cubes were also made for each batch to provide for unforeseen circumstances such as breakages etc. The schedule of mix is shown in Table 3.1 – 3.6. The mixes were designed to provide test samples that represents a wide variety of soils found in practice. The mixes prepared ranged from the 721 soil grade that has a mix proportion of 7:2:1 for Sand:clay:coarse

aggregate (by weight) to the 541 representing a sand, clay and coarse aggregate mix in the proportion 5:4:1 (by weight). It was designed so that the 721 grade represents very sandy soils, the 532 grade representing an evenly blended mix and the 451 grade represents a very clayey mix. A 622 grade soil (representing a mix of sand, clay and coarse aggregate in the proportion 6:2:2) was also prepared to investigate the effect of palm kernel shell on rammed earth when soil grade changed but volume of coarse aggregate remained constant.

Cube samples were made for each test. The tests were divided into four. The compressive test for effect of Pulverised Fuel Ash addition, the test for moisture migration, the ultrasonic pulse velocity (UPV) test and Thermal conductivity test. Three prisms were also made from each sample to test for linear shrinkage.

Table 3.1 Soil grade composition for Rammed Earth samples.

Soil Grade	Composition by weight (%)		
	Sand	**Clay**	**Coarse Aggregate**
721	70	20	10
451	40	50	10
532	50	30	20
622	60	20	20

Table 3.2 Mix schedule for 721 grade rammed earth with at various Pulverised Fuel Ash and cement contents

7:2:1 – sand:clay:coarse aggregate 721 samples containing No Pulverised Fuel Ash			
Sample No	**Sample ID**	**Cement Content Added (% of soil grade)**	**Pulverised Fuel Ash Content (%)**
1	**721-0FA0CE**	0	0
2	**721-0FA2CE**	2	0
3	**721-0FA4CE**	4	0
4	**721-0FA6CE**	6	0
5	**721-0FA9CE**	9	0
721 samples containing 10% (by weight) Added Pulverised Fuel Ash			
Sample No	**Sample ID**	**Cement Content Added (% of soil grade)**	**Pulverised Fuel Ash Content (%)**
6	**721-10FA0CE**	0	10
7	**721-10FA2CE**	2	10
8	**721-10FA4CE**	4	10
9	**721-10FA9CE**	9	10
721 samples containing 20% (by weight) Added Pulverised Fuel Ash			
Sample No	**Sample ID**	**Cement Content Added (% of soil grade)**	**Pulverised Fuel Ash Content (%)**
10	**721-20FA0CE**	0	20
11	**721-20FA2CE**	2	20
12	**721-20FA4CE**	4	20
721 samples containing 30% (by weight) Added Pulverised Fuel Ash			
Sample No	**Sample ID**	**Cement Content Added (% of soil grade)**	**Pulverised Fuel Ash Content (%)**
13	**721-30FA0CE**	0	30
14	**721-30FA2CE**	2	30
15	**721-30FA9CE**	9	30
721 samples containing 50% (by weight) Added Pulverised Fuel Ash			
Sample No	**Sample ID**	**Cement Content Added (% of soil grade)**	**Pulverised Fuel Ash Content (%)**
16	**721-50FA0CE**	0	50
16	**721-50FA2CE**	2	50
17	**721-50FA4CE**	4	50
18	**721-50FA9CE**	9	50

Table 3.3 Mix schedule for 451 grade rammed earth at various Pulverised Fuel Ash and cement contents

4:5:1 – sand:clay:coarse aggregate 451 samples containing No Pulverised Fuel Ash			
Sample No	**Sample ID**	**Cement Content Added (% of soil grade)**	**Pulverised Fuel Ash Content (%)**
19	**451-0FA0CE**	0	0
20	**451-0FA2CE**	2	0
21	**451-0FA4CE**	4	0
22	**451-0FA9CE**	9	0
451 samples containing 10% (by weight) Added Pulverised Fuel Ash			
Sample No	**Sample ID**	**Cement Content Added (% of soil grade)**	**Pulverised Fuel Ash Content (%)**
23	**451-10FA0CE**	0	10
24	**451-10FA2CE**	2	10
25	**451-10FA9CE**	9	10
451 samples containing 20% (by weight) Added Pulverised Fuel Ash			
Sample No	**Sample ID**	**Cement Content Added (% of soil grade)**	**Pulverised Fuel Ash Content (%)**
26	**451-20FA0CE**	0	20
27	**451-20FA2CE**	2	20
28	**451-20FA9CE**	9	20
451 samples containing 30% (by weight) Added Pulverised Fuel Ash			
Sample No	**Sample ID**	**Cement Content Added (% of soil grade)**	**Pulverised Fuel Ash Content (%)**
29	**451-30FA0CE**	0	30
30	**451-30FA2CE**	2	30
31	**451-30FA9CE**	9	30
451 sample containing 50% (by weight) Added Pulverised Fuel Ash			
Sample No	**Sample ID**	**Cement Content Added (% of soil grade)**	**Pulverised Fuel Ash Content (%)**
32	**451-50FA0CE**	0	50

Table 3.4 Mix schedule for 532 grade rammed earth at various Pulverised Fuel Ash and cement contents

5:3:2 – sand:clay:coarse aggregate 532 samples containing No Pulverised Fuel Ash			
Sample No	**Sample ID**	**Cement Content Added (% of soil grade)**	**Pulverised Fuel Ash Content (%)**
33	**532-0FA0CE**	0	0
34	**532-0FA2CE**	2	0
35	**532-0FA4CE**	4	0
36	**532-0FA5CE**	5	0
37	**532-0FA6CE**	6	0
38	**532-0FA9CE**	9	0
532 samples containing 10% (by weight) Added Pulverised Fuel Ash			
Sample No	**Sample ID**	**Cement Content Added (% of soil grade)**	**Pulverised Fuel Ash Content (%)**
39	**532-10FA0CE**	0	10
40	**532-10FA2CE**	2	10
41	**532-10FA4CE**	4	10
42	**532-10FA6CE**	6	10
43	**532-10FA9CE**	9	10
532 samples containing 20% (by weight) Added Pulverised Fuel Ash			
Sample No	**Sample ID**	**Cement Content Added (% of soil grade)**	**Pulverised Fuel Ash Content (%)**
44	**532-20FA0CE**	0	20
45	**532-20FA2CE**	2	20
46	**532-20FA4CE**	4	20
47	**532-20FA6CE**	6	20
48	**532-20FA9CE**	9	20
532 samples containing 50% (by weight) Added Pulverised Fuel Ash			
Sample No	**Sample ID**	**Cement Content Added (% of soil grade)**	**Pulverised Fuel Ash Content (%)**
49	**532-50FA0CE**	0	50
50	**532-50FA9CE**	9	50

Table 3.5 Mix schedule for 532 grade rammed earth containing PKS (No Pulverised Fuel Ash was added to mix containing PKS)

532 samples containing PKS			
Sample No	**Sample ID**	**Cement Content Added (% by weight of soil grade)**	**PKS replacement (% volume replacement of coarse aggregate fraction)**
51	**532-0KS0CE**	0	0
52	**532-10KS0CE**	0	10
53	**532-500KS0CE**	0	50
54	**532-90KS0CE**	0	90
55	**532-100KS0CE**	0	100
56	**532-100KS2CE**	2	100
57	**532-0KS5CE**	5	0
58	**532-100KS5CE**	5	100
59	**532-0KS9CE**	9	0
60	**532-100KS9CE**	9	100

Table 3.6 Mix schedule for 622 grade rammed earth containing PKS (No Pulverised Fuel Ash was added to mix containing PKS)

6:2:2 – sand:clay:coarse aggregate 622 samples containing PKS			
Sample No	**Sample ID**	**Cement Content Added (% of soil grade)**	**PKS replacement (% volume replacement of coarse aggregate fraction)**
61	**622-0KS0CE**	0	0
62	**622-10KS0CE**	0	10
63	**622-50KS0CE**	0	50
64	**622-90KS0CE**	0	90
65	**622-100KS0CE**	0	100
66	**622-0KS5CE**	5	0
67	**622-100KS5CE**	5	100

3.4 Incorporating Pulverised Fuel Ash and Palm Kernel Shell.

The amount of Pulverised Fuel Ash added was calculated as a mass proportion of the total amount of dry soil. For example, for 10kg of dry soil, an addition of 1kg of Pulverised Fuel Ash would equal 10% addition. In this example, the total mass of dry components for the mix becomes 11kg. The optimum moisture content (OMC) was always calculated as a percentage of

the total mass of the dry components (including the mass of cement where added). This means that in an unstabilised soil with a dry mass of 10kg, if the optimum moisture content is 8%, then 800g of water must be added to the mix. Sets of samples were produced using 9%, 6%, 4% and 2% cement stabilisation. Pulverised Fuel Ash was added in varying quantities ranging from 10% to 50%.

PKS was added as a replacement to coarse aggregate. Only the coarse aggregate fraction was changed as PKS was added as a replacement by volume. It should be noted that the PKS used was free of oil as it was washed and dried before use.

3.5 Cube Specimen Preparation

The laboratory based production of rammed earth samples should be a reflection of the onsite constriction technique used in making rammed earth walls. This has a net effect of providing results that are meaningful, useful and applicable to real life building situations. There are factors that are considered as important in relation to sample production and these include the level of compaction and total input energy. A manual hand rammer (Figure 3.2) was

Figure 3.2 Steel hand rammer used in compaction of the cube samples

used for the dynamic compaction of the soil in order to replicate field rammed earth production. For each of the rammed earth mix recipes produced, the optimum moisture content was found to be a value ranging from 7% to 9% moisture in relation to the dry mass of the soil. The optimum moisture content for each of the soils was determined in accordance with British Standard BS

1377 – Part 4: Compaction (BSI, 1990[4]) using the established proctor 'light' compaction method. NZS 4298 (Standards New Zealand, 1998) states that for rammed earth production, the moisture content should not fall below 3% of the optimum moisture content or rise above 5% of it. This standard was strictly adhered to. This standard was continually monitored by using the gravimetric method of moisture content determination (Oven drying and weighing). The mix was moistened to the appropriate moisture content and placed inside a mould (Figure 3.3).

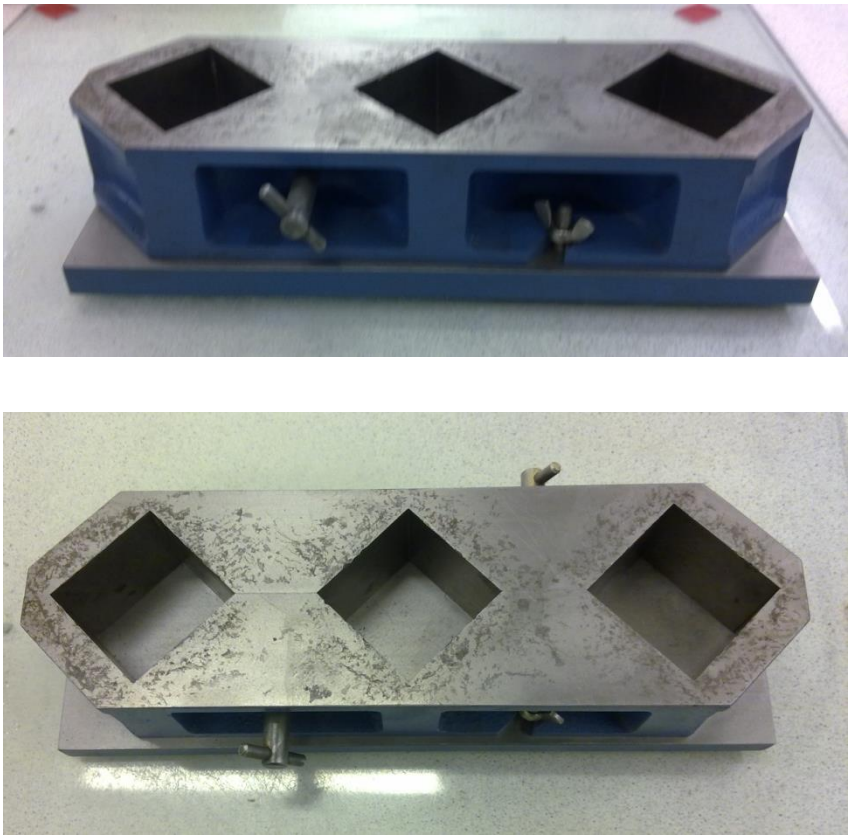

Figure 3.3 Hand rammed cube sample making mould

It was then compacted in two separate layers. The number of blows that ensures even compaction was soon observed to be roughly 36 blows. The rammer was a 4kg stainless steel solid cube tube with edges that ensure proper compaction at the cube corners. The mould used was a standard 50X50X50mm mould used in normal concrete cube making. The inside of the cube mould was painted with form-oil to ensure ease of removal of the cubes.

After compaction, a small quantity of compacted soil usually projects above the top of the mould. This is scraped away and a small amount of moist soil which was passed through a 1mm British Standard (BS 1377) sieve, sprinkled on top of the sample. This capping layer was then compacted with the hand rammer before being smoothed by the metal spatula to produce a perfectly flat surface. The resultant sample was a perfect 50mm rammed earth cube (Figure 3.4) with two even layers of compacted soil as shown in the figure below.

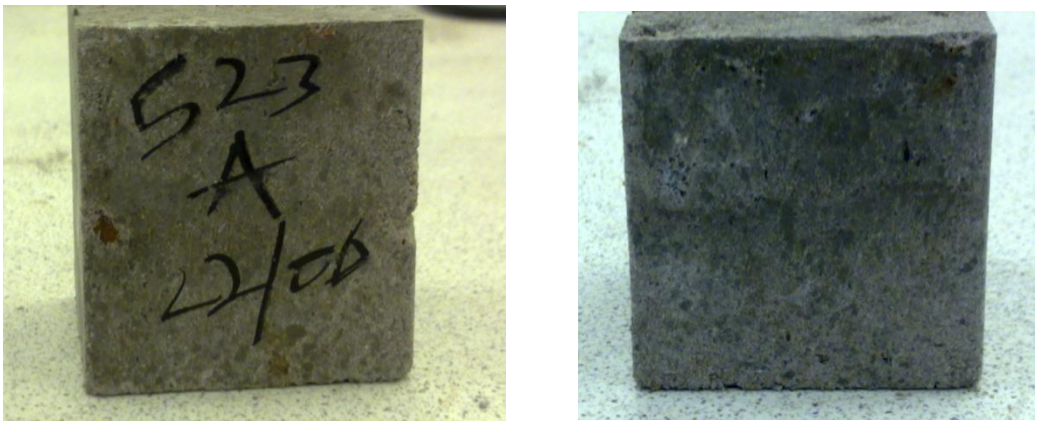

Figure 3.4 Completed rammed earth cube samples.

The cube samples were produced in specimen batches, each containing twenty cubes. A separate specimen batch was created to represent a control batch of unstabilised samples. Each of the cubes prepared was scheduled for a specific test.

3.6 Curing

The samples were stored in a sealed curing chamber (Figure 3.5 and Figure 3.6) at a temperature of 20^{o}C (±1^{o}) and a relative humidity of 75% (±5%). The curing chamber had a rotating drum humidifier and a digital monitoring equipment for monitoring the atmospheric conditions. The high relative humidity prevents the cubes from drying out too quickly thus minimising the chances of shrinkage cracks occurring. Samples scheduled for compression tests were taken out of the form work after 1 day.

Figure 3.5 Rammed earth samples left in mould for specified periods.

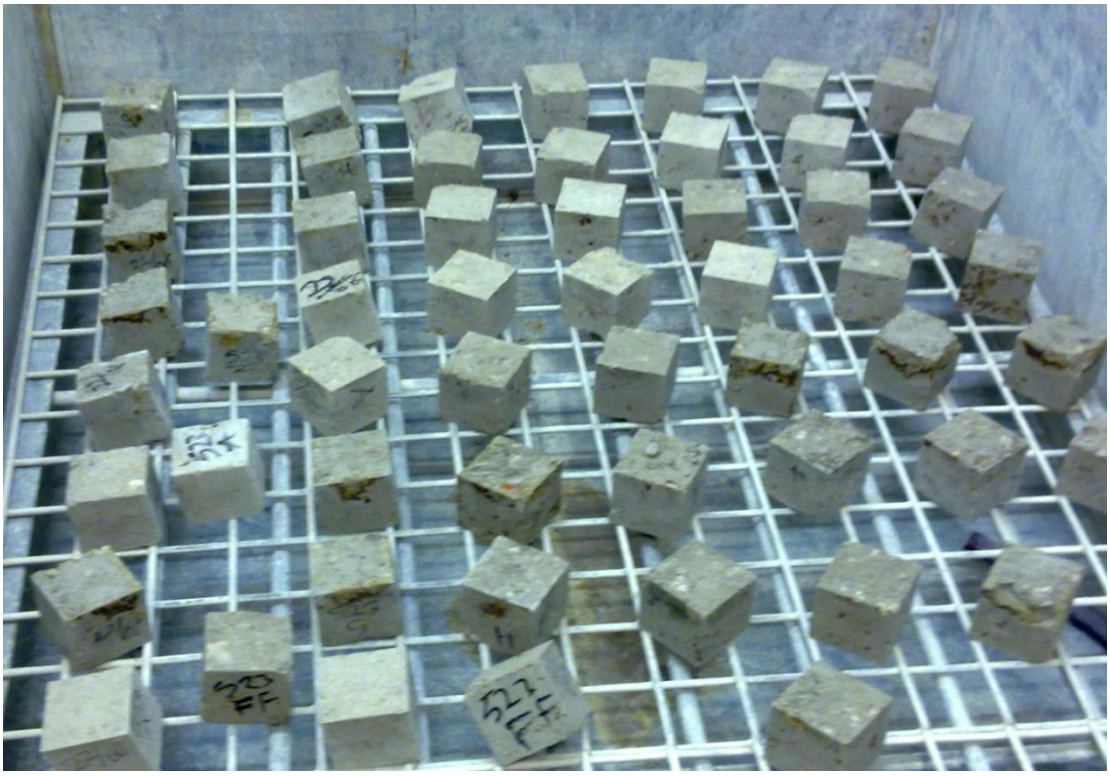

Figure 3.6 Collection of air dried rammed earth cube samples stored in a curing chamber under controlled conditions

3.7 Compressive Test Procedure

In order to compare rammed earth to other conventional masonry materials, compressive strength testing was carried out. The apparatus used for this was the 'Controls Sercomp 7' compression machine (Figure 3.7). A specimen was placed between the load platens of the test machine. The applied load rate was set at 50N/s. This ensured that failure of the sample occurred at a time typically between 30 and 90 seconds after the beginning of the test. This method is consistent with standard test procedure for conventional masonry materials such as concrete and mortar. A minimum of three rammed earth cube samples was required for compressive strength testing in order to give a good representative value for a particular soil type (Standards New Zealand, 1998). The machine provided values for the load at failure, and the corresponding stress.

Figure 3.7 The Controls Sercomp 7 compressive strength test machine

3.8 Capillary Test Procedure

The British Standard BS 3921 outlines the method for the test the Initial Rate of Suction (IRS) of Masonry Bricks. This test describes the behaviour of a material with regards to its ability to absorb water (by capillary action only) over time. The value for this is expressed in kg/m^2 min. However, this test requires the immersion of the sample in water, up to a depth of 3mm and is therefore inadequate for use in testing materials that slake on contact with water. The test requires that the solid mass of the porous sample be kept constant from the beginning of the test to the end. If mass loss occurs in the sample during testing, then the amount of absorbed water cannot be calculated accurately.

Another requirement from the BS 3921 is that the wetted face be whipped with a damp cloth to remove excess water. This presents a problem with materials that break up easily when wet.

To solve the problems highlighted above, Hall in Hall and Djerbib (2004) devised a method to test rammed earth using the modified IRS test called the IRS 'Wick' Test. This novel adaptation differed from the original test by lifting the sample off the water but maintaining hydraulic contact through a saturated wick. Usually, a wick is placed in the water and the sample placed on the wick. Care is taken to guarantee that the water level is kept constant always, ensuring that the wick is saturated and that there is very good contact between the sample and the wick.

What ensues is that free water is absorbed by the initially dry specimen from a saturated porous medium that offers little or no capillary resistance. Therefore, unstabilised Rammed Earth that slakes in contact with water remains stable throughout the test and negligible mass loss occurs as the inflow surface is retained by the self-weight of the sample acting on the solid surface of the wick.

3.8.1 The Modified Internal Rate of Suction (IRS) Test

The Modified IRS test is a modification of the BS 3921 IRS test apparatus perfected by Hall and Djerbib (Hall & Djerbib 2004a). Most elements of the original BS 3921 test are replicated with some major adjustments. The test procedure remains the same with the difference being observed in the test apparatus as seen in Figure 3.8. The most notable difference is that the sample is not immersed in water rather water is introduced to the base of the sample by a sponge which is immersed in water.

Rammed earth which is prone to slaking on contact with water remains intact through the testing period. The inflow surface is maintained in constant contact by the self-weight of the sample acting on the surface of the sponge.

3.8.2 Calibration of the Modified IRS Test

The Test procedure has been calibrated using materials that did not slake on contact with water by the developers. Hall and Djerbib (2004a) used a vibration compacted C30 concrete cube and 3 types of bricks to establish the fact that the modified IRS test produced consistent results which was in line with results obtained using the BS 3921 test procedure. It was however noted that the actual mass of sorbed water in the modified test (Figure 3.8) was about half of that observed using the BS 3921 test apparatus.

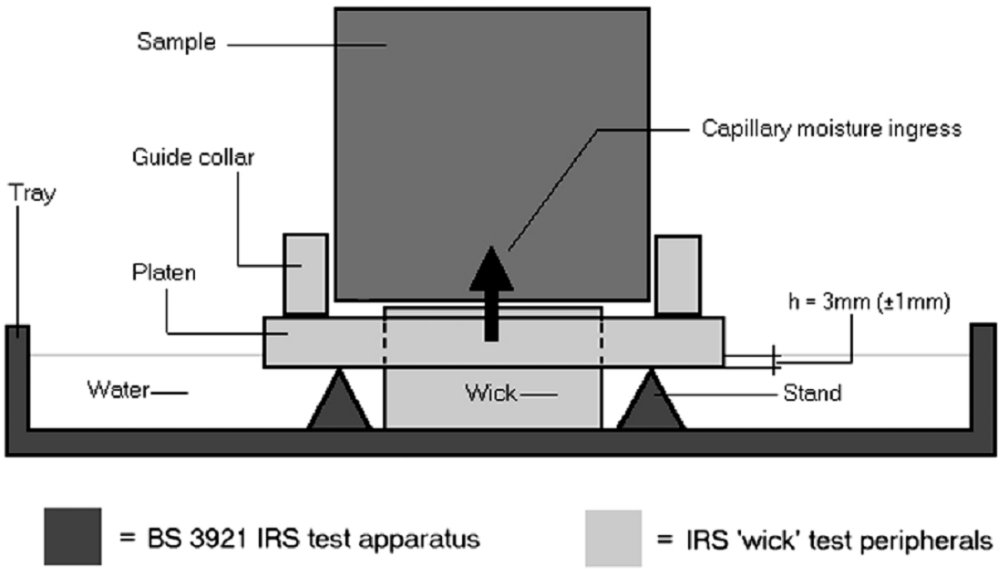

Figure 3.8 Modified IRS test apparatus (hall & djerbib 2004a).

Samples were dried to a constant mass then left to cool for 48hours. A trough was filled with water to the half-way point. A platen was then set on stands inside the trough. A sponge was placed in the middle of the platen reaching to the base of the trough well supplied with water. The sample was then placed on the platen making contact with the sponge. The sponge was observed to conduct moisture properly. The sample was picked up every minute and any excess moisture on the surface wiped off. It was then weighed and set back on the wick. Testing lasted 24 hours for each sample. Testing was carried out on concrete blocks and bricks first to test the accuracy and repeatability of the test and to compare them to results obtained when tested in accordance to the BS 3921 test procedure.

As the samples (Figure 3.9) completed the IRS test at 24 hours, it was subjected to further testing to determine the rate of loss of moisture from a wetted sample. As the moisture dissipation test commenced immediately after the IRS test, the mass of absorbed water is known. The cube is placed in a controlled environment an allowed to dry naturally at 20OC and 40%RH with the wetted surface pointing upward. Samples were weighed at set intervals.

Hall and Djerbib (2004a) agree that rammed earth generally has a low initial rate of suction compared to conventional masonry materials such as concrete and fired clay brick and absorbs much smaller amounts of water over a given time span. This is illustrated in Table 3.7

Table 3.7 Average amount of sorbed water during a 5-minute IRS test (hall & djerbib 2004a)

Masonry type	Dry $mass_{avg}$ (g)	Average w_m (g)	Average w_m (%)
London brick – Fletton	851.0	10.95	1.29
London brick – Dapple light	923.2	7.12	0.77
Engineering brick	1316.6	12.47	0.95
C30 concrete	2165.8	6.72	0.31
Rammed earth – 532	2136.9	3.17	0.15
Rammed earth – 622	2132.0	3.37	0.16
Rammed earth – 712	2068.8	8.45	0.41
Rammed earth – 802	2030.6	15.15	0.74
Rammed earth – 433	2180.5	3.42	0.16
Rammed earth – 523	2101.3	4.22	0.20
Rammed earth – 613	2120.0	4.15	0.20
Rammed earth – 703	2058.4	5.95	0.29
Rammed earth – 424	2067.3	5.92	0.28
Rammed earth – 514	2089.0	3.12	0.15

Tests were carried to determine the effect of adding Pulverised Fuel Ash to rammed earth. Also tests showed the impact of the addition of PKS to rammed earth on the moisture adsorption property of rammed earth.

Figure 3.9 Tested rammed earth samples

Results showed that although the total mass of water absorbed was higher for bricks and concrete, the percentage water absorbed as compared to the dry mass was similar to that of unstabilised rammed earth.

The total absorbed mass of water with time was plotted for each sample and comparisons made. Most of the samples were tested for 24 hours. Testing of a few samples did not get to 24 hours as those samples lost structural integrity as they absorbed water.

3.9 Shrinkage Test Procedure

Earth samples were rammed into a prism measuring 40x40x140mm (Figure 3.10). Three of each samples were made (Figure 3.11). Each sample was promptly labelled and studs attached. Each sample had 2 adjacent faces prepared for studs. The surface of the sample was inspected for impurities and any rough edge smoothed out by lightly scrapping protruding bits off the sample. High strength glue was attached sparingly to ensure that only the area the stud sits on has glue applied. The glue was tested on sample runs to ensure that they held properly over 100 days before the actual experimentation commenced. The studs were attached with a spacer and the length between the spacers measured .Measurement was taken over 90 days at regular intervals. Measurement was by a Mitutoyo Absolute Demec Gauge (Figure 3.12). The results for samples containing PKS and Pulverised Fuel Ash are presented below. Control samples containing none of the above additives were also prepared for each soil grade. Rammed earth containing cement as stabilisers was also prepared and tested to compare the effect of stabilisation on rammed earth shrinkage when Pulverised Fuel Ash or PKS was used in rammed earth preparation.

Figure 3.10 Sample preparation mould

Figure 3.11 Samples ready for testing

Figure 3.12 The Mitutoyo dial guage.

3.10 Thermal Conductivity Procedure

The sample was dried in a drying chamber at 75^{o}C until constant mass was achieved. It was then allowed to cool in an air tight environment to room temperature. The procedure was carried out using the Armfield heat conduction apparatus (Figure 3.13). Thermistors attached to the apparatus were not adaptable to the size of the sample so manual readings were taken using a digital thermometer. The thermometer was sensitive up to 2^{o}C.

It was determined that a wattage rating of 9 produced a desired stable 60^{o}C heat source after a few minutes. This was applied to one face of the sample. The attachment was fastened securely to ensure that no heat loss was recorded. This was checked using a thermal camera. The time interval between readings was determined. Temperature was recorded at various points along the side of the sample and at the opposite face.

Thermal conductivity was determined using the transient heat conduction calculation. The theoretical transient heat conduction curve was plotted for temperature against time using the effective thermal conductivity determined using simulation software. An assumption here is that all of the electrical power provided is converted to heat.

Figure 3.13 Armfield heat conduction apparatus

Chapter Four

Soil Classification

This chapter defines tests that were carried out in the course of the investigation. Several tests were carried out in an effort to classify the soil used in the procedures. These tests help characterise the soil and provide a source of comparison for soils found in any location.

4.1 Atterberg Limits.

The method of test used was the Cone Penetrometer. This is the British Standard (BS 1377:1975) preferred method for determining the liquid limit of soils. Here measurement is taken to determine the penetration of a standard cone of specified mass. At the liquid limit, the cone would penetrate to a depth of 20mm.

The material was sieved and sample selected from that passing the 425µm sieve. About 250g of the sample was set aside for the test according to procedures set out in BS 1377.

Liquid Limit: Selected material was mixed thoroughly with known volume of water until it was worked into a thick homogenous paste. This was then placed in an air tight container, sealed and left over for 24hrs. This allowed water to permeate through the soil mass. This process is known as maturing. The sample was then placed on a glass plate and remixed for a period of about 10 minutes. Care was taken to keep the material together in order to minimise loss of moisture.

The sample was then placed in a cup carefully to avoid trapping air. Care was also taken to ensure that the sample filled the cup evenly and the top surface smoothed off to level with the rim. The cone was then lowered until its tip just rested on the surface of the sample. The reading of the dial gauge was noted before the cone was allowed to fall. Reading was taken at the new level.

A moisture content sample was taken from the area penetrated by the cone and placed in a numbered moisture content container. The moisture content was then determined for the sample. Further tests were repeated with increase in moisture until a range of penetration values from about 15mm to

25mm was obtained (see Table 4.1 and 4.2). The cone penetration was then plotted against the corresponding moisture content (Figure 4.1)

Table 4.1 The liquid limit table

Try L1	Try L2	Penetration	Mass of empty	Mass of	Mass of	Water
17.7	17.5	17.6	46.73	81.79	72.56	35.73364
19	19	19	46.33	89.61	78.08	36.31496
21.5	21.1	21.3	46.08	88.74	76.86	38.59649
22.8	22.6	22.7	46.01	84	73.14	40.02949
24.5	24.1	24.3	45.99	96.38	81.53	41.78391
15.5	15.5	15.5	46.18	69.49	63.79	32.36797
17	16.8	16.9	45.95	70.67	64.45	33.62162
17.9	17.9	17.9	45.97	83.27	73.42	35.88342
16.5	16.5	16.5	45.91	76.58	68.56	35.40839
18.5	18.7	18.6	46.21	70.65	64.09	36.68904
19.8	19.4	19.6	46.36	65.33	59.94	39.69072
20.4	20.6	20.5	45.63	60.82	56.62	38.21656
21.4	21.2	21.3	45.89	60.59	56.38	40.13346
21.8	21.8	21.8	45.92	63.88	58.59	41.75217
15.2	15	15.1	46.47	69.93	64.11	32.9932
17.7	18.1	17.9	46.04	80.42	71.28	36.21236
20.6	21.1	20.85	45.63	70.33	63.64	37.14603
22.5	22.1	22.3	45.77	76.91	68.41	37.54417
25	24.8	24.9	46.2	83.67	72.89	40.38966
16.5	17	16.75	45.24	77.79	69.74	32.85714
18	17.6	17.8	45.48	76.68	68.78	33.90558
19.2	19	19.1	46.03	77.16	68.97	35.70183
21.2	21.6	21.4	45.72	75.03	67.29	35.88317
22.4	22	22.2	46	79.06	69.88	38.44221
23	22.8	22.9	45.72	72.51	64.96	39.24116
17.9	17.5	17.7	45.93	78.41	69.94	35.27697
15.8	15.5	15.65	45.53	72.93	66.03	33.65854
16.2	16.6	16.4	46.19	76.96	68.98	35.01536
23.8	23.6	23.7	46.2	76.74	68.13	39.26129
17.1	16.6	16.85	45.96	70.03	63.87	34.39419
19.4	19.4	19.4	45.88	72.24	65.18	36.58031
21.4	21.8	21.6	46.38	70.04	63.1	41.50718
22.4	22.1	22.25	45.64	70.05	63.02	40.44879
22.9	23.3	23.1	46.21	71.86	64.12	43.21608

Water content was determined using the equation

$$W = \frac{(M2-M3)}{(M3-M1)}\ x\ 100 \qquad 4.1$$

Table 4.2 The plastic limit table

Mass of empty container M1 (gm)	Mass of container + wet soil M2 (gm)	Mass of container + dry soil M3	Water Content W (%)
46.06	70.01	66.96	14.5933
46.2	67.14	63.82	18.84222
46.2	61.99	59.64	17.48512
45.85	70.48	66.84	17.34159
46.21	59.78	57.76	17.48918
46.08	61.56	59.22	17.80822
45.99	65.04	62.2	17.52005
46.09	59.7	57.71	17.12565
45.61	55.18	53.85	16.14078
46.47	61.02	58.76	18.38893
45.65	59.38	57.18	19.08066
49.94	60.31	58.18	25.84951
45.75	62.18	59.73	17.52504

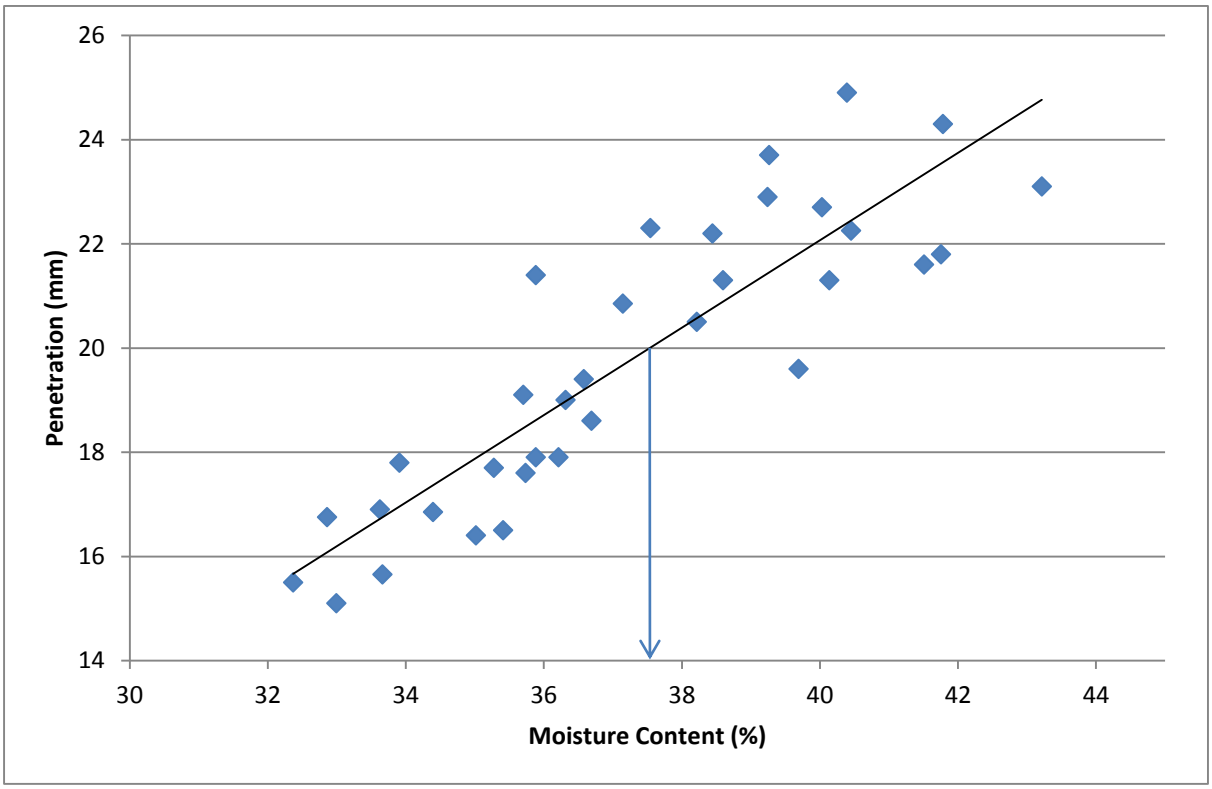

Figure 4.1 The Atterberg limit chart

The Atterberg Limits of the clay was determined. The clay had a plastic limit value of 18.09, and a liquid limit of 37.5. The Plasticity Index was determined to be 19.41. According to British practice, this clay can be termed as being of medium plasticity. This can be observed in the plasticity chart in figure 4.2.

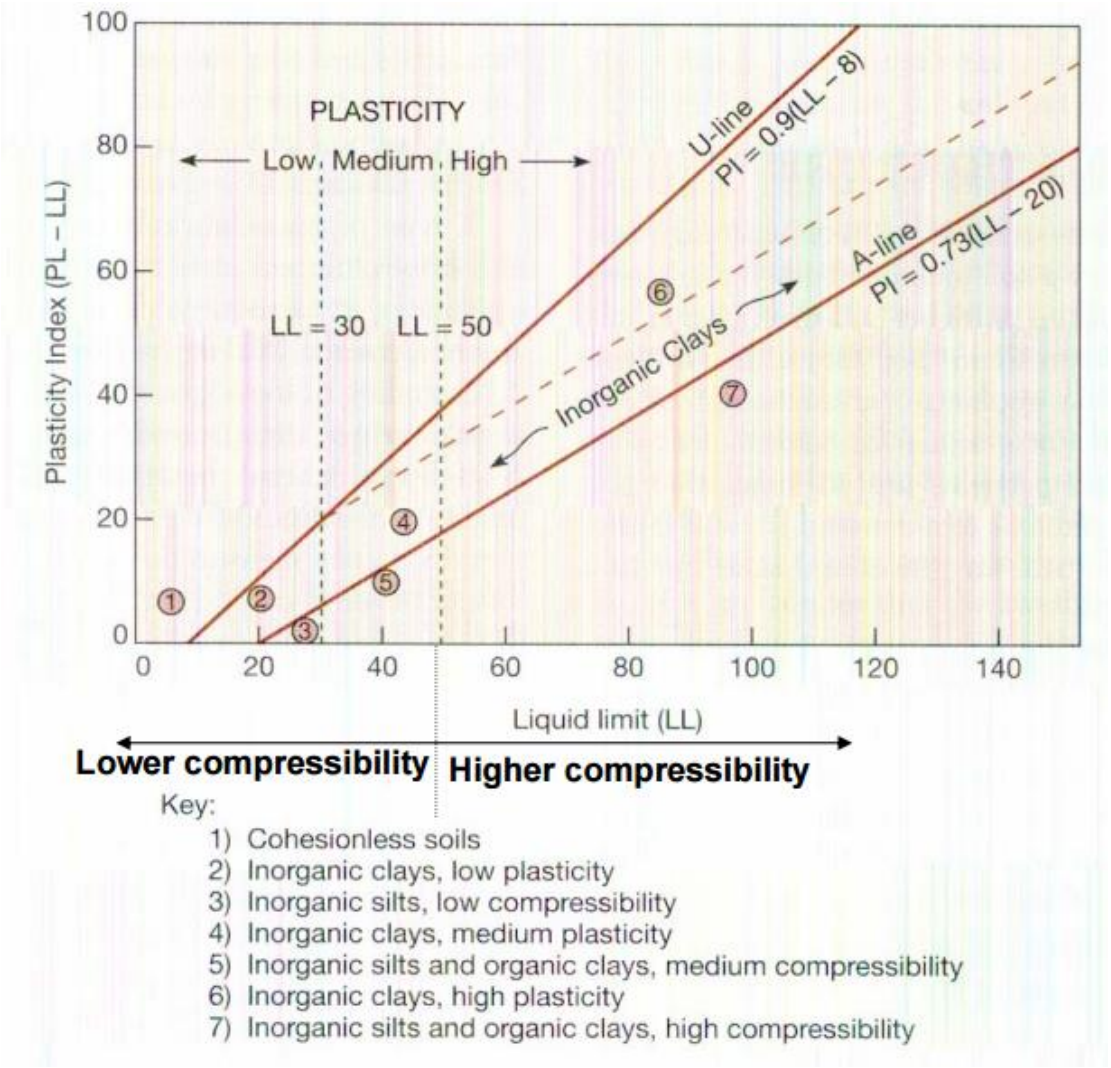

Figure 4.2 The plasticity Chart (Lanbo I. 2007)

4.2 Particle Size Distribution

Tests to determine particle sizes were carried out.

4.2.1 Soil Grading

2400g of oven dried soil was obtained by quartering. This was carried out as prescribed in BS 1377-1 (1990) and BS 1377-2 (1990). It was then placed in the oven again for 24 hours at 105^{o}C. The soil sample was then passed through sieves with sizes ranging from 10mm to 10µm. The sieve was agitated in a mechanical shaker. The mass of each material retained on each sieve was recorded. This was then represented as a percent of total mass of soil. The percentage passing the 63µm sieve was also recorded. The result obtained is represented in Figure 4.3.

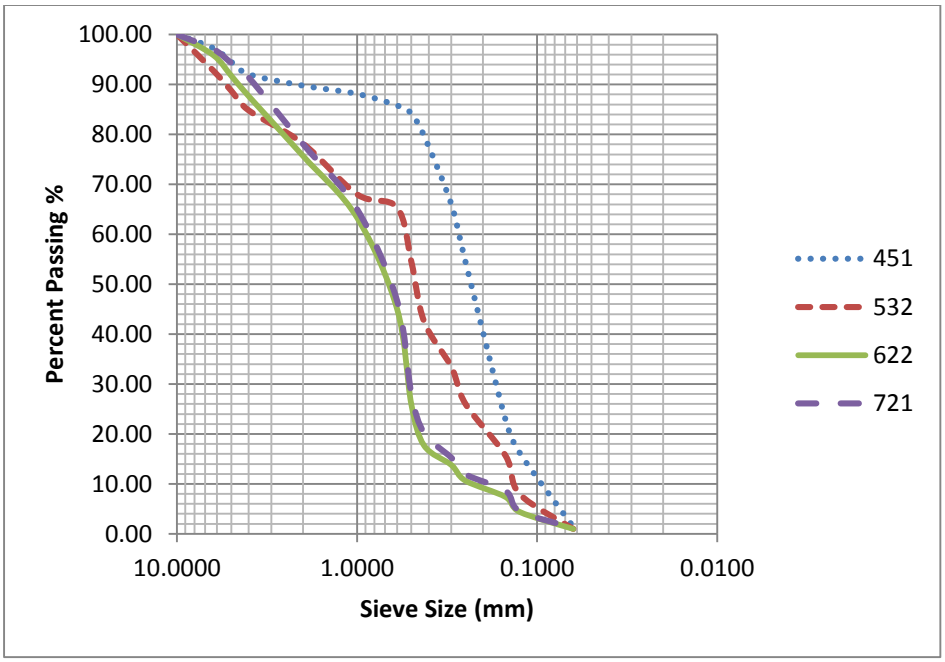

Figure 4.3 Particle size distribution for all four soil types.

4.2.2 Soil Type 451

Soil type 451 was obtained by blending sand clay and coarse aggregate in the ratio of 4:5:1. 4 parts sand was added to 5 parts of well blended clay and 1 part coarse aggregate less than 10mm in size. This soil sample was blended to represent a very clayey soil. The resulting blend appeared fine grained in texture, and can be described as a very clayey soil. This blend was developed to test the suitability of soils having very high clay content in rammed earth production. It was found to have a Cu of 2.84 and Cc of 1.13 (Figure 4.4). Here, C_u is the coefficient of uniformity and C_c is the coefficient of curvature and is obtained by the following formula

$$C_u = \frac{D_{60}}{D_{10}} \quad (4.2)$$

$$C_c = \frac{D_{30}^2}{D_{60} x D_{10}} \quad (4.3)$$

D_{60}, D_{30} and D_{10} refer to sieve sizes corresponding to % passing sieve size 60, 30 and 10 respectively.

4.2.3 Soil Type 532

This soil sample was obtained by blending 5 parts sand, 3 parts clay and 2 parts coarse aggregate. This represents a more even blend with a total specific surface area (SSA_t) to clay ratio of over 20%. It was found to have a C_u of 3.53 and C_c of 1.06.

4.2.4 Soil Type 622

622 soil grade was obtained by blending 6 part sand with 2 part clay and 2 part coarse aggregate. This blend had a slightly lower clay content than the 532 mix. The mix appeared medium to coarse in texture. It was found to have a C_u of 3.6 and C_c of 1.2.

4.2.5 Soil Type 721

This blend composed of 7 parts sand, 2 parts clay and 1 part coarse aggregate. This blend had a medium texture and was blended to represent most sandy soils with SSA_t/clay ratio of less than 15%. It was found to have a C_u of 5 and C_c of 1.8.

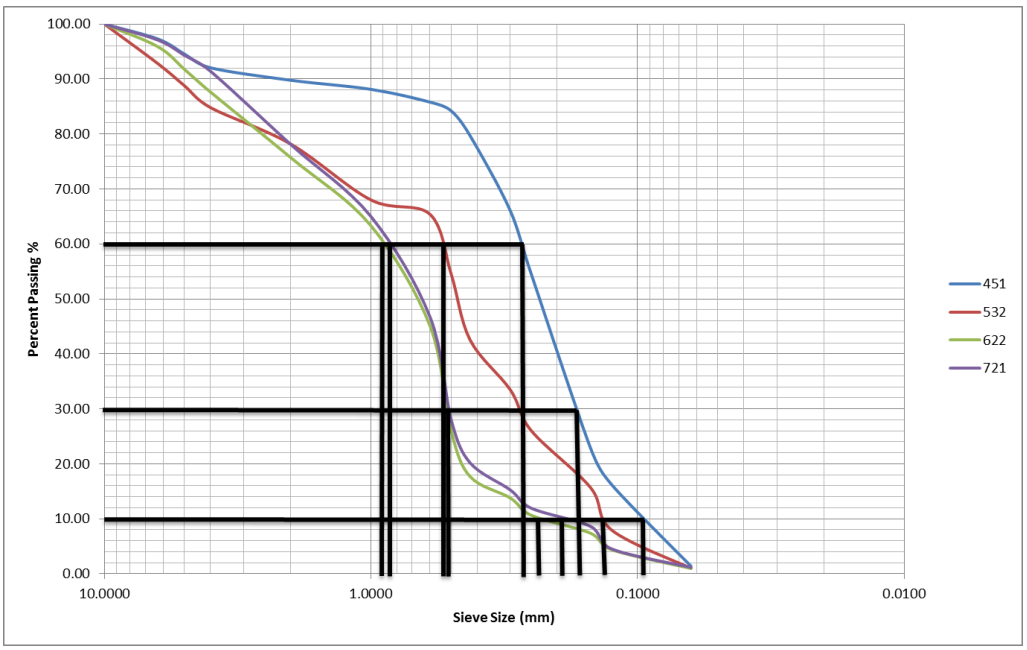

Figure 4.4 Soil grading chart highlighting D_{60}, D_{30} and D_{10}.

4.3 Composition of clay and fly ash particles

The clay and fly ash used in the experiments were analysed to determine the elemental composition and concentration. Silicon was found to be one of the most prominent element found in both samples. The other elements and concentration are shown in Table

Table 4.3 Clay Elemental Content

Na	Mg	Al	Si	P	S	Cl
%	%	%	%	%	%	%
< 0.35	0.221	8.161	24.26	0.0968	0.0212	0.0126
K	Ca	Ti	V	Cr	Mn	Fe
%	%	%	%	%	%	%
0.966	0.2064	0.7167	0.0127	0.0173	0.0181	1.834
Co	Ni	Cu	Zn	Ga	Ge	As
%	%	%	%	%	%	%
< 0.0025	0.00842	0.00229	0.00553	0.0028	0.00014	0.00045
Se	Br	Rb	Sr	Y	Zr	Nb
%	%	%	%	%	%	%
< 0.00011	0.00005	0.01016	0.00921	0.00348	< 0.050	< 0.0010
Mo	Ag	Cd	In	Sn	Sb	Te
%	%	%	%	%	%	%
< 0.0010	< 0.00050	0.0033	< 0.00050	< 0.00060	< 0.00060	< 0.00070
I	Cs	Ba	La	Ce	Hf	Ta
%	%	%	%	%	%	%
0.0053	0.0128	0.026	0.0263	0.038	0.00077	0.00414
W	Hg	Tl	Pb	Bi	Th	U
%	%	%	%	%	%	%
< 0.00071	< 0.00020	< 0.00032	0.00232	< 0.00020	0.00169	< 0.00061

Table 4.4 Fuel Ash Elemental Content

Na	Mg	Al	Si	P	S	Cl
%	%	%	%	%	%	%
< 0.37	0.394	8.656	19.48	0.164	0.6587	0.01374
K	Ca	Ti	V	Cr	Mn	Fe
%	%	%	%	%	%	%
1.205	2.885	0.592	0.0194	0.0231	0.1619	6.444
Co	Ni	Cu	Zn	Ga	Ge	As
%	%	%	%	%	%	%
0.0054	0.01652	0.01524	0.0243	0.00366	0.00189	0.00734
Se	Br	Rb	Sr	Y	Zr	Nb
%	%	%	%	%	%	%
0.00114	0.00103	0.0118	0.06182	0.00537	< 0.050	< 0.0016
Mo	Ag	Cd	In	Sn	Sb	Te
%	%	%	%	%	%	%
< 0.0050	< 0.00087	< 0.0013	< 0.00086	< 0.0020	< 0.0013	< 0.0020
I	Cs	Ba	La	Ce	Hf	Ta
%	%	%	%	%	%	%
< 0.0035	< 0.0048	0.1541	< 0.0100	0.0123	< 0.0013	0.0061
W	Hg	Tl	Pb	Bi	Th	U
%	%	%	%	%	%	%
< 0.0012	0.00057	< 0.00047	0.01876	0.00051	0.00175	0.00152

4.3 Determination of Optimum Moisture Content

To achieve maximum strength, rammed earth needs to be fully compacted. This is reflected in achieving the highest density possible. Density is determined by the amount of moisture in the material before compaction. The amount of water, expressed as a proportion by mass of the dry solid particles is known as the moisture content. The water content that enables a rammed earth sample to achieve maximum density is known as the optimum moisture content.

Optimum moisture content is achieved in the lab by adding a predetermined portion of water to a dry sample. Soil is ‘dry’ when no further water can be removed at a temperature not exceeding 110^{o}C.

While optimum moisture content can be determined in a number of ways, two methods were used in this experiment.

- The drop test method and
- The proctor light method.

While the drop test was used to determine the range of moisture content that was close to the optimum, the proctor light method was used to determine the exact optimum moisture content.

4.3.1 The Drop Test Method:

This method is used extensively in the field to ensure an even mix before ramming. However, it is also useful to determine a range for the optimum moisture content when new soils are encountered.

Soil was weighed out and the surface dry saturated moisture content determined. Water was added as a proportion of entire mass. Water was added from 4% up to about 17% depending on how fast result was fed back. For each moisture content, soil was squeezed into a ball 40mm in diameter. It was then dropped from a height of 1.5m. The pattern that resulted determined the water content of the sample. When the soil was too dry or too wet, it usually fragmented into many small pieces. When soil clumped together, it had just passed the optimum moisture content and is too wet. However, when the soil broke down into a few large pieces, it contained just the right amount of moisture.

The range at which the soil sample started to clump together until it started to break apart again was recorded and this range was subjected to the second test to determine the exact moisture content that would produce the highest dry density.

4.3.2 The Proctor Light Method

The soil was prepared and dried to constant mass. Water was added as a percent of total weight. 6% water content was a starting point for most soil mix. The resulting wet soil mass was then mix thoroughly. The mould was

weighed with the base plate attached. The extension collar was then applied only after weight had been taken to the nearest gram. Moist soil was then added to the mould and compacted in layers. It was discovered by repeat testing that 3 layers produced very similar results as 5 layers of compaction when the proctor machine was used and when each layer was of approximate mass as the others. The mould was affixed tightly to the proctor machine and 25 blows were delivered using a hammer that weighed 4.9kg, dropped from a height of 450mm above the soil. It was discovered that a manual hammer could be used to achieve the same result provided the blows were carefully distributed to ensure uniform compaction (BS 1377-4, 1990).

After compaction, the mould was taken down from the machine and the collar removed and the top of the mould levelled carefully using a straight edge. The mould containing the compacted earth was then weighed and the weight of the empty mould taken away from this. This was repeated for a number of moisture content ranging from 6% to 14% depending on soil type. The dry density of the material was then calculated and plotted for each water content in a graph of dry density vs water content (Figure 4.5). The highest point of the curve which is known as maximum dry density is marked off and the corresponding water content at which it occurs is known as the optimum moisture content as seen in figure.

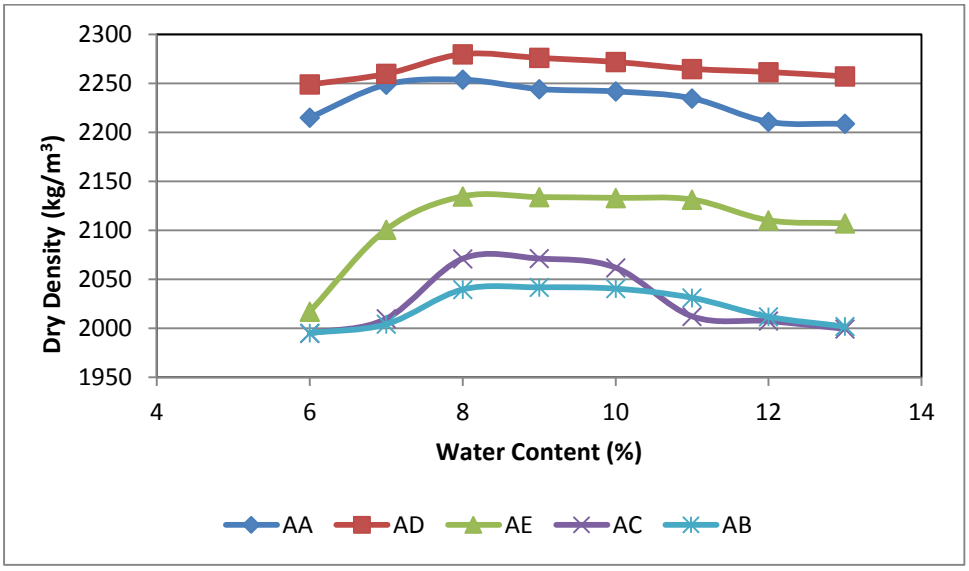

Figure 4.5 Optimum moisture determination for rammed earth sample AA: 622-OKS0CE, AD: 622-10KS0CE, AE: 622-50KS0E, AC: 622-90KS0CE, AB: 622-100KS0CE.

Chapter Five

Physical and Mechanical Properties of Rammed Earth Containing no Additives

Work has been carried out by previous researchers (Hall & Djerbib 2004b; Hall & Allinson 2009; Hall & Djerbib 2004a) on selection of rammed earth material based on properties observed for various grades. However, with the disposal of Pulverised Fuel Ash in rammed earth, these properties are greatly altered. The decision to utilise soil as it is found on site or to improve on it by importing and mixing with other soil type will depend on the property foremost in consideration. This chapter investigates the physical and material properties of various blends of rammed earth when no additives have been introduced. It should however be noted that these experiments consider the use of rammed earth as non-load bearing walls.

The soil grades being considered are the 721 (representing sandy soil), 532 (representing well blended soil) and 451 (representing very clayey soil).

5.1 Density Comparisons

Density did not vary much irrespective of the proportion of constituent material. Sample 451 had the lowest density. This is probably due to the low coarse aggregate content. Supporting this argument is the sample with the next lowest density containing the same proportion of coarse aggregate. All samples saw a sharp reduction in density in the first 7 days as seen in Figure 5.1. Density trend showed a general decline over 90 days.

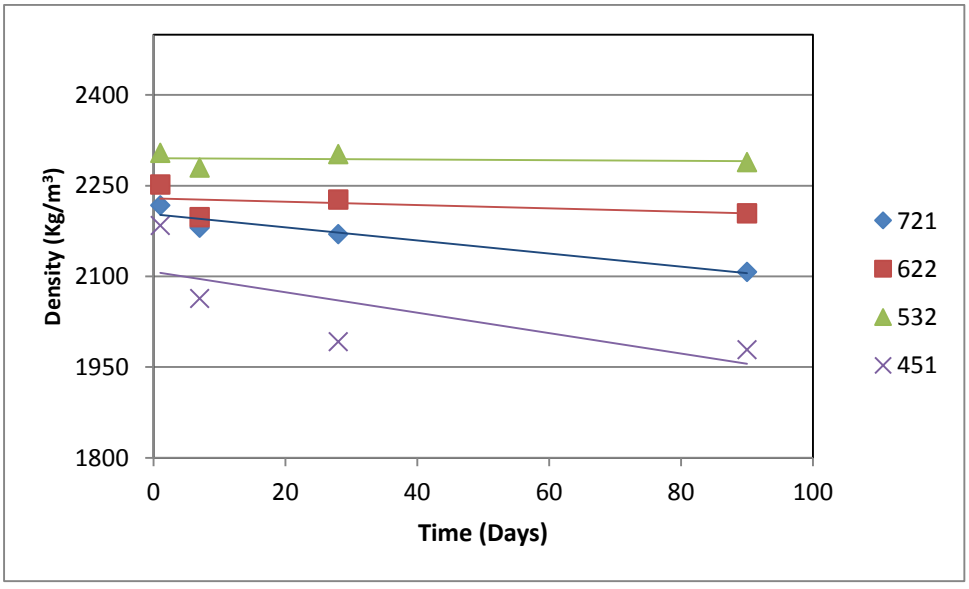

Figure 5.1 Density values for rammed earth soil samples

Values obtained are in agreement with previous work carried out by Hall and Gjerbib (2004b) as seen in Figure 5.3 and by other researchers (Venkatarama Reddy et al. 2010; Jaquin et al. 2009; Walker & Britain 2005) as seen in Table 5.1

Table 5.1 Density as related to soil composition (venkatarama reddy et al. 2010).

Properties	Soil designation					
	River sand	S1	S2	S3	S4	S5
Soil:sand (by weight)	0:1	1:0	1:0.5	1:1	1:1.5	1:2.5
Textural composition (% by mass)						
Sand (4.75–0.075 mm)	94.8	50.3	65.1	72.6	77.0	82.1
Silt (0.075–0.002 mm)	5.2	18.1	13.8	11.6	10.4	8.9
Clay (<0.002 mm)	–	31.6	21.1	15.8	12.6	9.0
Compaction characteristics						
Maximum dry density (kg/m³)	–	1835	1910	2000	1980	1950
Optimum moisture content (%)	–	15.6	10.8	9.4	9.4	9.4

5.2 Compressive strength Comparisons

Figure 5.2 shows that grade 451 which represents clayey soil has the lowest compressive strength figure over 90 days. 622 which represents soil with high sand content and high aggregate content showed the highest figures for compressive strength. While 532 blend which represents an evenly blended soil showed the highest compressive strength for day 1, 622 soil grade had a steady strength increase as the samples aged.

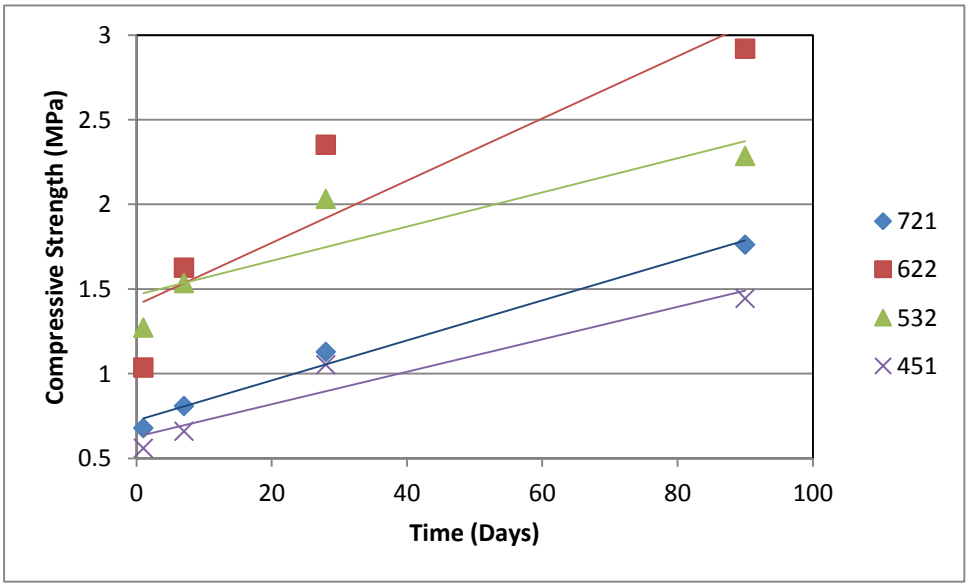

Figure 5.2 Compressive strength propagation for various soil grades over 90 days.

Comparing this to other recent research efforts (Figure 5.3 and 5.4), we note that clayey soil consistently have the worst compressive strength properties while sandy soil tends to have higher compressive strengths (Jayasinghe & Kamaladasa 2007; Hall & Djerbib 2004b).

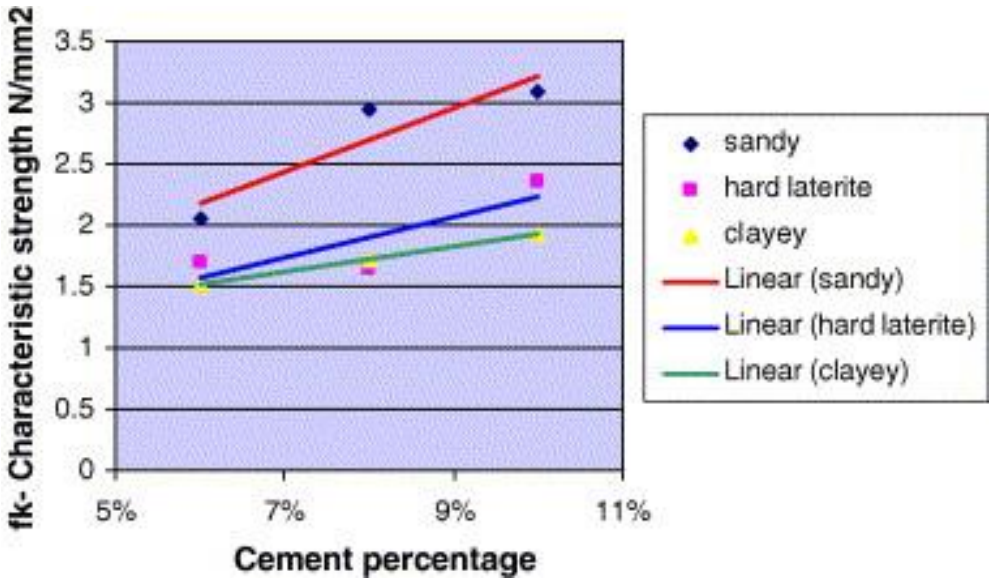

Figure 5.3 Compressive strength comparisons for different cement stabilised rammed earth walls (jayasinghe & kamaladasa 2007).

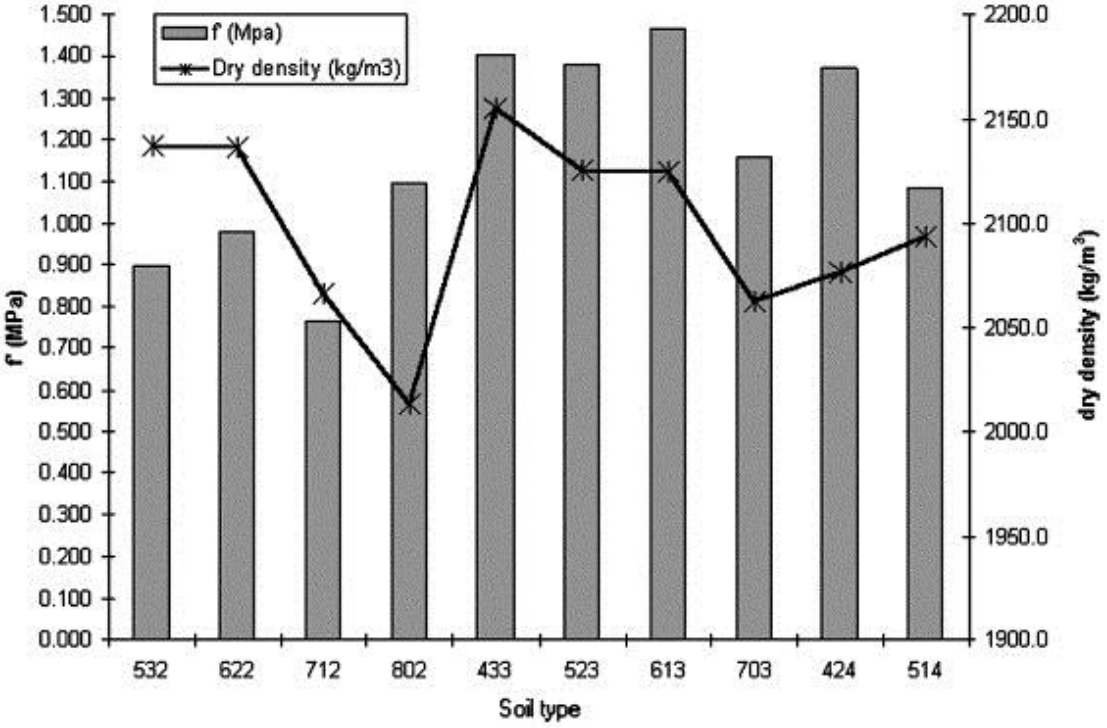

Figure 5.4 Compressive strength and density values for various rammed earth mixes (hall & djerbib 2004b).

5.3 Ultrasonic Pulse Velocity Comparisons.

Rammed earth soils made from different mixes showed differences in internal structure as measured by the ultrasonic pulse velocity. Samples having higher speed show a better packed internal structure. The 532 sample had the highest UPV values from day 7 up to the 90th day of testing. However, sample made from the 451 mix had the highest UPV value on day 1. It will be noted that these samples have the highest clay content. As seen in Figure 5.5, sample 721 had the worst velocity values. All samples recorded UPV value increase with age except for the 451 sample that recorded slightly lower values on the 28th day.

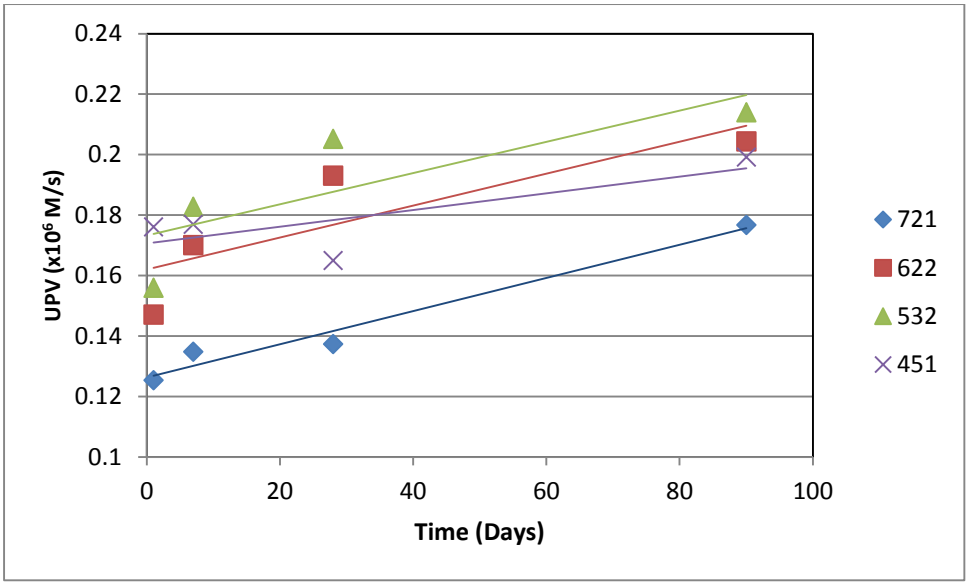

Figure 5.5 UPV values for rammed earth soil samples

Chapter Six

Physical and Mechanical Properties of Rammed Earth Containing Palm Kernel Shell (PKS)

Incorporating palm kernel shell in rammed earth will go a long way in increasing the overall utility of rammed earth. Not only will PKS find a safe disposal method, but regions that produce large quantity of PKS and have soils with poor coarse aggregate content (for example, the Eastern Region of Nigeria) can find the coarse aggregate needed to build rammed earth houses. PKS was introduced to the samples by replacing (by volume) parts or all of the coarse aggregate fraction in the rammed earth samples. The effect of incorporating PKS on rammed earth properties is discussed below.

6.1 Compressive strength

The compressive strengths obtained from the crushing of samples are shown in figures 6.1 and 6.2. The effect of PKS on compressive strength appeared not to follow a pattern of maximum replacement attaining the highest or lowest strength as compared to a zero content. PKS has been introduced by replacing the coarse aggregate component partially or wholly in defined proportions.

In the 622 mix, compressive strength on the first day increases as 10% of aggregates are replaced with PKS. The increase is a 19% increase from 1.04MPa which is the 1 day control strength for the 622 mix. Compressive strength starts to decrease with further replacement up to and beyond 50% (strength loss of 14%) replacement. The trend is reversed at 90% replacement (33% less strength compared to 20% replacement) where compressive strength shows significant improvement for 100% replacement (up 63% from 90% replacement). This trend is similar for 7 day strengths as shown in Figure 6.1. After 28 days however, there is very little difference in strengths for each replacement level. There is a gradual decrease in compressive strength as PKS replaces coarse aggregate. At 10% replacement the decrease is more marked at 9.6% when compared to further replacement of 50, 90 and 100% which stand at 14.3%, 14.7% and 16.1% reduction in compressive strength respectively.

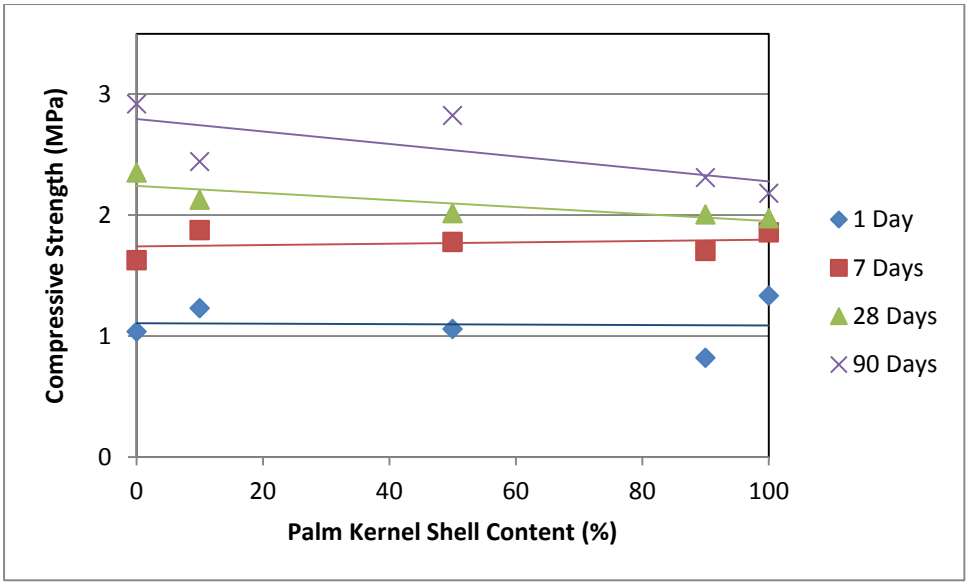

Figure 6.1 Compressive strength of 622 soil grade rammed earth

For the 532 mix, compressive strength falls by 10.2% when replacement is 10%, and then rises by 20.1% as compared to the strength obtainable after 10% replacement (Figure 6.2). A slight decrease in compressive strength of 5.6% can be observed when further replacement reaches 90%.

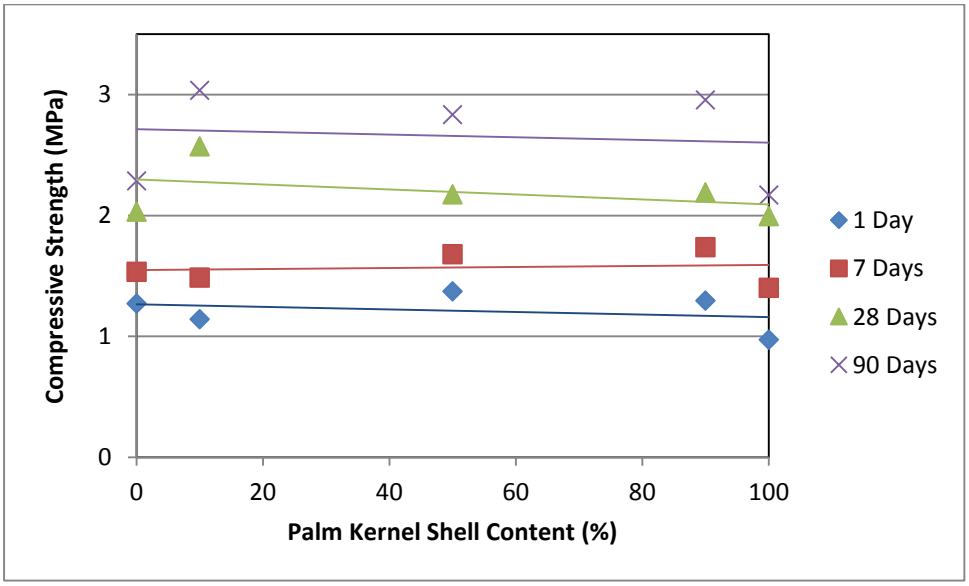

Figure 6.2 Compressive strength of 532 soil grade rammed earth

However total replacement of coarse aggregate will result in a reduction of compressive strength by 23.5% on the first day. This trend is closely repeated

on the 7th day. But by the 28th day, Compressive strength trend changes completely. A 10% replacement sees compressive strength increase by a massive 26.6%. However further increasing the PKS content to 50% results in a compressive strength loss of 15.4%. This however is still an increase of 7% when no PKS is present. This position is slightly improved to 7.9% upon further addition of PKS to 90%. Total replacement of coarse aggregate by PKS sees compressive strength fall by 1.8% as compared to zero PKS Compressive strength. Figure 6.3 shows a bar chart comparing the 28day strengths of 622 and 532 mixes.

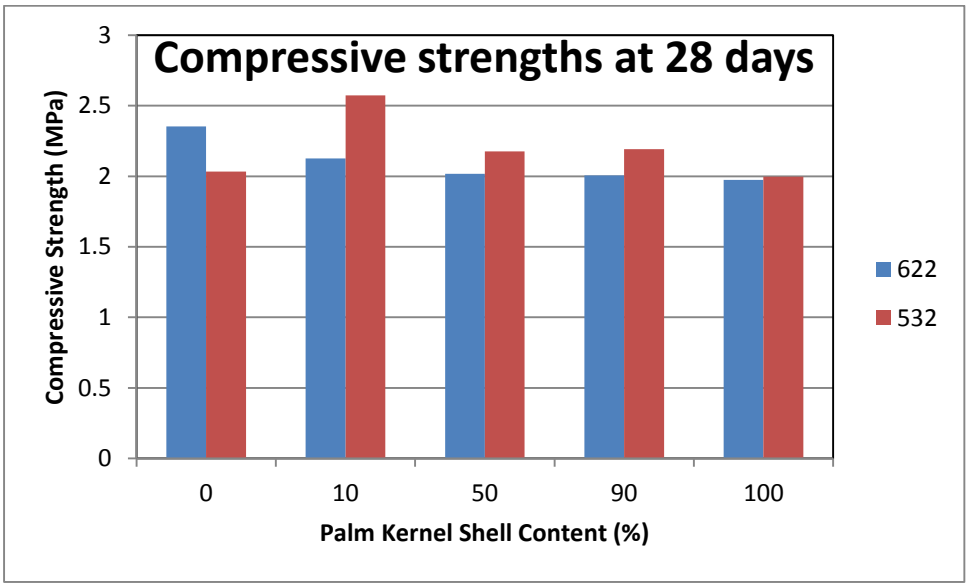

Figure 6.3 Compressive strength comparatives for 622 and 532 soil grade rammed earth at 28 days, at different PKS content.

When compressive strength development is viewed with respect to time, we see from figures 6.4 and 6.5 that strength increase is continuous. For 622 mix, Figure 6.4 shows that sample containing no PKS develop the most strength. On the other hand, sample containing 10% PKS was seen to develop the most strength for the 532 mixes. This is clearly seen in Figure 6.5.

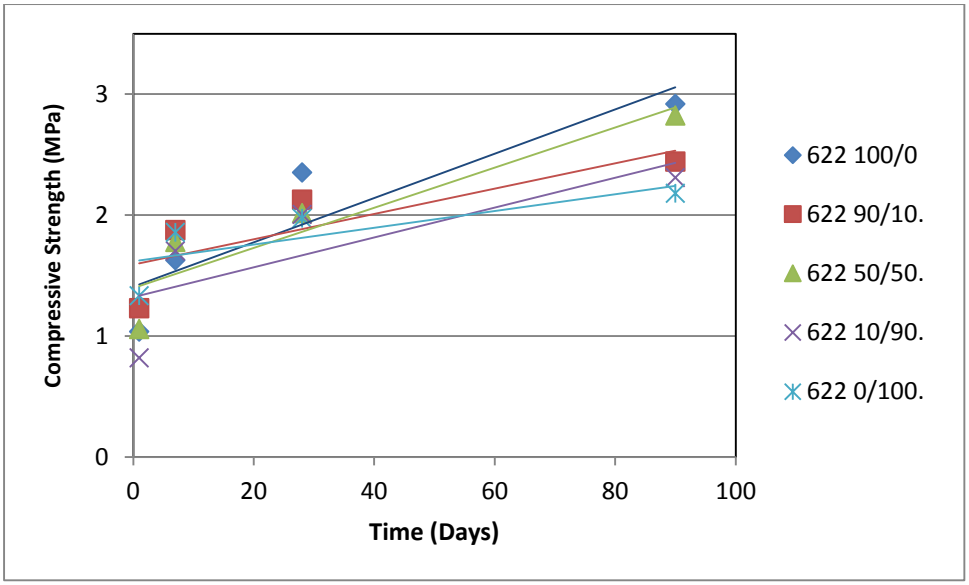

Figure 6.4 Compressive strength comparison for 622 soil grade rammed earth at different PKS content

Compressive strength develops in a similar pattern for all samples in the 622 mix for the first 7 days. For the sample containing no PKS, compressive strength goes from a 1 day strength of 1.04Mpa to a 90 day strength of 2.92Mpa, an increase of 182%. The sample containing 100% PKS on the other hand has strength increase from 1.33Mpa to 2.18Mpa, an increase of 64%. The sample containing 50% PKS showed remarkable strength increase after 28 days with an increase of 40% as opposed to a 14.9%, 15.1% and 10.5% for 10%, 90% and 100% replacements respectively.

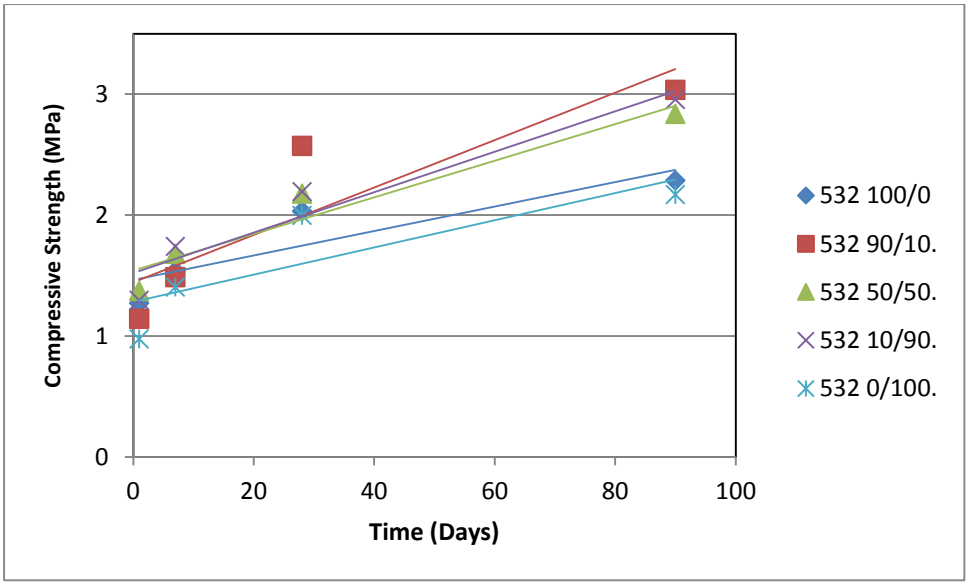

Figure 6.5 Compressive strength comparison for 532 soil grade rammed earth at different PKS content

The 532 mix paints a different picture. While a similar compressive strength gain trend is observed for 0 and 100% PKS replacement, and for 50% and 90% replacement, values for a 10% replacement is strikingly different. Compressive strength is gained very rapidly over the first 28 days and then starts to slow. There is a 73% rise in compressive strength between the 7th and 28th day strengths. This starts to slow and only an 18% increase is observed by the 90th day. For the sample containing 90% PKS, strength continues to increase at an increasing rate. Compressive strength increases from the 7th day strength to the 28th day strength by 26% and continues to rise to the 90th day strength by 34.8%.

The slope of the curve obtained when compressive strength is measured against time provides an insight into the rate of gain in compressive strength daily. When this value is compared to values obtained for various samples containing Palm kernel shell the result is a chart that shows how PKS content affects compressive strength propagation in rammed earth. From Figure 6.6, it can be seen that adding 10% PKS will increase the time it takes for the rammed earth sample to attain its highest compressive strength value in 90

days. Further addition of PKS is seen to decrease the time it takes the sample to build up compressive strength.

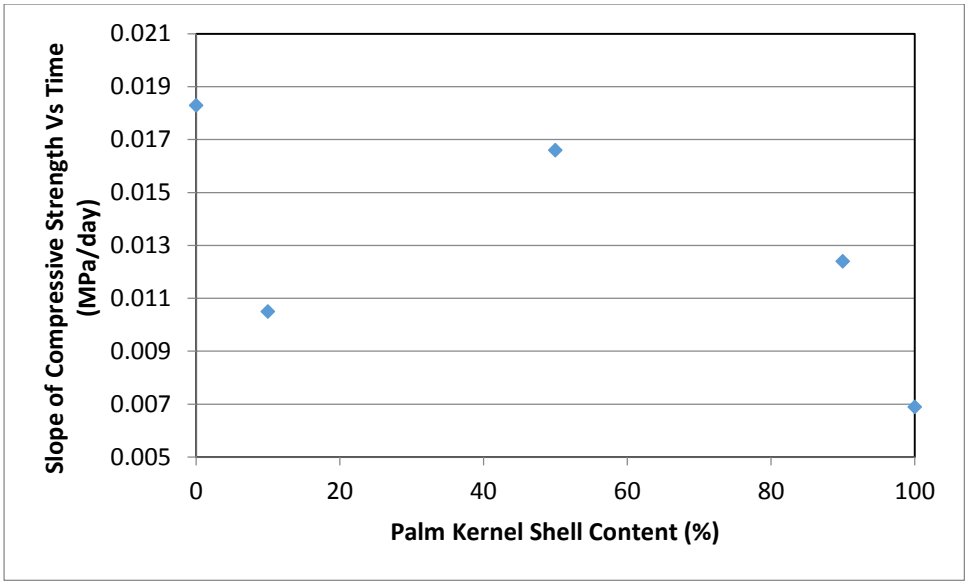

Figure 6.6 Plot of Compressive strength gain with time for 622 grade rammed earth at various PKS content

Sample containing 100% PKS is observed to attain the maximum 90 day strength at the longest time recorded. This could however be due to that fact that it has the lowest compressive strength value. This is however not the case for the 532 soil grade as seen in figure 6.7. There was no substantial difference in the time taken for samples containing either 100% crushed granite or 100% PKS to attain maximum compressive strength in 90 days.

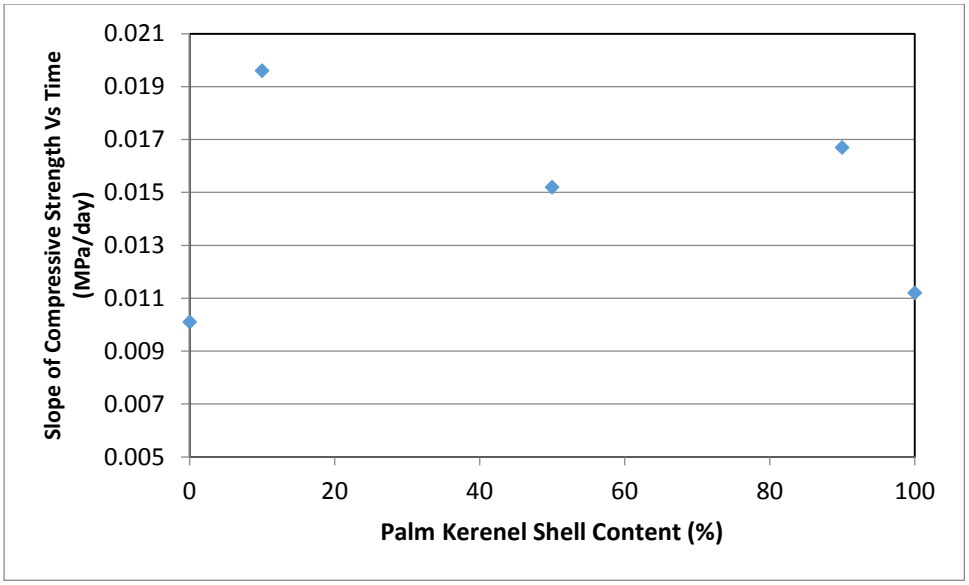

Figure 6.7 Plot of Compressive strength gain with time for 532 grade rammed earth at various PKS content

As observed in Figure 6.8, When cement is added to the same mix, sample containing only coarse aggregate gains strength at a faster rate than sample containing 100% PKS. However , compressive strength appears to peak after about 28 days while compressive strength continues to rise past day 90 in samples containing 100% PKS.

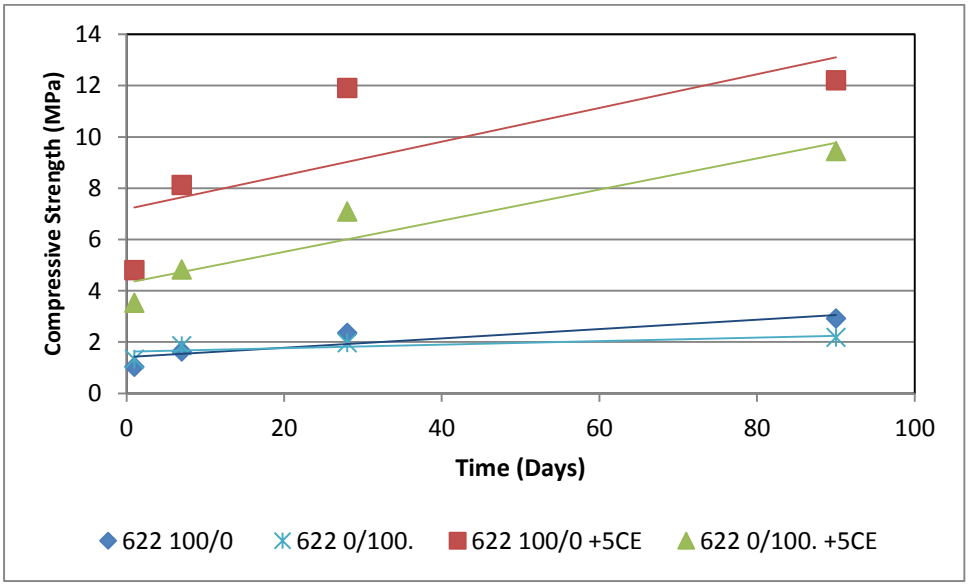

Figure 6.8 Compressive strength of 622 soil grade rammed earth containing 5% cement

This trend did not repeat for rammed earth made from 532 grade rammed earth. As seen in Figure 6.9, when the same proportion of cement (5%) was added to the mix, compressive strength values did not vary by much. While day 1 strengths for sample containing 100% PKS was the value with the most significantly different value, the sample gained compressive strength quickly enough to rank pari pasu samples containing 100% crushed granite at day 90.

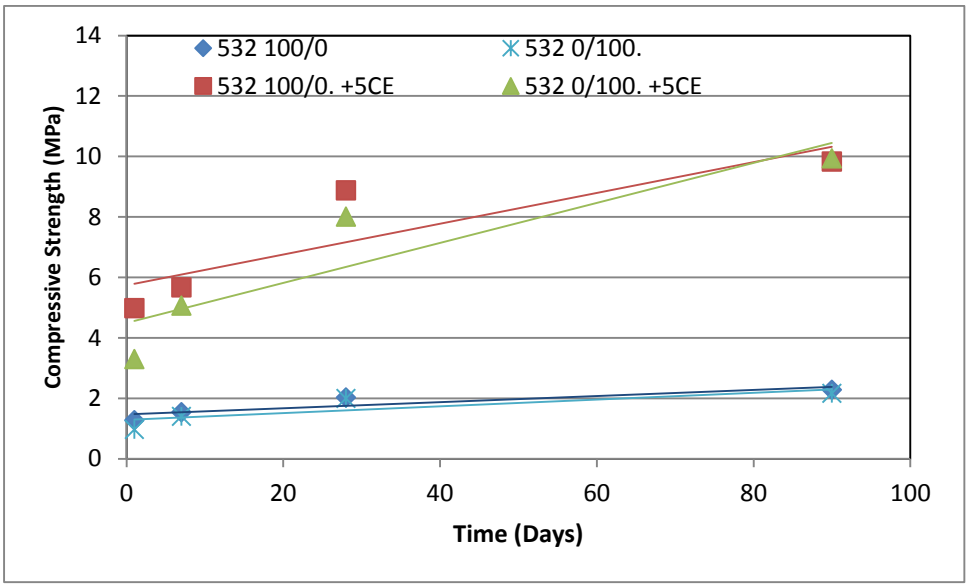

Figure 6.9 Compressive strength of 532 soil grade rammed earth containing 5% cement

6.2 Ultrasonic Pulse Velocity

The ultra-sonic pulse velocities provided an insight as to the internal mechanism of the structures. Figures 6.10 to 6.11 presents UPV values for both soil grades at different curing ages up to 90 days.

From Figure 6.12 and 6.13 it can be observed that UPV values tend to increase with time. The values observed on day one appear to be far lower than all the values observed on the 90th day. However speed differed greatly for samples as PKS was added.

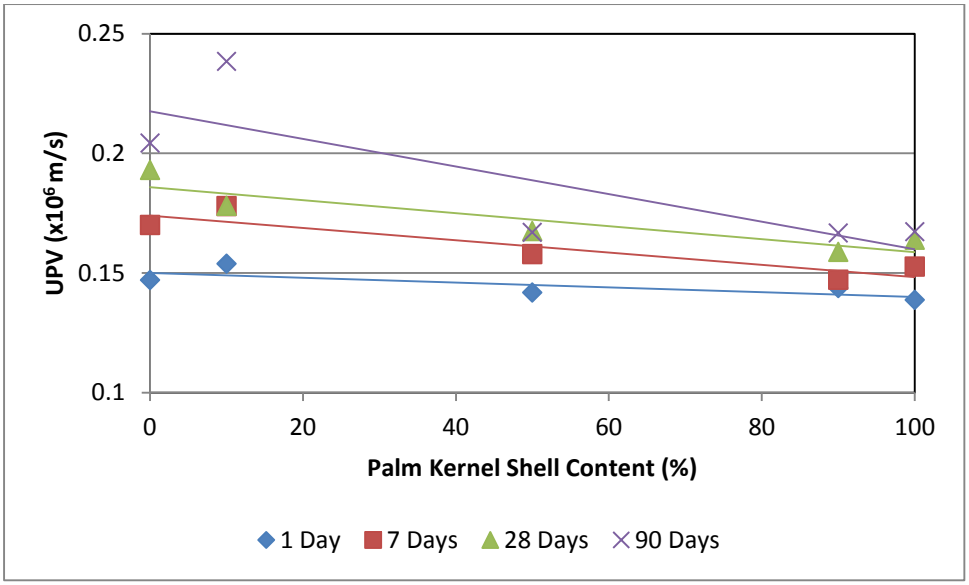

Figure 6.10 UPV of 622 soil grade rammed earth

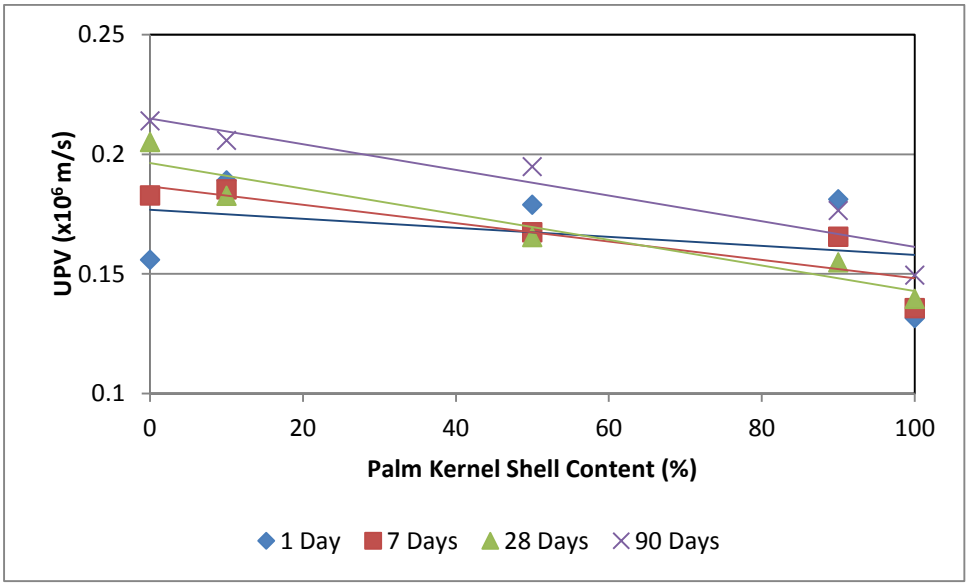

Figure 6.11 UPV of 532 soil grade rammed earth

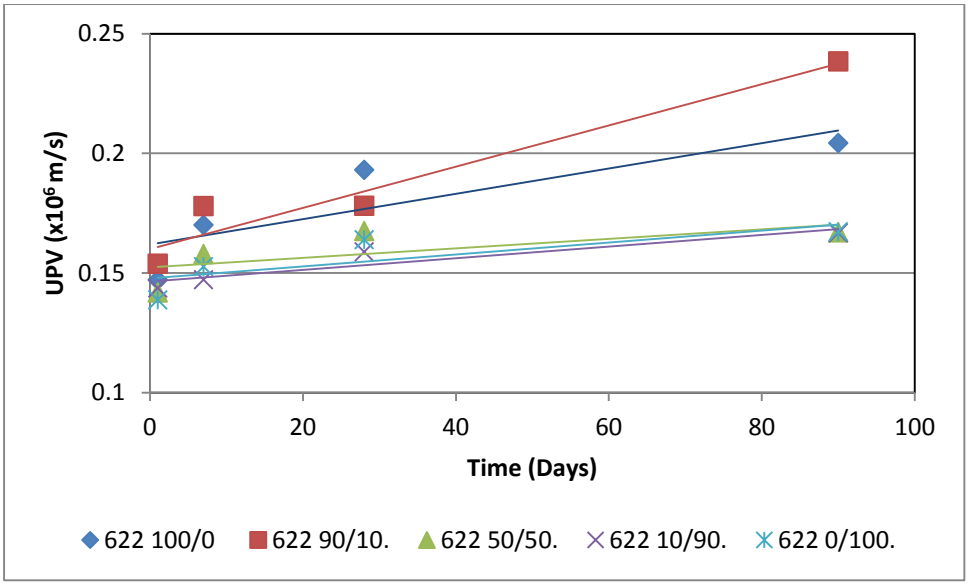

Figure 6.12 UPV comparison for 622 soil grade rammed earth at different PKS content

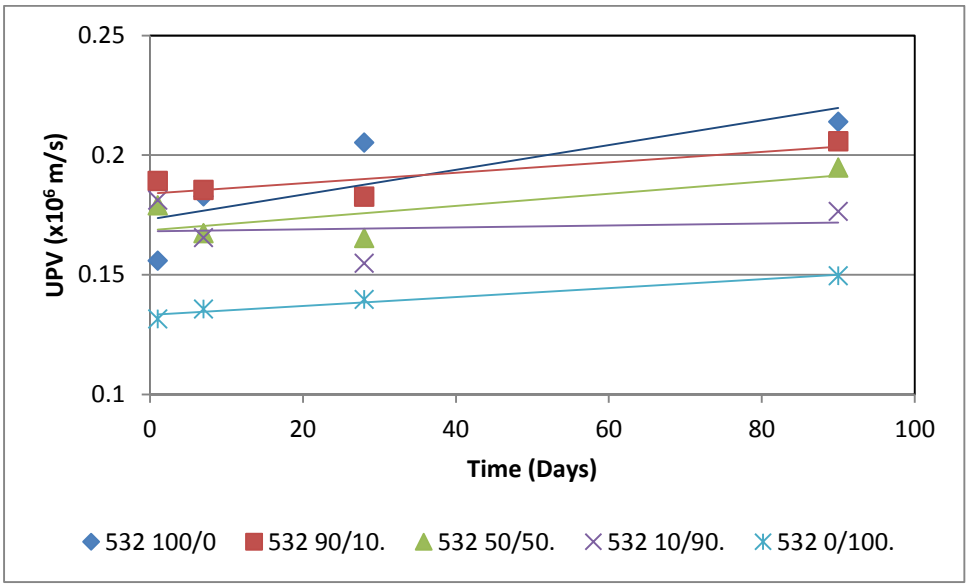

Figure 6.13 UPV comparison for 532 soil grade rammed earth at different PKS content

For the 622 mix, testing on day 1 revealed that UPV decreased as PKS was added. However there was an initial increase of 4.6% when 10% of aggregate was replaced by PKS. Further replacement (upto a total of 50%) resulted in fall in UPV values of 7.8%. When replacement reached 90%, UPV values

increased slightly by 1.25%. Using 100% PKS as aggregate saw UPV values fall by 5.6% when compared to 100% coarse aggregate.

This trend remained similar at day 7 testing with the difference in UPVbetween 100% coarse aggregate and 100% PKS aggregate increasing to 10%. After 90 days, the initial increase in UPV value that was observed at 20% had increased to 16.7%. Further increase in replacement quantity (up to 50%) however lowered UPV values by 30%. 90% replacement saw a further reduction of 0.2%. 100% replacement with PKS showed an observable reduction in UPV of 18% when compared with 100% coarse aggregate.

The 532 mix showed a similar falling trend. As seen in figure Day 1 testing showed an initial rise in UPV similar to that seen in 622 mix before a subsequent fall in value. 10% aggregate replacement resulted in a 21% rise in UPV value. This quickly reduced by 5.4% as replacement reached 50%. At 100% replacement, UPV had fallen by 15.6%.

At day 7, UPV values increased for the initial 20% replacement by 1.4%. A fall in velocity of 10% was then recorded at 50% replacement. This fell further by 1.1% at 90% replacement. At 100% replacement, the UPV value had fallen by 26% when compared to values observed for 100% coarse aggregate.

At 90 days, 20% aggregate replacement results in a decrease in UPV value of 3.85%. This reduces further by 5.3% when replacement reaches 50%. Further replacement (upto 90%) results in even further decrease in UPV by 9.4%. UPV values fall by 30% in total when 100% of coarse aggregates are replaced with PKS.

While 622 grade samples containing either PKS or crushed granite witnessed a rise in UPV values with time, stabilising with 5% cement appeared to produce samples that didn't undergo any internal restructuring over 90 days. The sample containing only crushed granite saw a slight decline in UPV values as seen in Figure 6.14.

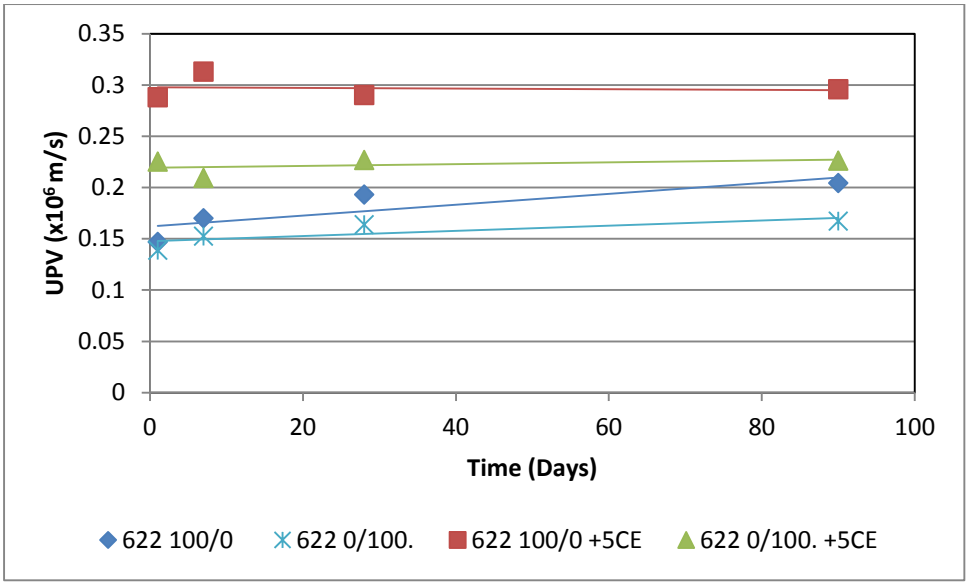

Figure 6.14 UPV values for 532 soil grade rammed earth containing 5% cement

When the same quantity of cement was added to samples made from the 532 soil grade, the result was quite similar with just a slight increase in the early age values for UPV. This can be seen in Figure 6.15.

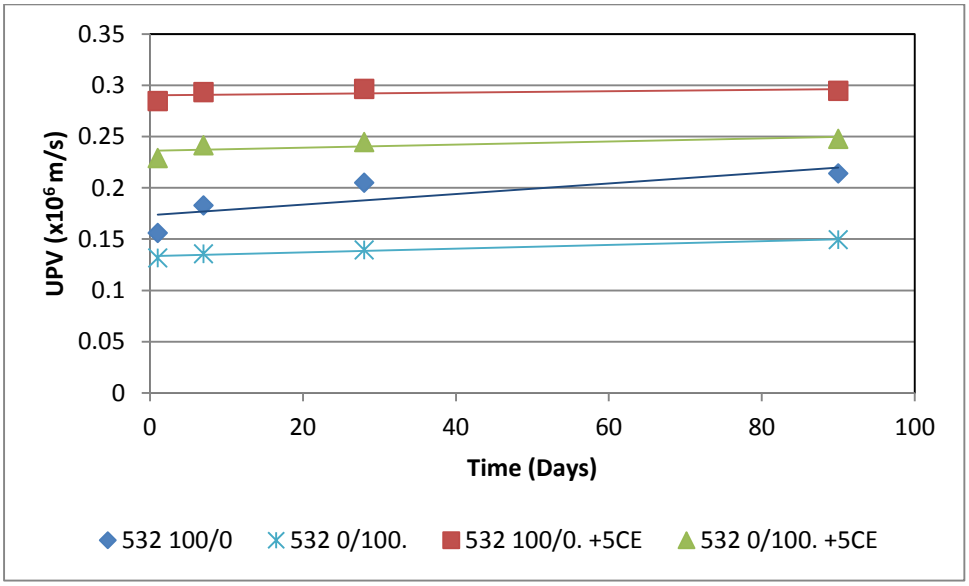

Figure 6.15 UPV values for 532 soil grade rammed earth containing 5% cement

6.3 Density

Experimental results reveal that density was affected by replacement of coarse aggregate with Palm Kernel Shell. Daniel (2012) reports that density

followed the same pattern for replacement by weight and replacement by volume. Figure 6.16 and 6.17 show the density of two soil mixes up to a 100% replacement.

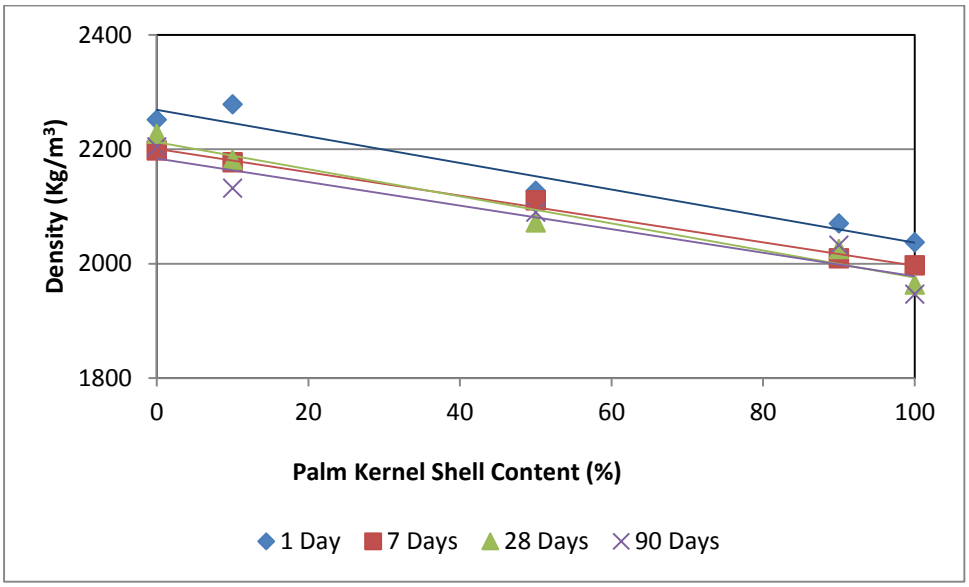

Figure 6.16 Density of 622 soil grade rammed earth

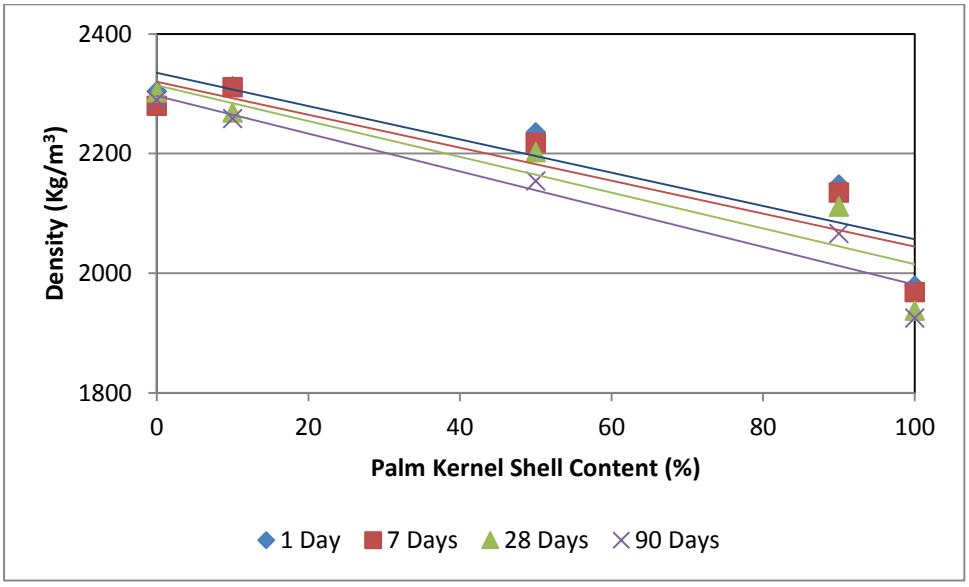

Figure 6.17 Density of 532 soil grade rammed earth

In both soil grades, density is seen to ultimately decrease with time. In the 622 mix, on day 1, density rises initially by 1.2% when coarse aggregate is replaced by 10%. Density starts to fall with further replacement. It falls to 5.5%

and 8% of initial density when replacement reaches 50% and 90% respectively. On the first day, at 100% replacement, density had fallen by 10% of initial density. This trend is observed in Figure 6.17 for soil grade 532. On the first day, 10% replacement resulted in a slight increase in density of 0.4%. Further replacement of 50% and 90% saw a reduction of initial density by 3% and 7% respectively. At 100% replacement, density had fallen by 14%.

Density however reduced at different rates over time for each replacement level. In the 622 grade soil, the control sample saw a decrease in density over time at a fairly steady rate for the first 7 days, witnessed a shallow spike by the 28th day, then a much slower loss rate up to 90 days. As can be seen in Figure 6.18, density fell by 2.5% in the first 7 days then started to rise. It had increased by 1.5% on the 28th day. By the 90th day, density was seen to have reduced by 2.1%. At 10% replacement, density fell by 4.5% then started to rise. It rose by 0.2%. At 90 days, Density had fallen by 6.5%.

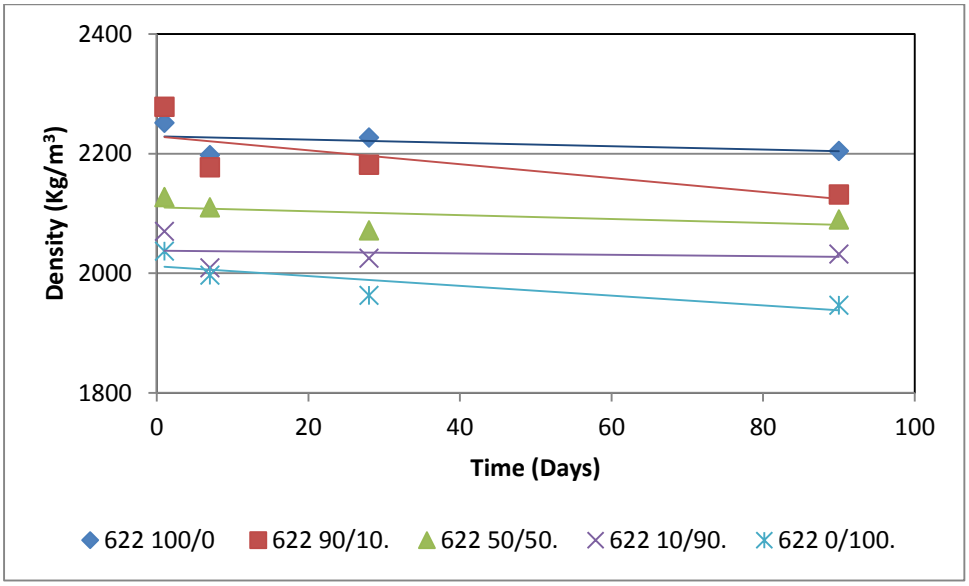

Figure 6.18 Density comparisons for 622 soil grade rammed earth at different PKS content

The sample containing 100% PKS however, showed a steady decrease in density. This steady decrease was also mirrored in the 532 mix (Figure 6.19).

The 622 mix saw a decline of 2%, 3.6%, and 4.5% at 7 days, 28 days and 90 days respectively. The 532 mix saw a reduction to density of 0.5%, 2%, 2.74% also a 7days, 28 days and 90 days as seen in Figure 6.19.

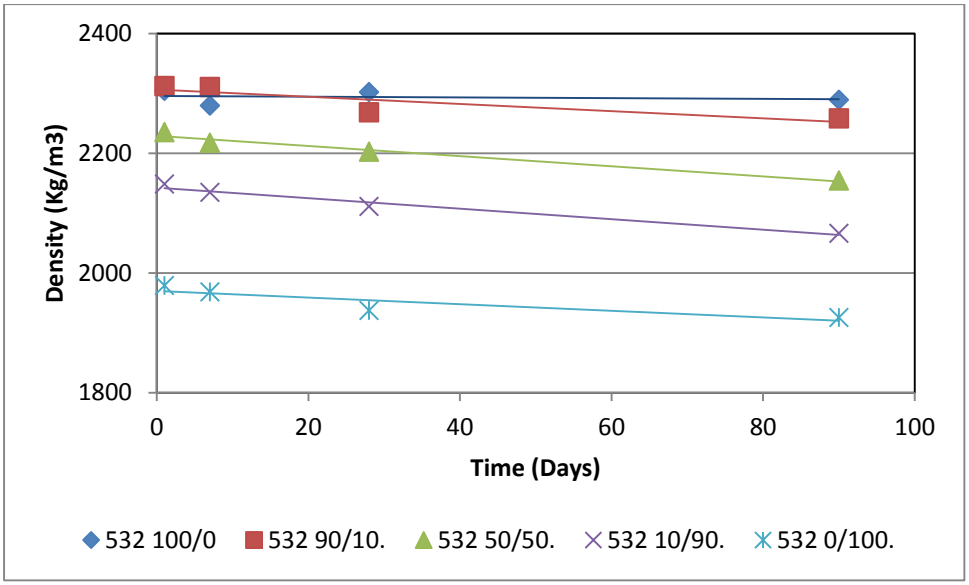

Figure 6.19 Density comparisons for 532 soil grade rammed earth at different PKS content

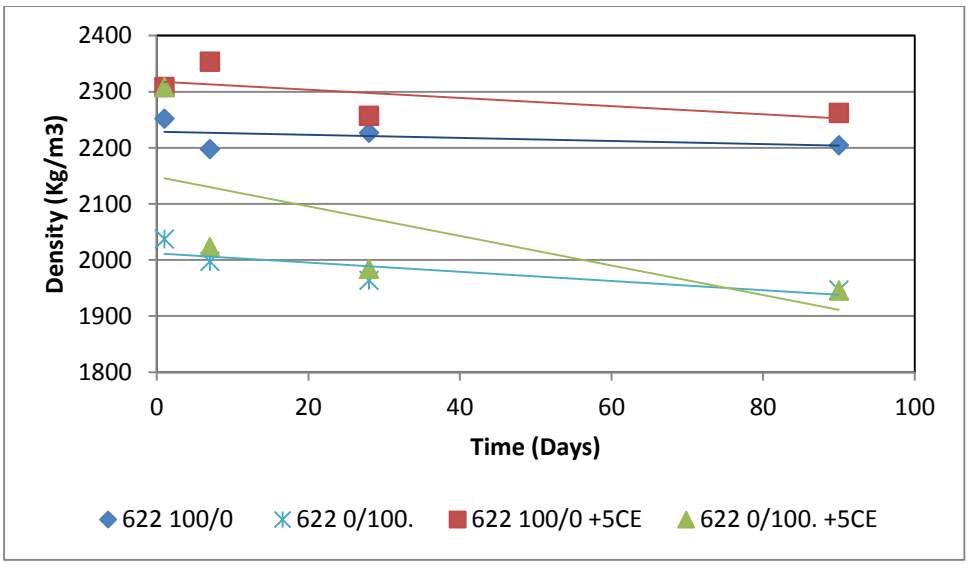

Figure 6.20 Density values for 622 soil grade rammed earth containing 5% cement

Figure 6.20 shows that while stabilisation by 5% cement resulted in an increase in density, density dropped at a far greater rate over time. Density

was higher for cement stabilised rammed earth samples containing PKS by 13% as opposed to 3% recorded for cement stabilised rammed earth containing only crushed granite.

When the 532 soil grade was stabilised, the rammed earth showed a difference in density that was not as pronounced as it was for the 622 soil grade rammed earth. While cement stabilisation raised density, the rate of decline in density as similar for samples containing only PKS but different for samples containing only crushed aggregate as the unstabilised sample did not change much in density over time (Figure 6.21).

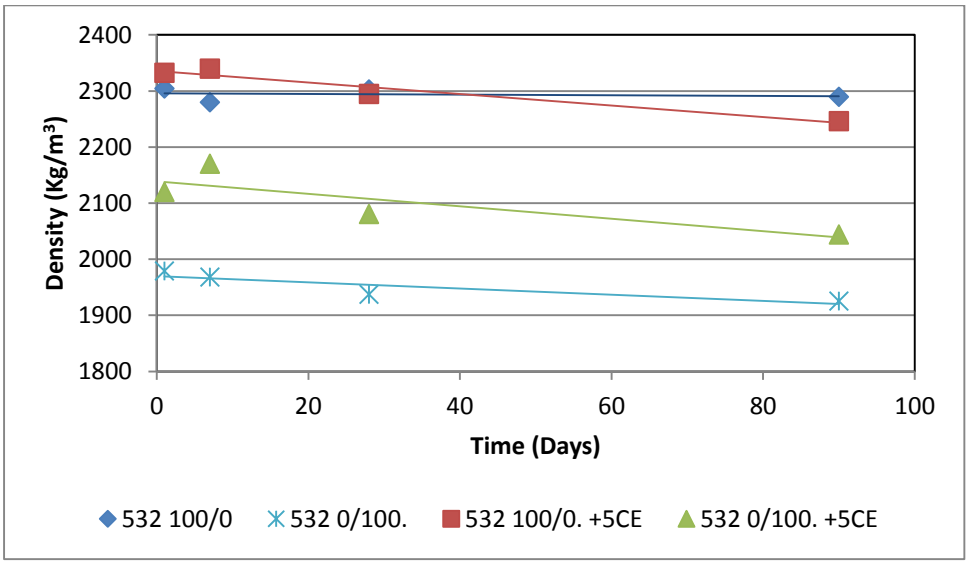

Figure 6.21 Density values for 532 soil grade rammed earth containing 5% cement

6.4 Initial Rate of Sorption (IRS)

Two soil types had PKS replacements for aggregate. 622 and 532. The full results for stabilised samples are shown in Figure 6.22.

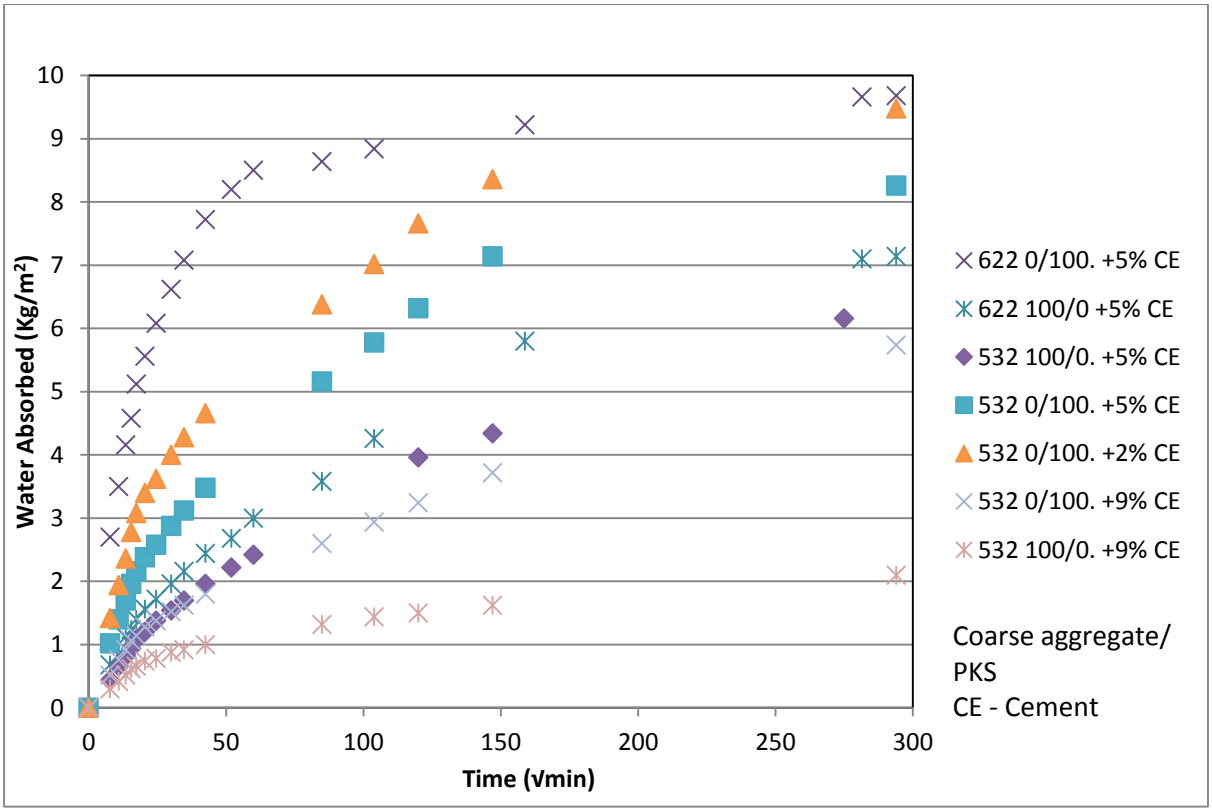

Figure 6.22 Moisture ingress in rammed earth samples containing PKS and cement

It appears from the figure that samples containing more cement absorbed less moisture while samples containing less cement had a much greater initial absorption rate. Also it is obvious from the figure that samples containing only coarse aggregate had far lower absorption rates than samples containing only palm kernel shells. This is better represented in figures 6.22 and 6.23.

Figure 6.23 shows that soil grade 622, containing PKS as aggregate and 5% cement as stabiliser exhibits the highest capacity for absorbing water. Water absorption after 24 hours peaked at just under 10 kg/m^2. Initial slope representing the greater influence of capillary action stood at 8.5. Soil grade 532 having a similar composition of PKS and Cement had the second highest absorption rate. This sample's water absorption peaked after 24 hours at 8.3 kg/m^2. This represents a decrease of 14% in total absorbed water.

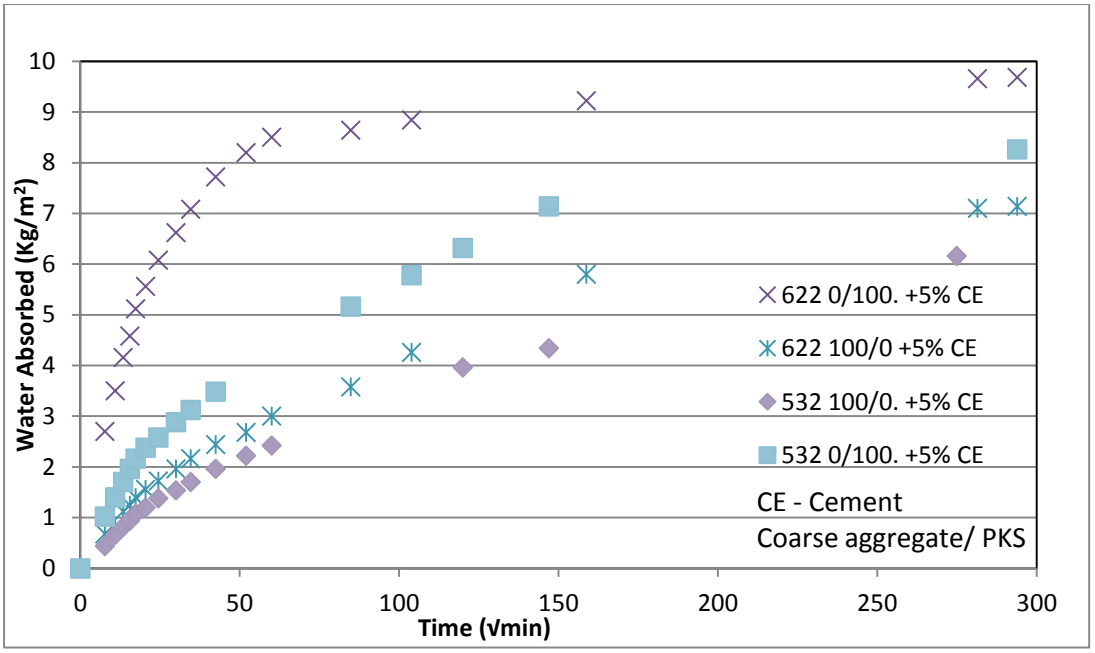

Figure 6.23 Comparison of moisture absorption of two soil grades containing only PKS or coarse aggregate and 5% cement.

The sample in figure 6.23 with the lowest sorbed water is the 532 grade soil containing 0% PKS. Although there were no readings obtained at 24 hours, the total amount of water absorbed after 21 hours was 6.16 kg/m2.

This was significantly lower than the 622 sample containing 100% PKS and 5% Cement, at the same time, by 36%. This leads us to conclude that 532 soil grade absorbs less water than 622 soil grade in the same time frame. Also adding PKS to both soil grades has the effect of increasing the water absorption property.

Figure 6.24 shows the impact of changing the amount of cement used in stabilisation. The sample with the least water absorption is the sample having the most cement and least PKS content. After 24hours, only an average of 2.1 kg/m^2 of water was absorbed. For the same mix containing PKS rather than granite, water absorption rises to 5.74 kg/m^2 representing an increase of 173%. When 5% cement is added to a sample containing granite, water absorption rises past 6.16 kg/m^2 as compared to the same sample containing 9% cement. The worst performing sample was the sample containing 100%

PKS and stabilised with 2% cement. The average total absorption stood at 9.48 kg/m^2 which represents an increase of 351% when compared to the sample having the least absorption.

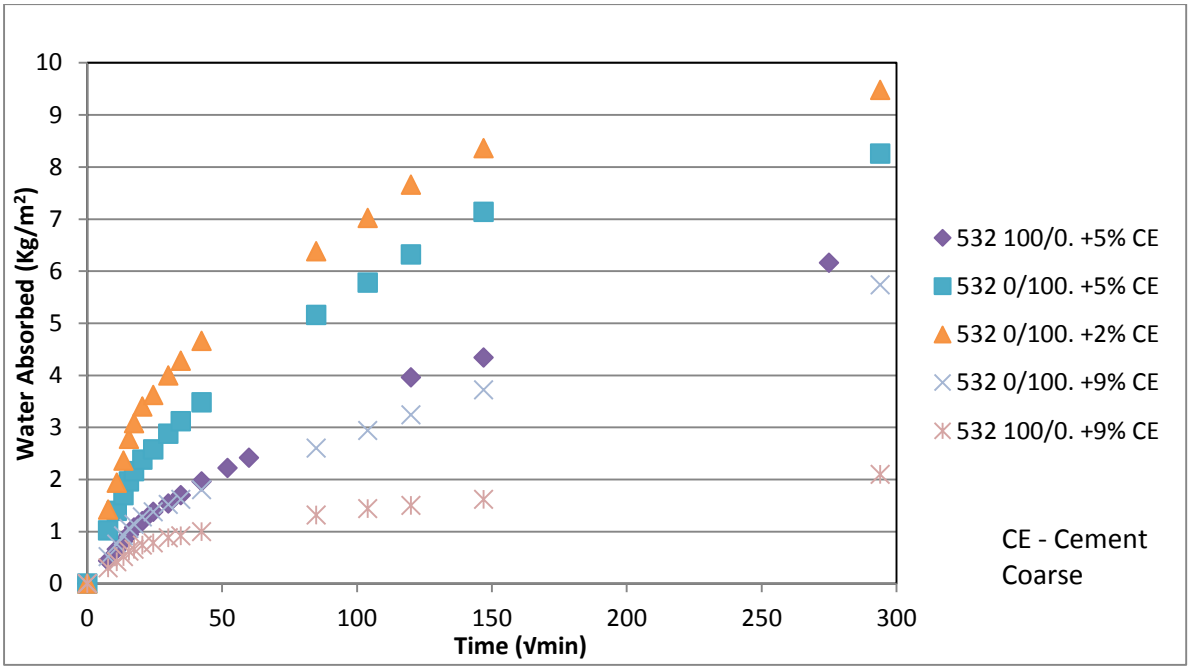

Figure 6.24 Comparison of the moisture absorption of 532 soil grades containing various cement contents

The process of Water ingress described above relates to the total conditions that aid in the propagation of moisture between solid particles. This includes the actions of diffusion combined with capillary action. Sorptivity however relates only to capillary action. This is the major driving force for the initial absorption of water as diffusion only takes effect after the ingress of moisture. The term that describes the action of Sorptivity in experimentation is known as the Initial Rate of Sorption and is measure over the first 5 minutes of the modified IRS test. Sorptivity is obtained experimentally by taking the slope of the graph of initial rate of sorption.

Mass of water absorbed is plotted against the square root of elapsed time (in seconds). While figures 6.25 and 6.26 provide us with maximum mass of

moisture absorbed after 5 minutes, it is easier to compare the effect of replacement of coarse aggregate when Sorptivity values are plotted. Sorptivity is measured by taking the gradient of each curve the values relate to.

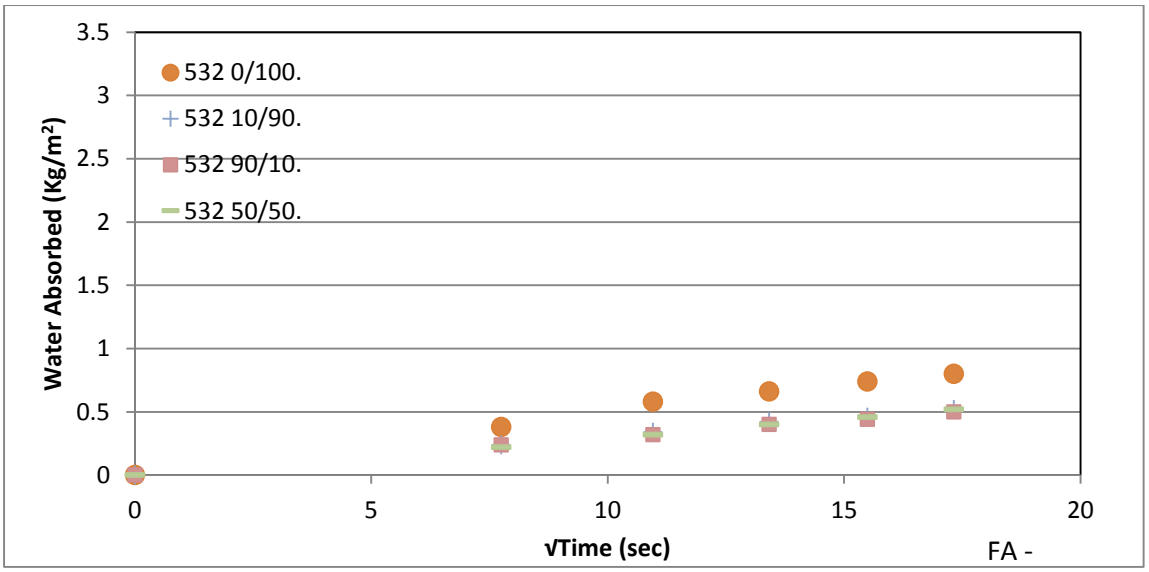

Figure 6.25 Initial rate of suction for rammed earth grade 532 containing PKS

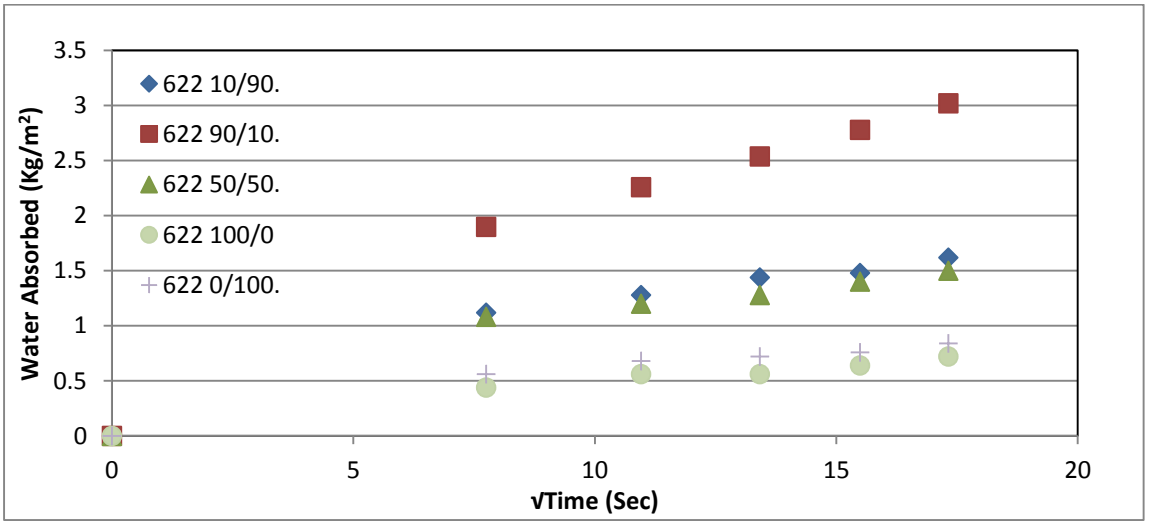

Figure 6.26 Initial rate of suction for rammed earth grade 622 containing PKS.

Figure 6.27 shows the changes in sorptivity as PKS is replaced as coarse aggregate in both 622 and 532 soil grades. It can be observed that Sorptivity

is generally greater in the 622 soil grade than the 532 soil grade. For the 622 soil grade, it can be concluded that a mix of Palm Kernel Shells and granite results in a higher sorption rate. There appears to be little change (19% as opposed to 130% when 10% coarse aggregate is PKS) when PKS completely replaces granite as coarse aggregate. For the 532 soil grade, a mixture of the two aggregate types resulted in marginally higher rate of sorption (42%) which remained fairly constant regardless of mix proportion. At 100% replacement, Sorptivity was at its highest with values rising by 132%.

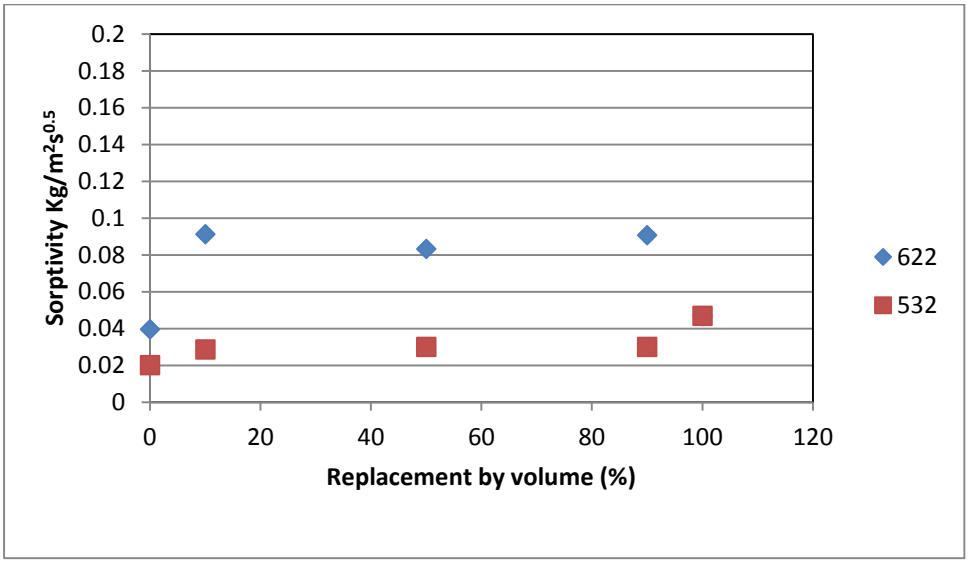

Figure 6.27 Sorptivity values for 532 and 622 soil grades containing various proportion of PKS

Cement was added to stabilise the mix. The effect of this is observed in Figure 6.28 and 6.29.

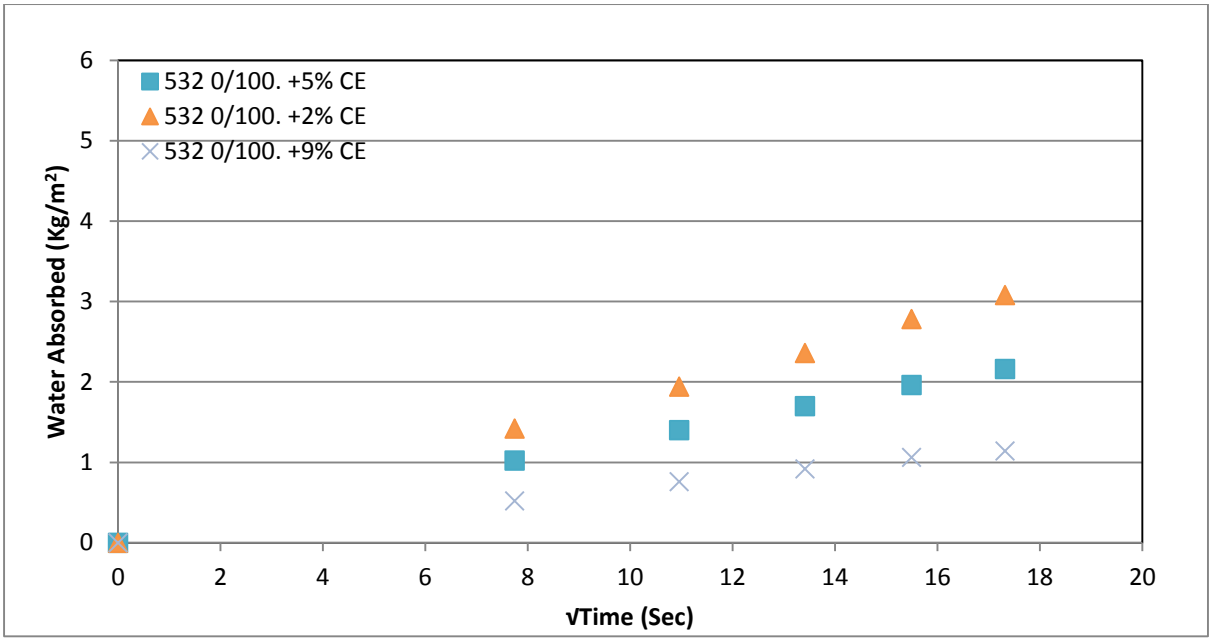

Figure 6.28 IRS of stabilised 532 grade rammed earth

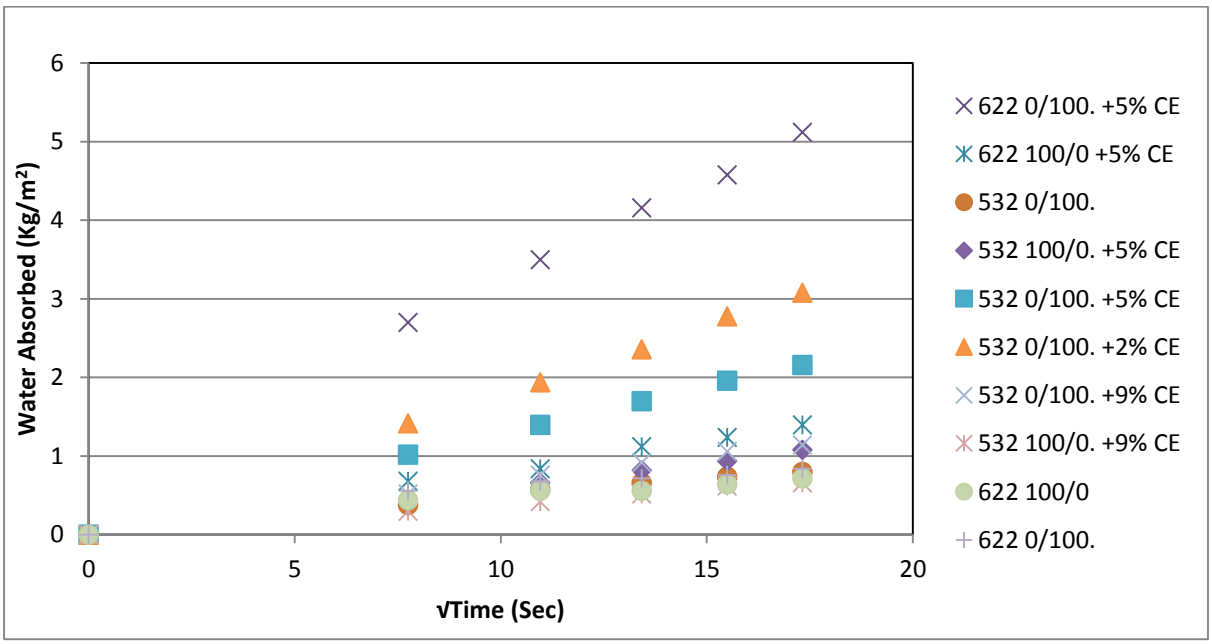

Figure 6.29 IRS of stabilised rammed earth

It can be observed from Figures 6.28 that stabilising Rammed Earth with cement leads to an initial increase in sorptivity. Sorptivity however reduced for greater amounts of stabilisation. A 2% cement content resulted in increasing sorptivity by 277%. Further stabilisation to 5% however reduced sorptivity but was still higher than unstabilised sorptivity by 166%. This trend was repeated

when stabilisation reached 9% Cement with a further reduction in sorptivity but still not sufficient enough to bring sorptivity down to initial unstabilised conditions (Figure 6.30). Sorptivity at 9% stabilisation was 43% greater than sorptivity obtainable for unstabilised grade 532 Rammed Earth.

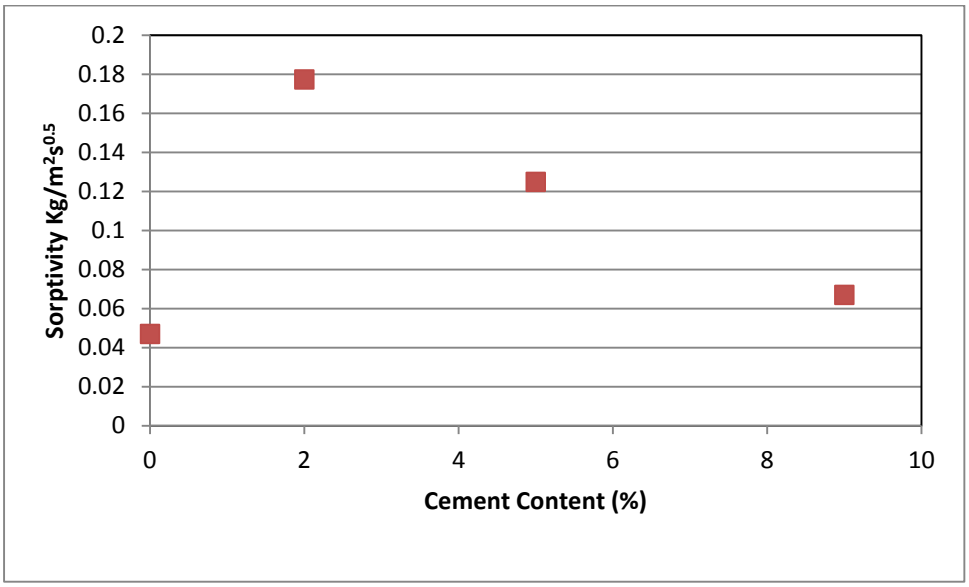

Figure 6.30 Sorptivity measurements in stabilised 532 grade rammed earth

6.5 Moisture Dissipation

The same samples that were tested in the Modified IRS test were used in the moisture dissipation test. This was a test carried out to determine the rate at which the rammed earth samples lost moisture through the process of diffusion and evaporation. The total mass of absorbed water is known at the initial start of the test. The sample is then allowed to dry out naturally in a controlled environment. The temperature was monitored and remained at 21OC (±10) and the relative humidity was observed to remain between 44% and 48%. The samples were weighed at 5 minutes, 15 minutes, 30 minutes, 1 hour up till 48 hours for most samples.

The results obtained when samples containing PKS was left to dry out naturally are shown below. Figure 6.31 and 6.32 show the results obtained

when the samples are unstabilised while figure 6.33 and 6.34 show the results when 5% cement is added.

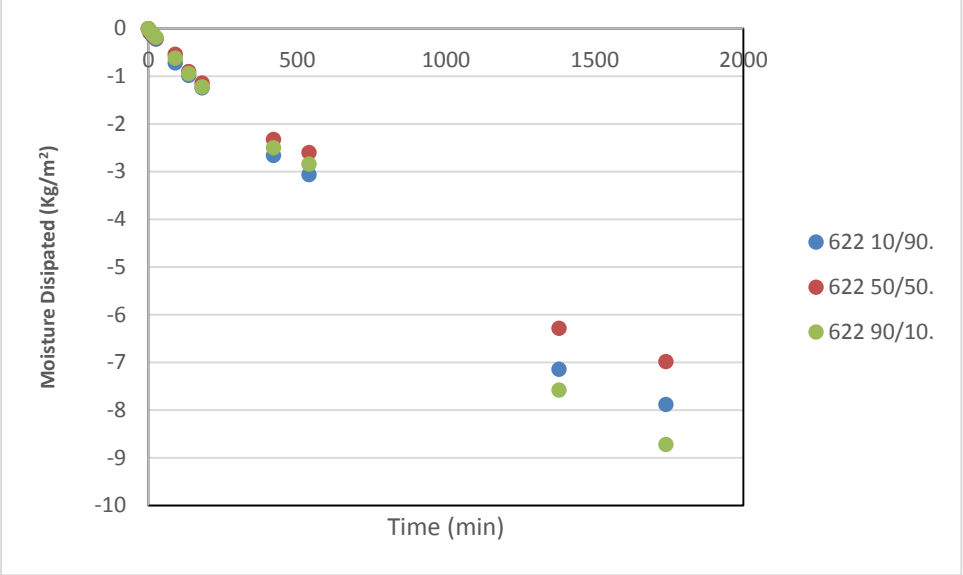

Figure 6.31 Moisture dissipation results for 622 samples containing PKS

As can be observed in figure 6.31, 622 samples containing an even blend of PKS and coarse aggregate held onto the most moisture. Sample containing 90% coarse aggregate lost the most moisture over time. While sample containing coarse aggregate lost more moisture initially, the rate of moisture dissipation reduced over time to end up lower than the sample containing 90% coarse aggregate.

Figure 6.32 shows results for 532 samples containing PKS. Unlike the 622 samples, 532 samples containing PKS shed more moisture over the same period of time than samples containing more coarse aggregate. There was no significant difference in the amount of lost moisture when PKS was increased from 10% to 50%. However, as PKS was increased to 90%,

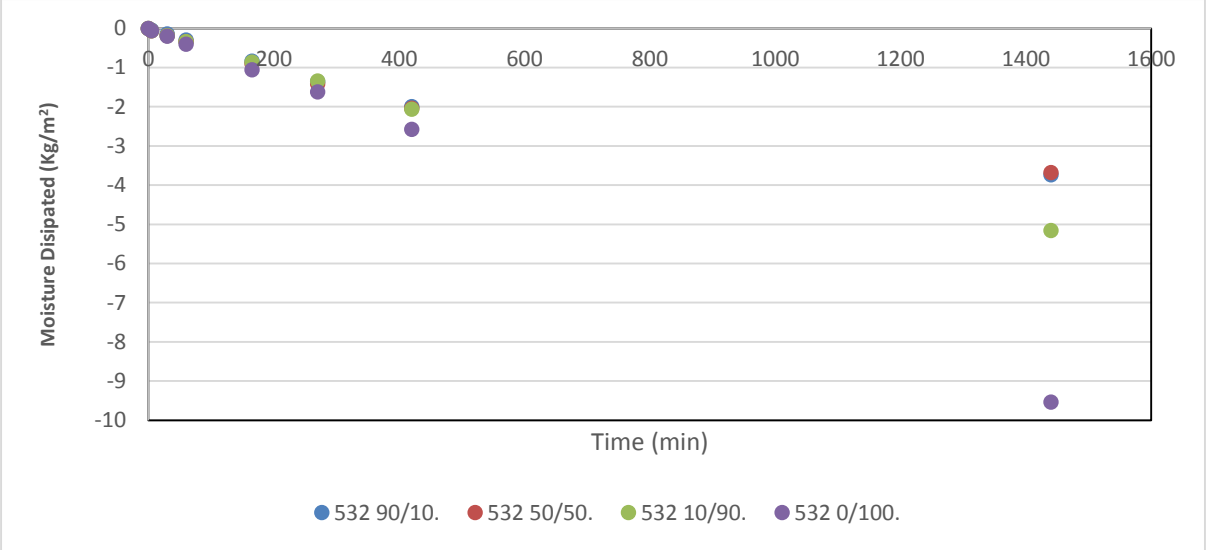

Figure 6.32 Moisture dissipation results for 532 samples containing PKS

Maximum moisture lost increased by 40%. Samples containing 100% PKS lost 160% more moisture compared to samples containing 10% PKS.

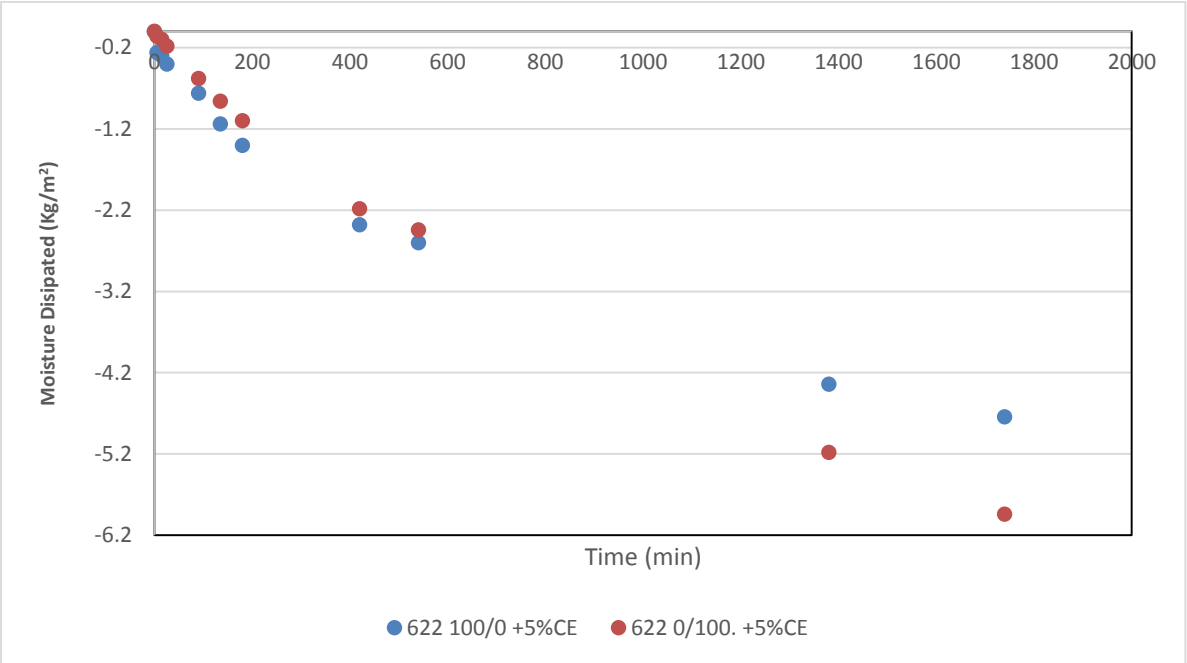

Figure 6.33 Moisture dissipation results for stabilised 622 samples containing PKS

When cement was added to stabilise the sample, the water retention property changed significantly. Figure 6.33 shows that the stabilised 622 soil grade

sample containing PKS lost more moisture than the sample containing only coarse aggregate. This is a reverse of conditions observed for unstabilised 622 samples. It was also observed that the addition of cement also resulted in an overall decrease in moisture loss.

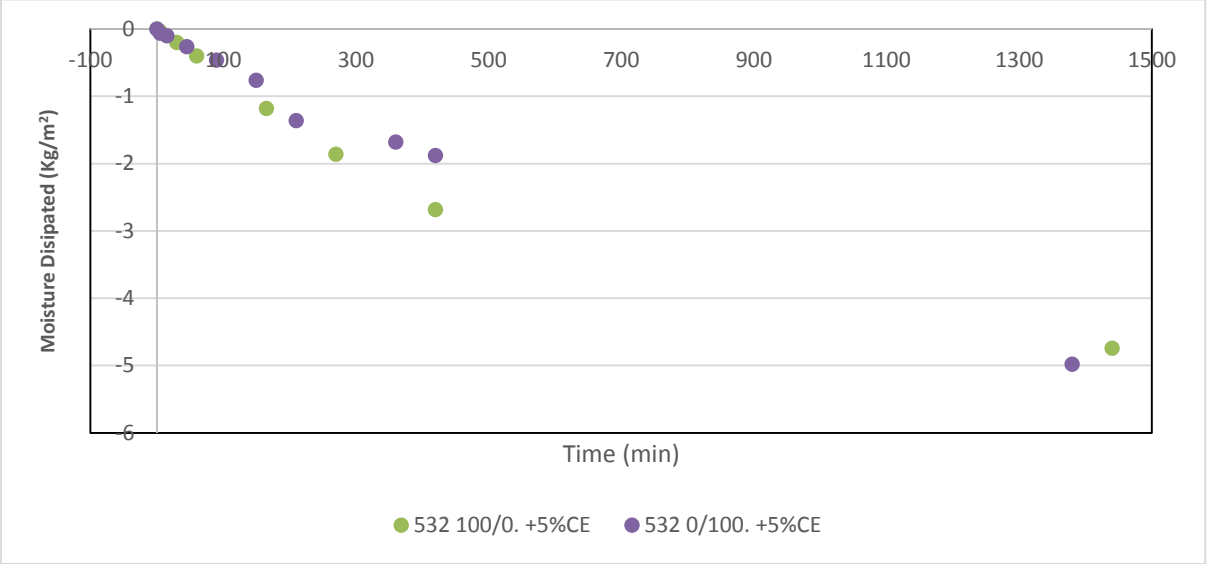

Figure 6.34 Moisture dissipation results for stabilised 532 samples containing PKS

It can be observed that sample containing only coarse aggregate showed a higher initial loss in moisture and only slowed with time to end up with a lower total mass of lost moisture. This trend is also observed for stabilised 532 samples (Figure 6.34). However the total mass of moisture lost is lower for stabilised 532 samples than for stabilised 622 samples.

6.6 Further Discussions

It is evident that soil grading affects all the properties of rammed earth. As any soil used for rammed earth manufacture can be modified by supplementing grade soil at a cost, emphasis should be placed on what property of rammed earth is most desirable.

Figure 6.35 shows the sorptivity of both 622 and 532 mixes as PKS replaces coarse aggregate. The 622 mix shows a surge in sorptivity of 130% as PKS is introduced up to 10%. Further replacement up to 50% reduces sorptivity by

8.6%. At 90% replacement, sorptivity increases by 8.9% eliminating any gain observed at 50%. However, complete replacement with PKS reduces sorptivity by 48% compared to sorptivity at 90% replacement. However, this represents an overall increase in sorptivity of 17% as compared to 0% PKS content.

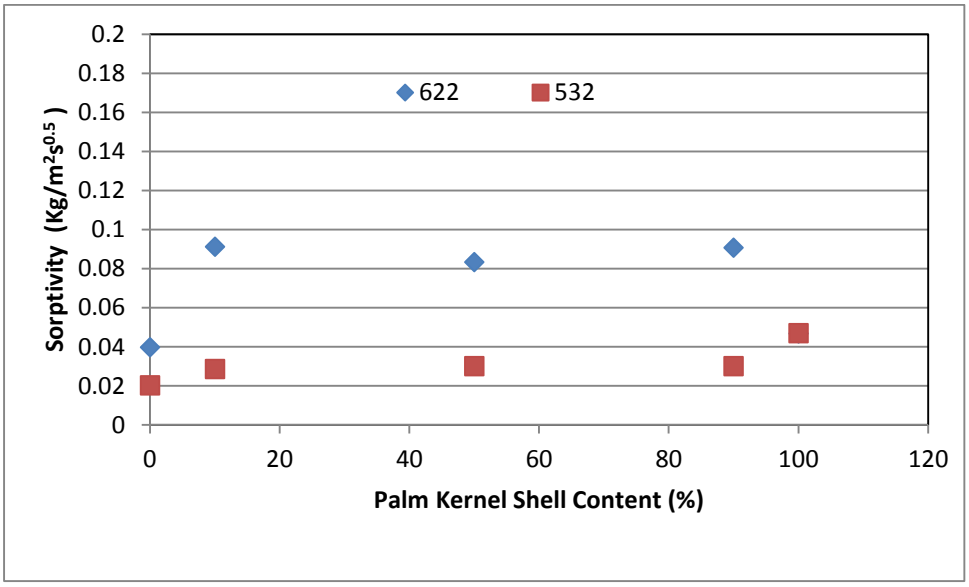

Figure 6.35 Sorptivity comparatives for 622 and 532 soil grade rammed earth.

The 532 mix shows a much slower increase in sorptivity as PKS replaces coarse aggregates. When PKS represents 10% coarse aggregate, there is a 41% increase in sorptivity. At 50%, sorptivity increases by 5%. A further increase of 0.3% is observed when PKS content is increased to 90%. However at 100% PKS content, sorptivity rises by 57%. This represents an increase of 133% when compared to a 0% PKS content. This is explained in more detail in later chapters.

Compressive strength followed a close pattern as seen in figure 6.36. Of note however is that compressive strength for 532 grade first rises before it starts to fall again.622 grade rammed earth witnessed a steady strength loss with increase in PKS content. It is also noteworthy that very little difference exists

between 622 and 532 soil grades when rammed earth contains 100% PKS as coarse aggregate.

Figure 6.37 shows that rammed earth made from 532 soil grade regardless of PKS content will find its values nested between strengths obtained with 622 grade samples containing crushed granite or coarse aggregate.

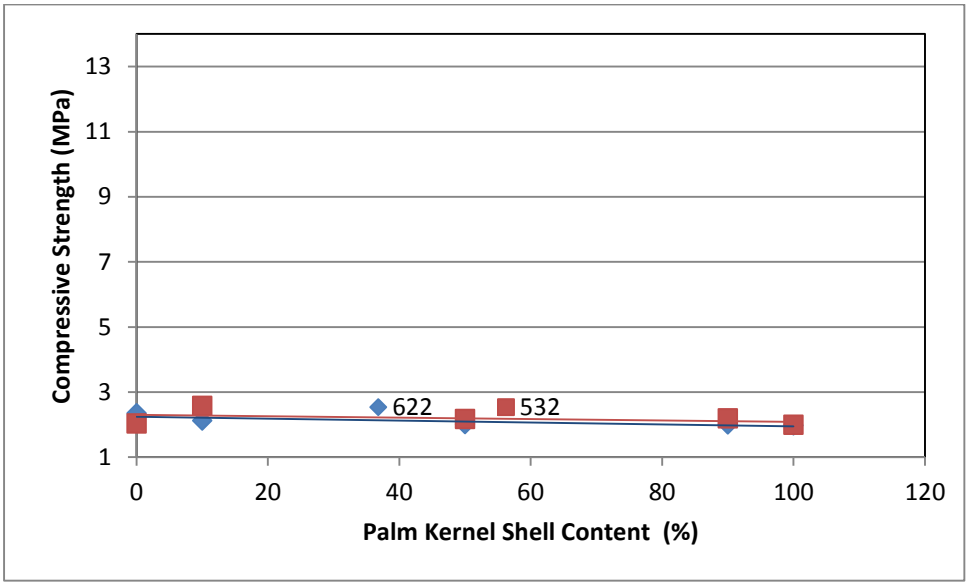

Figure 6.36 Compressive strength comparatives for 622 and 532 soil grade rammed earth at 28 days.

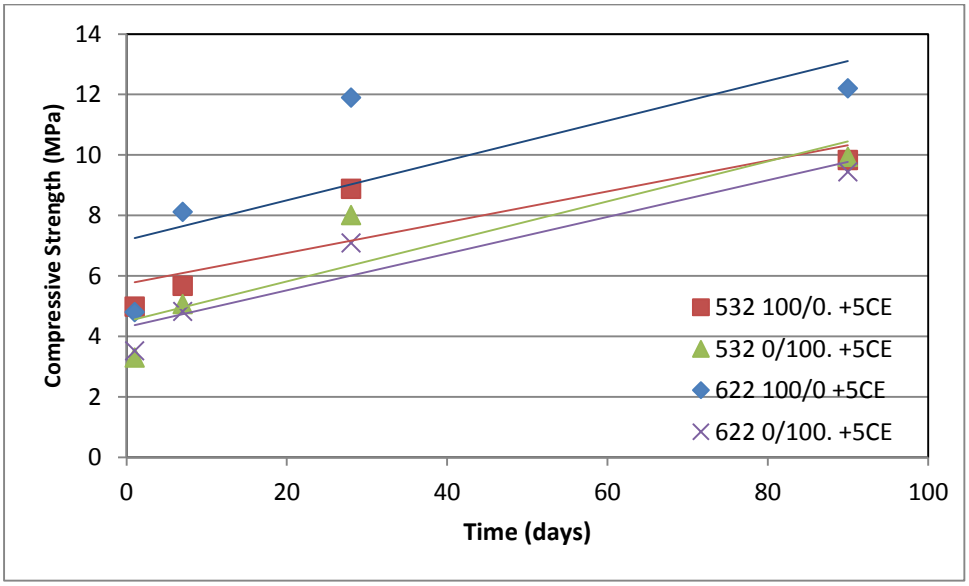

Figure 6.37 Compressive strength of cement stabilised rammed earth containing palm kernel shell

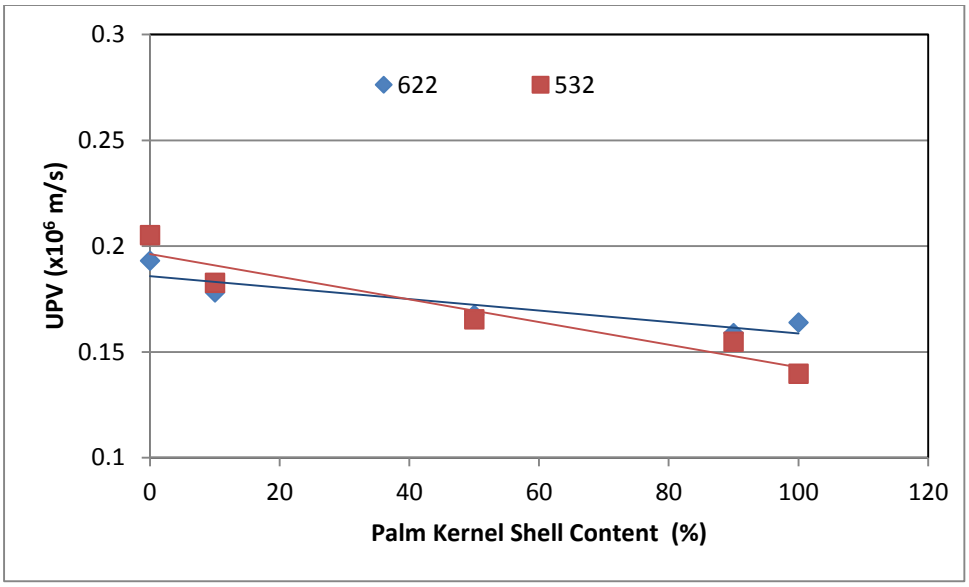

Figure 6.38 UPV comparatives for 622 and 532 soil grade rammed earth at 28 days.

As seen in figure 6.38 UPV values of both soil grades stay similar over all PKS contents although there was a divergence observed at 100% PKS use. Figure 6.39 shows that 622 grade rammed earth consistently has lower density than the 532 grade. This is probably due to the fact that the higher clay content releases moisture more slowly over 28days. However, rammed earth having 100% PKS had slightly lower density for 532 grade than rammed earth having similar PKS content with a 622 grading.

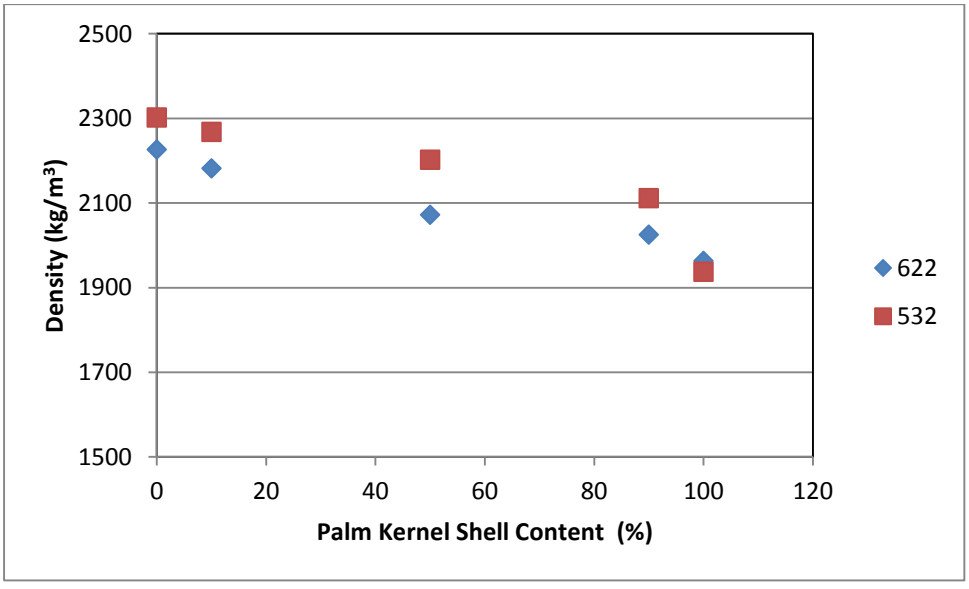

Figure 6.39 Density comparatives for 622 and 532 soil grade rammed earth at 28 days.

6.6.1 Correlation between Compressive Strength and UPV

Figures 6.40 and 6.41 show the relationship between UPV and compressive strength. We observe a positive correlation between the two properties regardless of the soil mix. The 532 mix displays a more sensitive relationship as compressive strength is observed to increase at a faster rate with each unit increase in UPV.

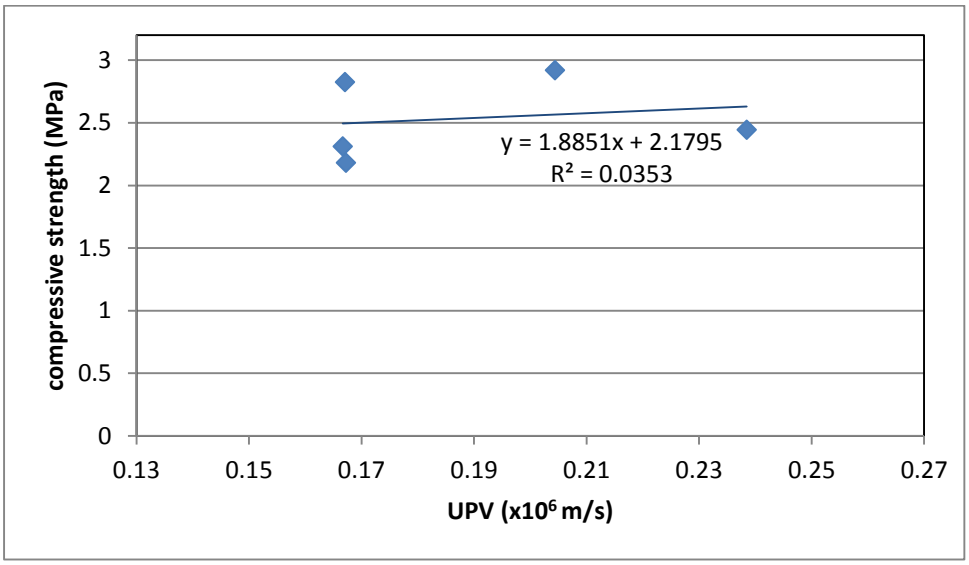

Figure 6.40 Compressive strength vs UPV for 622 soil grade

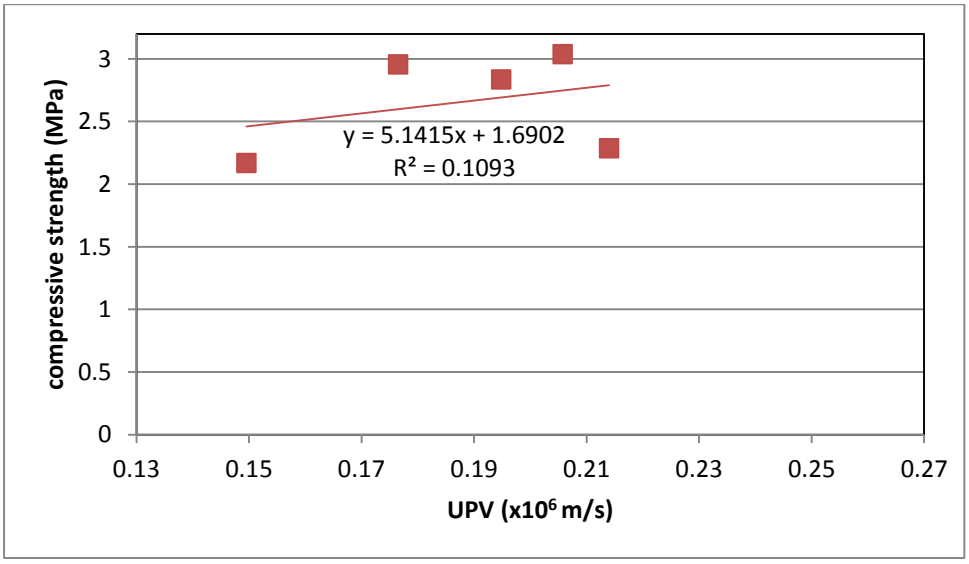

Figure 6.41 Compressive strength vs UPV for 532 soil grade

6.6.2 Correlation between Compressive Strength and Density

Compressive strength tends to increase with an increase in density. Figures 6.42 and 6.43 show that there is a positive correlation between density and compressive strength. It would appear that the 622 grade rammed earth mix gained compressive strength for each unit increase in density when compared to the 532 mix.

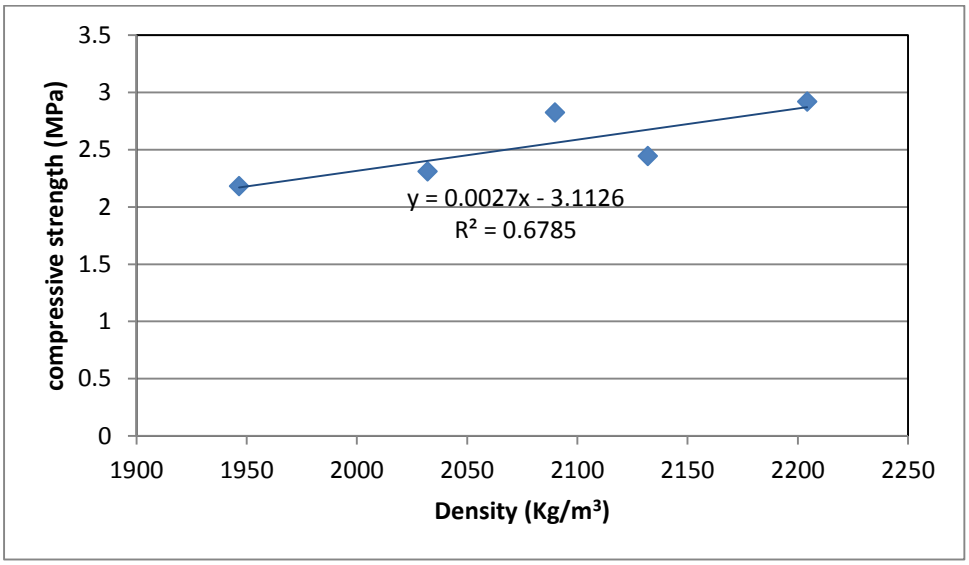

Figure 6.42 Compressive strength vs density for 622 soil grade

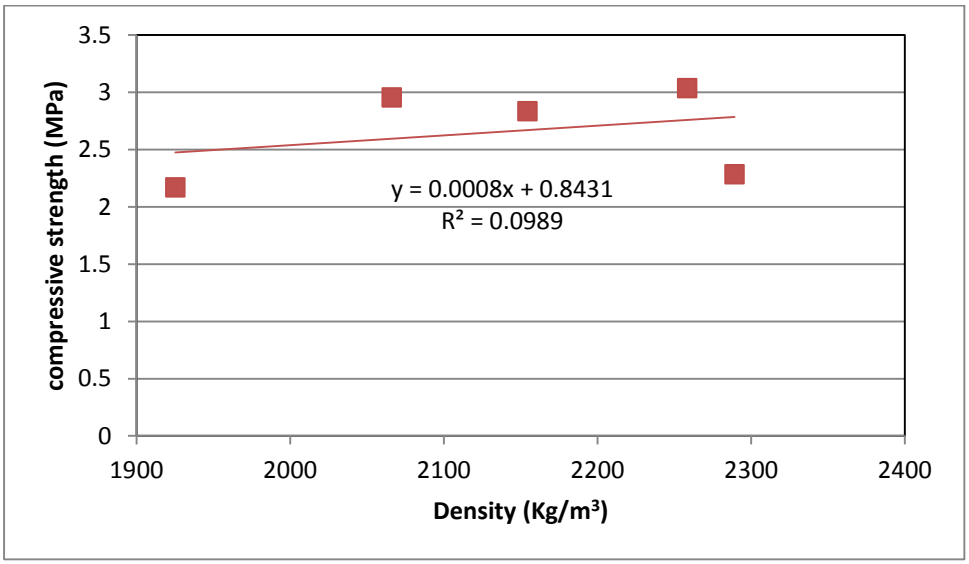

Figure 6.43 Compressive strength vs density for 532 soil grade

6.6.3 Correlation between Compressive Strength and Sorptivity

From figure 6.44 and 6.45, it would appear that there is a negative correlation between compressive strength and Sorptivity. The more a sample is prone to absorb water, the lower its compressive strength is expected to be. Rammed earth made from a 532 soil mix would be expected to lose more compressive strength as Sorptivity increases when compared to rammed earth made from 622 soil grade.

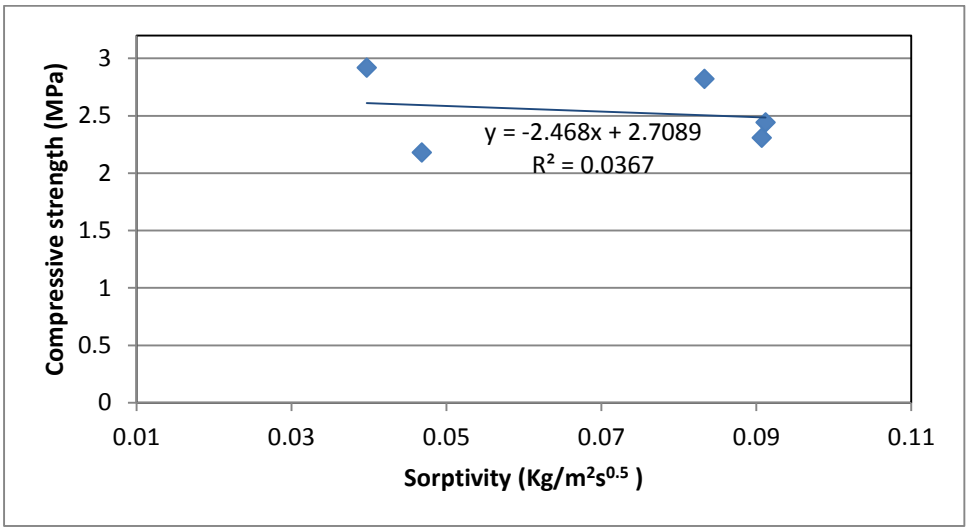

Figure 6.44 Compressive strength vs Sorptivity for 622 samples

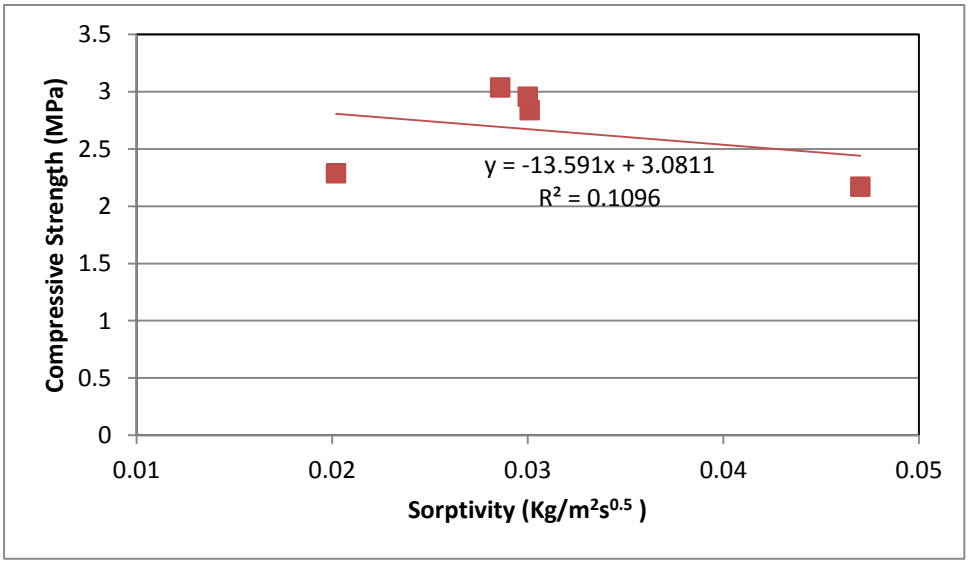

Figure 6.45 Compressive strength vs sorptivity for 532 samples

Chapter Seven

Physical and Mechanical Properties of Rammed Earth Containing Pulverised Fuel Ash

The physical and mechanical properties of rammed earth containing Pulverised Fuel Ash has been described in detail and is presented according to soil grade in this chapter. It should be noted that Pulverised Fuel Ash has been added to the mixes as a percentage of the mass of the sample it is added to.

7.1 721 Soil Grade

The 721 soil grade is made by bending soil in the proportion of 7:2:1 comprising Sand:Clay:Coarse aggregate.

7.1.1 Compressive Strength

Figure 7.1 shows how compressive strength develops over 90 days when Pulverised Fuel Ash is disposed of in rammed earth. From this figure, it would appear that rather than have an adverse effect on rammed earth strength property, Pulverised Fuel Ash actually increases the compressive strength of rammed earth. It is clear from figure that there is no net difference in the long term Compressive strength of rammed earth at low dosage of Pulverised Fuel Ash as compressive strength figures are similar at 90 days.

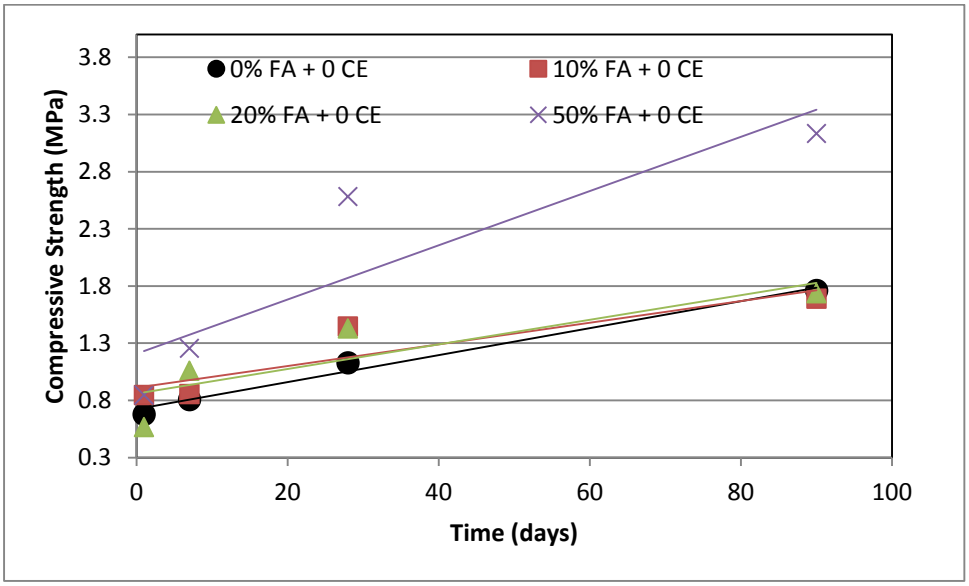

Figure 7.1 Compressive strength development for 721 grade soils over 90 days at zero cement content

Figure 7.2 shows the variation in 28 and 90 day compressive strength when Pulverised Fuel Ash is added from 0 -50%. While 50% Pulverised Fuel Ash content results in a 129% and 78% compressive strength gain at 28 and 90 days respectively, 10% and 20% Pulverised Fuel Ash content resulted in 28% and 26.5% strength gain on the 28th day and 4% and 1.5% strength loss on the 90th day.

When the same samples are stabilised with 2% cement as seen in figure 7.3, compressive strength gain can still be observed on the disposal of Pulverised Fuel Ash. The pattern for compressive strength gain is consistent when unstabilised rammed earth is stabilised with 2% cement. On the first day, there is a 81% compressive strength gain on day one. The effect of cement seems to decline at 7 days with a 61% gain in compressive strength. At 28 days, the effect of adding 2% cement is 64.6% and 30% on the 90th day. It would appear that a 2% stabilisation provides a rammed earth wall with very early strength rather than having any great long lasting advantage in strength gain.

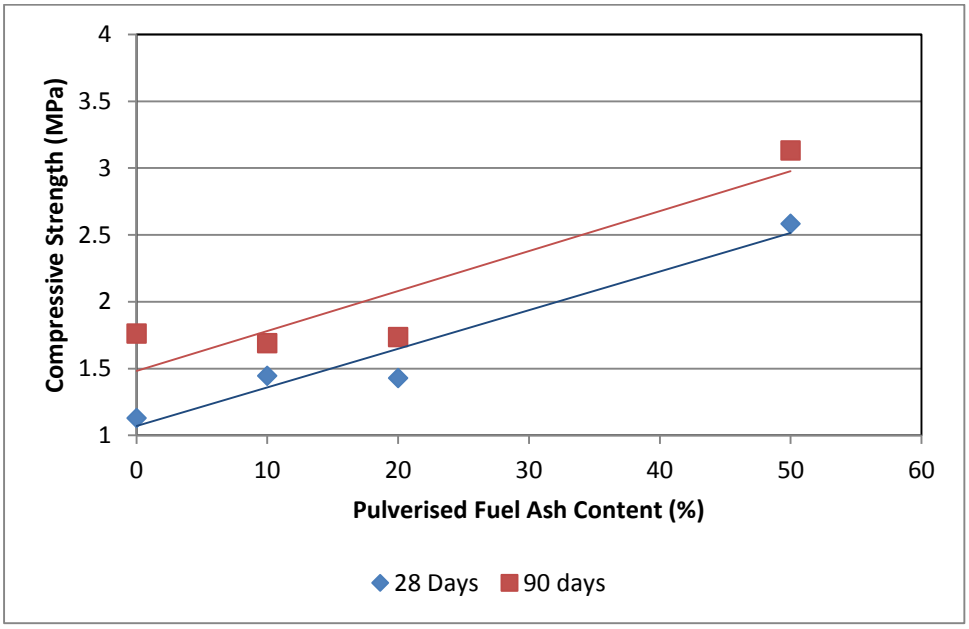

Figure 7.2 Compressive strength variation with Pulverised Fuel Ash content

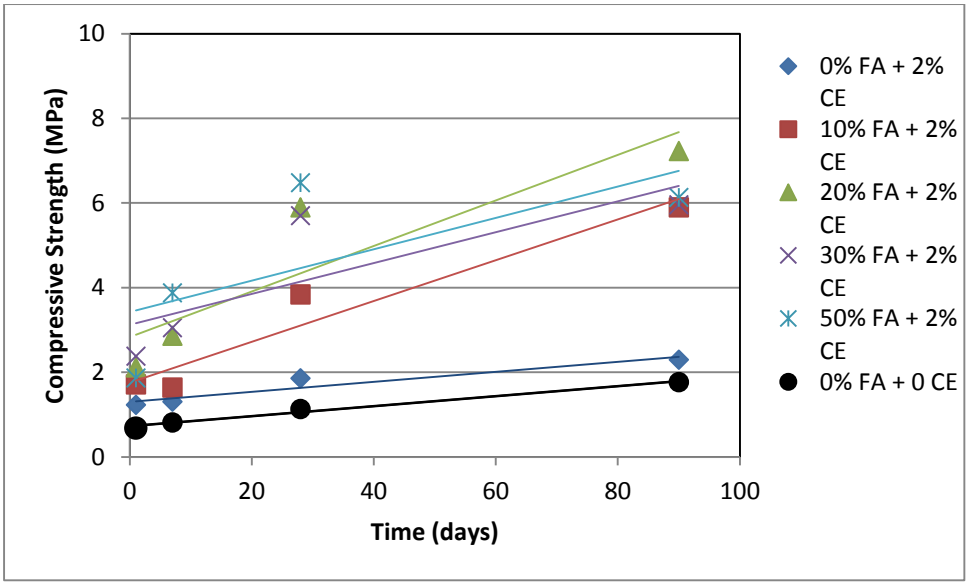

Figure 7.3 Compressive strength propagation for 721 grade soils over 90 days at 2% cement content

Adding Pulverised Fuel Ash up to 50% appears to also accelerate compressive strength gain progressively over 28 days but makes little significant difference in the long run as compressive strength appeared to converge at 6MPa. This represents a 205% gain in compressive strength. An exception was 20% Pulverised Fuel Ash content where compressive strength rose beyond 7MPa, a 214% compressive strength increase.

Figure 7.4 shows compressive strength results at 4% cement stabilisation. This trend is very similar to that seen in 2% stabilisation except compressive strengths are higher for each trend. 4% cement stabilisation produces an almost uniform rise in compressive strength as compared to unstabilised rammed earth. On the first day, there is a 209% strength gain which increases to 286% on day 7. However by day 90, strength gain stood at 128%. This is in tandem with the observations with a 2% stabilisation where stabilisation is seen to provide more significant advantage in providing early compressive strength for rammed earth.

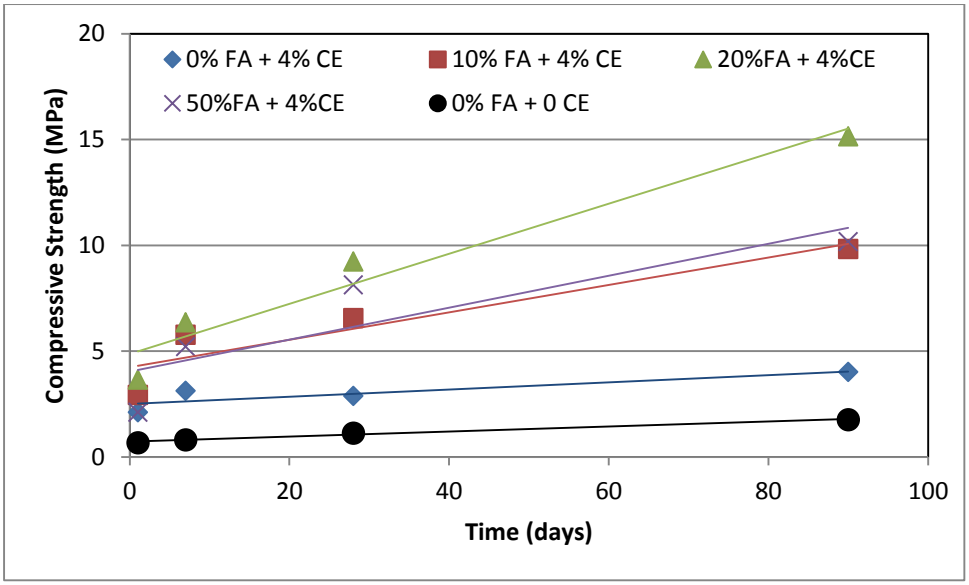

Figure 7.4 Compressive strength propagation for 721 grade soils over 90 days at 4% cement content

Again, compressive strength appears to increase significantly faster as more Pulverised Fuel Ash is introduced, but then starts to converge with age. At 90 days compressive strength appears to max out at 10MPa representing a 150% gain in compressive strength. Here 20% Pulverised Fuel Ash content again seem to perform best and does not converge by the 90th day.

9% cement stabilisation produces very high compressive strength gain. As seen in figure 7.5 compressive strength rises by 840% after 90 days. However there is further strength gain with the addition of Pulverised Fuel Ash. Again there is an increasing strength gain with increasing Pulverised Fuel Ash with compressive strength converging by the 90th day. 20% Pulverised Fuel Ash content again is the exception with compressive strength increasing at a faster rate.

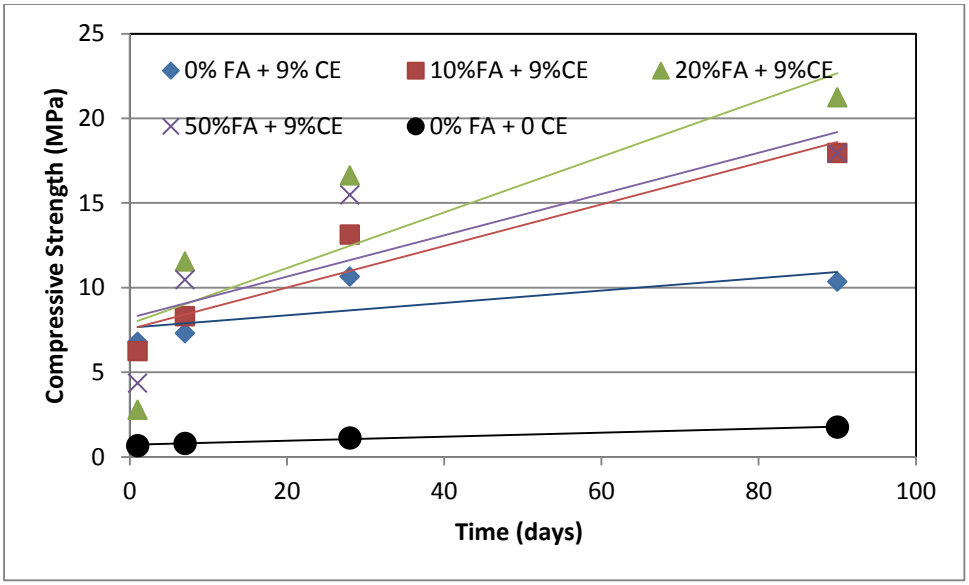

Figure 7.5 Compressive strength propagation for 721 grade soils over 90 days at 9% cement content

The chats in figure 7.6 to 7.8 show clearly the effect of Pulverised Fuel Ash has on stabilised rammed earth at 28 days. The results for 90 days are also included to compare and confirm the trend. For all degree of cement stabilisation, Pulverised Fuel Ash appears to increase compressive strength up to 20% and then further addition of Pulverised Fuel Ash appears to have a diminishing effect to compressive strength. It is noteworthy however that at 50% addition, compressive strength is consistently higher than at 0% for all degrees of stabilisation.

When cement is added to a rammed earth sample, strength gain is seen to rise significantly with cement content. While stabilisation by 2% results in compressive strength gain of 30%, a 4% stabilisation resulted in compressive strength rising by 128% when compressive strength was measured on the 90th day. In Figure 7.9, we see that when 9% stabilisation was applied, compressive strength rose by 495% as compared to unstabilised strengths on the same day.

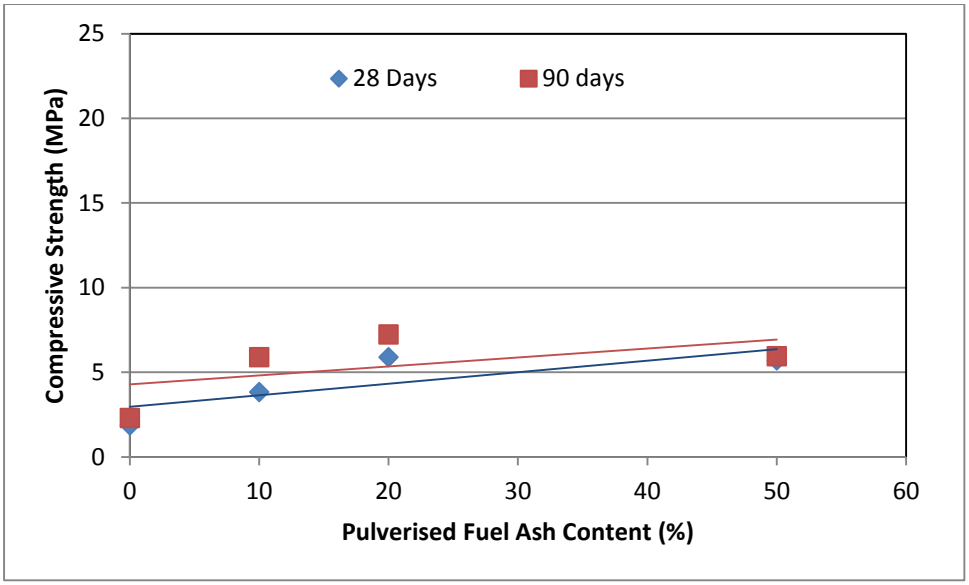

Figure 7.6 Effect of Pulverised Fuel Ash on compressive strength for 721 grade soils with 2% cement content.

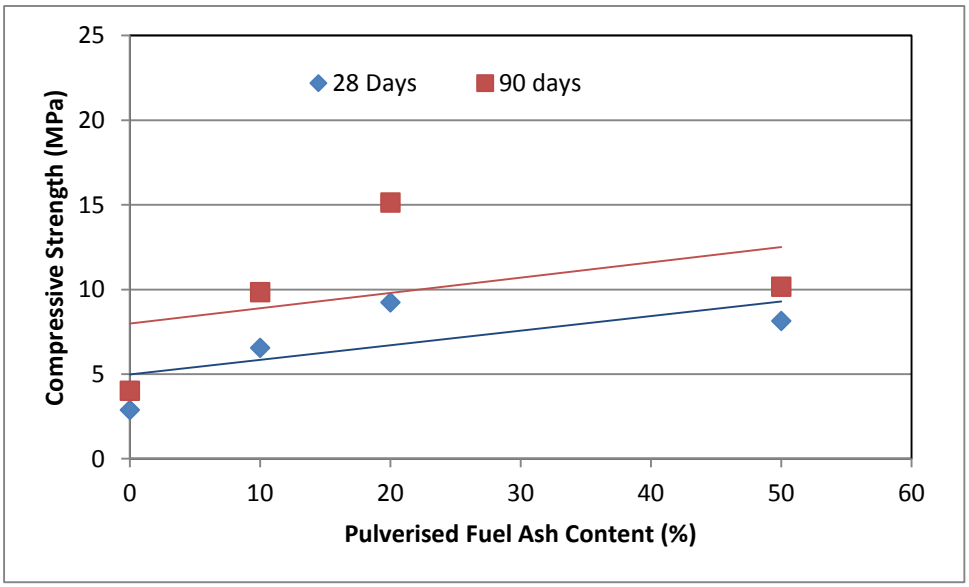

Figure 7.7 Effect of Pulverised Fuel Ash on compressive strength for 721 grade soils with 4% cement content.

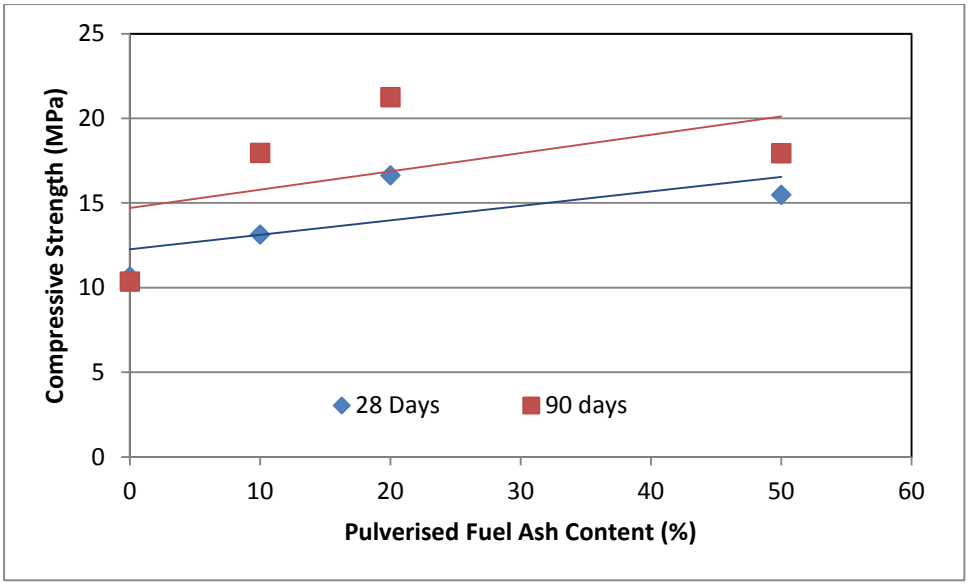

Figure 7.8 Effect of Pulverised Fuel Ash on compressive strength for 721 grade soils with 9% cement content.

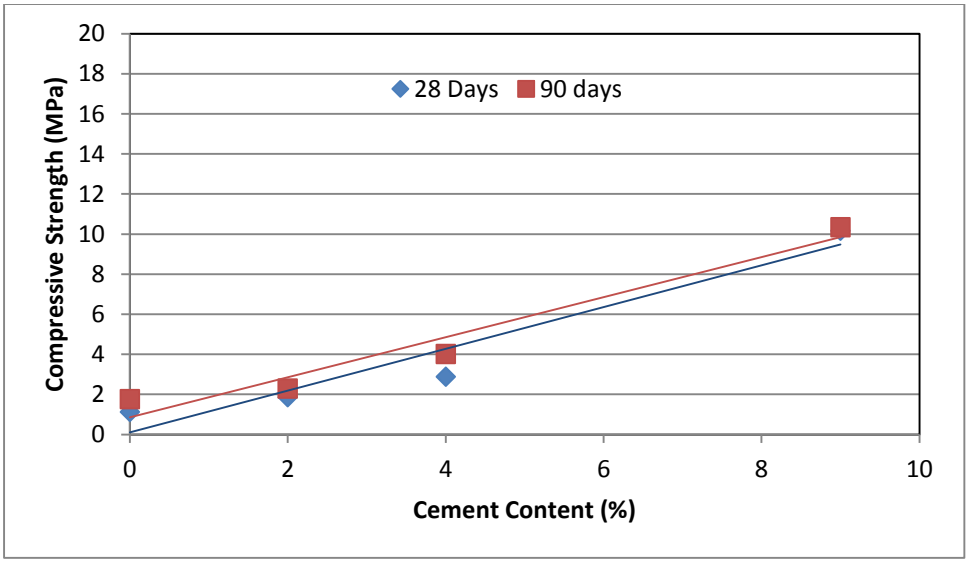

Figure 7.9. Effect of cement stabilisation on compressive strength in 721 soil grade rammed earth containing no Pulverised Fuel Ash

When Pulverised Fuel Ash is added, there appears to be a jump in values obtained for stabilisation. While testing samples containing 0% cement content revealed comparatively very little difference in compressive strength, when 10% Pulverised Fuel Ash is added, stabilising by 2% cement resulted in a higher compressive strength gain than for samples that didn't contain any Pulverised Fuel Ash at every day of testing. Figure 7.10 shows that after 90

days, and at 9% cement stabilisation, compressive strength was 73% higher for samples that contained Pulverised Fuel Ash.

Figure 7.11 shows that further addition of Pulverised Fuel Ash did not improve compressive strength when measured at 90 days. Further Pulverised Fuel Ash content however helped speed up the process of strength gain. The effect of increasing stabilisation on compressive strength was found to increase faster over 90 days when 50% Pulverised Fuel Ash was added to the mix.

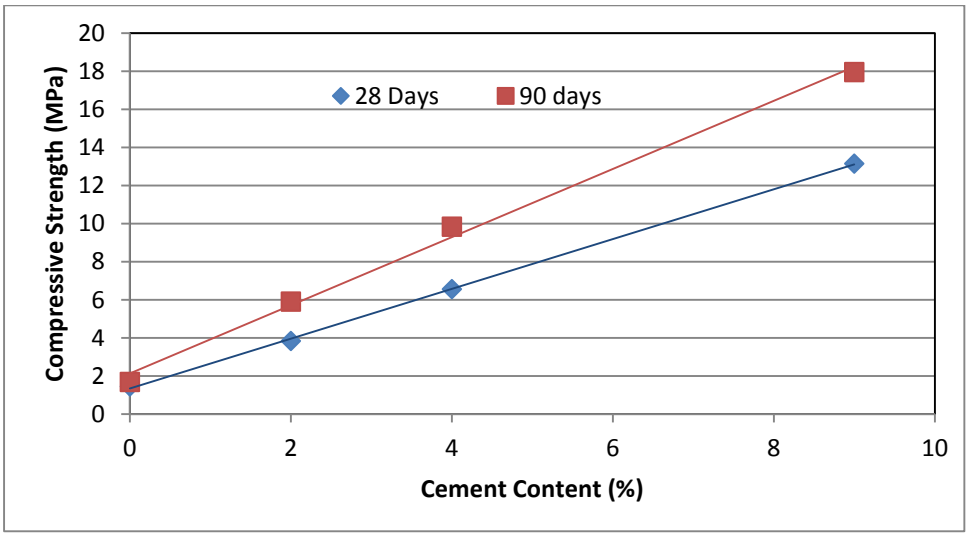

Figure 7.10. Effect of cement stabilisation on compressive strength in 721 soil grade rammed earth containing 10% Pulverised Fuel Ash

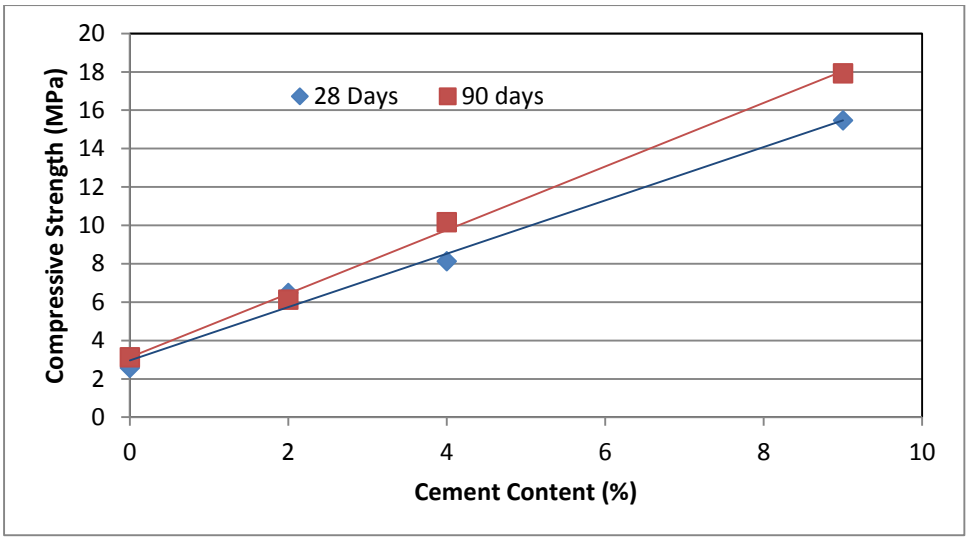

Figure 7.11. Effect of cement stabilisation on compressive strength in 721 soil grade rammed earth containing 50% Pulverised Fuel Ash

7.1.2 Ultrasonic Pulse Velocity

UPV readings revealed that Pulverised Fuel Ash has significant effect on the internal structure of Rammed earth. UPV appeared to rise with time for unstabilised rammed earth regardless of Pulverised Fuel Ash content.

As seen from figure 7.12, UPV for unstabilised rammed earth containing no Pulverised Fuel Ash rises by 7.5% after 7 days then by 2% by day 28. This further increase by 28.6% at the final day of testing. Adding 10% Pulverised Fuel Ash produced a similar trend. But increasing this to 20% reversed the trend with the first 7 days seeing a fall in UPV of 9% before a rise of 25% on the 28th day and a further 75 on the 90th day. This resulted in rammed earth having a 20% Pulverised Fuel Ash content having a UPV value 5.6% less than unstabilised rammed earth after 90 days. Rammed earth having Pulverised Fuel Ash content of 50% showed the highest improvement in UPV over 90 days. UPV value rose 20% after the first 7 days then a further 20% at 28 days. By the 90th day, UPV had risen by a total of 43% from first day values.

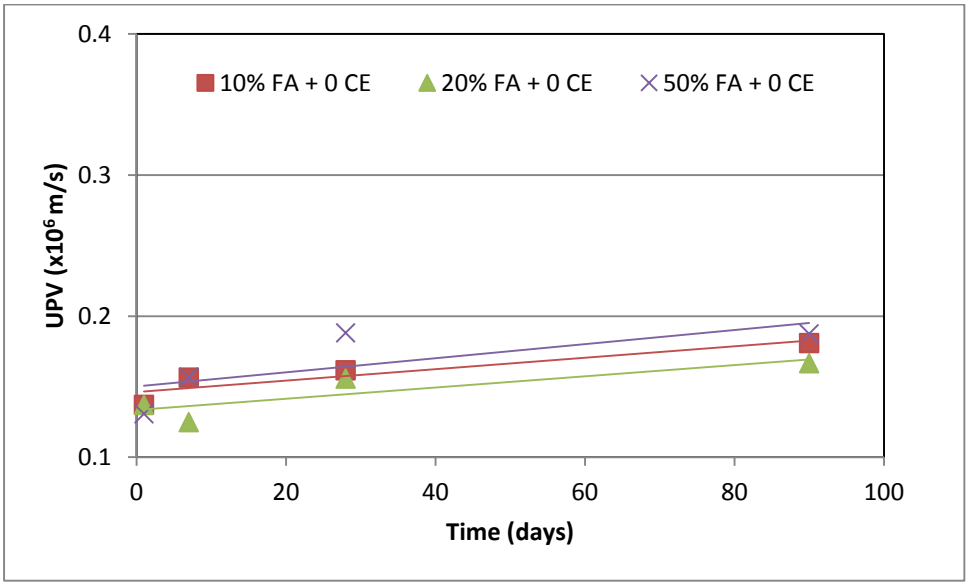

Figure 7.12 UPV for 721 grade soils over 90 days at zero cement content

When 2% cement is introduced, this pattern changes completely. Where UPV for an unstabilised sample rose consistently over time, adding 2% cement resulted in a higher initial UPV value which declined over time. 10% Pulverised Fuel Ash added to the mix resulted in smoothing out the difference as UPV values stayed fairly constant over time. Adding further quantities of Pulverised Fuel Ash however, while improving the increasing the overall UPV value had the effect of lowering it as the sample aged. This is shown in figure 7.13.

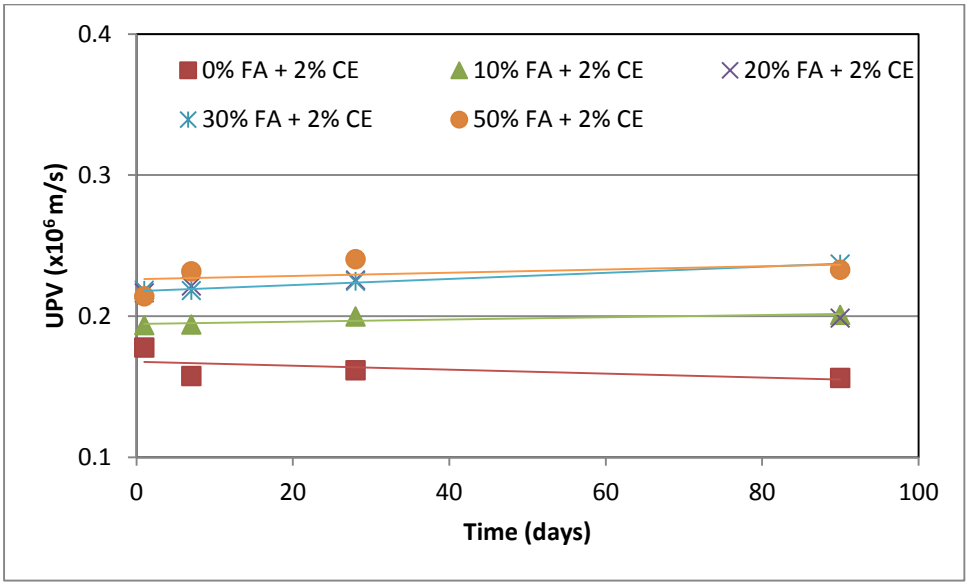

Figure 7.13 Ultrasonic pulse velocities for 721 grade soils over 90 days at 2%cement content

At 4% cement stabilisation, UPV values fall by a total of 16% from initial values but 90 days value were still 7% higher than unstabilised values. Increasing the quantity of Pulverised Fuel Ash resulted in further increase in UPV values. However, UPV values did not vary significantly with age for greater Pulverised Fuel Ash content. From Figure 7.14 it can be observed that UPV values for 10% Pulverised Fuel Ash content fell slightly (3.7%) after 28 days.

At 9% stabilisation, UPV value drops 3.6% then starts to rise. By the 90th day, UPV values had risen by 30%. Addition of Pulverised Fuel Ash resulted in a steep slope in the value of UPV for the first 7 days after which there was no significant change in value.

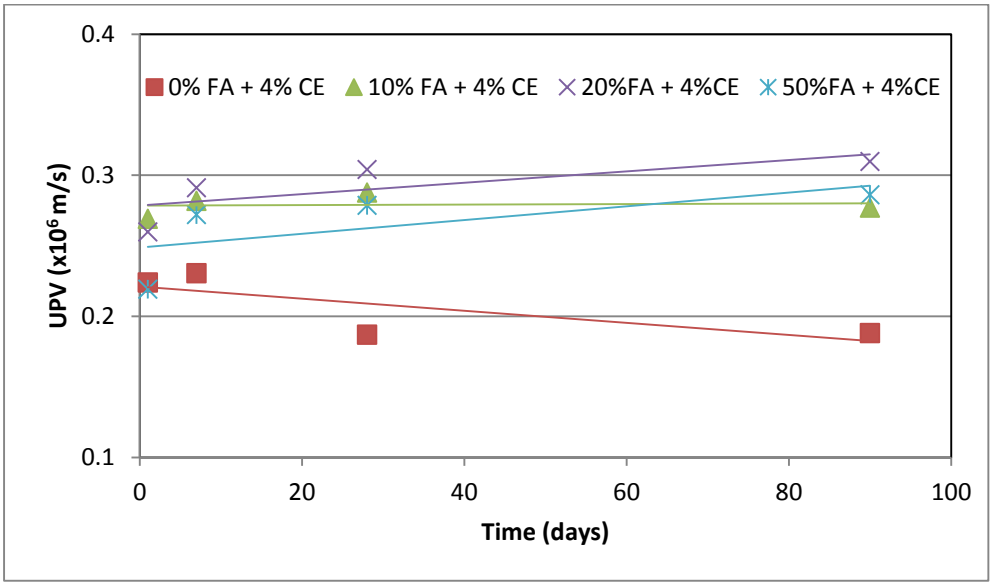

Figure 7.14 UPV for 721 grade soils over 90 days at 4% cement content

Cement added to stabilise 721 grade rammed earth resulted in an increase in UPV values. Figures 7.15 to 7.17 show however, that there is no appreciable change in ultrasonic pulse velocity values when Pulverised Fuel Ash is added to cement is stabilised rammed earth.

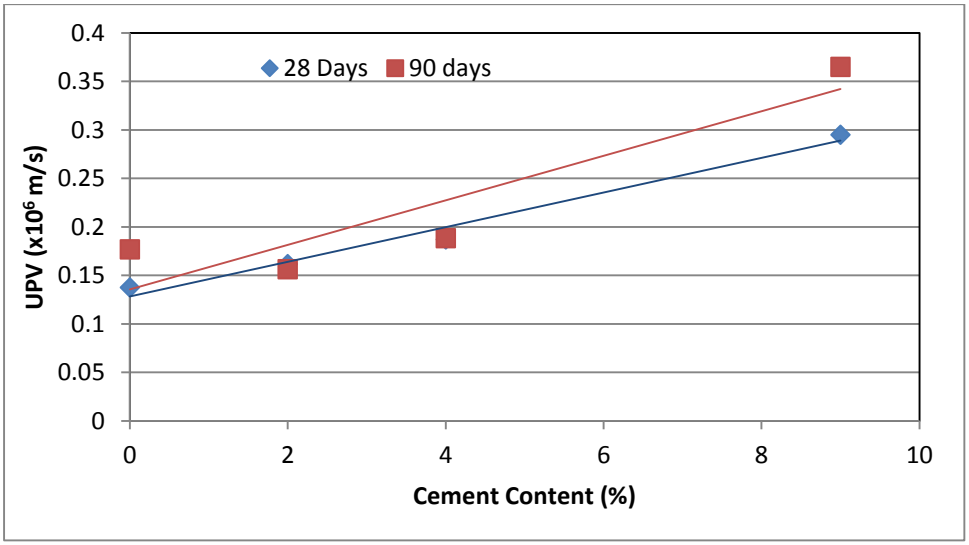

Figure 7.15 Effect of cement stabilisation on UPV in 721 soil grade rammed earth containing no Pulverised Fuel Ash

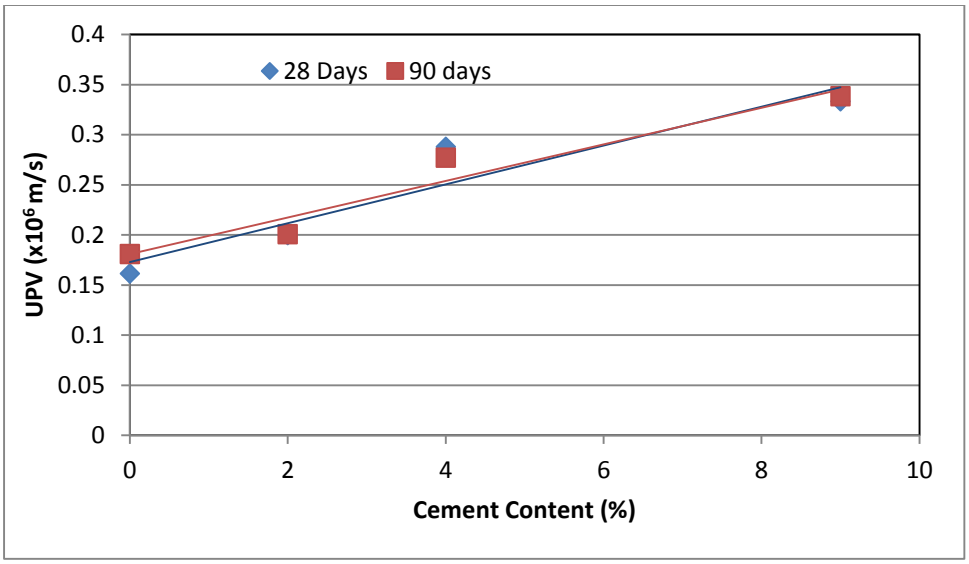

Figure 7.16 Effect of cement stabilisation on UPV in 721 soil grade rammed earth containing 10% Pulverised Fuel Ash

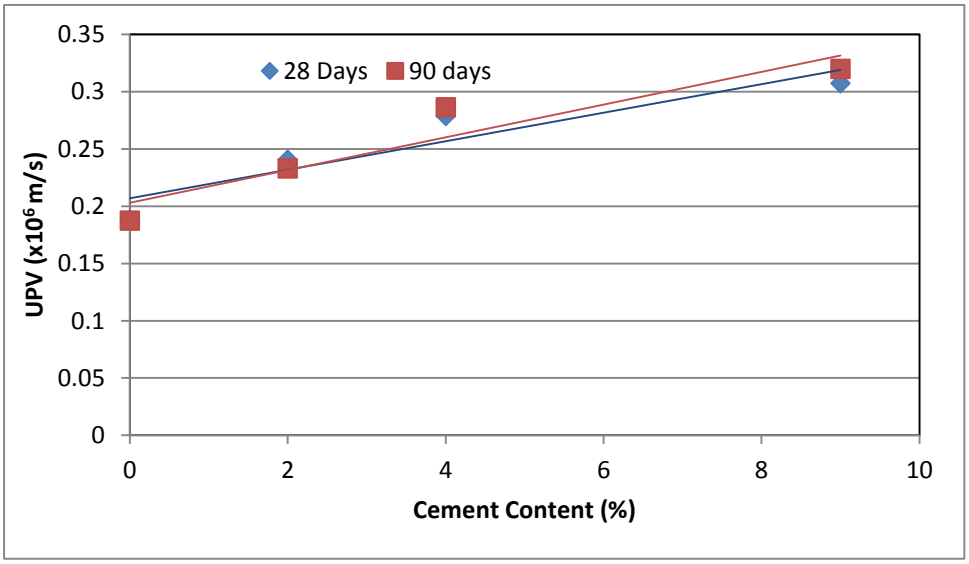

Figure 7.17. Effect of cement stabilisation on UPV in 721 soil grade rammed earth containing 50% Pulverised Fuel Ash

7.1.3 Density.

Density appeared to decrease as Pulverised Fuel Ash content increased. On day one, samples containing no Pulverised Fuel Ash had the highest recorded density. As observed in Figure 7.18, this unstabilised sample had an average

density of 2217.6Kg/m^3. Density fell slightly at 10% Pulverised Fuel Ash content. There was a 0.6% fall in density. However, further addition of Pulverised Fuel Ash resulted in much higher drop in density. A 20% Pulverised Fuel Ash content resulted in a drop in density of 8% when compared to first day densities. Further addition of Pulverised Fuel Ash did not result in any further appreciable decrease in density. This trend was maintained at all days of testing.

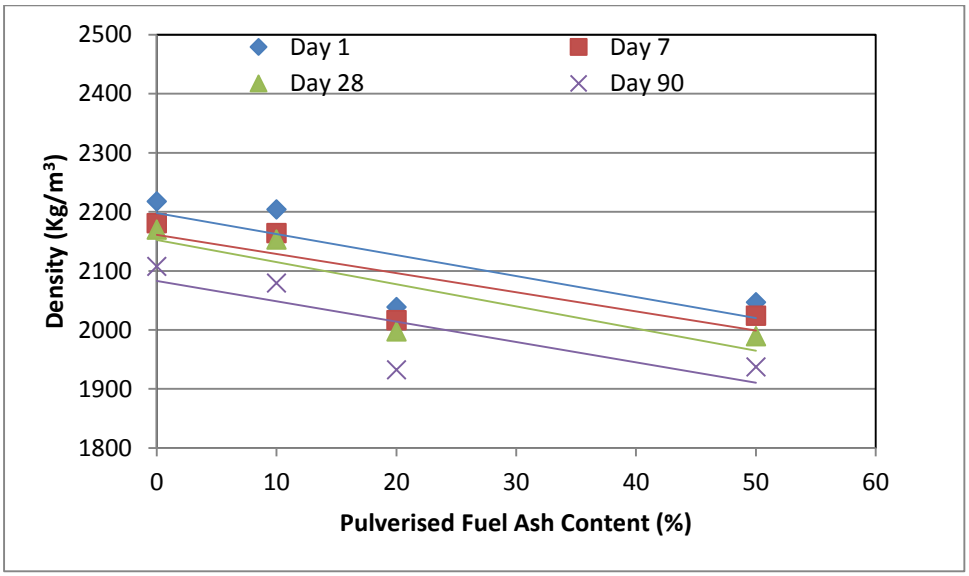

Figure 7.18 Density variation with Pulverised Fuel Ash content in 721 grade rammed earth

Density also reduced with time. At each day of testing, density was seen to have dropped slightly. Unstabilised rammed earth had a density drop of 1.7% after 7days while rammed earth containing 10% Pulverised Fuel Ash had a density loss of 1.9%. Rammed earth containing 20% and 50% Pulverised Fuel Ash both had a density loss of 1.1%. Figure 7.19 shows that density dropped at a declining rate after the 7th day.

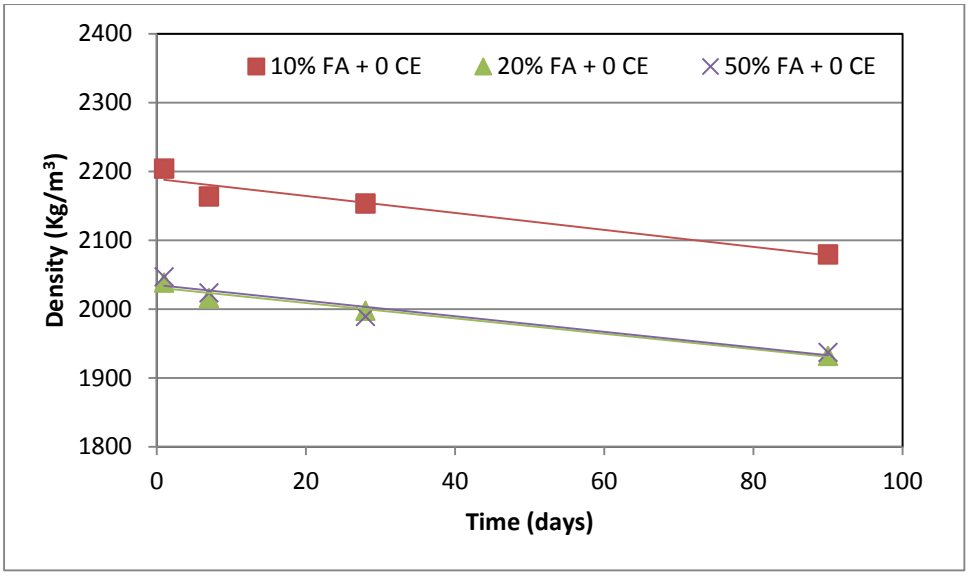

Figure 7.19 Density variation with time for 721 grade rammed earth containing Pulverised Fuel Ash

Adding cement to the mix also caused a drop in density. As can be seen in Figure 7.20, 2% cement content had a drastic effect on density. Density decreased by 6.6% on the first day when rammed earth was stabilised by 2%. Further stabilisation acted to reduce density up to a point where diminishing returns set in. 9% stabilisation had a consistently higher density on all days of testing than rammed earth that was stabilised by 2% cement. However samples stabilised by 9% cement still had lower densities at all days of testing than samples that were unstabilised.

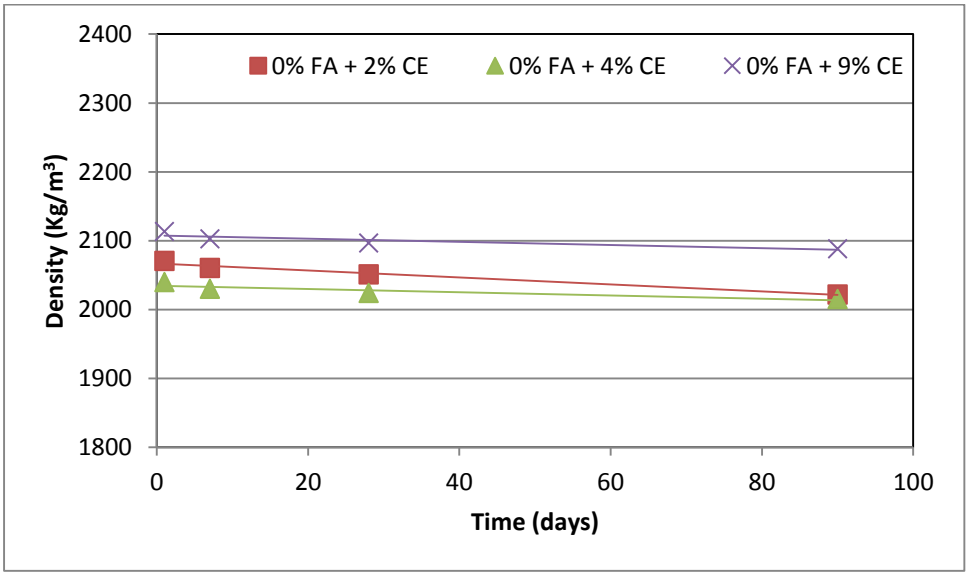

Figure 7.20 Density variation with time for cement stabilised 721 grade rammed earth

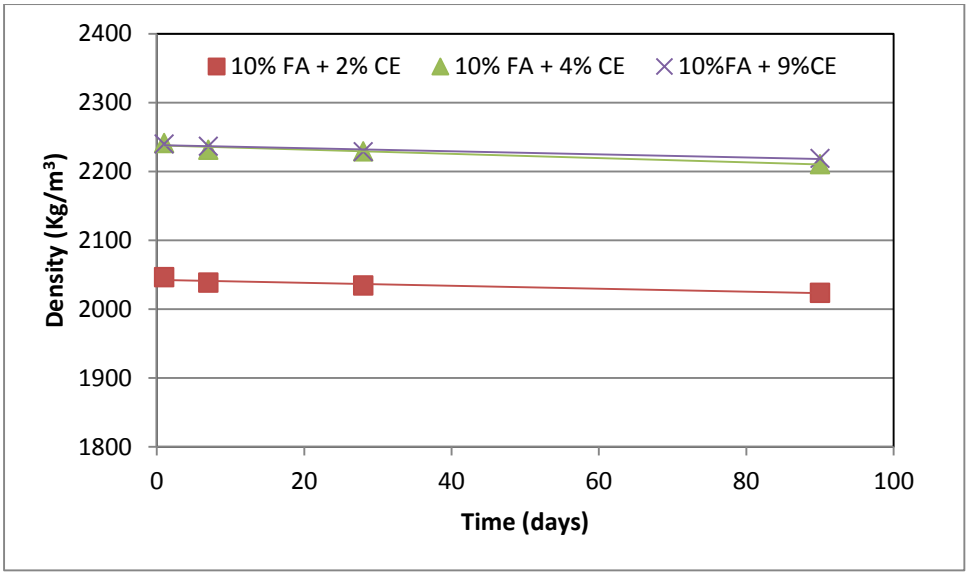

Figure 7.21 Effect of stabilisation on grade 721 rammed earth having 10% Pulverised Fuel Ash

When various proportions of cement was added to rammed earth containing 10% Pulverised Fuel Ash by mass, density was seen to rise above unstabilised values at 4% and (5 stabilisation. Density values were very close at those levels of stabilisation. However density was observed to be lower by 7% at 2% stabilisation on the first day of testing. While density reduced over time for the unstabilised samples, density was fairly constant at all the tested levels of stabilisation. This is observed in Figure 7.21.

At higher levels of Pulverised Fuel Ash content, 2% stabilisation still results in the least levels of density. However, 9% cement stabilisation results in lower density values for the first 60 days. Figure 7.22 shows that when testing was carried out on the 90th day, density values for unstabilised rammed earth containing 50% Pulverised Fuel Ash had fallen below the level of samples stabilised with 9% cement.

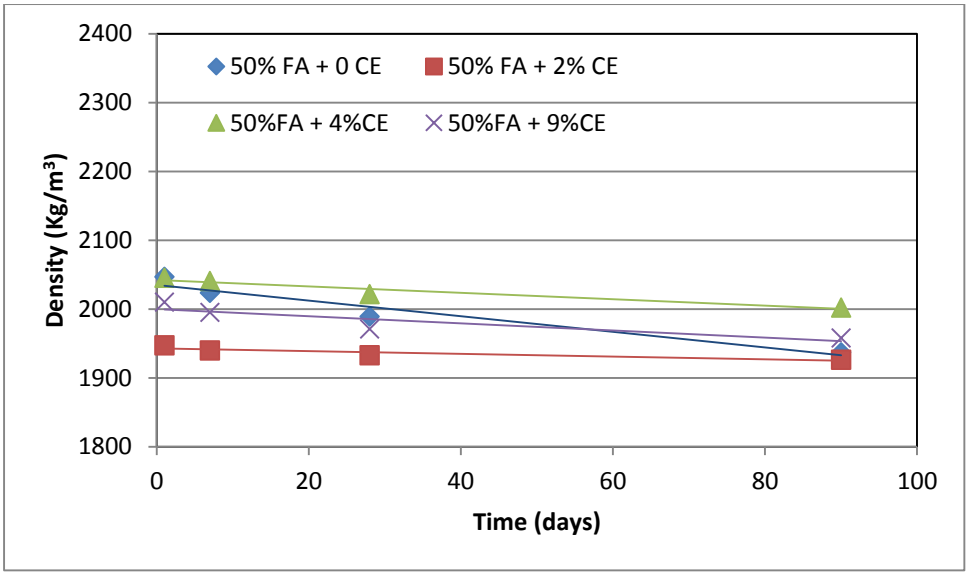

Figure 7.22 Effect of stabilisation on grade 721 rammed earth having 50% Pulverised Fuel Ash

Figure 7.23 shows the effect of cement stabilisation on density. As cement content increased, there was a marginal increase in density. Density however increased more rapidly when Pulverised Fuel Ash was added to cement stabilised rammed earth (Figure 7.24).

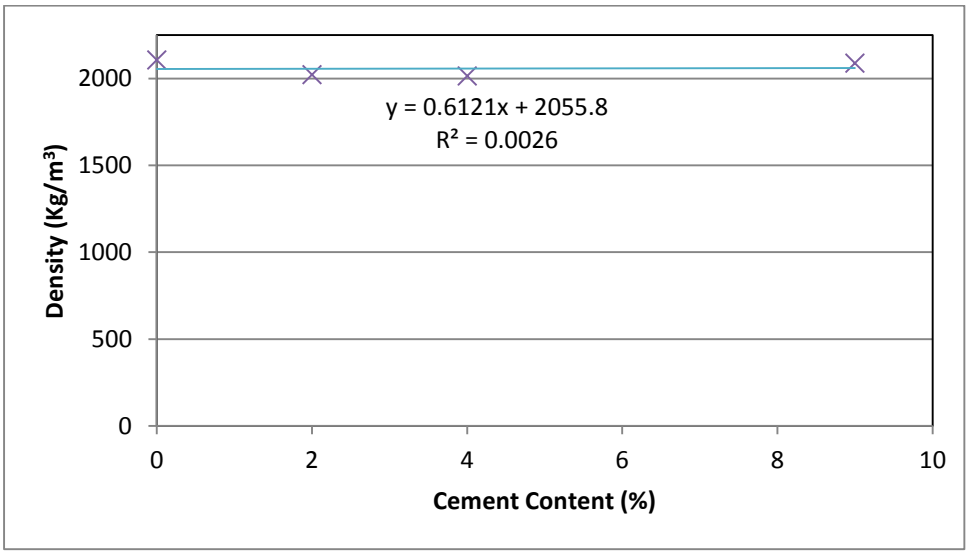

Figure 7.23 Effect of cement stabilisation on density in 721 soil grade rammed earth containing no Pulverised Fuel Ash

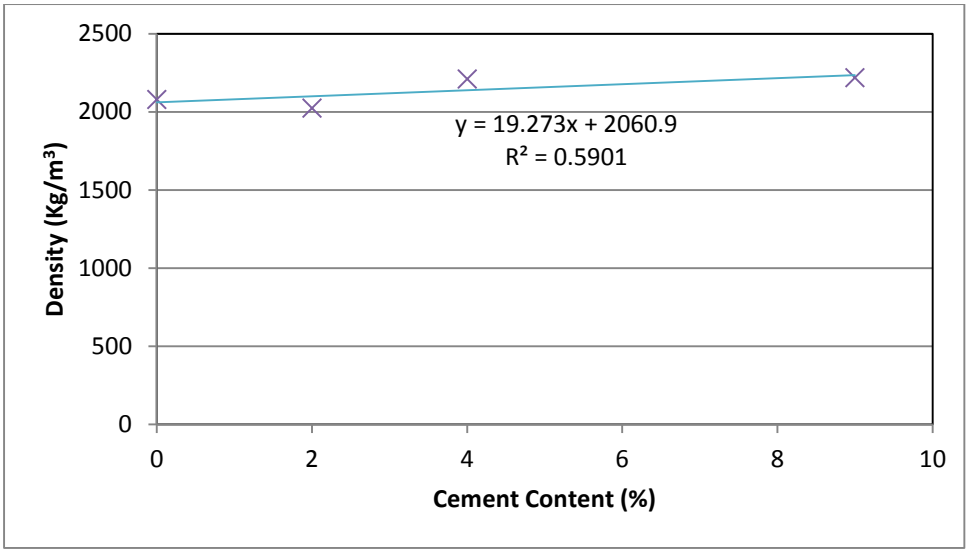

Figure 7.24 Effect of cement stabilisation on density in 721 soil grade rammed earth containing 10% Pulverised Fuel Ash

7.1.4 Initial Rate of Suction

The 721 grade Rammed earth sample as seen in Figure 7.25 showed an increase in sorptivity as Pulverised Fuel Ash content increased. However, sample containing 10% Pulverised Fuel Ash showed significantly lower initial absorption than the sample having no Pulverised Fuel Ash. However, as seen in Figure 7.26, this sample quickly absorbed more moisture after the first 2 minutes.

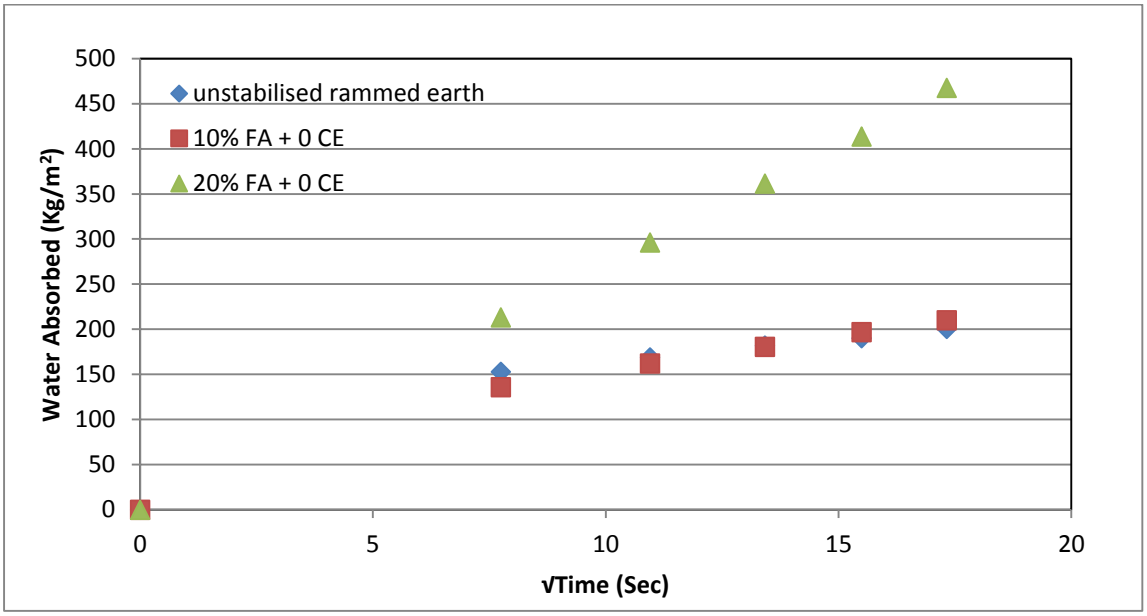

Figure 7.25 Initial rate of suction for unstabilised rammed earth made from 721 soil mix

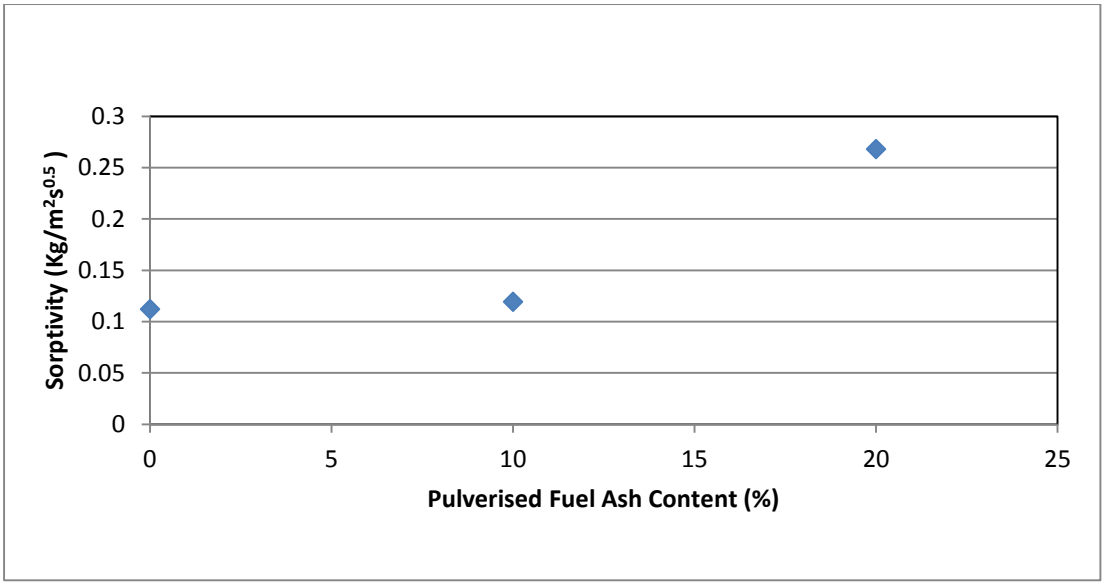

Figure 7.26 Sorptivity trend with increased Pulverised Fuel Ash content in a rammed earth 721 mix

7.1.5 Further Discussions

Compressive strength was measure against several properties. When compared against ultrasonic pulse velocity, there was a very strong positive correlation between all the samples made from the 721 soil mix regardless of cement or Pulverised Fuel Ash content (Figure 7.27 to 7.29). When the trend was looked at with respect to Pulverised Fuel Ash content, it can be observed from figure that there was an almost even distribution of points. This would indicate that the distribution is not dictated by Pulverised Fuel Ash content but rather by cement content. Here we see that increased cement content would result in increase in UPV and compressive strength.

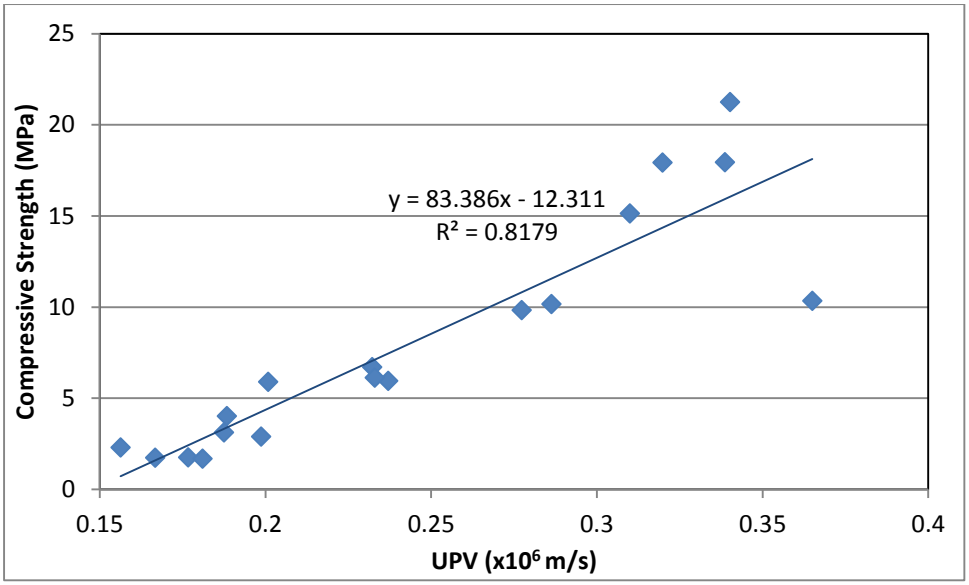

Figure 7.27 Compressive strength vs UPV in 721 soil grade

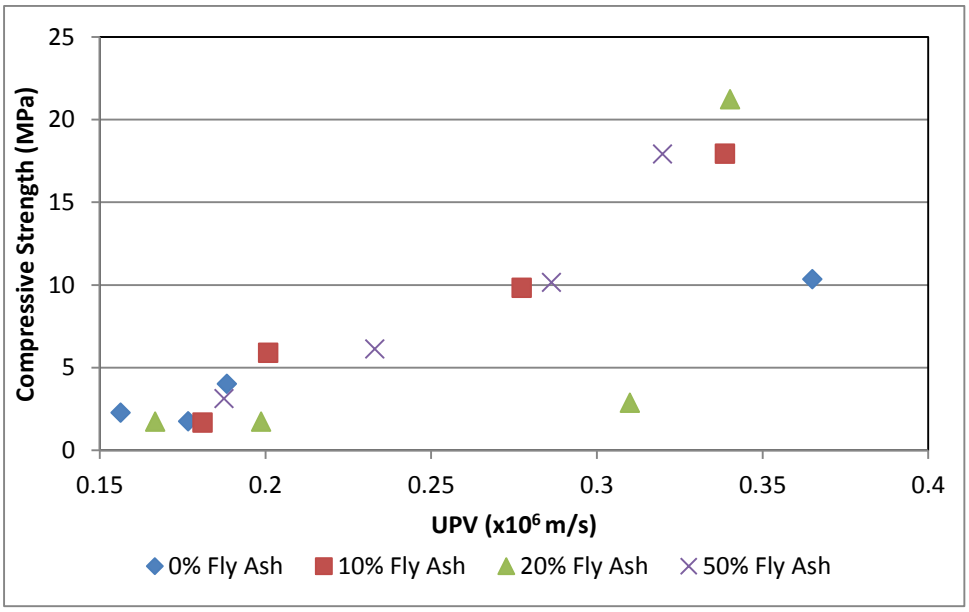

Figure 7.28 Compressive strength vs UPV in 721 soil grade (showing Pulverised Fuel Ash content distribution)

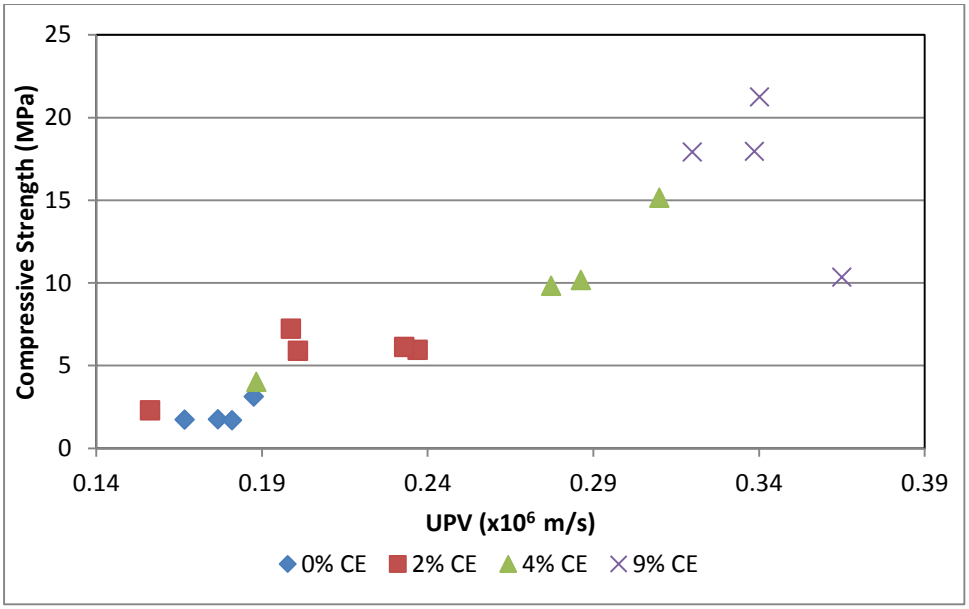

Figure 7.29 Compressive strength vs UPV in 721 soil grade (showing cement content distribution)

Comparing compressive strength and density reveals a weak negative correlation. Cement content and Pulverised Fuel Ash did not appear to have any significant effect on the distribution. Samples contain 9% cement showed highest compressive strength values but this happed regardless of the density value and can only be attributed to strength gained from hydrolysis of cement.

While there was a negative correlation between compressive strength and sorptivity, it was much stronger than what existed between compressive strength and density. Pulverised Fuel Ash content did however appear to affect the distribution as opposed to cement content. Very large Pulverised Fuel Ash additions appeared to increase sorptivity without increasing compressive strength.

Figures 7.30 to 7.35 shows how compressive strength relates to other properties of rammed earth. A positive correlation exists when compressive strength is measured against ultrasonic pulse velocity. However, an inverse relationship is observed when compressive strength is measured against density or Sorptivity.

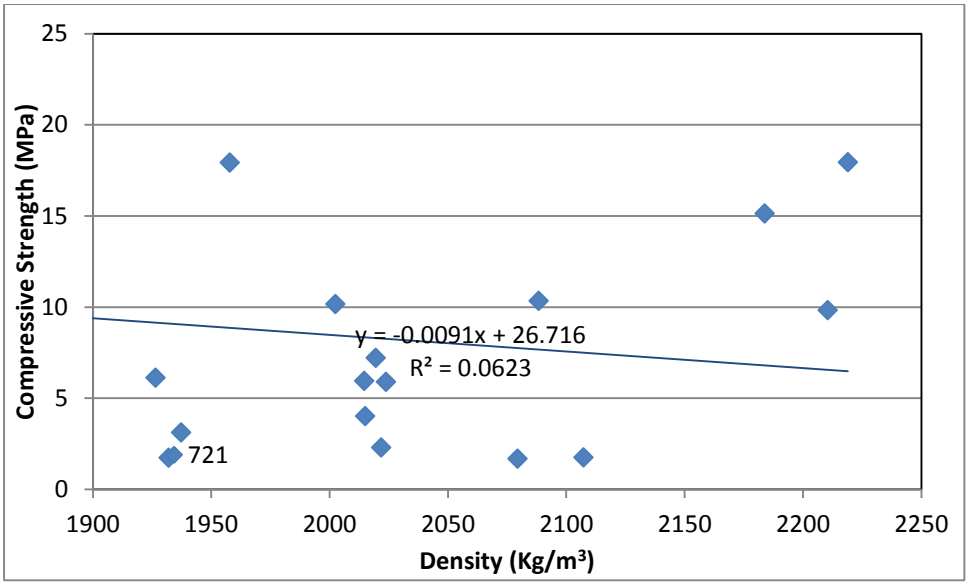

Figure 7.30 Compressive strength vs density in 721 soil grade

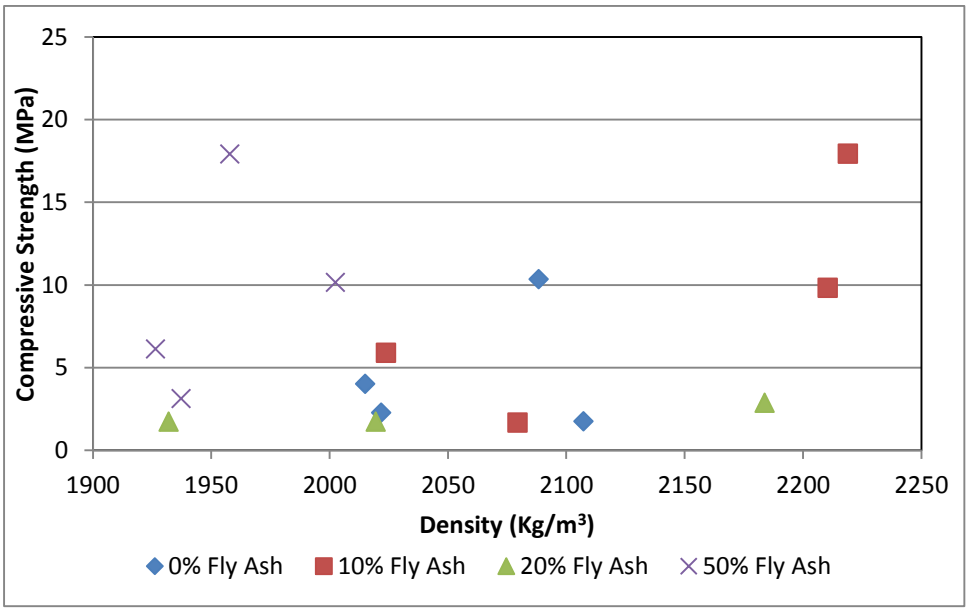

Figure 7.31 Compressive strength vs density in 721 soil grade (showing Pulverised Fuel Ash content distribution)

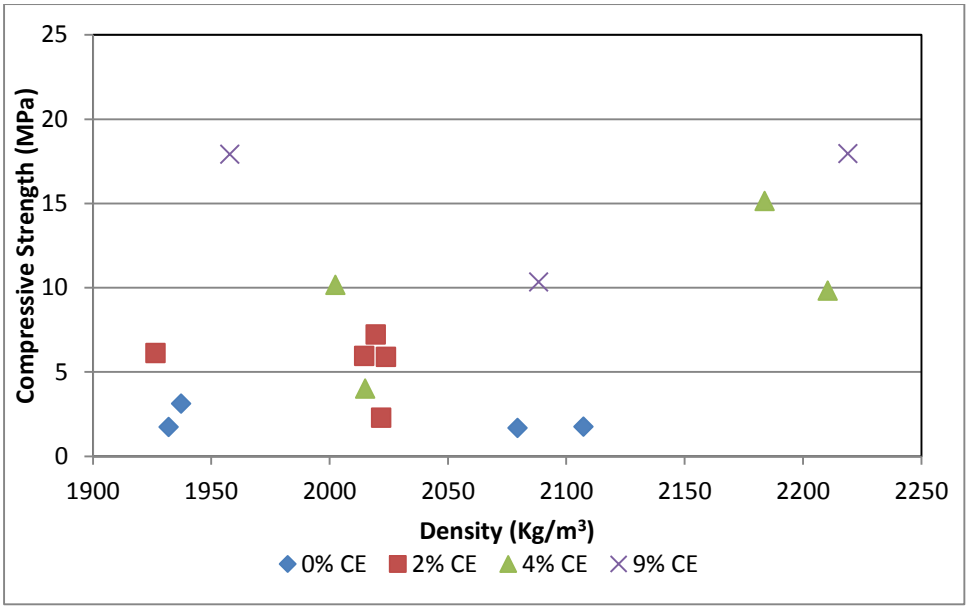

Figure 7.32 Compressive strength vs density in 721 soil grade (showing cement content distribution)

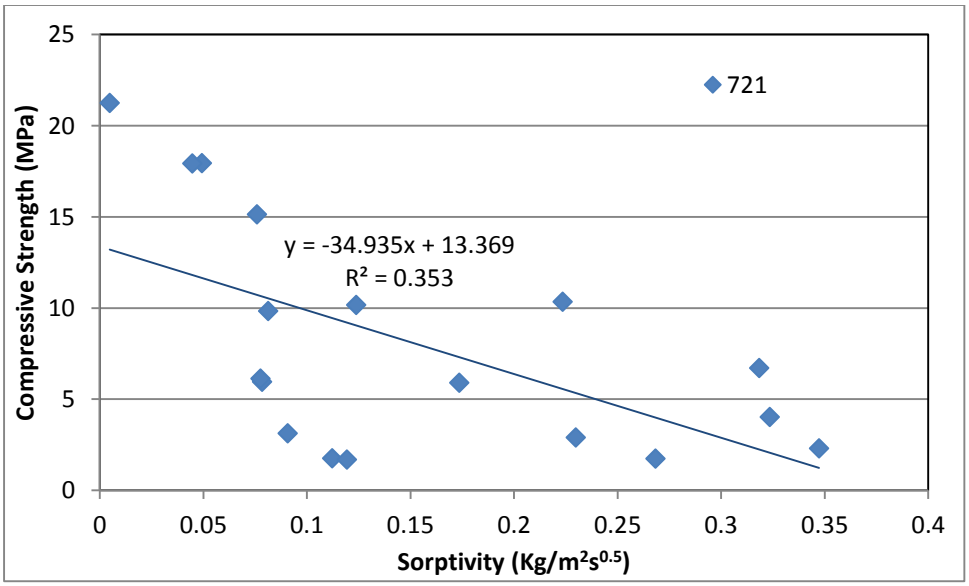

Figure 7.33 Compressive strength vs sorptivity in 721 soil grade

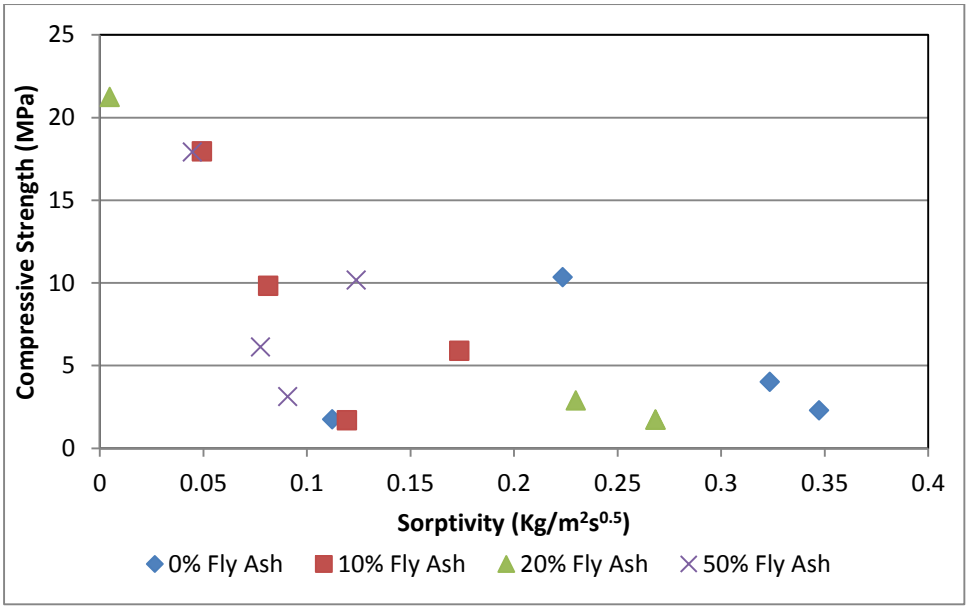

Figure 7.34 Compressive strength vs sorptivity in 721 soil grade (showing Pulverised Fuel Ash content distribution)

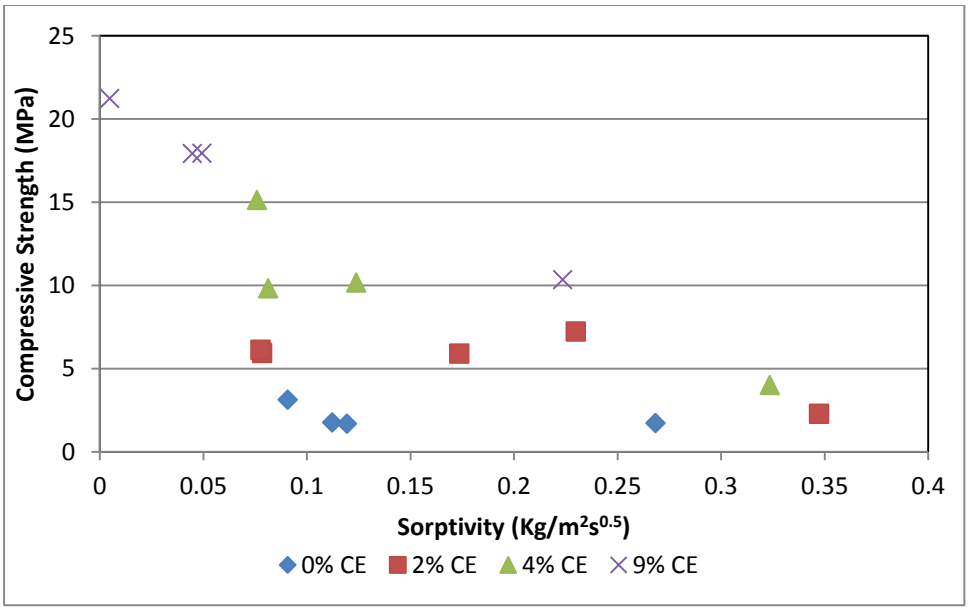

Figure 7.35 Compressive strength vs sorptivity in 721 soil grade (showing cement content distribution)

7.2 451 Soil Grade

The 451 soil grade is made by bending soil in the proportion of 4:5:1 comprising Sand:Clay:Coarse aggregate.

7.2.1 Compressive Strength

Figure 7.36 shows the effect of adding Pulverised Fuel Ash to soil that is classified as clayey. Soil type 451 consisting 4 part sand, 5 part clay and 1 part coarse aggregate showed increase in compressive strength when Pulverised Fuel Ash was added. 10% Pulverised Fuel Ash addition showed the best consistency in strength gain. While 20% Pulverised Fuel Ash produced the highest compressive strengths after 28 days, there was much strength gain after 7 days. Strength however rose by 76% when testing was carried out by the 28th day. 90 day testing revealed a further strength gain of 42%. Further addition of Pulverised Fuel Ash resulted in diminishing returns as 28 day compressive strengths of rammed earth containing 30% Pulverised Fuel Ash reported 2% less compressive strength than samples containing 10% Pulverised Fuel Ash on the same day.

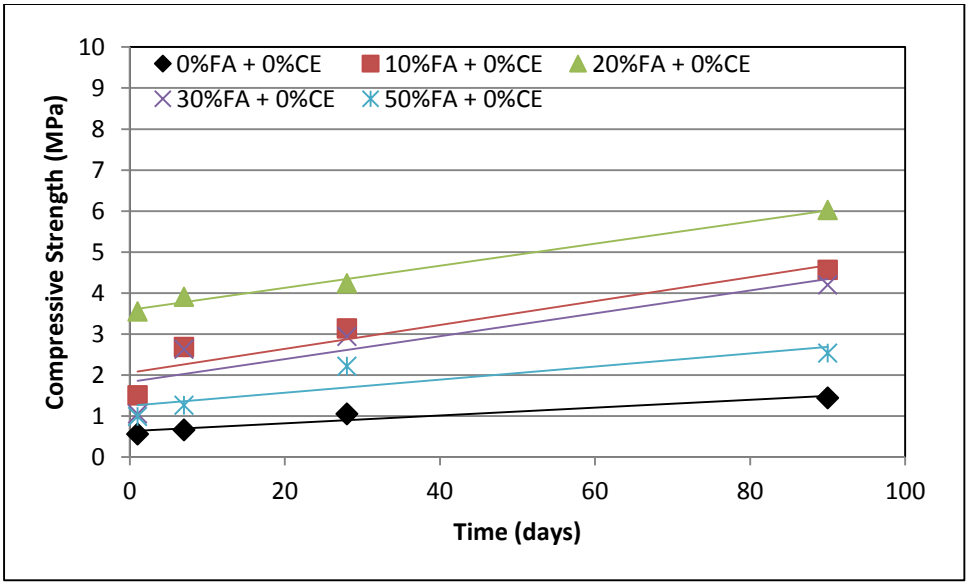

Figure 7.36 Compressive strength propagation for 451 grade soils over 90 days at zero cement content

Figure 7.37 gives a clear view of strength over the days. At 28 days, compressive strength rises by a hefty 198% when 10% Pulverised Fuel Ash was added. Compressive strength continued to rise by a further 35% when Pulverised Fuel Ash was increased by a further 10%. Increasing Pulverised

Fuel Ash by another 10% (30% total) results in a loss in compressive strength of 30.5%. Further increasing Pulverised Fuel Ash content to ta total of 50% resulted in further compressive strength loss of 25%. However this position was still 110% greater than compressive strength recorded at zero Pulverised Fuel Ash content.

When cement is added to rammed earth the effect of Pulverised Fuel Ash changes. While compressive strength appears to increase, addition of Pulverised Fuel Ash appears to have a negative impact on compressive strength as seen in figure 7.38. Adding 2% cement increases compressive strength increasingly over time. First day strengths increase by 201% while 7 day strengths show an increase of 375%. The difference in compressive strength shrinks to 272% by the 28th day, but widens again at day 90 to 461%. There appears to be no significant difference in compressive strength at day 1 when 10% Pulverised Fuel Ash is added to rammed earth. However as the sample aged, the Pulverised Fuel Ash in the sample appeared to retard the development of compressive strength in the sample. This is observed in figure 7.38 and 7.39. There was a 12.6% decrease in compressive strength by day 7, 11.4% decrease by day 28 and 17.8% decrease by day 90. While first day strength appeared to improve on further addition of Pulverised Fuel Ash (by 10%), compressive strength did not improve significantly with age.

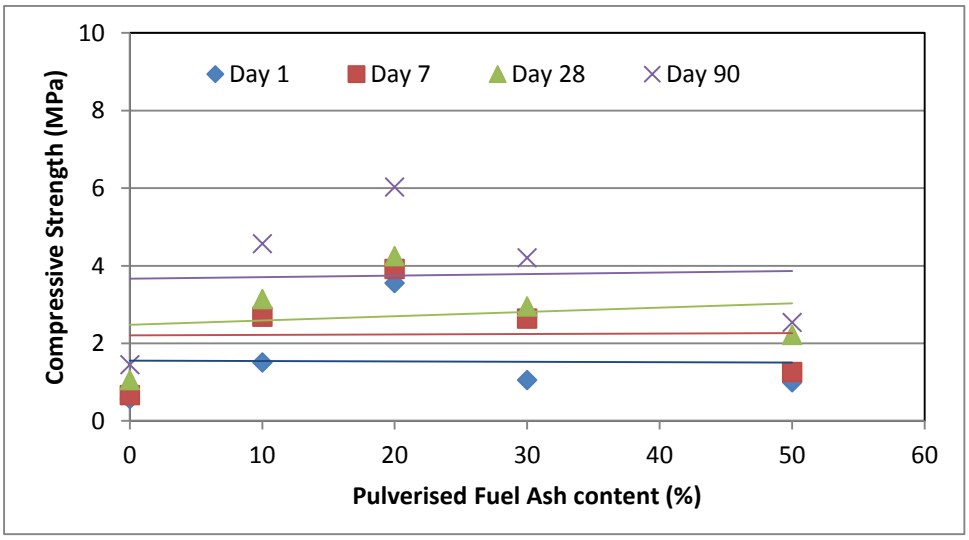

Figure 7.37 Effect of Pulverised Fuel Ash on compressive strength for 451 grade soils.

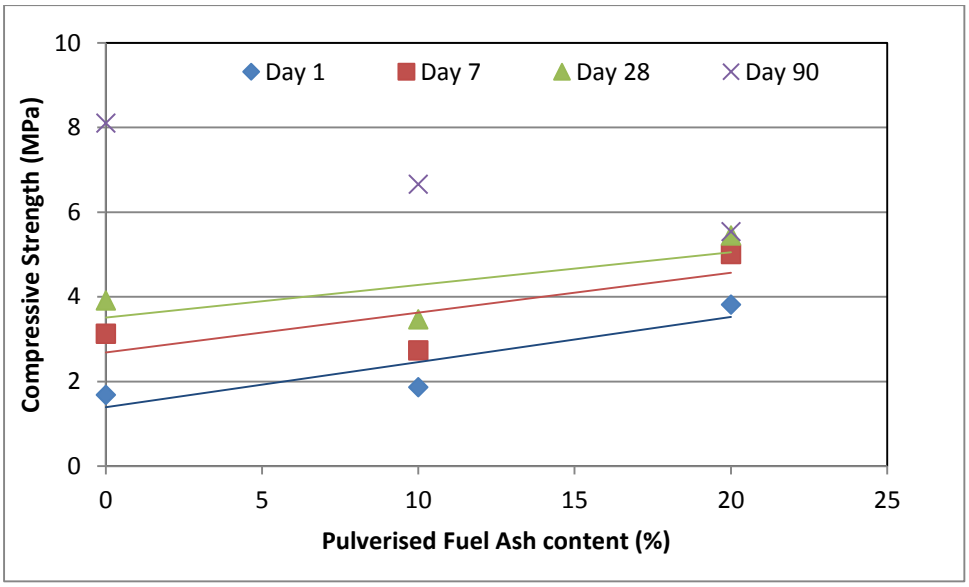

Figure 7.38 Effect of Pulverised Fuel Ash on compressive strength for 451 grade soils with 2% cement content.

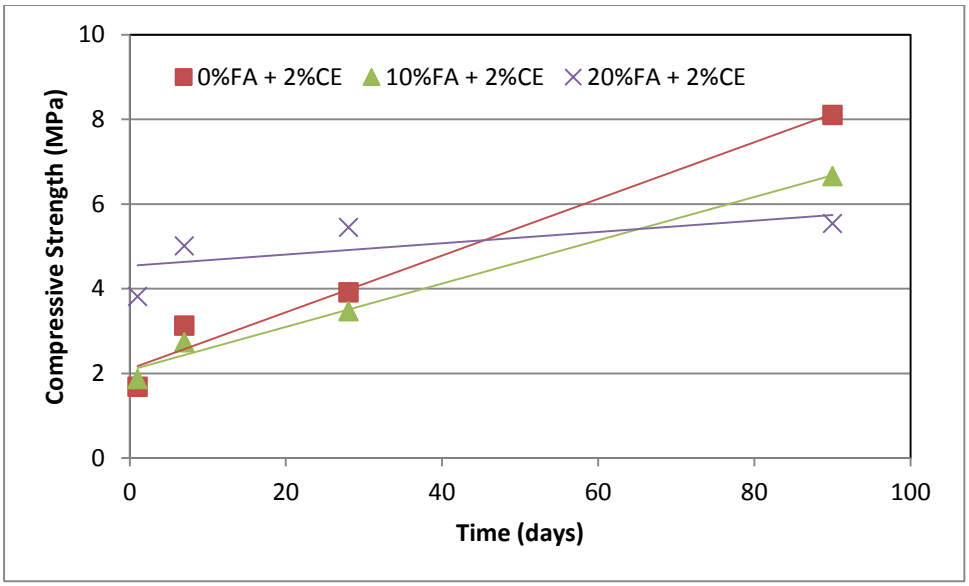

Figure 7.39 Compressive strength propagation for 451 grade soils over 90 days at 2% cement content

At 9% cement content, compressive strength is improved. While it can be argued if this improvement is proportional to cement content, the effect on added Pulverised Fuel Ash is more pronounced. 10% Pulverised Fuel Ash added to the mix improved compressive strength very significantly for the first 7 days but not by much by the 28th day. It would appear that Pulverised Fuel Ash in the mix provided initial strength but delayed the hydrolysis reaction of

cement. This as seen in figure7.40 results in a much lower strength up to 90 days. There is a similar initial quick compressive strength gain over the first 7 days for 9% cement stabilised rammed earth when 20% Pulverised Fuel Ash is added and just as seen with 10% samples, compressive strength doesn't rise by any significant margin after this time. Adding Pulverised Fuel Ash up to 30% appears to result in consistently lower compressive strengths as seen in figure 7.41. It should be noted that while the strength figures were significantly lower than figures obtained for 9% cement stabilised rammed earth with no Pulverised Fuel Ash, they were still higher than figures obtained for unstabilised rammed earth without Pulverised Fuel Ash.

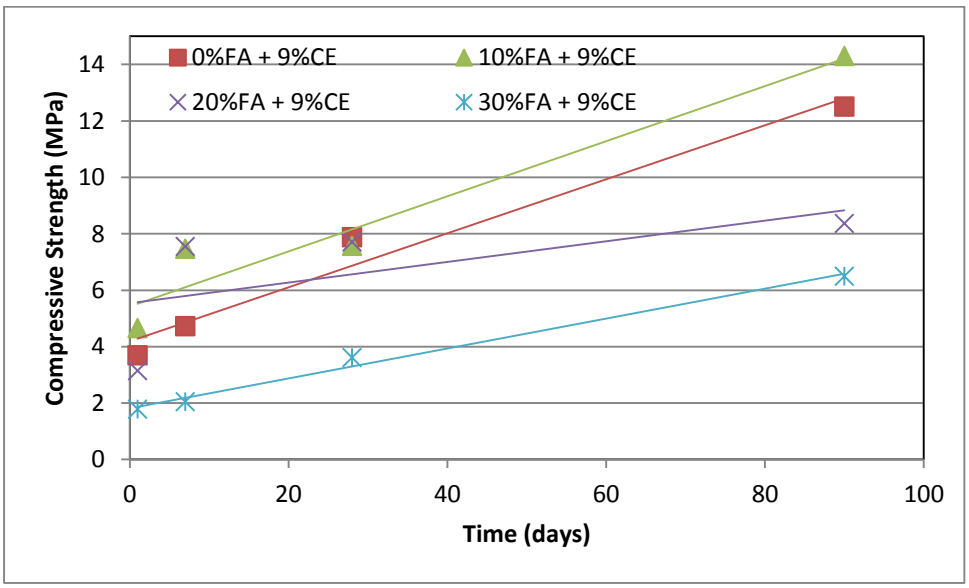

Figure 7.40 Compressive strength propagation for 451 grade soils over 90 days at 9% cement content

Figure 7.42 to 7.44 shows how cement stabilisation affects compressive strength when various amounts of Pulverised Fuel Ash was present in the mix. At 0% Pulverised Fuel Ash content, compressive strength increased steadily as cement content increased. There was a 766% increase in compressive strength when cement stabilisation rose from 0 to 9%. Compressive strength at this age peaked at about 13MPa. This was comparable to compressive strengths obtained when 10% Pulverised Fuel Ash was added to similar samples. However, compressive strength increased

by only 213% when 10% Pulverised Fuel Ash was added. This is due to the fact that Pulverised Fuel Ash increased the unstabilised strength of rammed earth. This translates to the fact that cement stabilisation does not go very far in increasing compressive strength of rammed earth containing Pulverised Fuel Ash. This is further illustrated in figure 7.44 where the maximum compressive strength recorded for 9% cement stabilised rammed earth containing 20% Pulverised Fuel Ash was 8.37MPa. Here, compressive strength increased by 39% when stabilisation increased from 0 to 9%

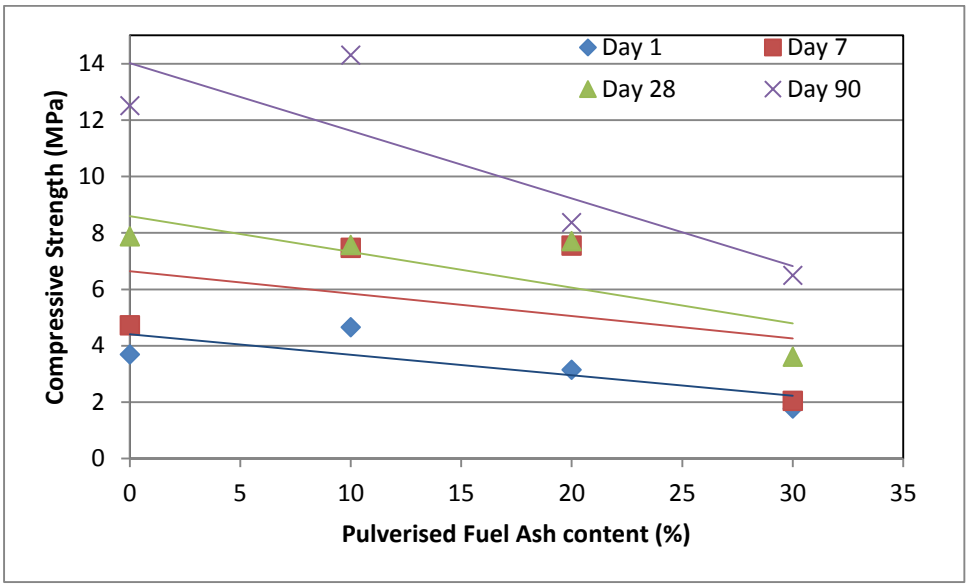

Figure 7.41 Effect of Pulverised Fuel Ash on compressive strength for 451 grade soils with 9% cement content.

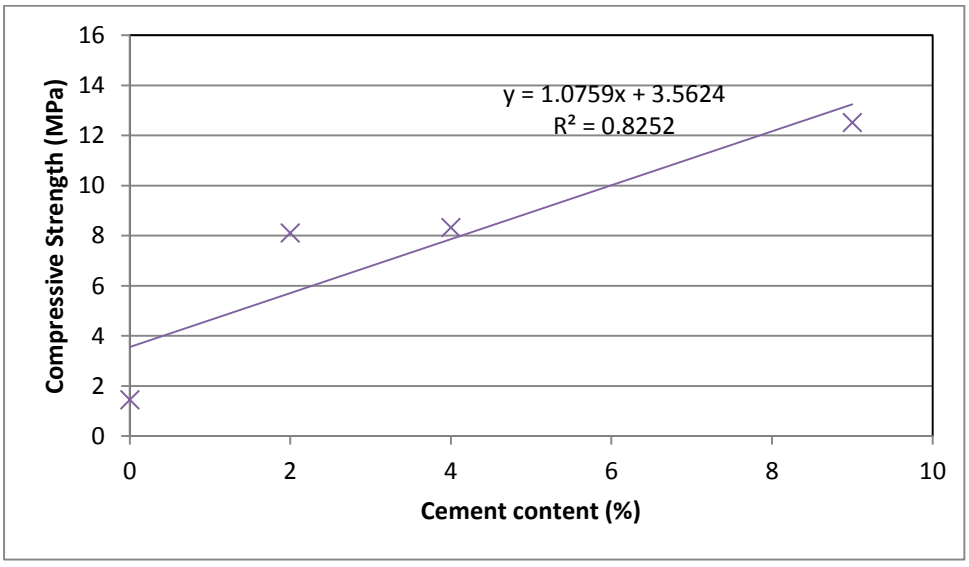

Figure 7.42 Effect of cement stabilisation on compressive strength in 451 soil grade rammed earth containing no Pulverised Fuel Ash

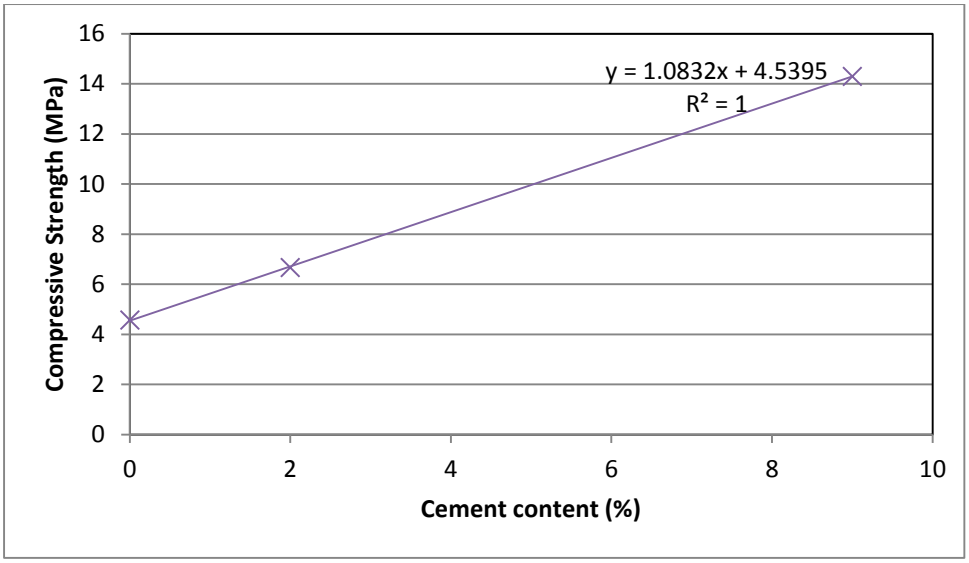

Figure 7.43. Effect of Cement stabilisation on compressive strength in 451 soil grade rammed earth containing 10% Pulverised Fuel Ash

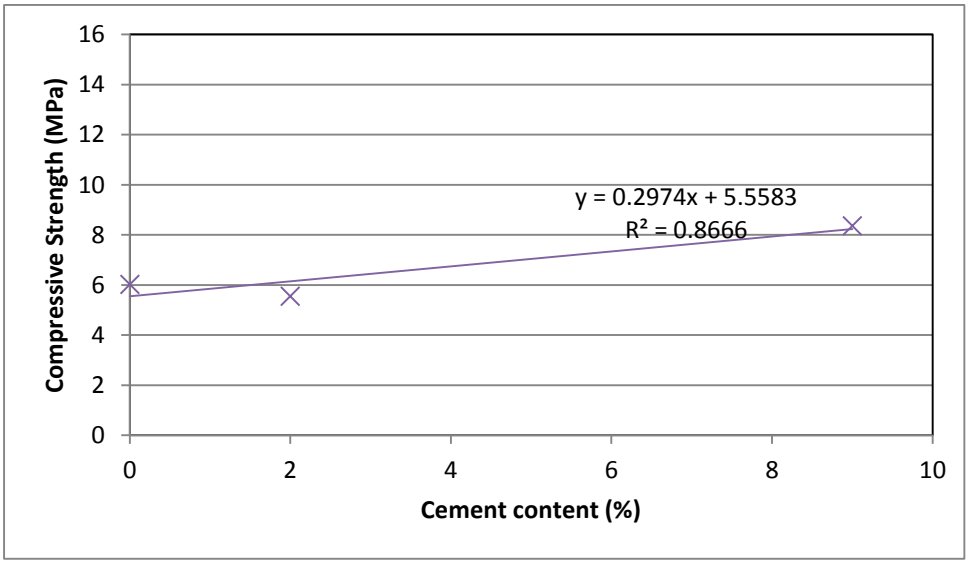

Figure 7.44 Effect of cement stabilisation on compressive strength in 451 soil grade rammed earth containing 20% Pulverised Fuel Ash

7.2.2 Ultrasonic Pulse Velocity

The speeds at which pulses travelled seemed to increase with time. This indicated that the internal structure of the material changed significantly as moisture found its way out of the core of the material. Figure 7.45 shows that unstabilised rammed earth took longer to settle out internal moisture migration.

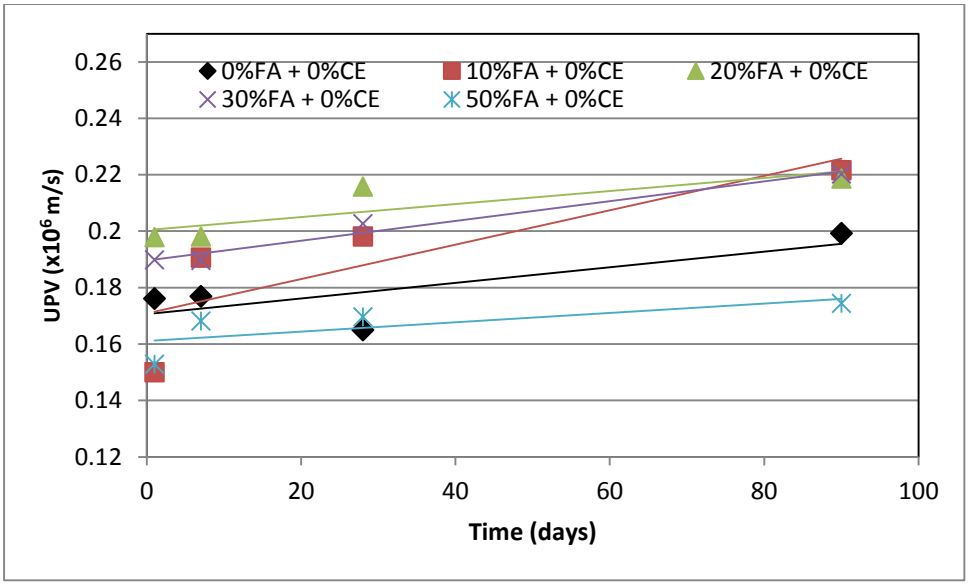

Figure 7.45 Time controlled variation in UPV of 451 grade rammed earth containing various quantities of Pulverised Fuel Ash

UPV dropped by 4% by the 28th day of testing. This drop was observed quite earlier (7 days) for samples containing 20% and 30% Pulverised Fuel Ash. For these samples, UPV seemed to approach its peak by the 28th day as there was very little increase by the 90th day. Unstabilised rammed earth was still showed signs of improvement by the 90th day of testing.

When the effect of adding Pulverised Fuel Ash was investigated, Figure 7.46 shows that on almost all days tested, Pulverised Fuel Ash content had very little effect on the UPV values. Maximum gain or drop in UPV was observed to be 15%.

On addition of cement to the mix, UPV appeared to improve at much the same rate at all ages. Figure 7.47 shows that the addition of 2% cement produced the best improvement in the rammed earth samples. Stabilising by 2% resulted in a 38% rise in UPV value. Further stabilisation up to 4% resulted in a much smaller improvement of 13% in UPV. Further stabilisation to 9% resulted in UPV value improvement of 0.2%.

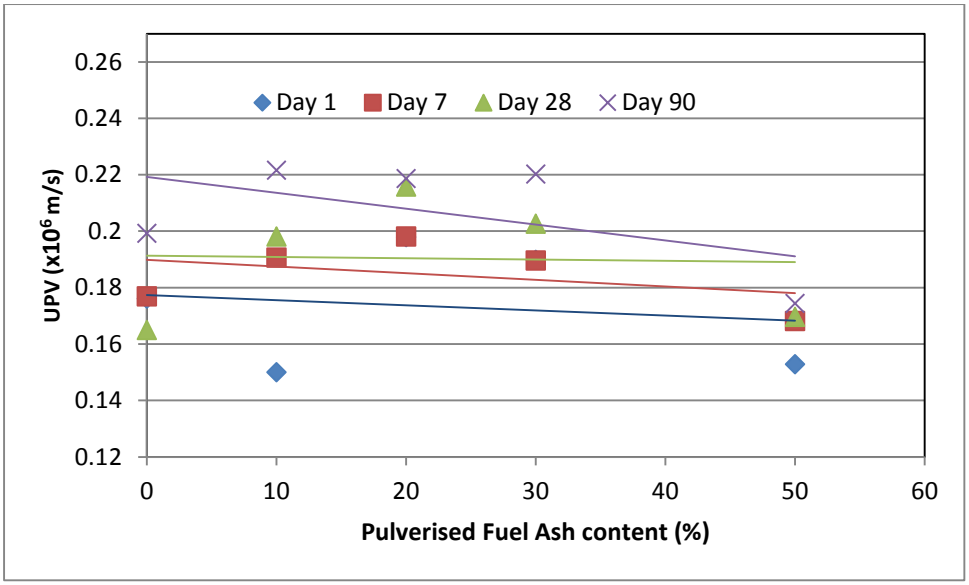

Figure 7.46 Effect of Pulverised Fuel Ash on UPV values of 451 grade rammed earth

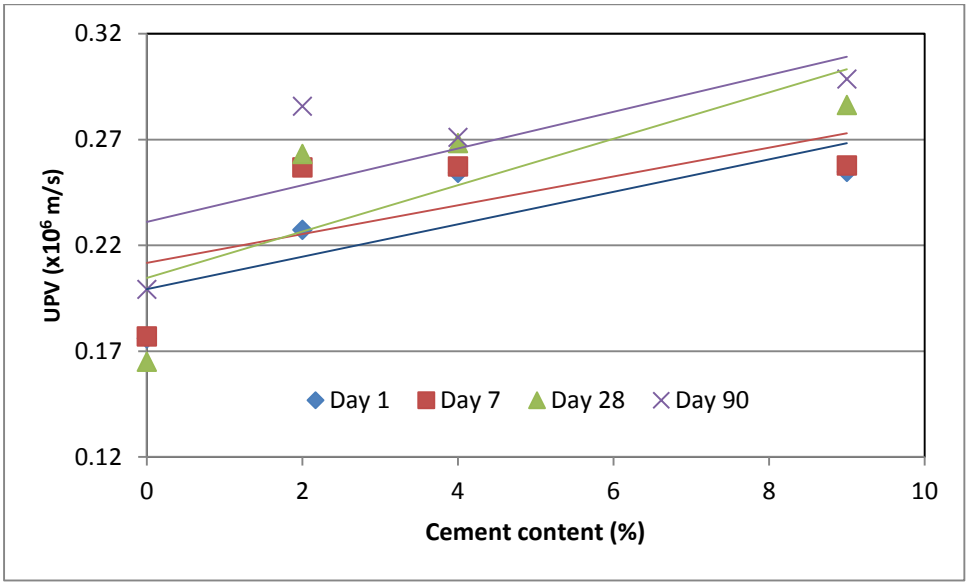

Figure 7.47 Effect of cement content on UPV values of 451 grade rammed earth

As 2% cement stabilisation produced the best UPV results, Pulverised Fuel Ash was added to the mix and tested over 90 days. Results obtained are plotted in figure 7.48 and 7.32 shows that although all the combinations had UPV values greater than unstabilised rammed earth, addition of Pulverised Fuel Ash to cement stabilised rammed earth reduced the UPV value.

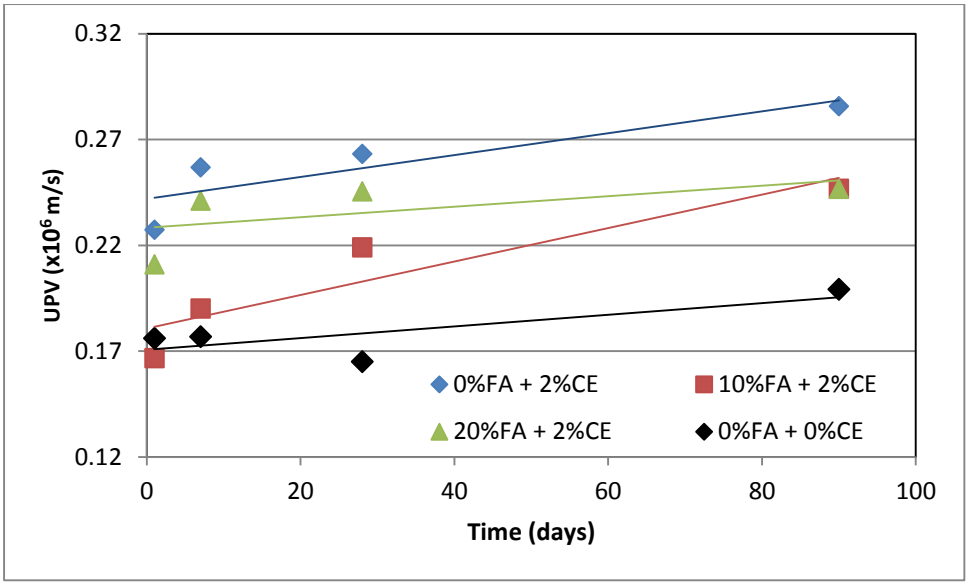

Figure 7.48 UPV effect of adding Pulverised Fuel Ash to 451 grade rammed earth stabilised with 2% cement

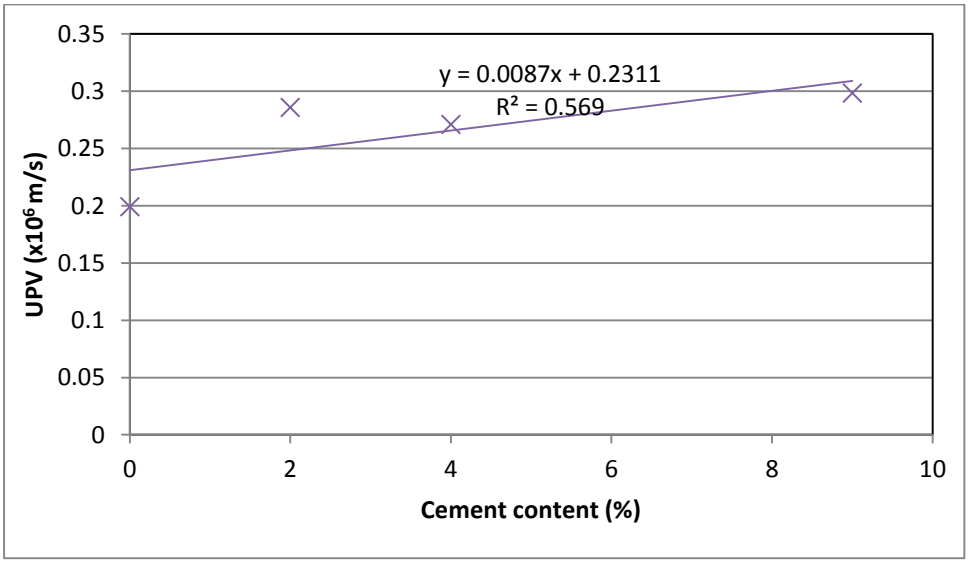

Figure 7.49 Effect of cement stabilisation on UPV in 451 soil grade rammed earth containing no Pulverised Fuel Ash

Figure 7.49 to 7.51 shows that stabilisation of 451 soil grade rammed earth leads to increase in UPV. When stabilisation goes from 0 to 9%, UPV increases by about 50%. It is also clear to see that this does not change significantly when 10% or 20 % Pulverised Fuel Ash is added to the mix.

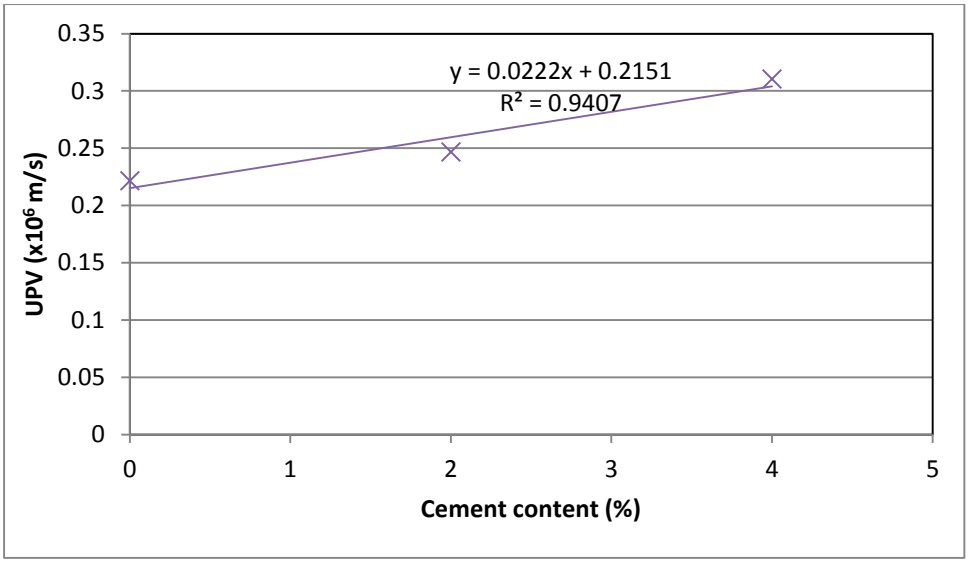

Figure 7.50 Effect of cement stabilisation on UPV in 451 soil grade rammed earth containing 10% Pulverised Fuel Ash

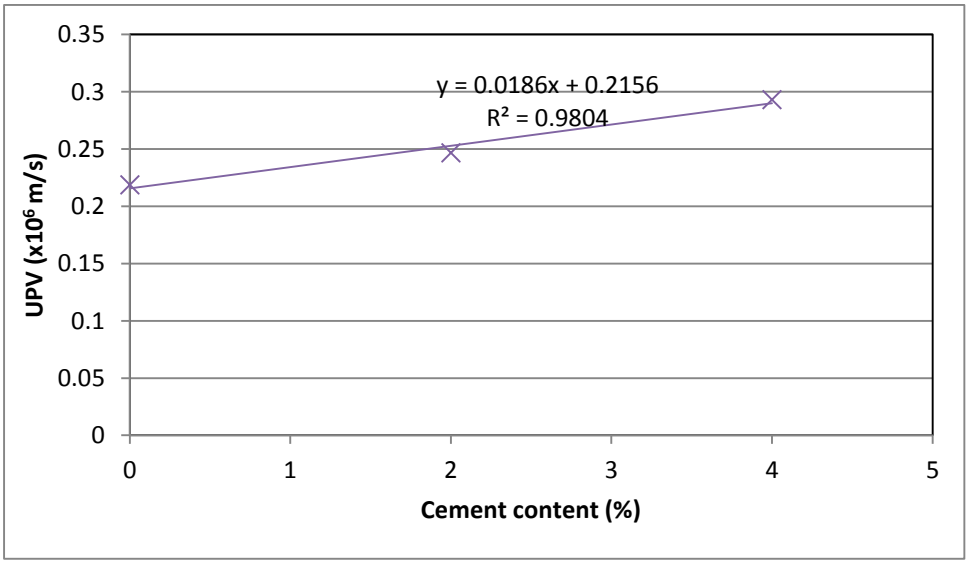

Figure 7.51 Effect of Cement stabilisation on UPV in 451 soil grade rammed earth containing 20% Pulverised Fuel Ash

7.2.3 Density

Rammed earth made from 451 soil mix exhibited very little change in density with time. Figure 7.52 shows that while the unstabilised sample saw a reduction in density of 5% after 7 days, sample containing 50% Pulverised Fuel Ash saw a reduction in density values of only 4% on the same day. Density didn't change very much after the 7th day.

Figure 7.53 provides a clear picture on how adding Pulverised Fuel Ash affects rammed earth made from a 451 mix of soils. It can be seen that as Pulverised Fuel Ash is added to the mix, there is a reduction in density. On the first day of testing, adding 10% Pulverised Fuel Ash to the mix resulted in density falling by 0.7%. Further addition of Pulverised Fuel Ash (up to 20%) resulted in density falling by another 1.5%. Increasing Pulverised Fuel Ash content to 30% results in a further decrease in density by 4.8%. The highest degree of fall in density was observed in rammed earth with a Pulverised Fuel Ash content of 50%.

When cement was used to stabilise the mix, the effect on density was variable depending on the amount of cement used in stabilisation. A 2% cement stabilisation resulted in a minor increase of 0.2% in density. Further stabilisation saw a massive fall in density of 7%. Further stabilisation to 9% appeared to however increase density again by 5%. This is observed in Figure 7.54.

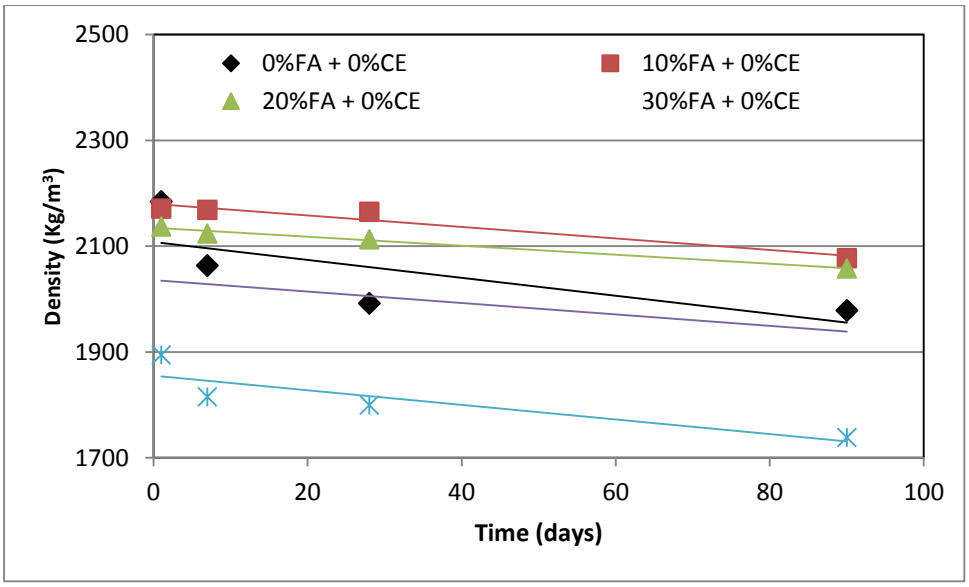

Figure 7.52 Density change with age in 451 grade rammed earth

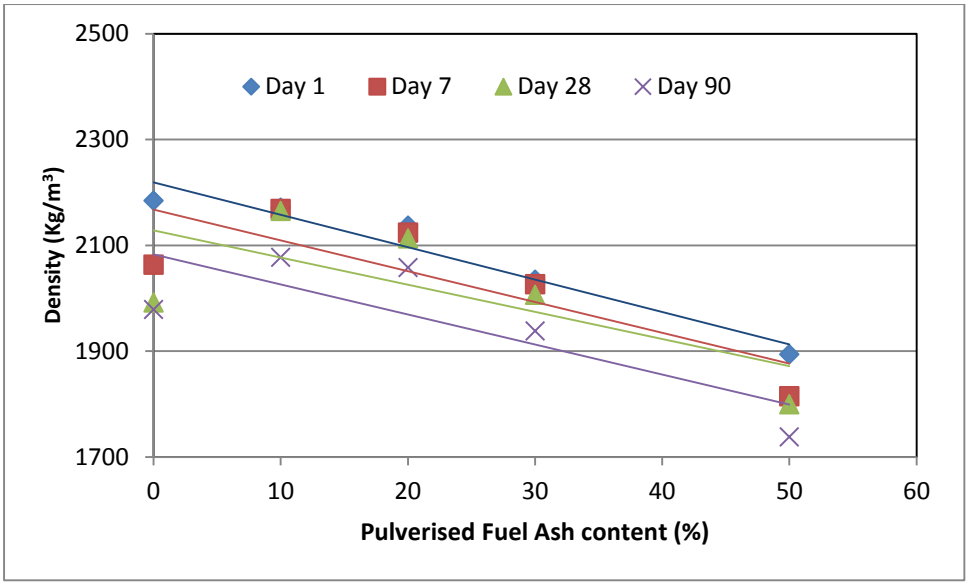

Figure 7.53 Effect of Pulverised Fuel Ash on density for 451 grade rammed earth.

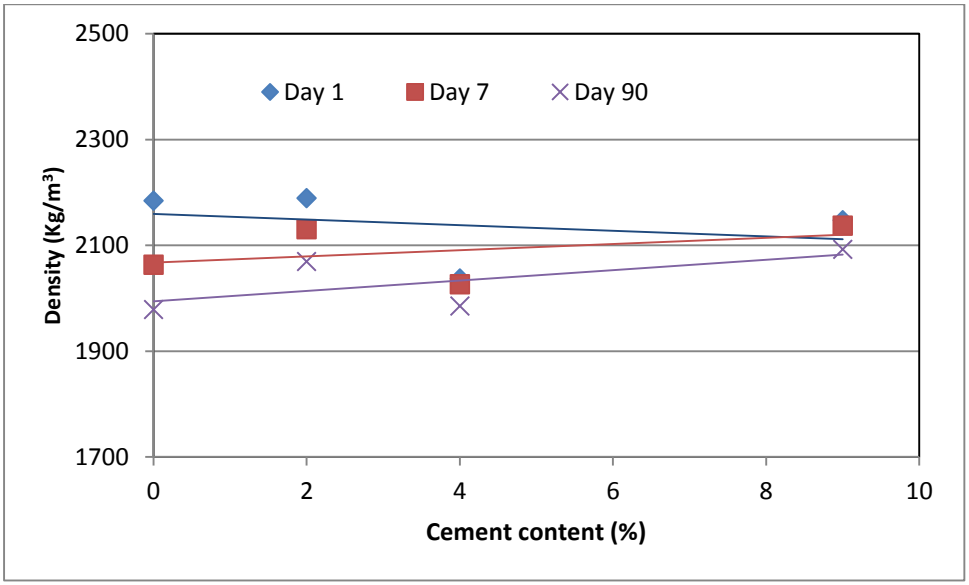

Figure 7.54 Effect of cement stabilisation on density of 451 grade rammed earth samples

A combination of Pulverised Fuel Ash and cement produced results that are shown in Figure 7.55. 10% and 20% Pulverised Fuel Ash was added to samples that were stabilised by 2% cement. Sample containing 10% Pulverised Fuel Ash had the same density as unstabilised rammed earth on day one. However, while density values dropped off rapidly with time for the unstabilised sample, the sample containing 20% Pulverised Fuel Ash and 2%

cement didn't change as much in density thus density was noted to be higher at day 90. Sample containing 20% Pulverised Fuel Ash and 2% cement did not show much variation in density either but had significantly less density at day 1.

Figure 7.56 to 7.58 show the effect of cement stabilisation on rammed earth samples made from 451 soil grade. Figure 7.56 shows a relationship between density and increasing stabilisation when the samples contained no Pulverised Fuel Ash. Density can be seen to be rising with cement content. There was a 5.8% increase in density as stabilisation went from zero to 9%. This trend was however reversed with the introduction of Pulverised Fuel Ash. When the samples contained 10% Pulverised Fuel Ash, increasing stabilisation resulted in a decrease in density. This is probably due to the fact that Pulverised Fuel Ash increased the density of the sample. It can be concluded then that cement stabilisation helped reverse the effect of increased density when Pulverised Fuel Ash is present in a 451 rammed earth mix.

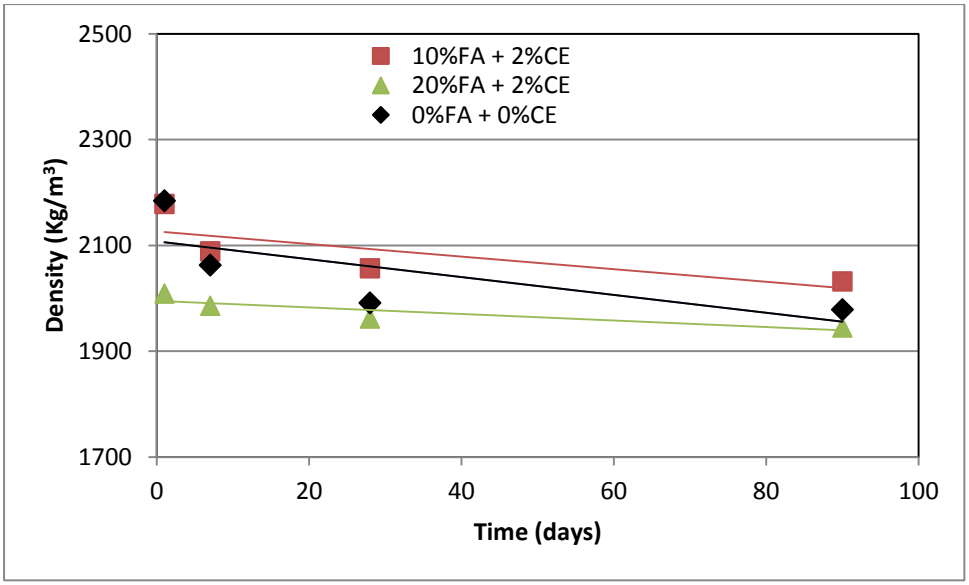

Figure 7.55 Effect on UPV when Pulverised Fuel Ash is added to a 2% cement stabilised 451 grade rammed earth

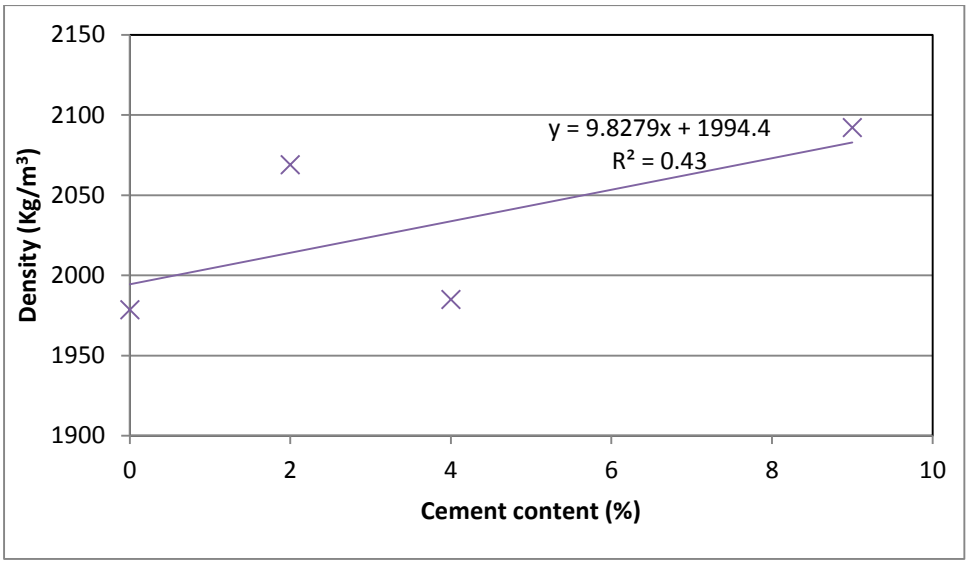

Figure 7.56 Effect of Cement stabilisation on Density in 451 soil grade rammed earth containing no Pulverised Fuel Ash

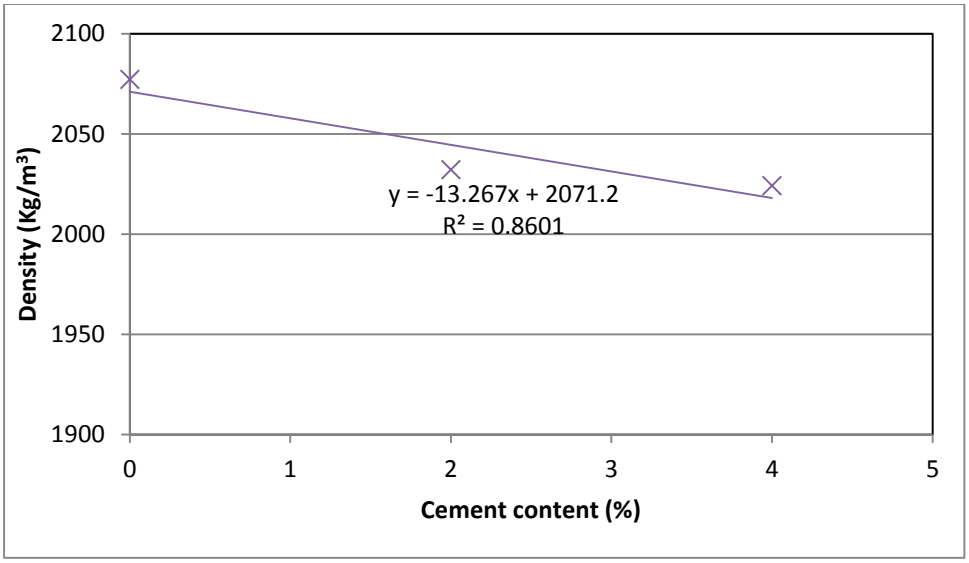

Figure 7.57 Effect of Cement stabilisation on Density in 451 soil grade rammed earth containing 10% Pulverised Fuel Ash

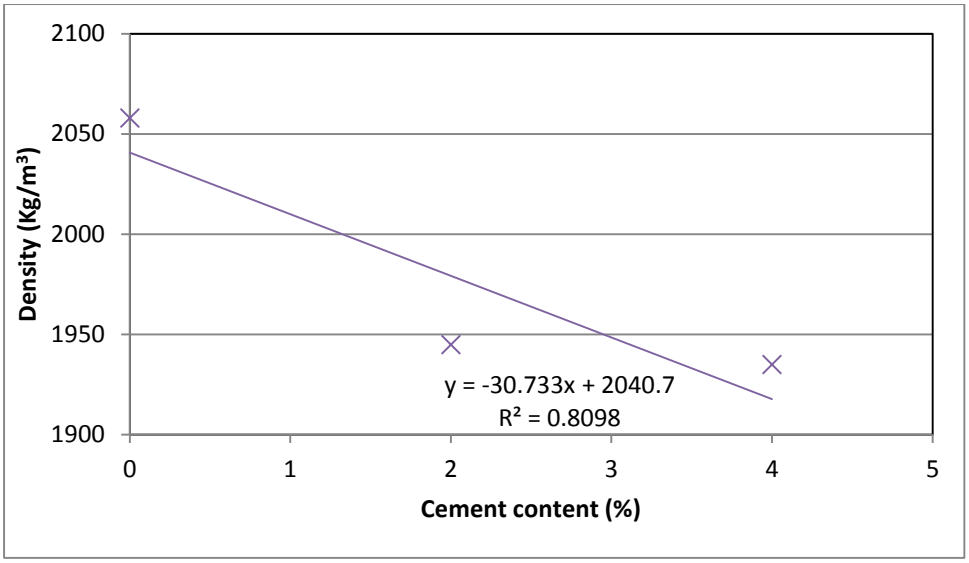

Figure 7.58. Effect of Cement stabilisation on Density in 451 soil grade rammed earth containing 20% Pulverised Fuel Ash

7.2.4 Initial Rate of Suction

Initial rate of suction for Rammed Earth of grade 451 containing Pulverised Fuel Ash shows that Sorptivity was reduced when only 10% Pulverised Fuel Ash was added to the sample. As can be seen in Figure 7.59, further addition of Pulverised Fuel Ash resulted in a huge increase in the rate of suction. This gradually reduced with increase in Pulverised Fuel Ash content. The total quantity of sorbed moisture is still recorded for the sample containing 50% Pulverised Fuel Ash even though there was a gradual lull in initial capillary intake.

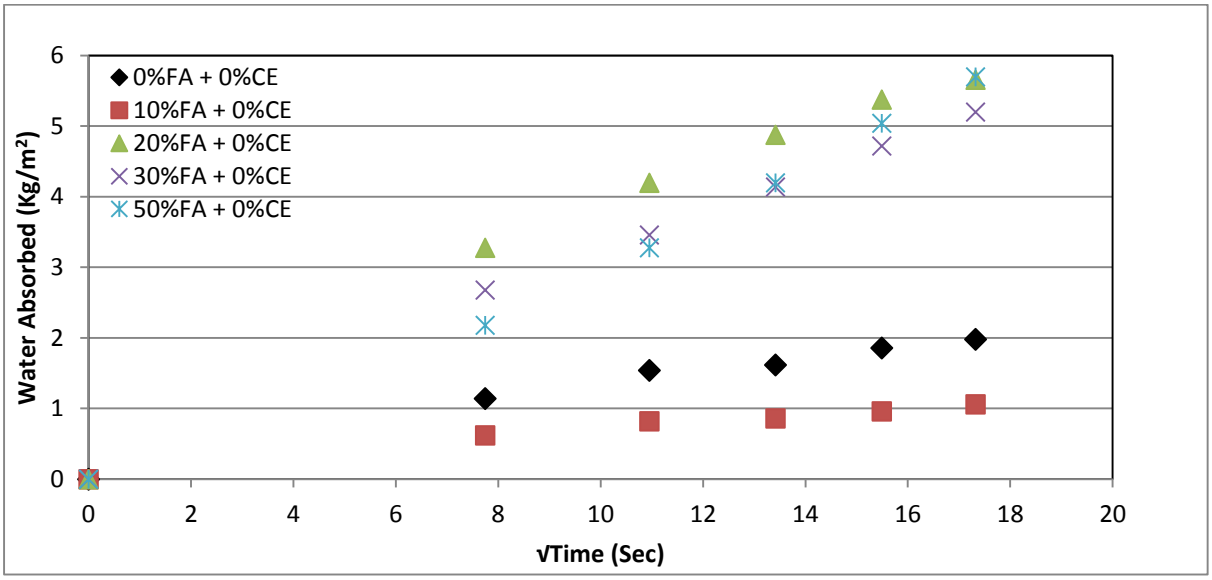

Figure 7.59 Initial rate of sorption in 451 rammed earth at various Pulverised Fuel Ash content

Figure 7.60 provides a clear picture of the influence of Pulverised Fuel Ash on the Sorptivity value. It becomes immediately obvious that 10% Pulverised Fuel Ash content provides positive results as Sorptivity reduces by 47%. However, further addition of Pulverised Fuel Ash tends to increase Sorptivity greatly. A 20% Pulverised Fuel Ash content will result in a jump in absorption values of over 450%.

The point at which Sorptivity starts to reduce when rammed earth is stabilised with cement cannot be estimated by the data presented above. Further checks need to be carried out to determine the point at which rising Sorptivity turns around and starts to fall. What our data does point to however is that 2% cement content would increase Sorptivity when Pulverised Fuel Ash is added to rammed earth (Figure 7.61). It also appears that further cement stabilisation would at some point lead to fall in Sorptivity. At 9% stabilisation, Sorptivity was still higher than values obtained for unstabilised samples

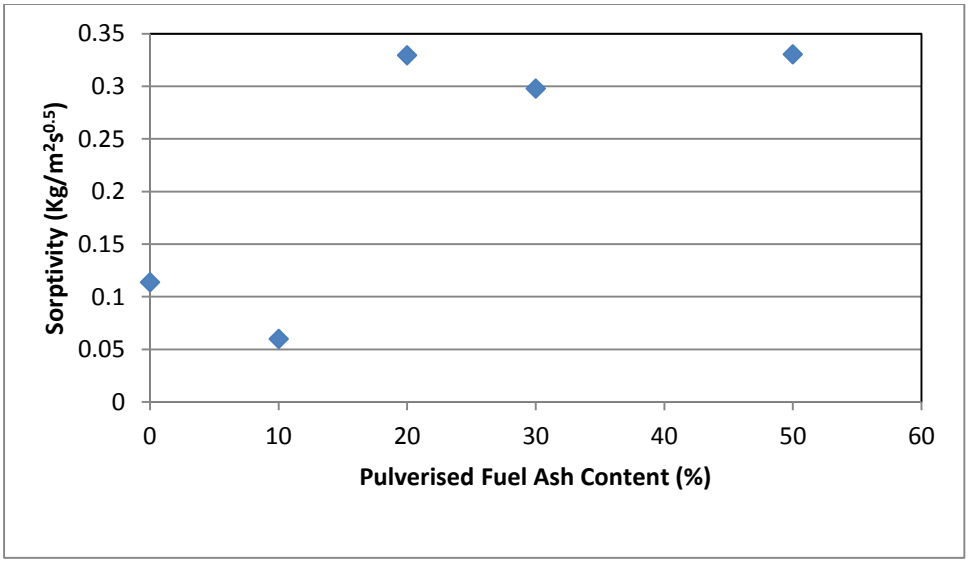

Figure 7.60 Effect of Pulverised Fuel Ash content on sorptivity in unstabilised 451 rammed earth

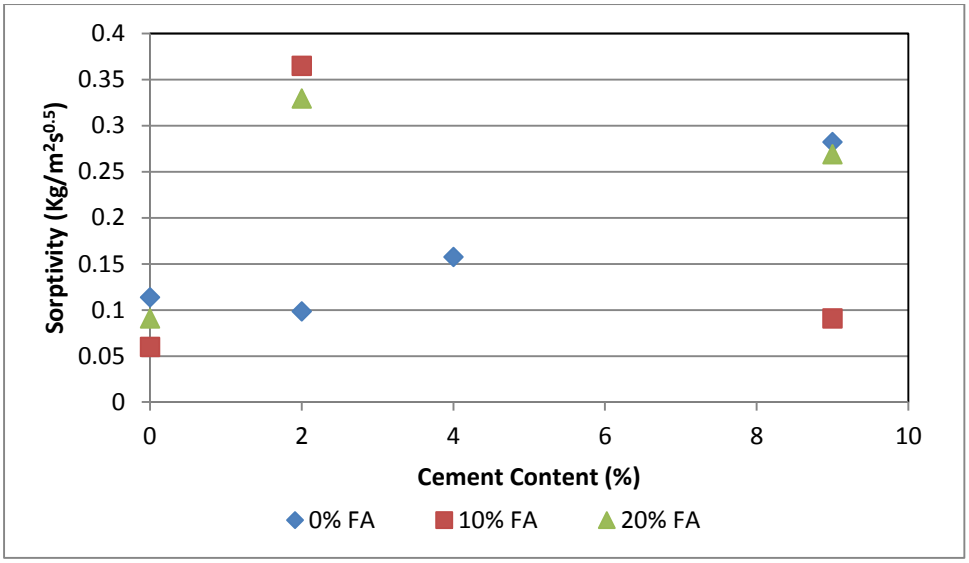

Figure 7.61 Effect of stabilisation on 451 rammed earth containing Pulverised Fuel Ash.

.

7.2.5 Further Discussions

Compressive strength increased with increase in ultrasonic pulse velocity as did it, with increasing density. The reverse was the case however when compressive strength was measured against Sorptivity. The more susceptible a sample was to water ingress, the lower the compressive strength achieved. Figures 7.62 to 7.70 show the distribution of points with respect to Pulverised Fuel Ash content and cement content. The UPV distribution when compared to compressive strength for the various Pulverised Fuel Ash contents are similar. There is an even spread between the samples irrespective of Pulverised Fuel Ash content. When density is compared against compressive strength however, it appears that samples having no Pulverised Fuel Ash had higher density and exhibited higher compressive strength. This was however surpassed by samples containing 10% Pulverised Fuel Ash.

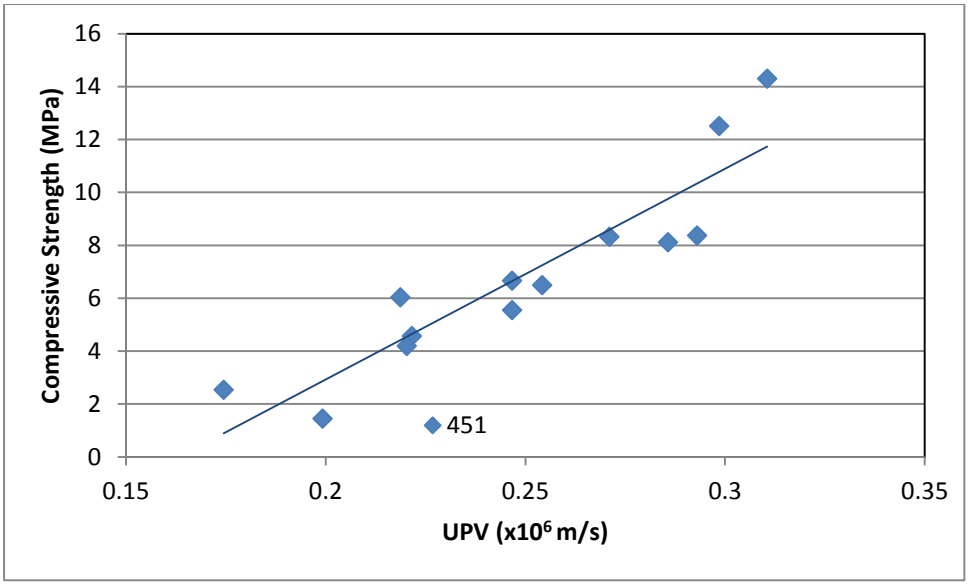

Figure 7.62 Correlation between compressive strength and UPV in 451 soil grade

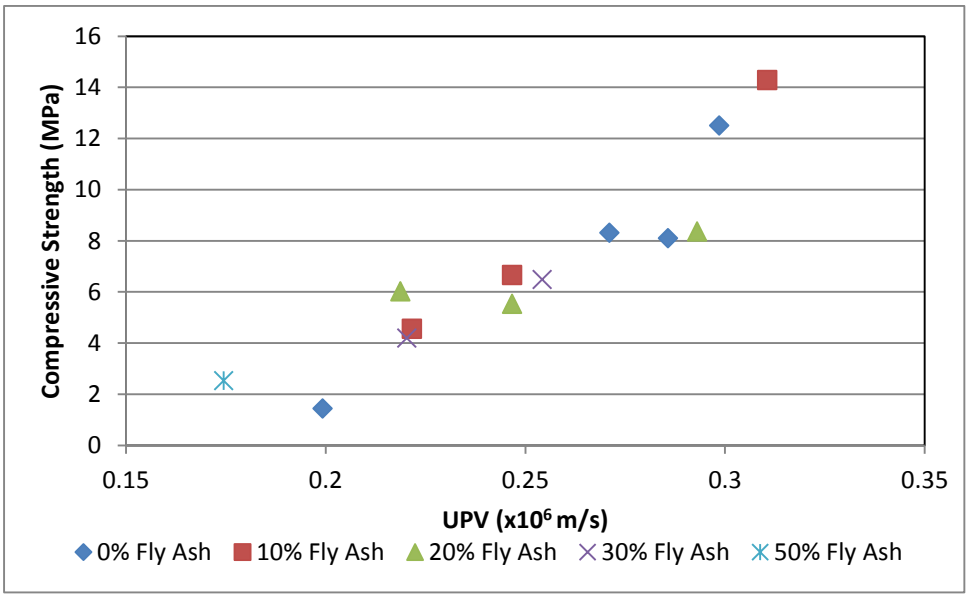

Figure 7.63 Compressive strength vs UPV in 451 soil grade (showing Pulverised Fuel Ash content distribution)

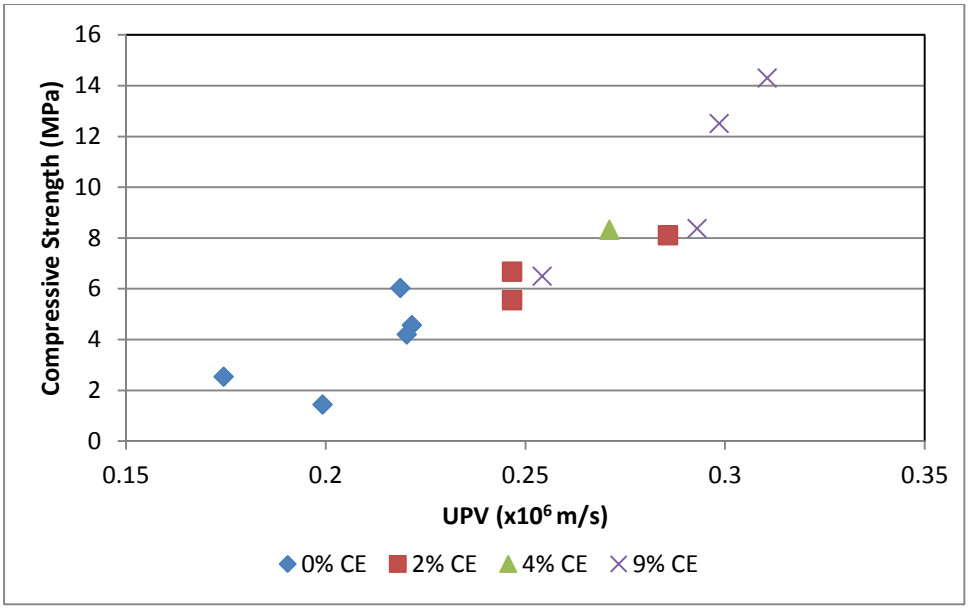

Figure 7.64 Compressive strength vs UPV in 451 soil grade (showing cement content distribution)

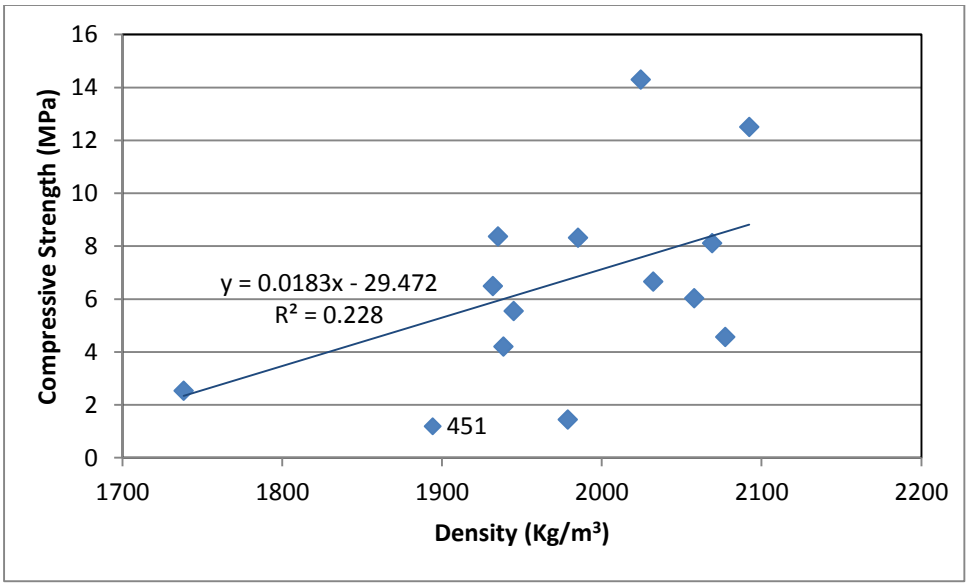

Figure 7.65 Correlation between compressive strength and density in 451 soil grade

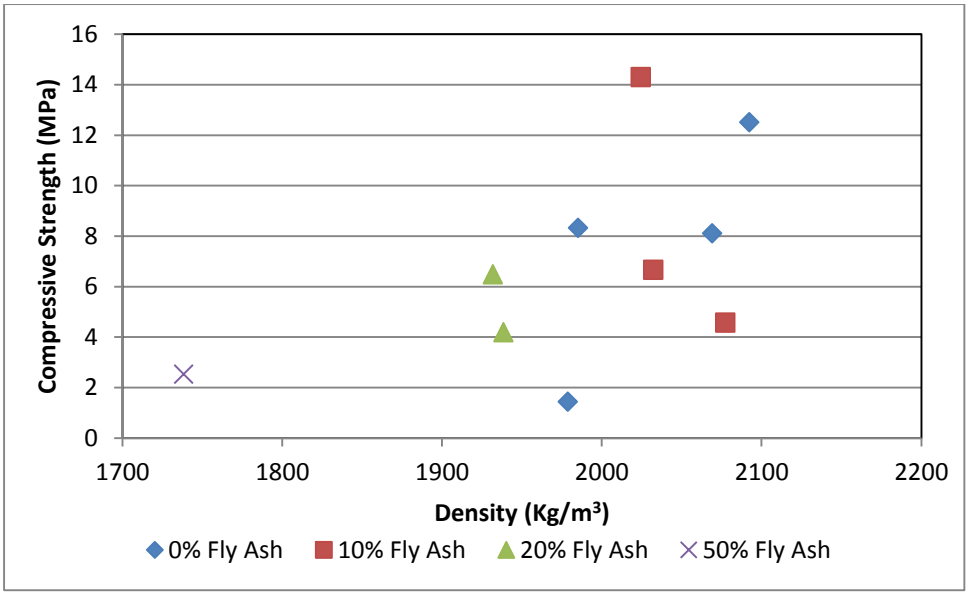

Figure 7.66 Compressive strength vs density in 451 soil grade (showing Pulverised Fuel Ash content distribution)

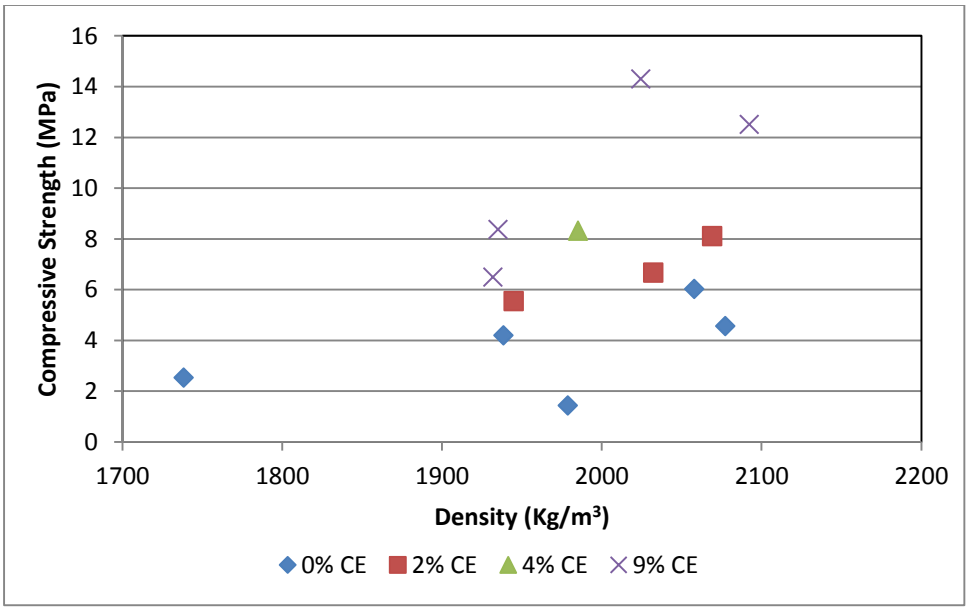

Figure 7.67 Compressive strength vs density in 451 soil grade (showing cement content distribution)

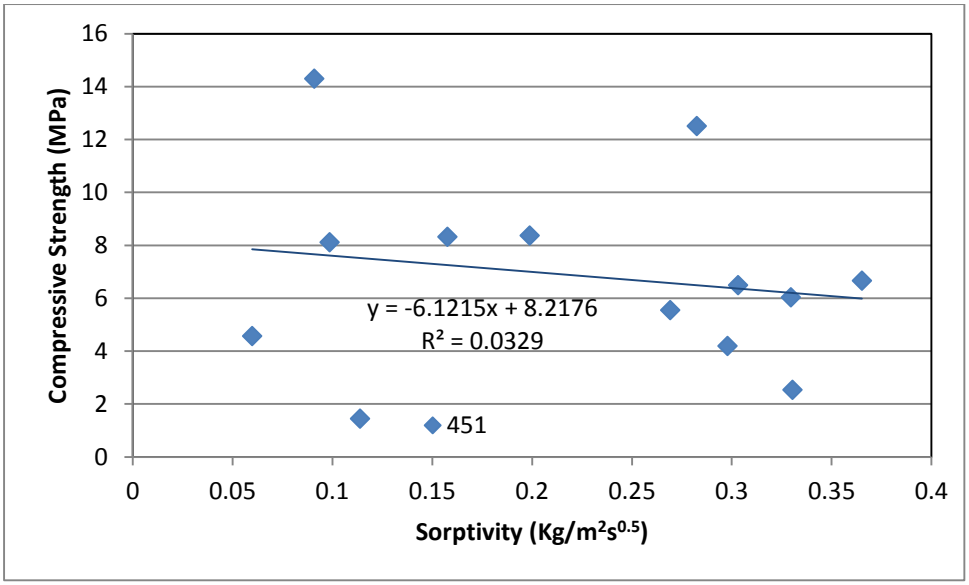

Figure 7.68 Correlation between compressive strength and sorptivity in 451 soil grade

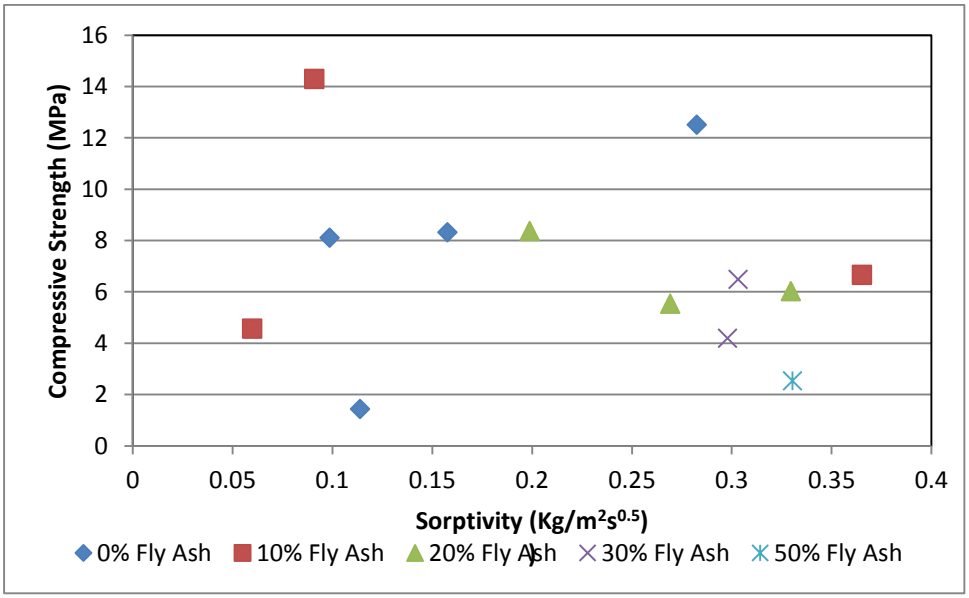

Figure 7.69 Compressive strength vs sorptivity in 451 soil grade (showing Pulverised Fuel Ash content distribution)

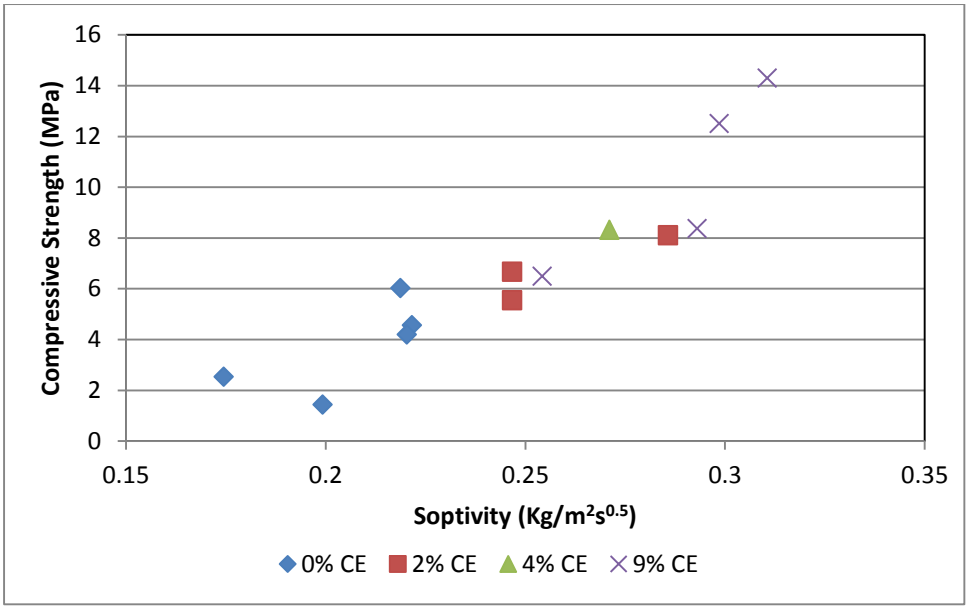

Figure 7.70 Compressive strength vs sorptivity in 451 soil grade (showing cement content distribution)

7.3 532 Soil Grade

The 532 soil grade is made by bending soil in the proportion of 5:3:2 comprising Sand:Clay:Coarse aggregate.

7.3.1 Compressive strength

For smaller quantities of Pulverised Fuel Ash, there appeared to be very little difference in compressive strength for the first 7 days (Figure 7.71). At 10% and 20% Pulverised Fuel Ash content, compressive strengths were similar to rammed earth samples having no Pulverised Fuel Ash. While rammed earth containing 20% Pulverised Fuel Ash showed compressive strength rising by 128% samples containing 10% Pulverised Fuel Ash gained compressive strength of 42% in tandem with unstabilised rammed earth with no Pulverised Fuel Ash content. However, after 28 days, rammed earth with 10% Pulverised Fuel Ash displayed a steady rise in compressive strength and ends 90 days similar to the strength of 20% Pulverised Fuel Ash samples. Samples having 50% Pulverised Fuel Ash consistently exhibited lower compressive strength than samples without any Pulverised Fuel Ash. 50% Pulverised Fuel Ash

caused a loss in compressive strength of 61%, 40%, 36% and 10% at 1, 7, 28 and 90 days respectively.

Figure 7.72 shows this relationship more clearly. While there is a general trend of decline in compressive strength, it would appear that an initial strength gain up to and including 20% Pulverised Fuel Ash still exists. This is more defined with the age of the material.

Looking at Figure 7.74, compressive strength on the first day declines steadily with the addition of Pulverised Fuel Ash. 10% Pulverised Fuel Ash addition resulted in a 32% decrease in compressive strength. Adding another 10% Pulverised Fuel Ash resulted in a further decrease of 53%. With age however this trend tends to change. At 28 days, the effect of 10% Pulverised Fuel Ash was positive as compressive strength rose by 11% and by a further 75% when 20% Pulverised Fuel Ash was added. While 90 day strength showed remarkable strength increase from a 28 day position of 84% for 10% Pulverised Fuel Ash content, 20% Pulverised Fuel Ash content did not produce any significant compressive strength gain.

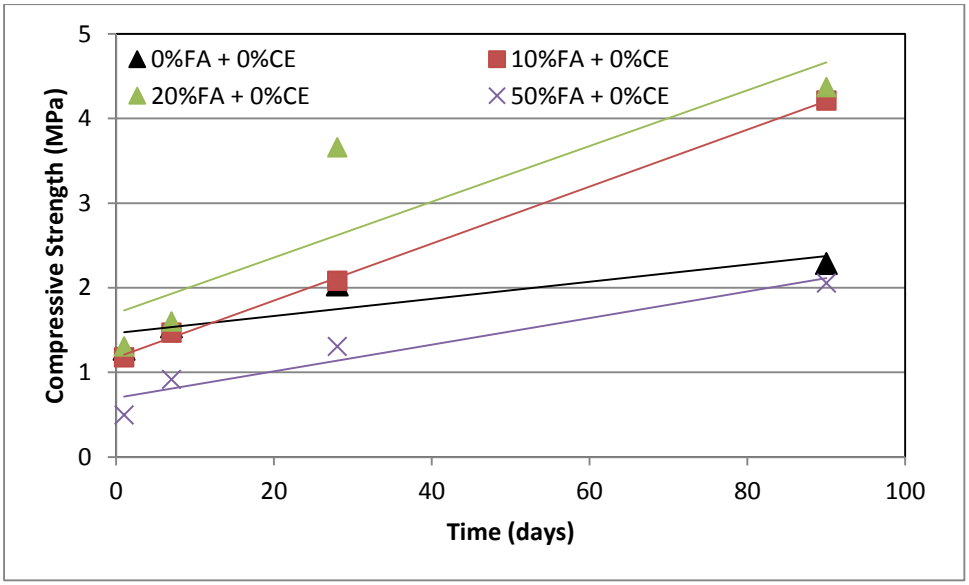

Figure 7.71 Compressive strength propagation for 532 grade soils over 90 days at zero cement content

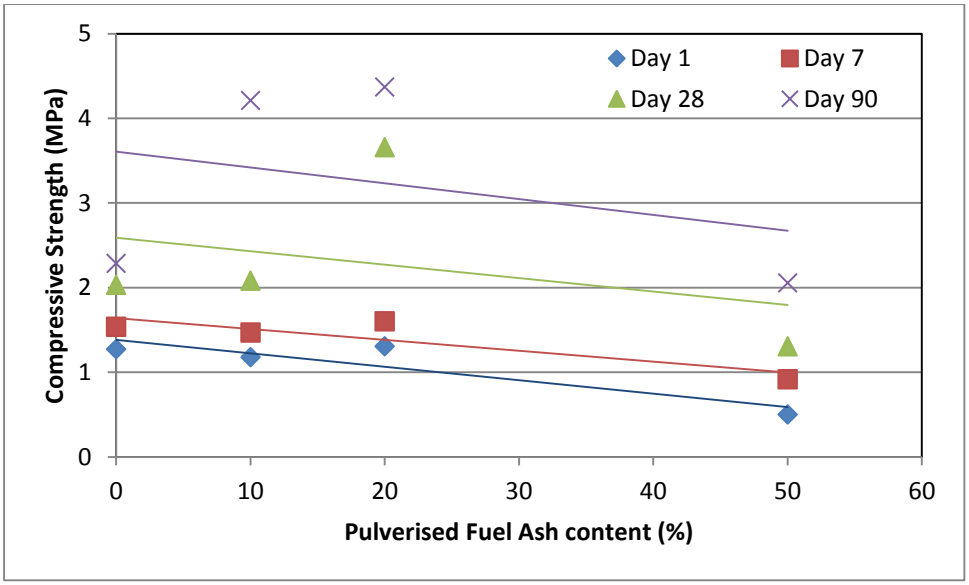

Figure 7.72 Effect of Pulverised Fuel Ash on compressive strength for 532 grade soils.

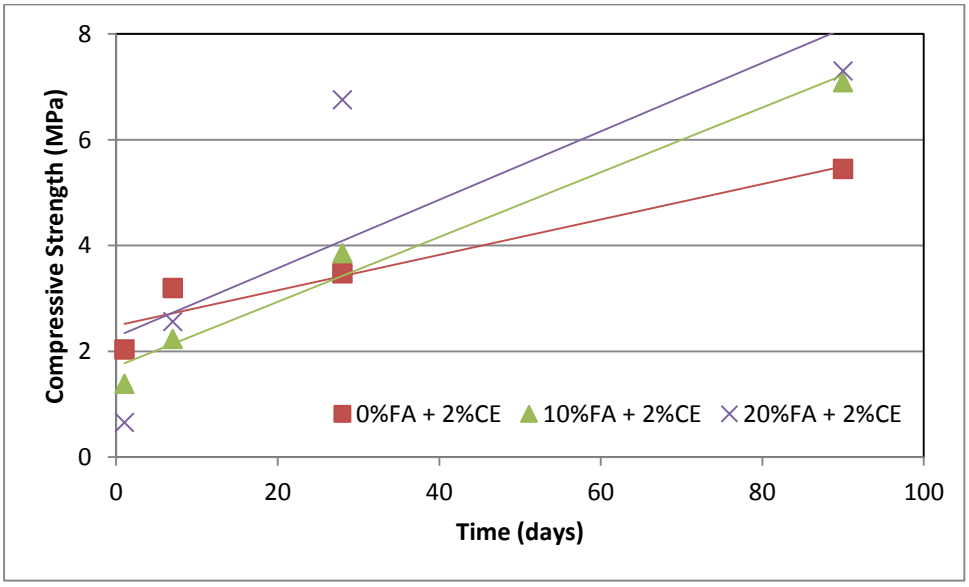

Figure 7.73 Compressive strength propagation for 532 grade soils over 90 days at 2% cement content

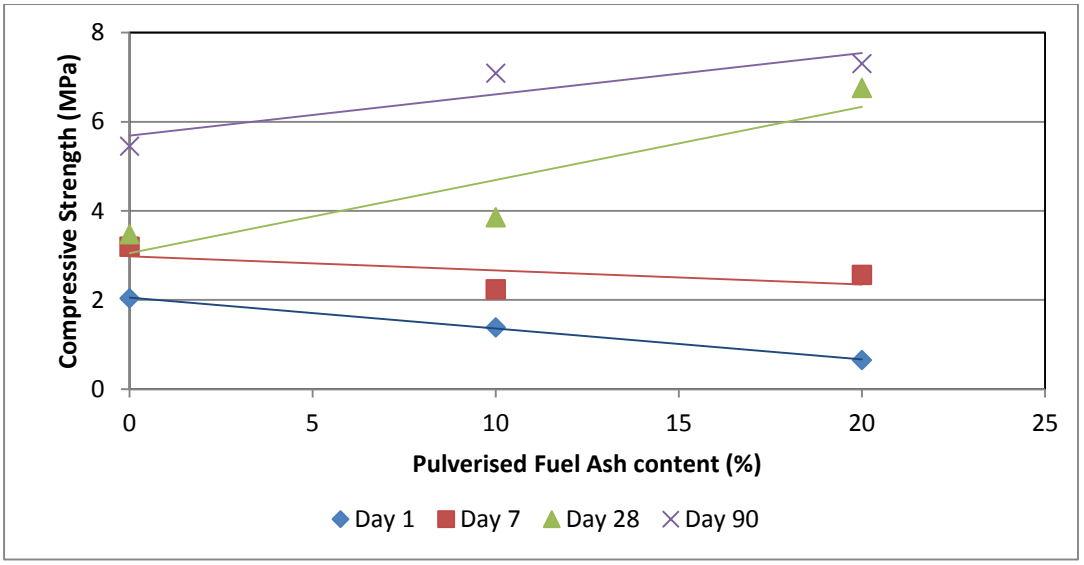

Figure 7.74 Effect of Pulverised Fuel Ash on compressive strength for 532 grade soils with 2% cement content.

At 4% cement stabilisation, compressive strength is increased by 255% on the first day (Figure 7.75). This increase continues at a steady rate as the sample aged. Adding Pulverised Fuel Ash however reduced initial compressive strength but this quickly rose to surpass day 7 strengths for 4% stabilised samples containing no Pulverised Fuel Ash. Compressive strength appeared to be highest at 90 days for rammed earth containing 10% Pulverised Fuel Ash.

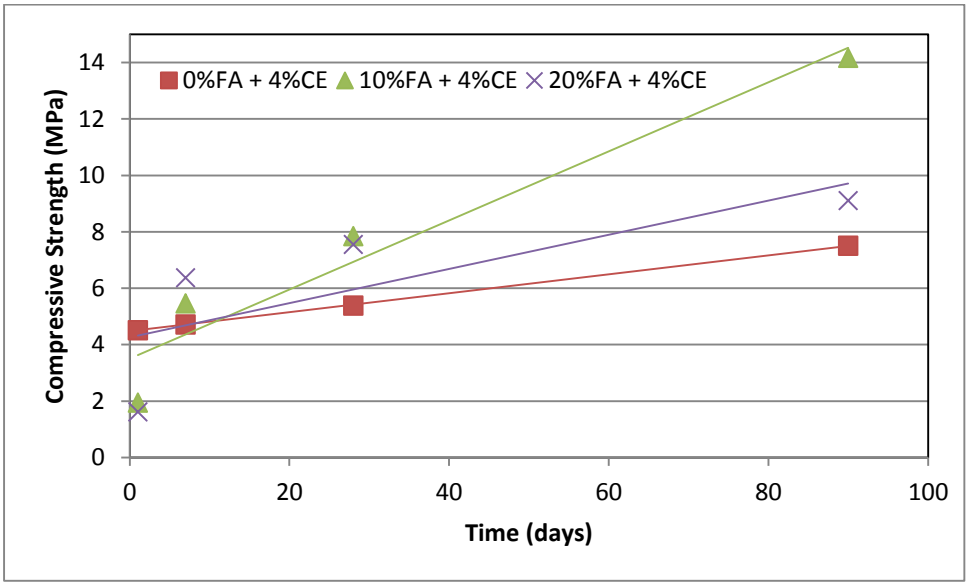

Figure 7.75 Compressive strength propagation for 532 grade soils over 90 days at 4% cement content

Figure 7.76 provides an insight to the effect of Pulverised Fuel Ash over 90 days. Except for 7 day results, 20 % Pulverised Fuel Ash content results in lower compressive strength than 10% Pulverised Fuel Ash content. After 28 days, compressive strength rose by 46% on adding Pulverised Fuel Ash. Increasing Pulverised Fuel Ash to 20% reduced compressive strength by 3.7%.

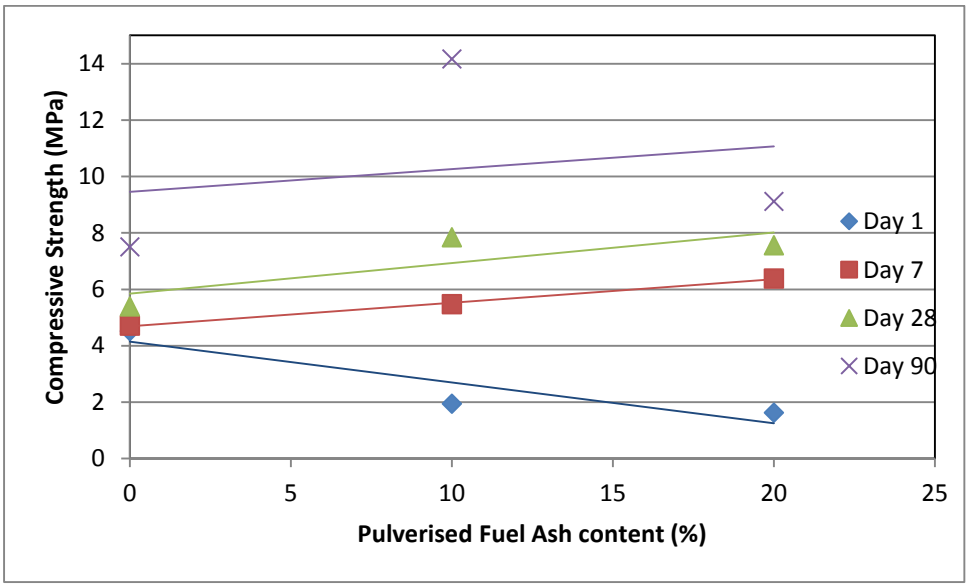

Figure 7.76 Effect of Pulverised Fuel Ash on compressive strength for 532 grade soils with 4% cement content.

At 6% cement stabilisation (Figure 7.77), 10% Pulverised Fuel Ash content shows the highest propagation of compressive strength over 90 days. 20% Pulverised Fuel Ash performed marginally less than 6% stabilised rammed earth containing no Pulverised Fuel Ash. All the samples performed better than unstabilised rammed earth.

At all ages, 10% Pulverised Fuel Ash content resulted in compressive strength gain while further addition of 10% resulted in strength loss. As seen from Figure 7.78 there was very little strength gain from day 7 to day 28 for 6% stabilised rammed earth with no Pulverised Fuel Ash content. At 28 days, compressive strength rose by 70.8% with 10% added Pulverised Fuel Ash. At 20% content, strength fell by 44%. As the sample aged to 90 days,

compressive strength difference at 10% Pulverised Fuel Ash content had reduced to 50% and 20% Pulverised Fuel Ash content had risen to 62%.

Figure 7.79 provides compressive strength comparatives for 9% stabilised rammed earth samples containing up to 50% Pulverised Fuel Ash. It is immediately obvious to see that while 9% cement stabilised rammed earth with 50% Pulverised Fuel Ash results in much higher compressive strength than unstabilised rammed earth, it performs worse than any other combination of Pulverised Fuel Ash pictured above. While 10% Pulverised Fuel Ash content performed better than 9% cement stabilised rammed earth without Pulverised Fuel Ash, 20% Pulverised Fuel Ash performed poorly to start with and then proceeded to gain more compressive strength after 28 days.

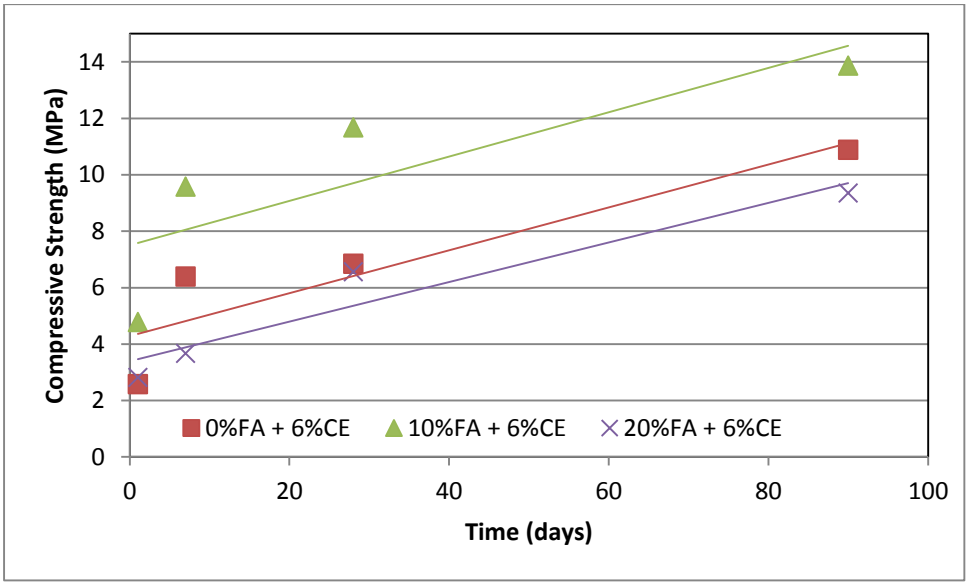

Figure 7.77 Compressive strength propagation for 532 grade soils over 90 days at 6% cement content

At all ages, compressive strength first rose on addition of 10% Pulverised Fuel Ash and then started to fall with further addition. Figure 7.80 shows that this difference was minor at early ages but compressive strength differences increased as the samples gained strength with age. At 28 days, compressive strength first rose by 56% at 10% Pulverised Fuel Ash content then started to

fall. Compressive strength had fallen by 38% at 20% content and a further 12% by 50% Pulverised Fuel Ash content.

Figure 7.81 shows the effect of the addition of cement to 532 grade rammed earth. A 2% cement stabilisation resulted in a compressive strength gain of 70.8%. Compressive strength rose further with further stabilisation. At 4% stabilisation, compressive strength had risen by 165% as compared to an initial unstabilised position. Comparing unstabilised samples with 5% cement stabilised samples showed a compressive strength gain of 337%. When compared to 9% stabilised rammed earth, compressive strength appears to have risen by a significant 443%.

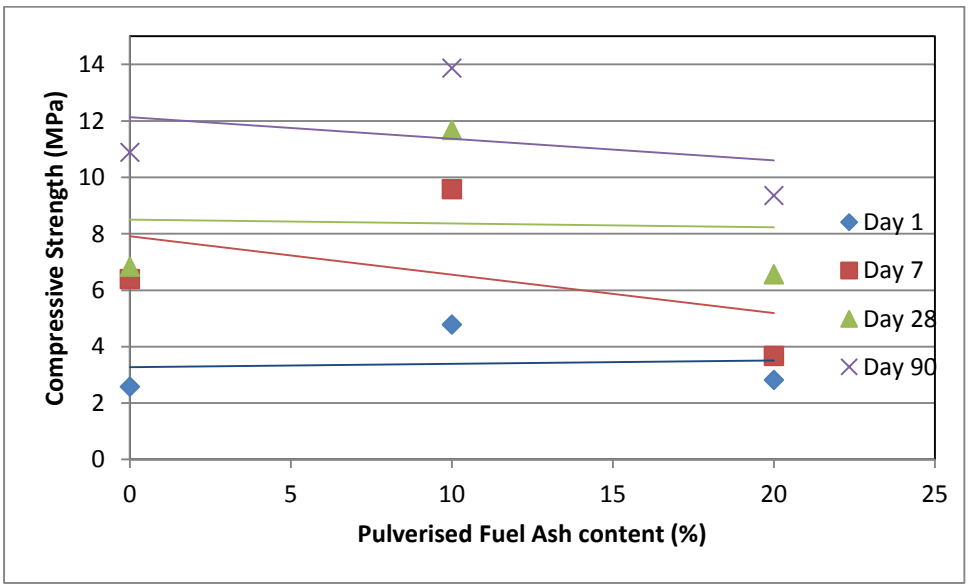

Figure 7.78 Effect of Pulverised Fuel Ash on compressive strength for 532 grade soils with 6% cement content.

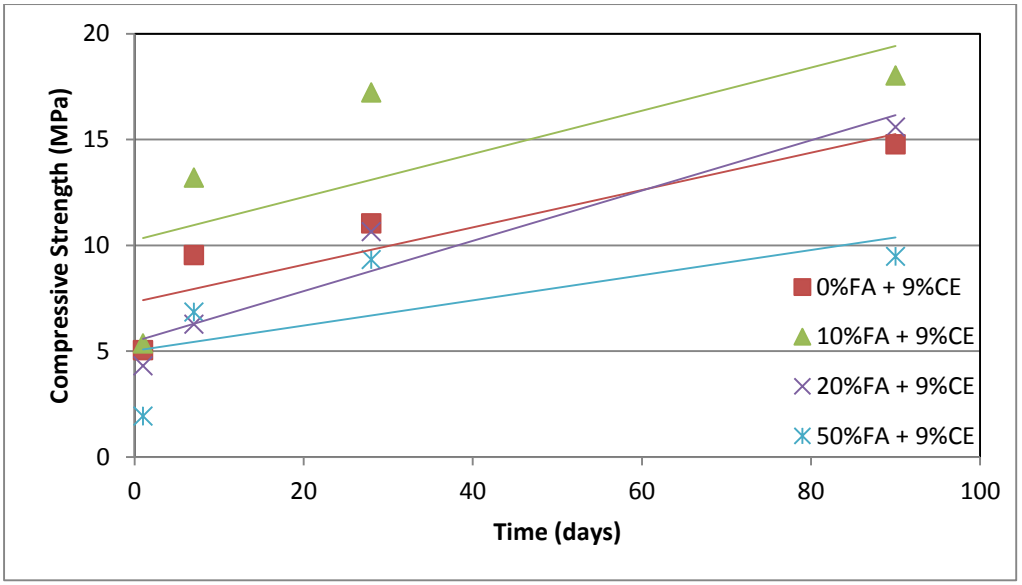

Figure 7.79 Compressive strength propagation for 532 grade soils over 90 days at 9% cement content

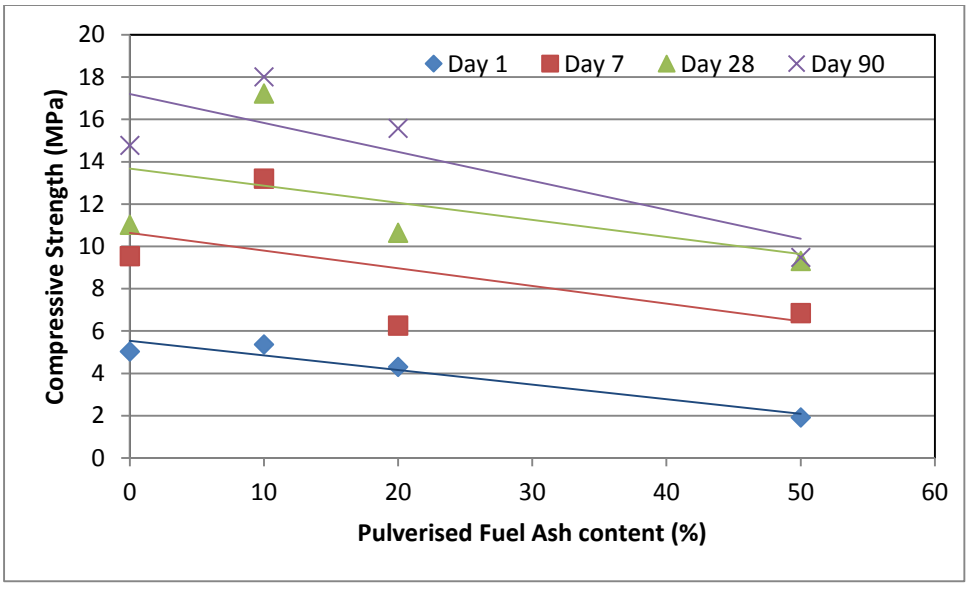

Figure 7.80 Effect of Pulverised Fuel Ash on compressive strength for 532 grade soils with 9% cement content.

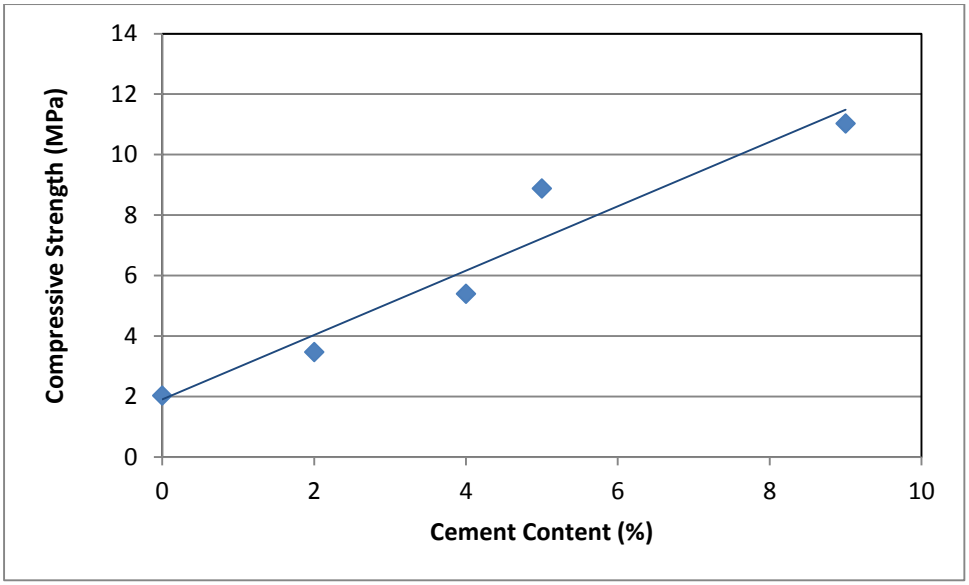

Figure 7.81 Effect of cement stabilisation on compressive strength for 532 grade rammed earth at day 28.

Figures 7.82 to 7.84 show the effect of cement stabilisation on compressive strength. Compressive strength when measured on the 90th day showed a progressive improvement as cement content was increased. Compressive strength grew by 546% when stabilisation was moved from 0% to 9%. Pulverised Fuel Ash was added to the mix (10% and 20%) and this did not seem to have a significant difference on compressive strength.

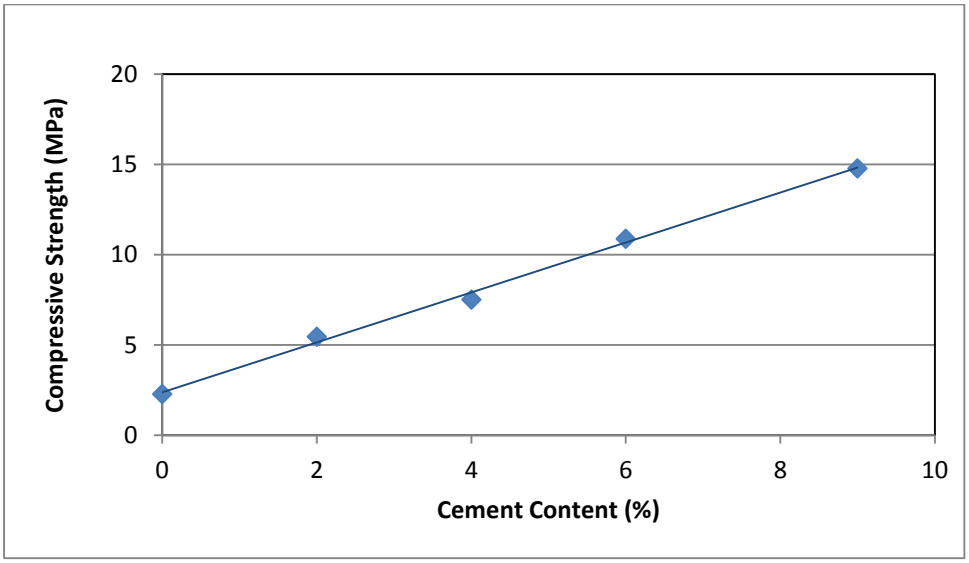

Figure 7.82 Effect of Cement stabilisation on Compressive Strength in 532 soil grade rammed earth at day 90.

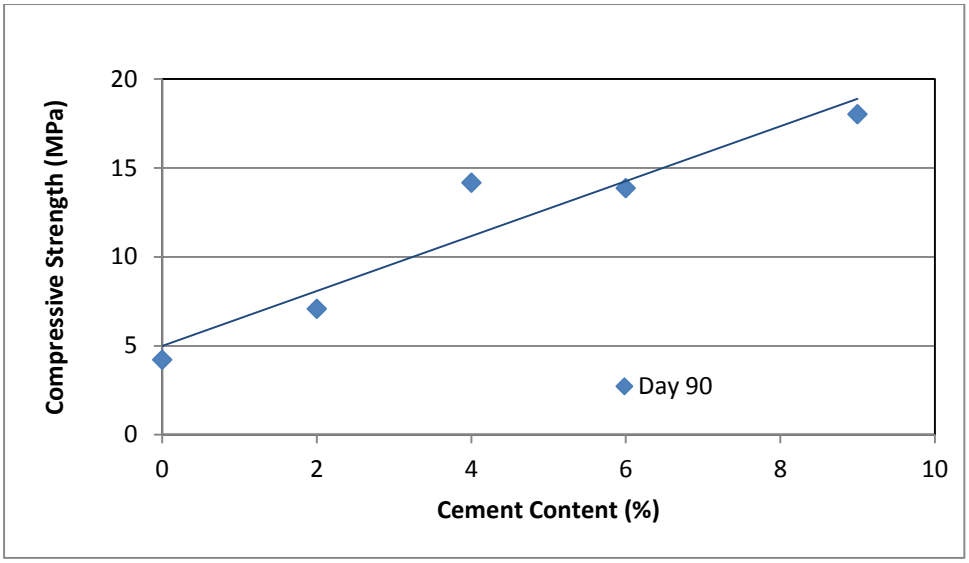

Figure 7.83. Effect of cement stabilisation on compressive strength in 532 soil grade rammed earth containing 10% Pulverised Fuel Ash

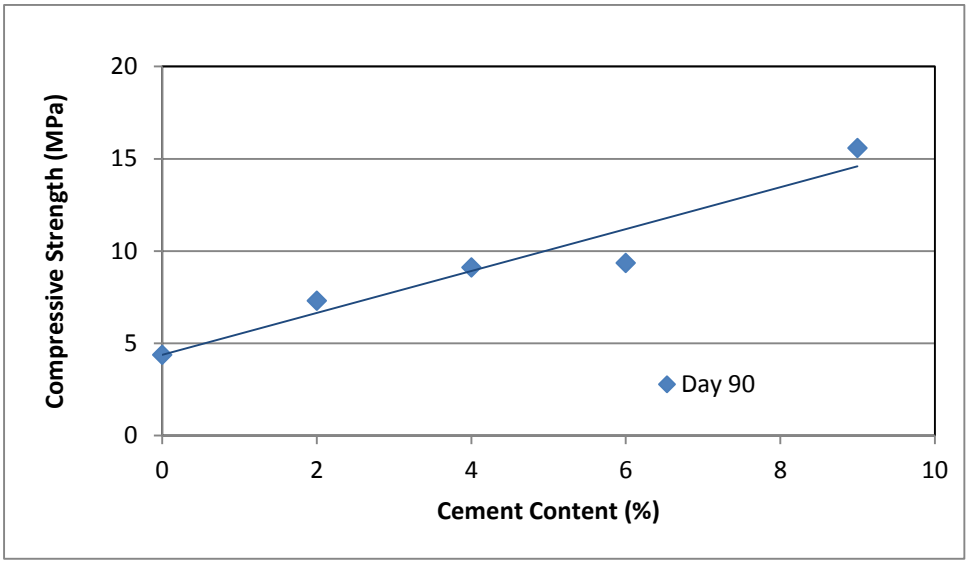

Figure 7.84. Effect of cement stabilisation on compressive strength in 532 soil grade rammed earth containing 20% Pulverised Fuel Ash

7.3.2 Ultra Sonic Pulse Velocity

The UPV values for rammed earth increased with age. Velocities for unstabilised rammed earth increased by 21% by the 7th day of testing. This slowed to 1.5% by the 28th day. Velocity did not improve appreciably after this day. Figure 7.85 shows the sample containing 20% Pulverised Fuel Ash

however showed tremendous improvement in UPV values between day 7 and day 28.

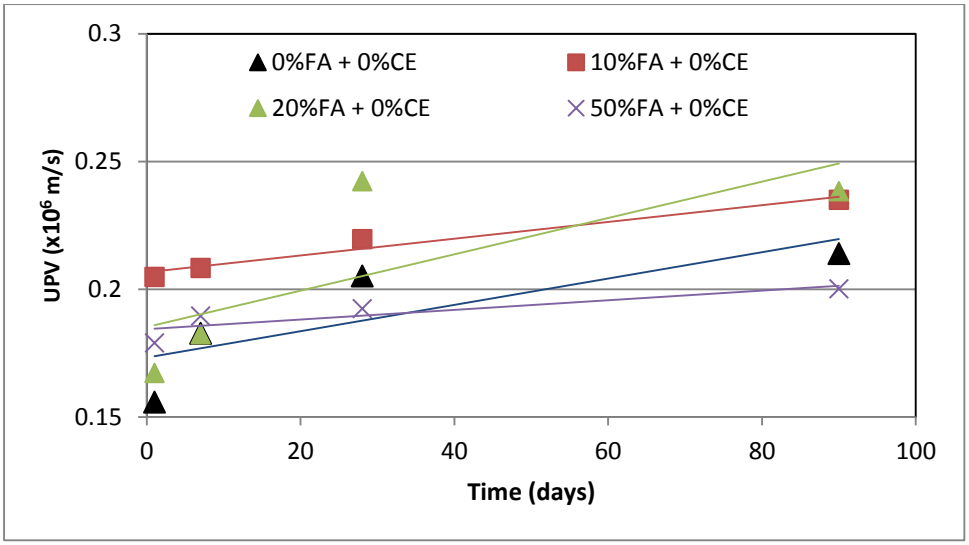

Figure 7.85 UPV values for 532 grade soils over 90 days at zero cement content

When Pulverised Fuel Ash was added to the sample, velocity was observed to increase (Figure 7.86). A 10% Pulverised Fuel Ash content resulted in a 33.6% increase in the UPV value. Increasing Pulverised Fuel Ash further to 20% caused a slight decrease in UPV value after which UPV values started to rise again. Gains in UPV caused by further addition of Pulverised Fuel Ash did not persist past the 7th day.

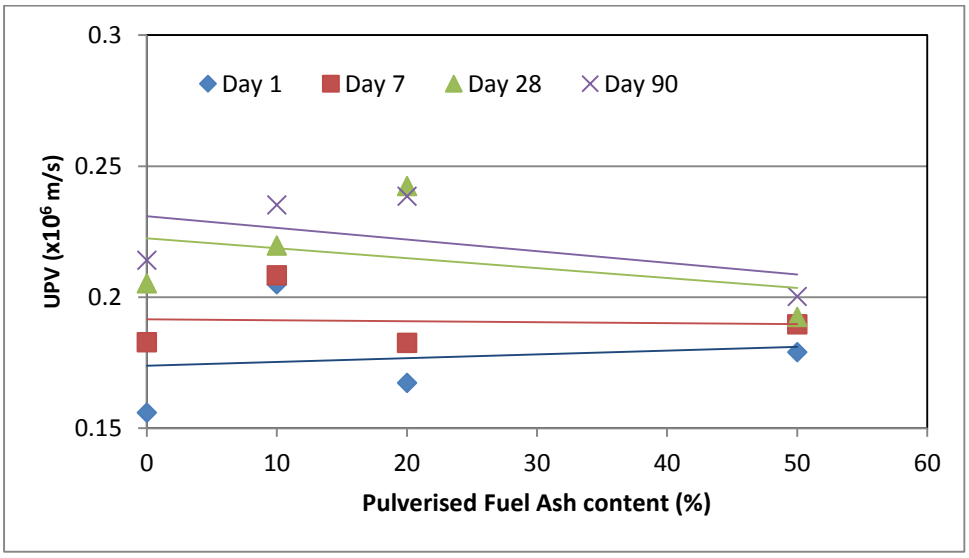

Figure 7.86 Effect of Pulverised Fuel Ash content on UPV in rammed earth made from 532 soil grade

Adding cement to 532 grade rammed earth increased the UPV value at all level of stabilisation. There was no appreciable improvement at higher level of stabilisation (Figure 7.87). While there was a marginal level of improvement at the first day of testing, the 7th day testing revealed very similar results at all levels of stabilisation tested.

When Pulverised Fuel Ash was added to cement stabilised rammed earth, there appeared to be a dampening effect on the improvements that come with cement stabilisation. Increasing Pulverised Fuel Ash content contributed to reducing UPV values. However, velocity values obtained was still higher than that observed for unstabilised rammed earth containing no Pulverised Fuel Ash (Figure 7.88).

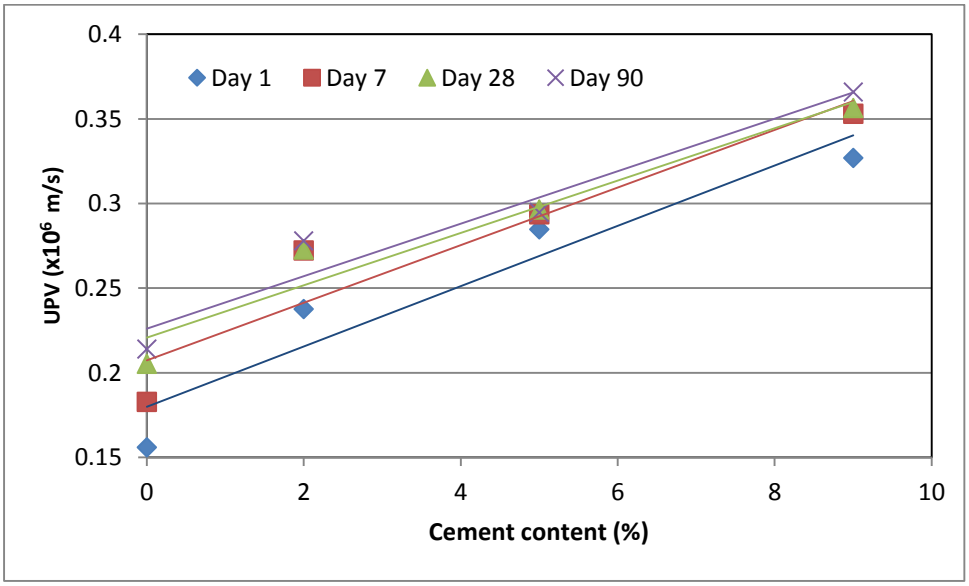

Figure 7.87 Effect of cement stabilisation in UPV in 532 soil grade rammed earth

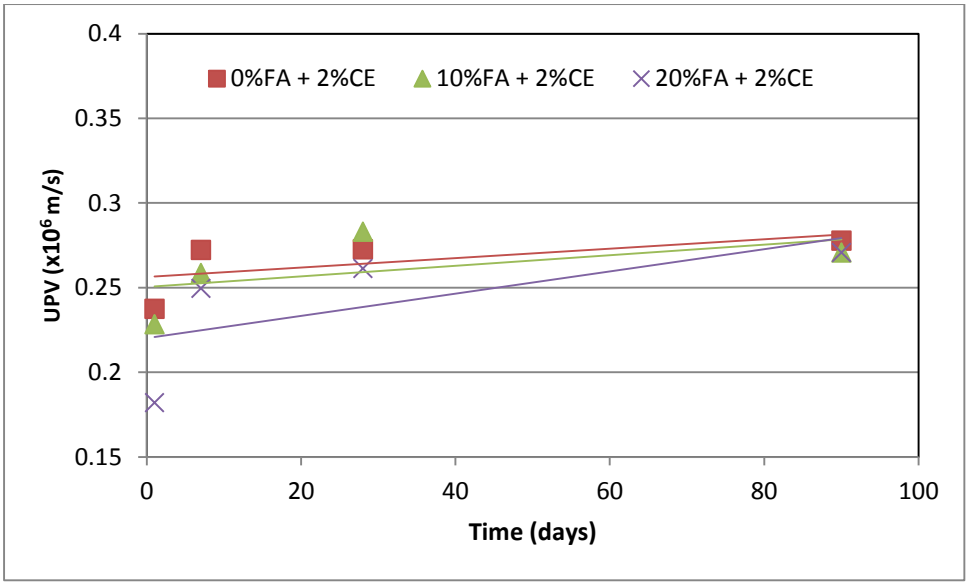

Figure 7.88 Effect on UPV when Pulverised Fuel Ash is added to a 2% cement stabilised 532 grade rammed earth

UPV figures for various cement content and Pulverised Fuel Ash content can be found in figures 7.89 to 7.91. Stabilisation was seen to increase UPV as cement content rose. Adding Pulverised Fuel Ash did not appear to cause any significant difference to the effect stabilisation had on rammed earth made from 532 soil grade.

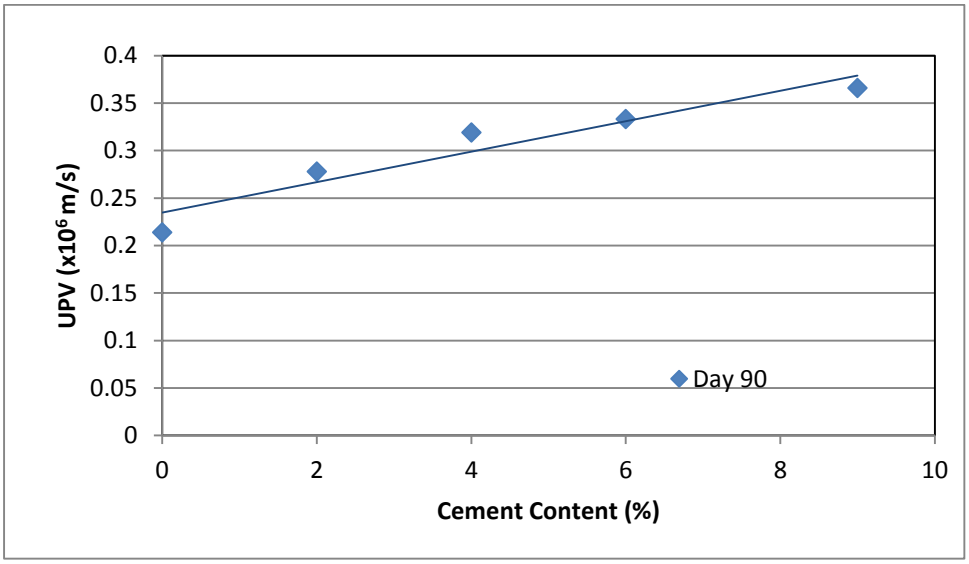

Figure 7.89 Effect of Cement stabilisation on Ultrasonic Pulse Velocity in 532 soil grade rammed earth containing no Pulverised Fuel Ash

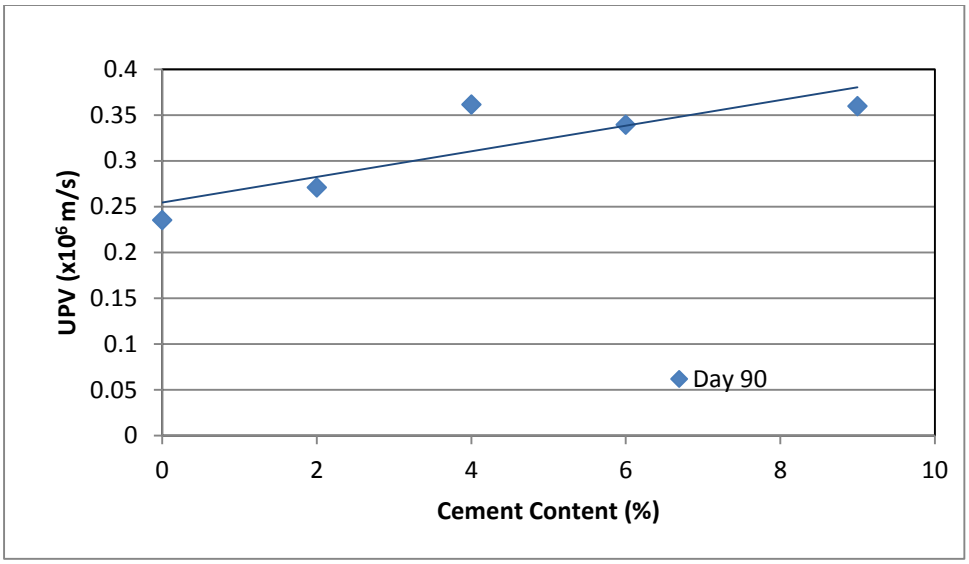

Figure 7.90. Effect of Cement stabilisation on Ultrasonic Pulse Velocity in 532 soil grade rammed earth containing 10% Pulverised Fuel Ash

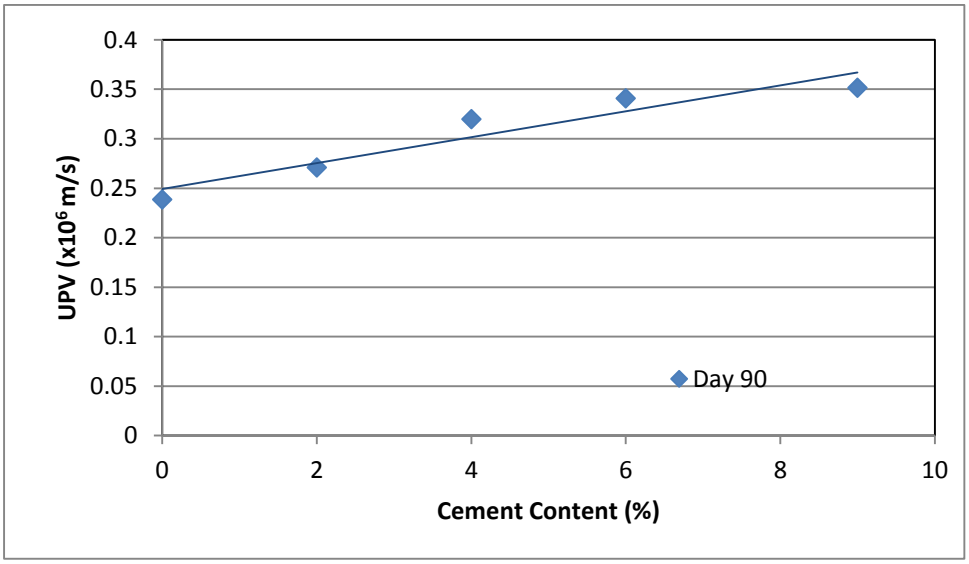

Figure 7.91. Effect of Cement stabilisation on Ultrasonic Pulse Velocity in 532 soil grade rammed earth containing 20% Pulverised Fuel Ash

7.3.3 Density

As expected, adding Pulverised Fuel Ash to 532 grade rammed earth served to reduce density. As the samples aged, density fell but not by a large margin. From demoulding up to day 90 of testing, the unstabilised rammed earth sample had a density drop of only 0.65% (Figure 7.92). The sample containing 10% Pulverised Fuel Ash had a reduction in density of 0.32% after 90 days. 20% Pulverised Fuel Ash content resulted in 3% density reduction over 90 days and adding 50% Pulverised Fuel Ash resulted in rammed earth having 5.9% less density after 90 days.

Density fell by 3.8% when 10% by mass of total sample comprised Pulverised Fuel Ash (Figure 7.93). This figure rose to 8.6% when another 10% of Pulverised Fuel Ash was added to make a total of 20% Pulverised Fuel Ash content. At 50% Pulverised Fuel Ash content, density had fallen by 23.7%.

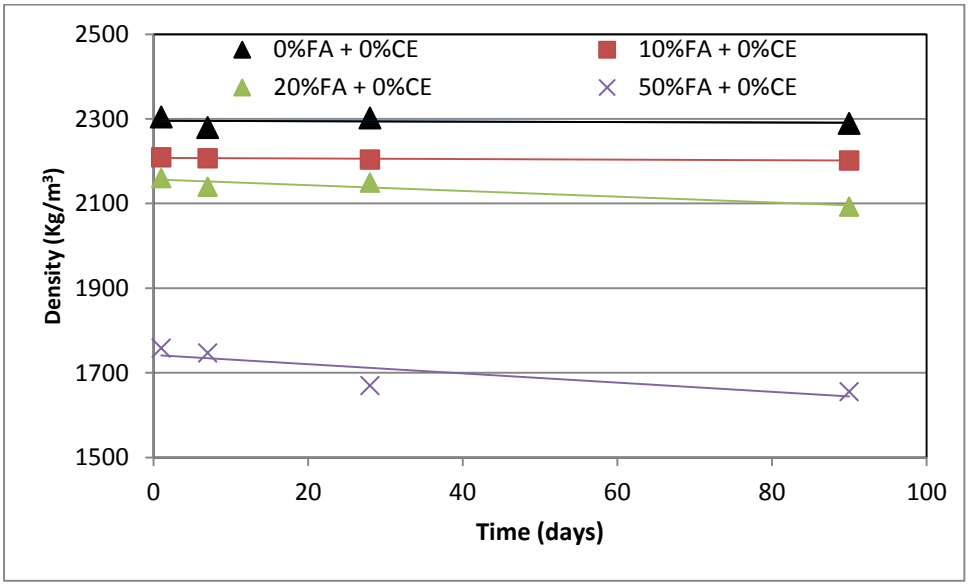

Figure 7.92 Density change with age in 532 grade rammed earth

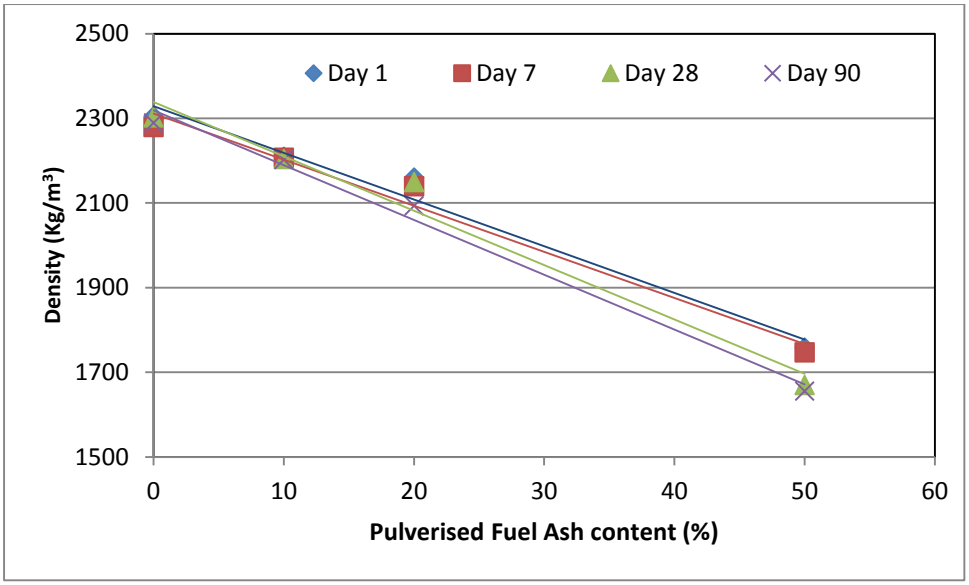

Figure 7.93 Effect of Pulverised Fuel Ash content on density in rammed earth made from 532 soil grade

Adding Cement to the mix resulted in lowering density until a point where further addition of cement resulted in increasing density. From Figure 7.94, it can be seen that 2% cement stabilisation resulted in decreasing density by 3.5% when tests were carried out at day 90. Further stabilisation resulted in a more dense material. Stabilising by 9% cement resulted in increasing density by 2.6%.

For samples made from 532 soil grade material, density increased with stabilisation marginally (1%) when no Pulverised Fuel Ash was present. Adding Pulverised Fuel Ash to the sample had a different effect depending on how much Pulverised Fuel Ash was added. At 10% Pulverised Fuel Ash content, increasing stabilisation results in a decrease in density of 1.4% when stabilisation goes from 0 to 9%. At 20% Pulverised Fuel Ash content however, density remained relatively unchanged. This can be observed in figures 7.95 to 7.97.

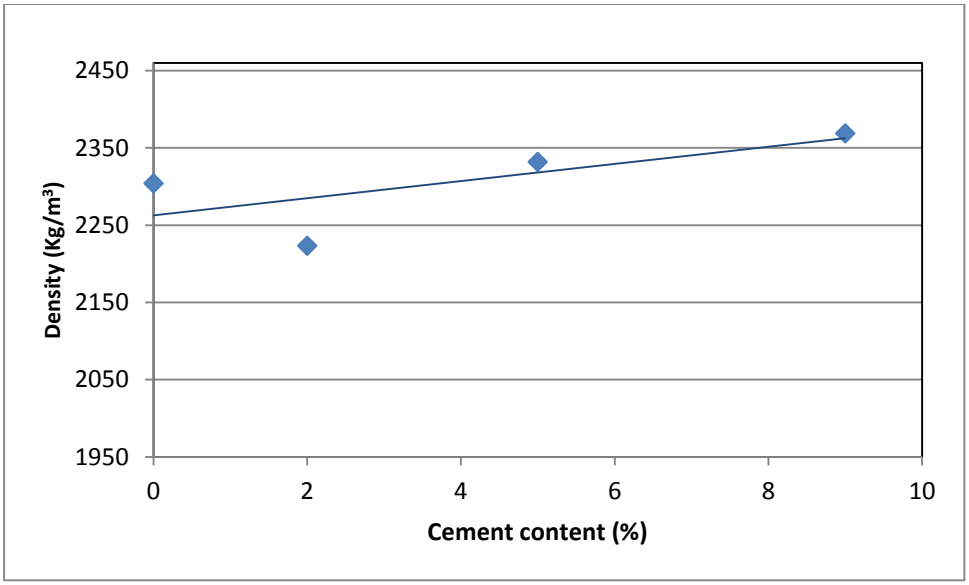

Figure 7.94 Effect of cement stabilisation in density in 532 soil grade rammed earth

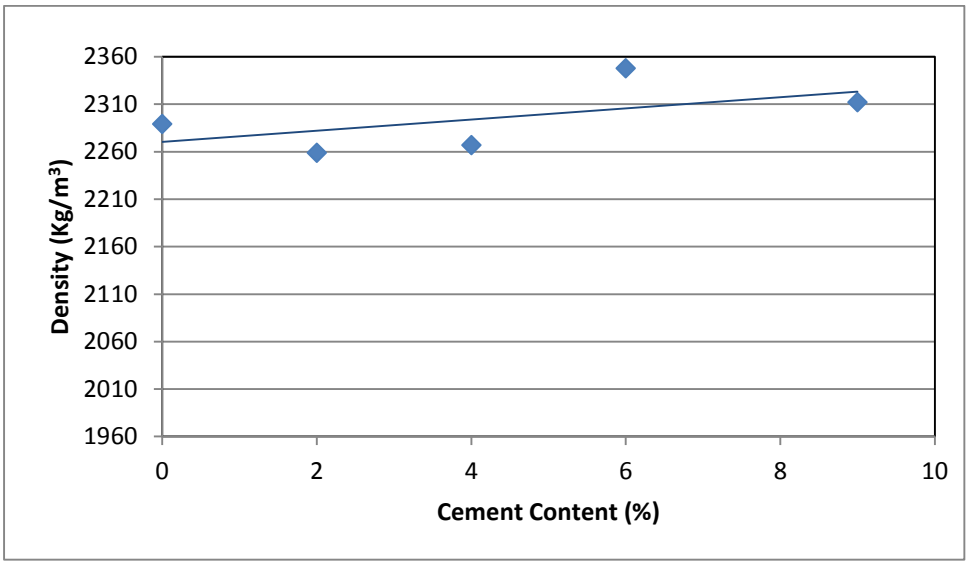

Figure 7.95. Effect of Cement stabilisation on Density in 532 soil grade rammed earth containing no Pulverised Fuel Ash

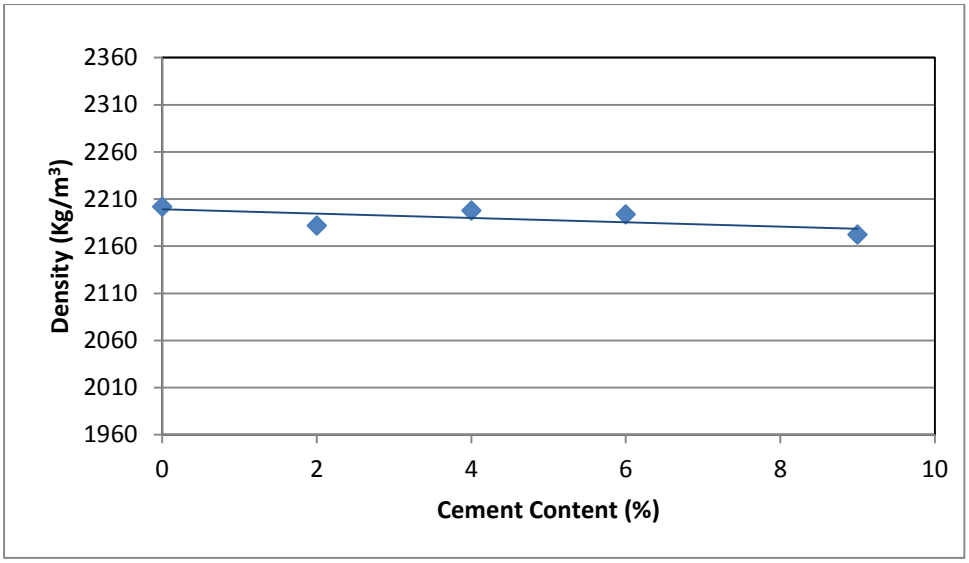

Figure 7.96. Effect of Cement stabilisation on Density in 532 soil grade rammed earth containing 10% Pulverised Fuel Ash

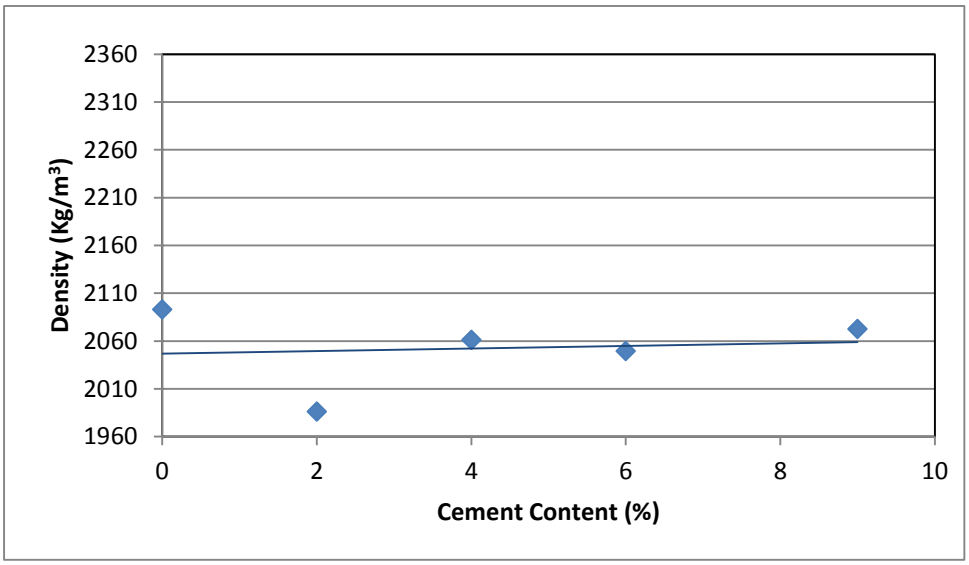

Figure 7.97. Effect of Cement stabilisation on Density in 532 soil grade rammed earth containing 20% Pulverised Fuel Ash

7.3.4 Initial Rate of Suction

Water absorption tests were carried out for samples that contain Pulverised Fuel Ash. Figures 7.98 to 7.100 show the test result for soil grade 532

containing various proportions of Pulverised Fuel Ash and stabilised to different degrees.

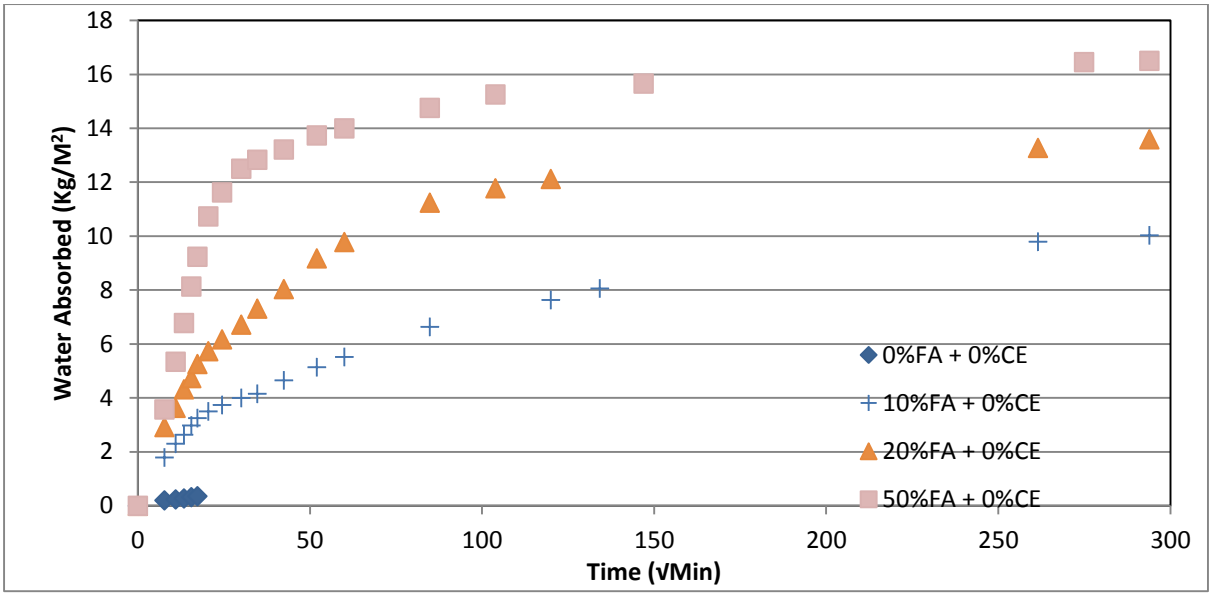

Figure 7.98 Comparison of the water absorption properties of 532 soil with increasing Pulverised Fuel Ash.

Increasing the content of Pulverised Fuel Ash also served to increase the total average amount of water absorbed. As can be observed in figure 9.6, the samples without Pulverised Fuel Ash did not retain structural integrity up to the maximum testing time of 24 hours. However, it can be seen to have a lower initial rate of sorption. The sample tested at 24 hours with the least total average absorbed water was the sample containing the lowest quantity of Pulverised Fuel Ash. At 24 hours, the sample containing 10% Pulverised Fuel Ash had a total average water absorption of 10.04 kg/m^2. Increasing the Pulverised Fuel Ash quantity to 20% and 50% respectively also increases the total average absorption to 13.6 kg/m^2 and 16.5 kg/m^2 respectively. This represents an increase of 35.5% and 64% respectively. Results were similar when cement was used to stabilise the sample.

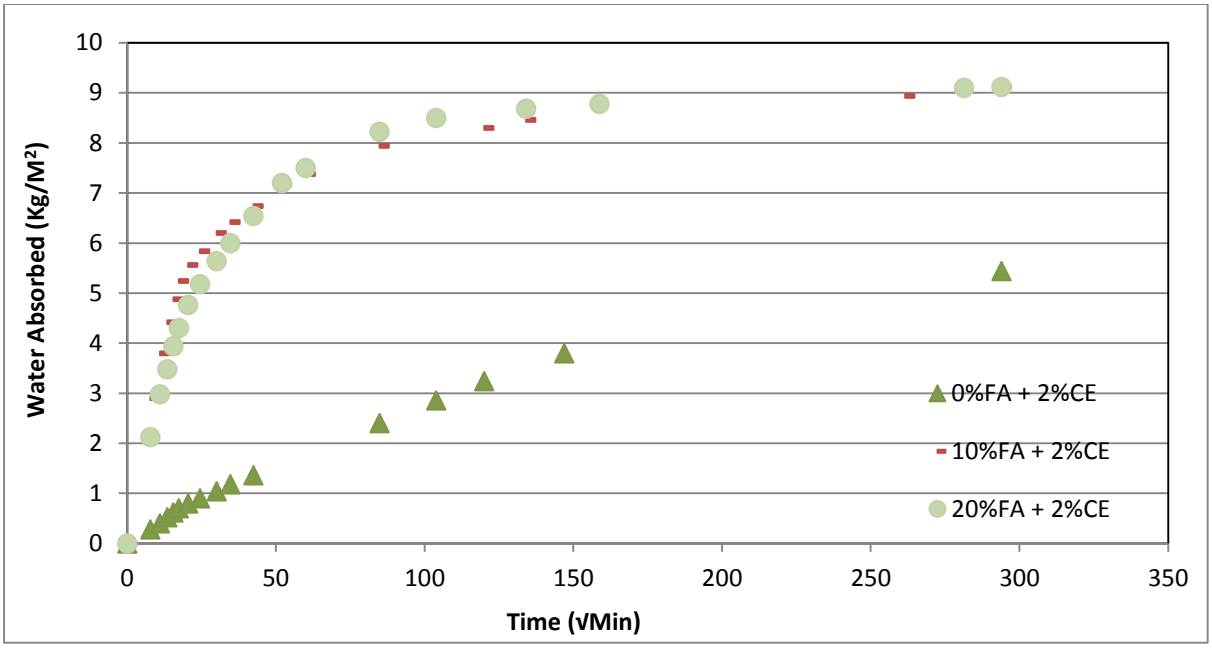

(a)

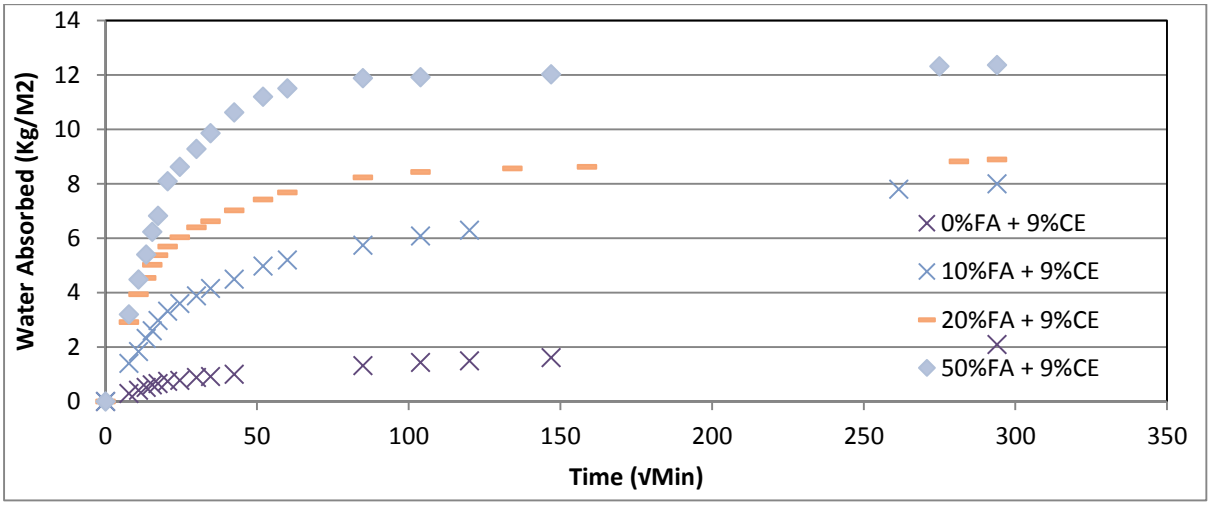

(b)

Figure 7.99 Comparison of the water absorption properties of 532 soil with increasing Pulverised Fuel Ash at (a) 2% cement stabilisation, (b) 9% cement stabilisation.

It can be observed from figure 7.98 that at low levels of cement stabilisation (2%), water absorption increases as Pulverised Fuel Ash content increases. This trend continues even at higher levels of stabilisation (9%). It can also be observed that just as has been mentioned in an earlier section, total average

amount of sorbed water reduces with increasing levels of stabilisation. Figure 7.99 however shows that the difference in absorbed water is less with cement stabilisation.

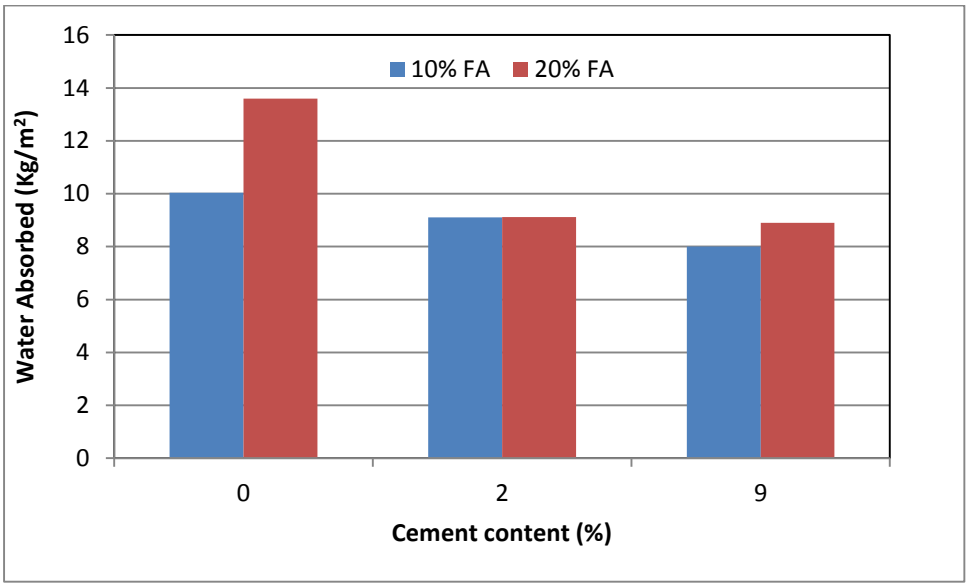

Figure 7.100 Effect of cement content on water absorption on 532 soil grade samples.

It can be seen from figures that sorptivity tends to increase with increase in Pulverised Fuel Ash content as observed in the total value of sorbed moisture after 5 minutes of testing time.

Given the fact that Pulverised Fuel Ash is made up of clay size particles without the adhesive properties, it can be argued that the micro pore structure that forms as a result of increase in Pulverised Fuel Ash content provides better capillary channels through which moisture migrates into the sample.

Addition of 10% Pulverised Fuel Ash has a profound effect on sorptivity as it is increased by 821%. Further raising the Pulverised Fuel Ash content by 10% to a total of 20% results in a further increase in the measure of sorptivity by 60%. A 50% addition of Pulverised Fuel Ash appeared to raise sorptivity further by 79% as observed in Figure 7.101 and 7.102.

When the 532 grade sample was stabilised with cement, we observe that the sorptivity properties were affected by the blend of cement to Pulverised Fuel Ash. Figure 9.17 shows very little difference

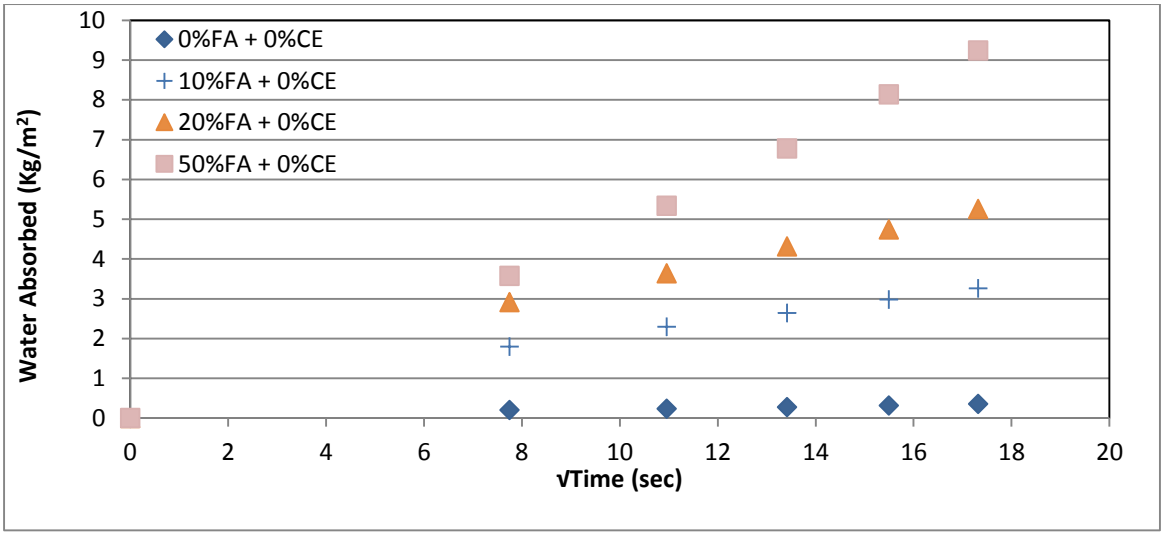

Figure 7.101 Initial rate of sorption for rammed earth, grade 532 containing Pulverised Fuel Ash

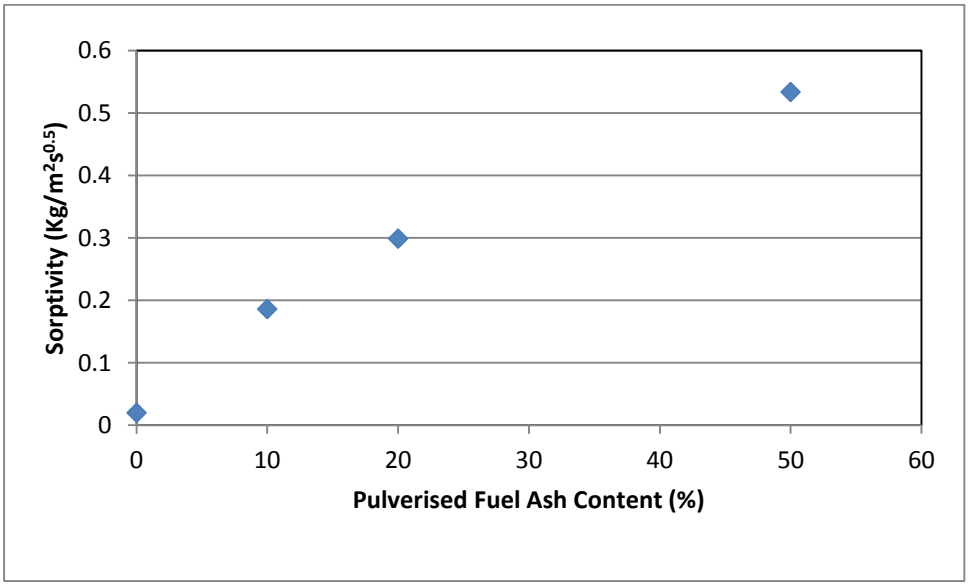

Figure 7.102 Sorptivity at various Pulverised Fuel Ash content for unstabilised 532 grade rammed earth

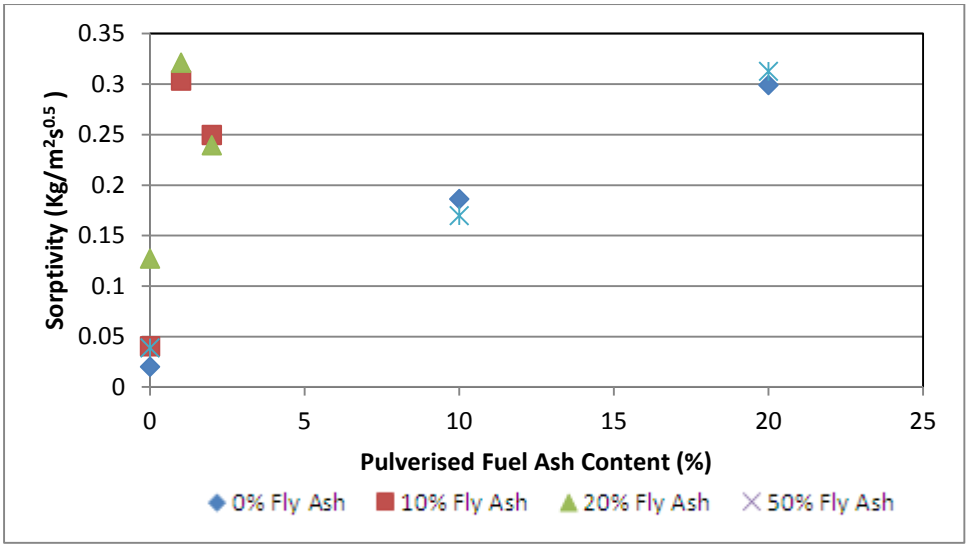

Figure 7.103 Effect of Pulverised Fuel Ash content on cement stabilised grade 532 rammed earth

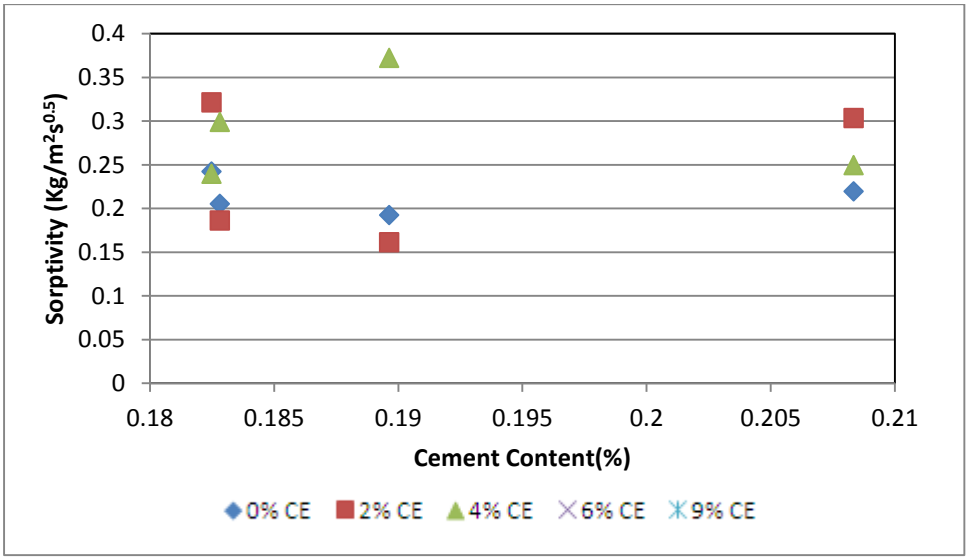

Figure 7.104 Effect of Cement content on Grade 532 Rammed Earth containing Pulverised Fuel Ash

7.3.5 Further Discussions

Figures 7.105 to 7.113 show the correlation in various properties of 532 soil grade rammed earth. When compressive strength was measured against ultrasonic pulse velocity, a positive correlation was found to exist.

For sorptivity values for unstabilised rammed earth and rammed earth stabilised by 9% Cement content. In Figure 7.103, we observe that sorptivity

values became more unpredictable as Pulverised Fuel Ash content increased. When the sample contained no Pulverised Fuel Ash, sorptivity rose and crested at 6% cement content then fell to a level very close to that obtainable for unstabilised samples.

When cement was added to samples that contained 10% Pulverised Fuel Ash, the pattern was almost repeated except sorptivity was generally higher and crested closer to 4% cement content. At 6% stabilisation, sorptivity appeared to be better than an unstabilised position with sorptivity falling by about 13%. However further addition of cement stabiliser seemed to increase stabilisation further. Adding cement to rammed earth having 20% Pulverised Fuel Ash appeared to have the same effect as further stabilising a 10% Pulverised Fuel Ash filled sample beyond the 9% stabilised position. Sorptivity is seen to fall with increased dosage of cement up to about 4% where it starts to rise upon further addition of cement. There is another crest at 6% cement content where sorptivity starts to fall again. At 9% cement stabilisation, sorptivity is once again very close to the unstabilised value.

It would appear that for all samples of rammed earth, stabilising with 9% cement does not change the sorptivity value significantly from the unstabilised position regardless of the level of Pulverised Fuel Ash in the sample.

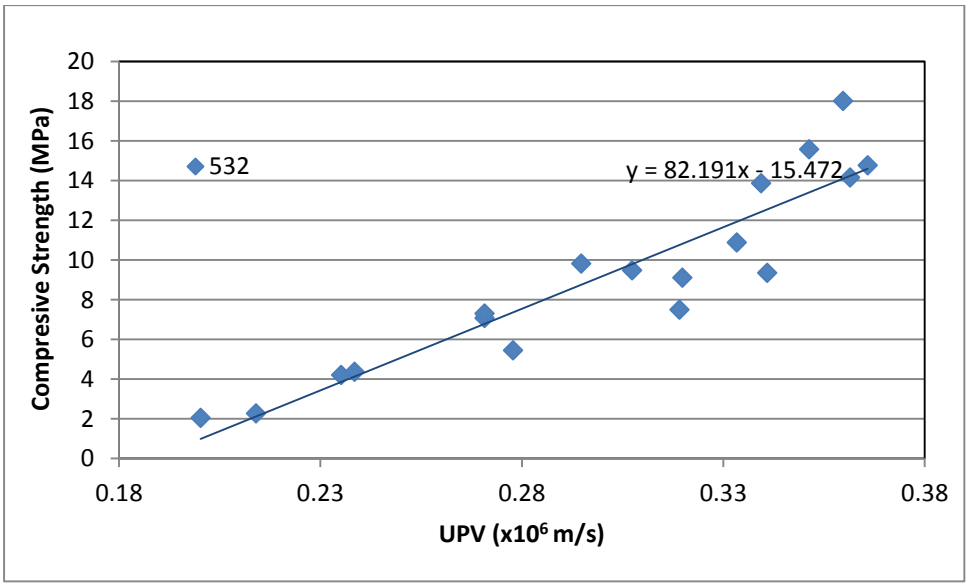

Figure 7.105 Correlation between compressive strength and UPV in 532 soil grade

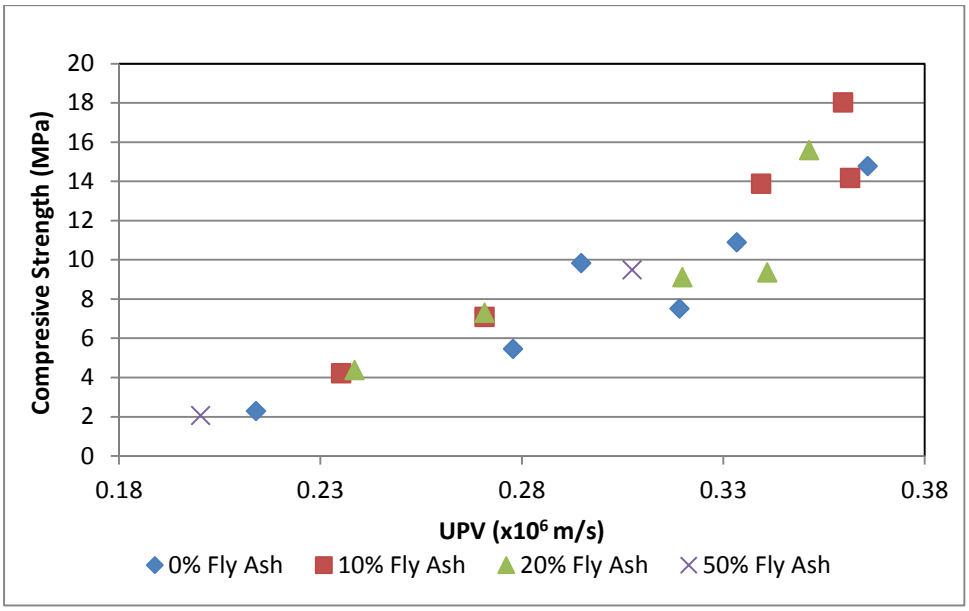

Figure 7.106 Compressive strength vs UPV in 532 soil grade (showing Pulverised Fuel Ash distribution)

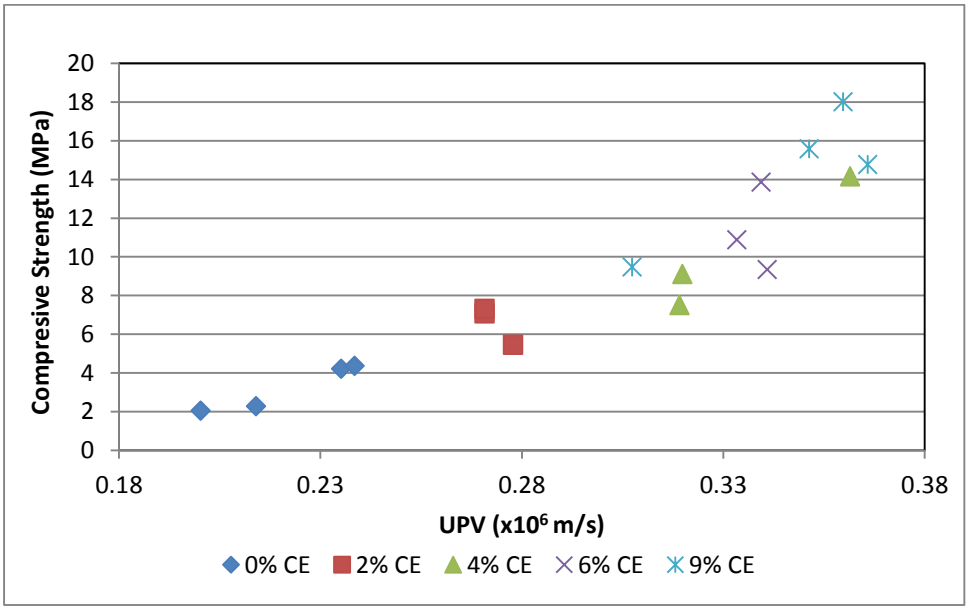

Figure 7.107 Compressive strength vs UPV in 532 soil grade (showing cement distribution)

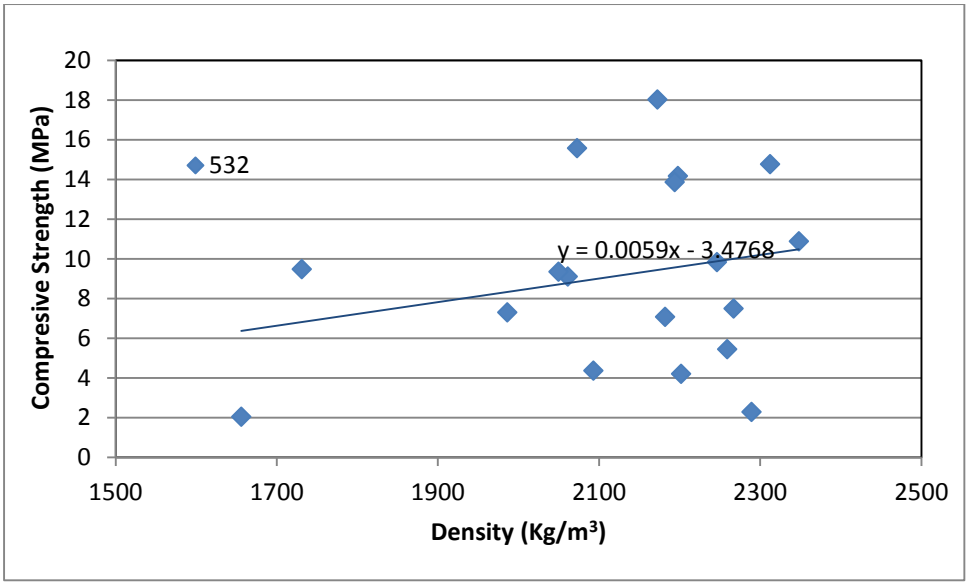

Figure 7.108 Correlation between compressive strength and density in 532 soil grade

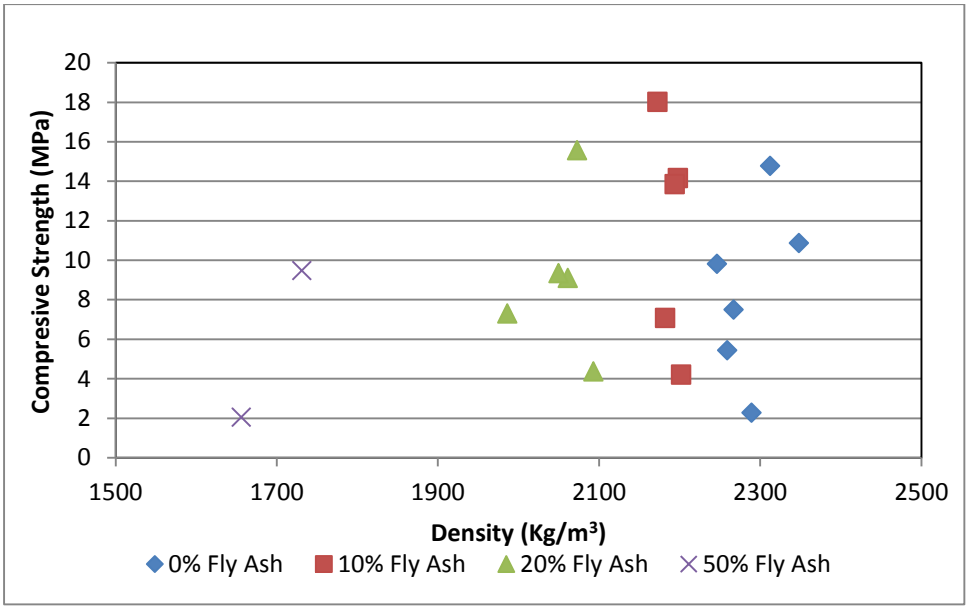

Figure 7.109 Compressive strength vs density in 532 soil grade (showing Pulverised Fuel Ash distribution)

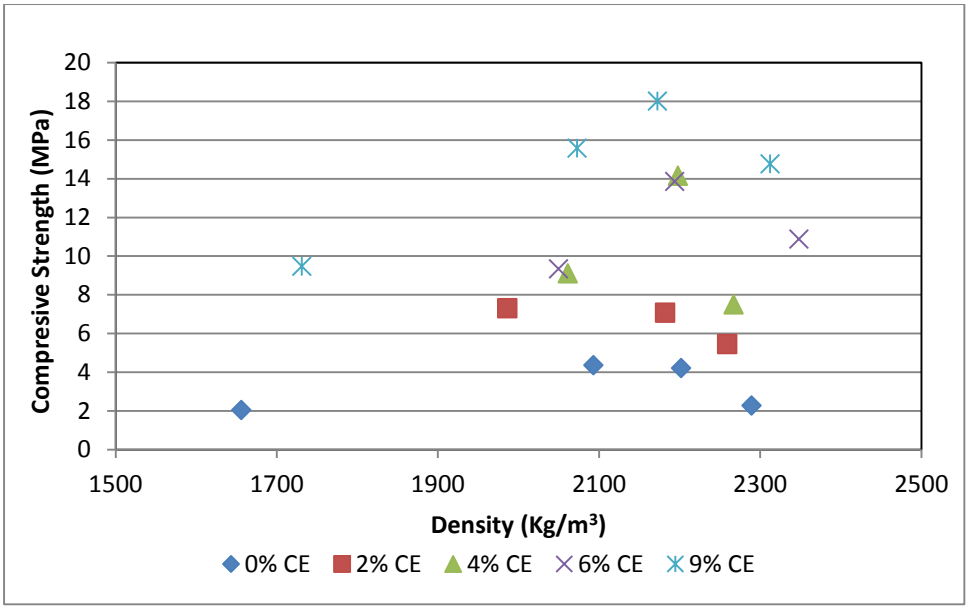

Figure 7.110 Compressive strength vs density in 532 soil grade (showing cement distribution)

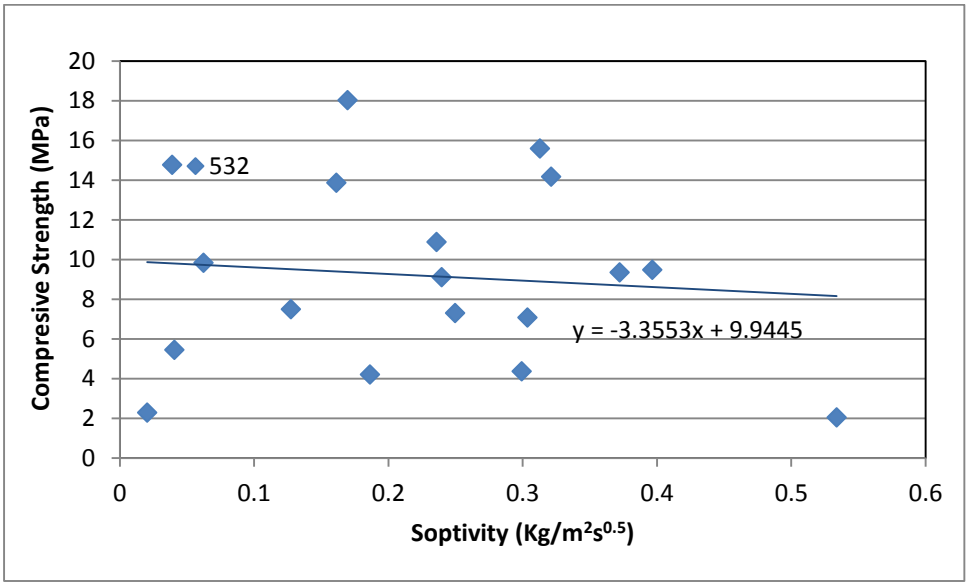

Figure 7.111 Correlation between compressive strength and sorptivity in 532 soil grade

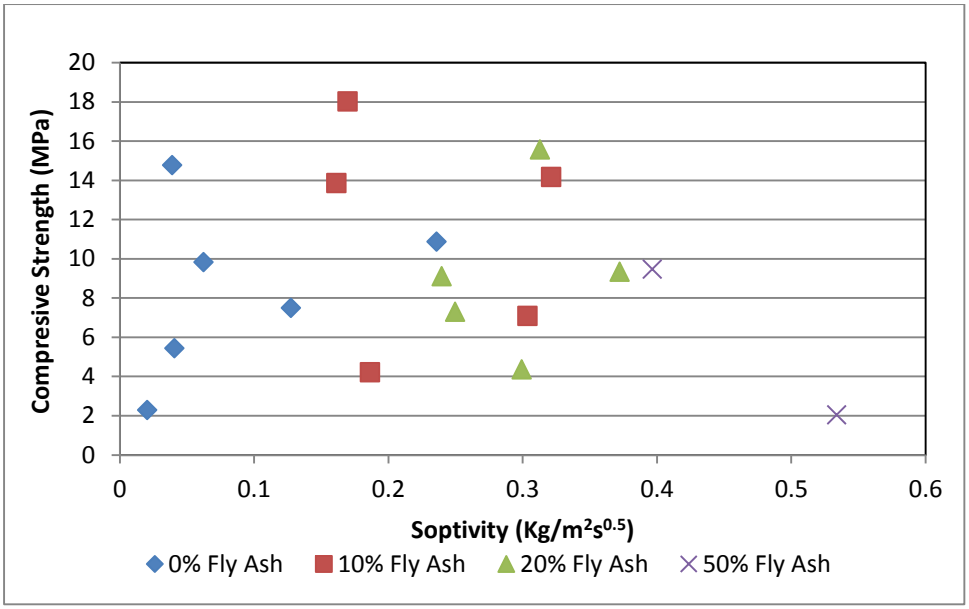

Figure 7.112 Compressive strength vs density in 532 soil grade (showing Pulverised Fuel Ash distribution)

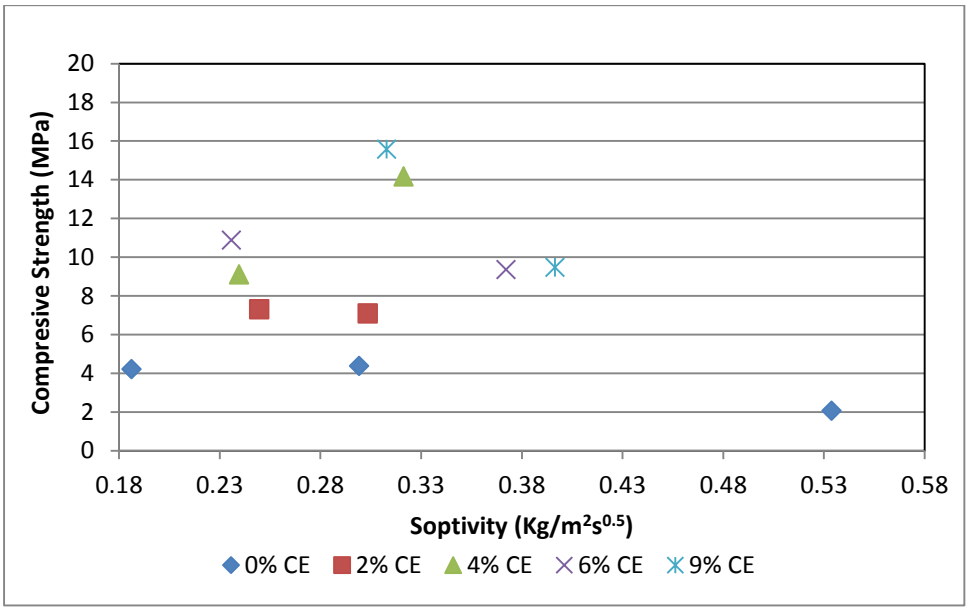

Figure 7.113 Compressive strength vs density in 532 soil grade (showing cement distribution)

The faster a sound wave could travel through the sample, the higher the compressive strength was expected to be. For this same sample, increasing density was also found to have a positive effect on compressive strength.

Compressive strength however correlates negatively with Sorptivity and suggests that samples that are more prone to water ingress will be expected to have a corresponding decline in compressive strength when measured on the 90th day. There is an even spread across the spectrum when compressive strength is measured against ultrasonic pulse velocity. When density and sorptivity were each measured against compressive strength, the results show clear cut boundaries between samples at different Pulverised Fuel Ash content. Higher Pulverised Fuel Ash content results in lower density but also lower compressive strength. The highest compressive strength is observed sample containing 10% Pulverised Fuel Ash having the lowest density. Samples containing no Pulverised Fuel Ash have maximum compressive strength at maximum density. Sorptivity increased with increase in Pulverised Fuel Ash content. At low or zero Pulverised Fuel Ash content, sorptivity was lowest for samples that had the highest compressive strengths.

Chapter Eight

Prediction of Water Ingress in Rammed Earth

It is possible to predict capillarity and diffusion using the Capillary-Diffusive Theory as discussed in section 2.11 of chapter 2, this chapter verifies that rammed earth produced in these test conforms to the curve generated when the formula is represented graphically. This section also looks to determine if the addition of PKS or Pulverised Fuel Ash distorts the expected outcome in any way.

Formula (villar-cocina et al. 2002) presents the equation to be replicated

$$\frac{M}{A} = N\rho\left(1 - exp\left(\frac{-St^{\frac{1}{2}}}{N\rho}\right)\right)$$

$$+C_0 L\left(1 - \frac{8}{\pi^2}\sum_{n=0}^{\infty}\frac{1}{(2n+1)^2}exp\left(-\frac{(2n+1)^2\pi^2 Dt}{4L^2}\right)\right) \qquad (8.1)$$

Here,

N = Constant related to the distance from the concrete surface over which capillary pores control the initial sorption

P = Density of water

D= Diffusion coefficient

S= Sorptivity coefficient

C = Water concentration

t = Time.

C_0 = invariance of water concentration

The first part of the equation (equation 8.2) refers to the part of water ingress that is primarily controlled by capillary absorption.

$$N\rho\left(1 - exp\left(\frac{-St^{\frac{1}{2}}}{N\rho}\right)\right) \qquad (8.2)$$

This part of the equation strongly influences moisture migration in the first few minutes and is usually measured for using the initial rate of suction procedure.

$$C_0 L\left(1-\frac{8}{\pi^2}\sum_{n=0}^{\infty}\frac{1}{(2n+1)^2}exp\left(-\frac{(2n+1)^2\pi^2 Dt}{4L^2}\right)\right) \quad (8.3)$$

The second part of the equation (equation 9.3), defines the parameters responsible for diffusion within the sample. This part of the equation controls moisture migration over a longer period of time.

These values are used in the tables below.

8.1 Prediction by soil Grade

Various soil grades without any additives were tested using the model described above.

Table 8.1 Predictive values for unstabilised soils using the capillary-diffusive model

Sample name	Soil type	N	S	Co	D	R2
532-0FA0CE	532	1.999762	0.497531	100.0004	0.00005	0.983006
622-0KS0CE	622	9.994451	1.571418	4.904603	0.208824	0.991767
451-0FA0CE	451	49.99915	1.660599	29.85893	3.808802	0.975399
721-0FA0CE	721	49.19337	2.909074	23.19685	0.292386	0.999977

Table 8.1 Shows the values obtained using the Capillary-Diffusive model. Parameters as described above are derived from the model and when plugged into the equation, provide curves that can be compared to that obtained experimentally. These are shown in figures 8.1 to 8.4.

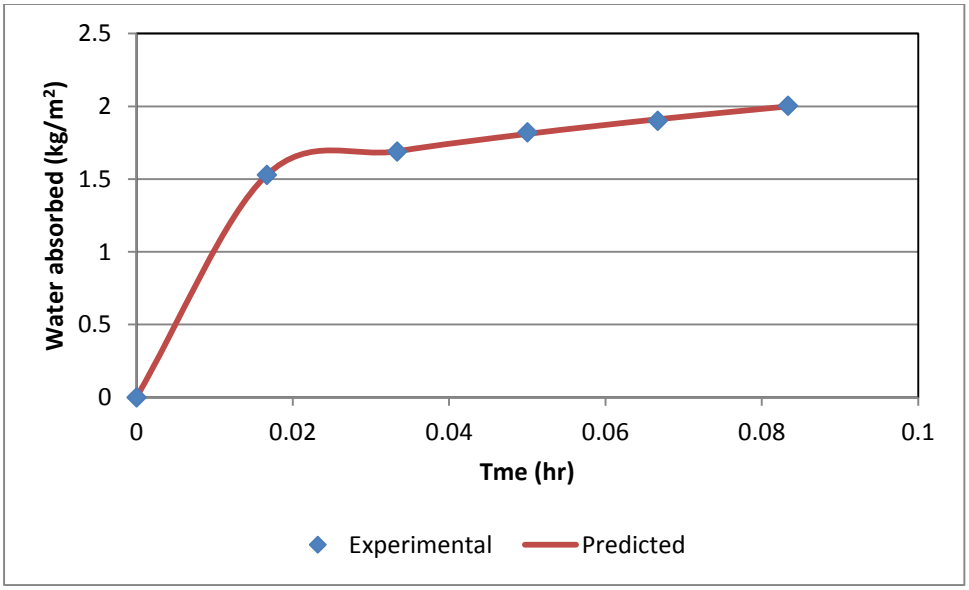

Figure 8.1 Sample 721-0FA0CE time dependent water absorption. Theoretical and experimental

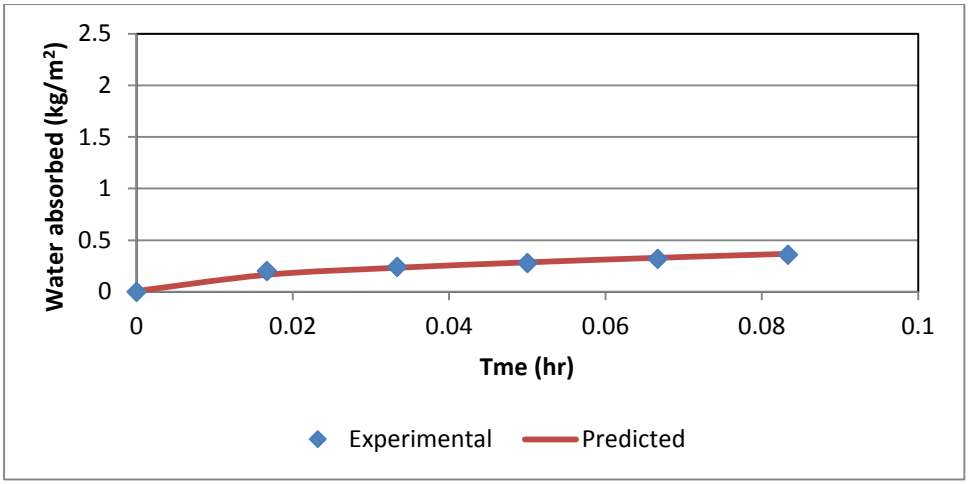

Figure 8.2 Sample 532-0FA0CE time dependent water absorption. Theoretical and experimental

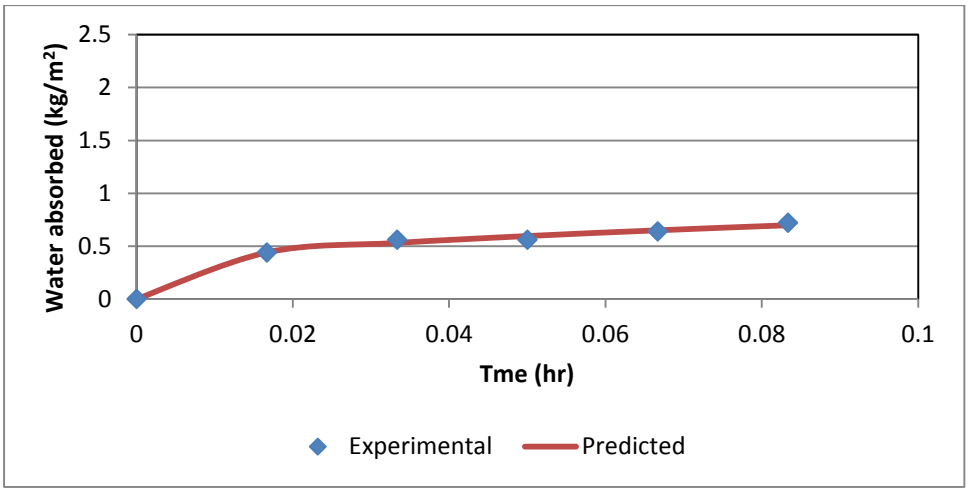

Figure 8.3 Sample 622-0KS0CE time dependent water absorption. Theoretical and experimental

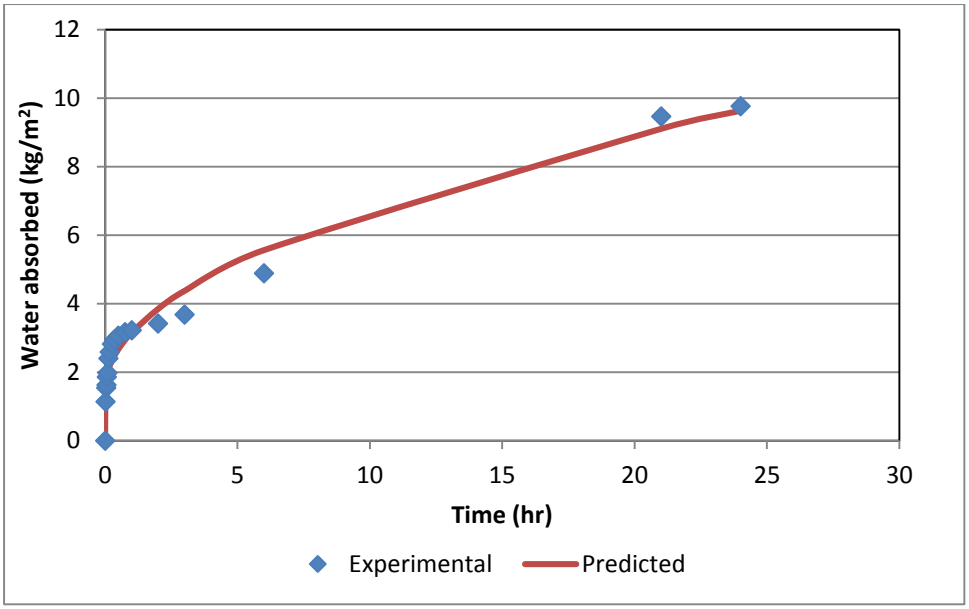

Figure 8.4 Sample 451-0FA0CE time dependent water absorption. Theoretical and experimental

It can be seen from Figures 8.1 to 8.4 that unstabilised rammed earth samples closely follow the prescribed model. Maximum absorption for the test period cannot be compared between all samples as most of them did not retain structural integrity at 24 hours of testing. However, actual Sorptivity has been compared to 'S' – the constant relating to the coefficient of Sorptivity as observed in Figure 8.5 and 8.6.

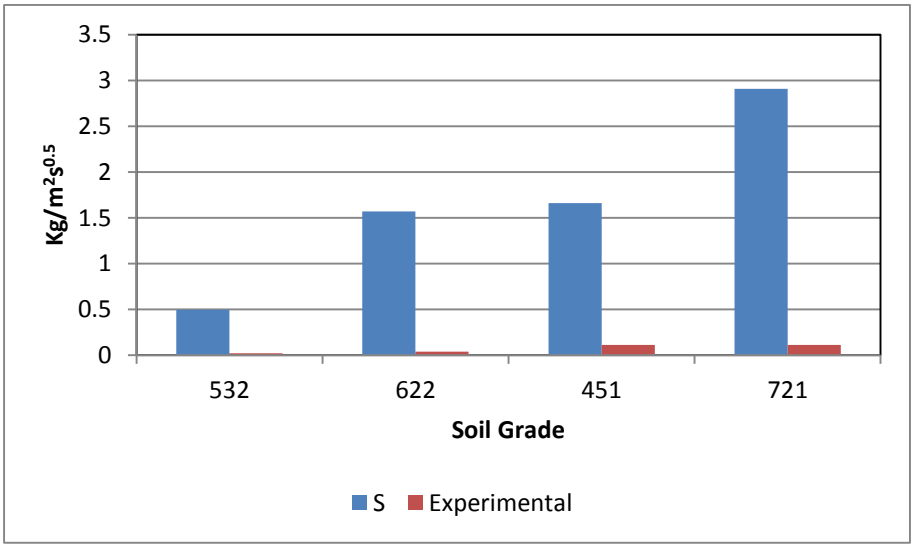

Figure 8.5 Comparison between Sorptivity and 's' values in various rammed earth mixes

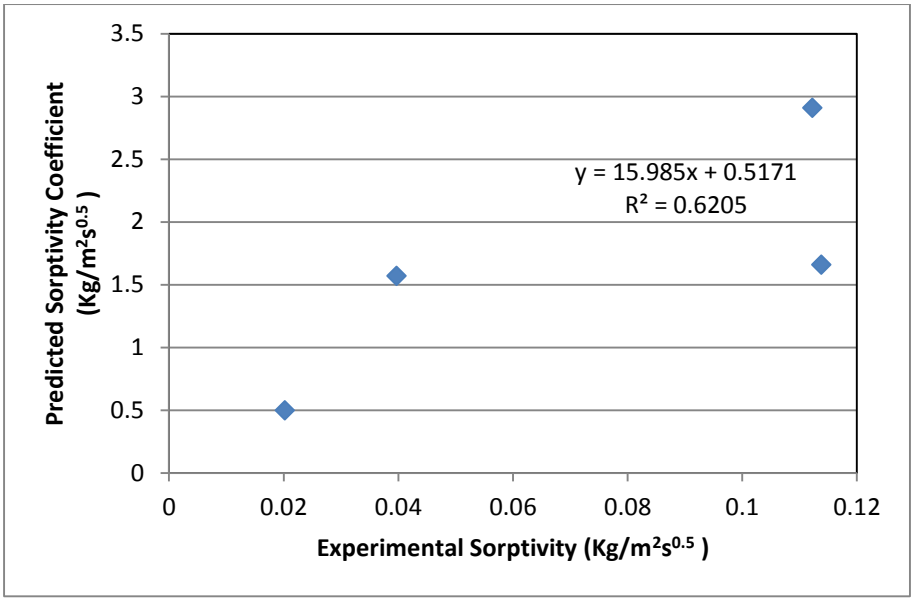

Figure 8.6 Correlation between experimental Sorptivity and theoretical 's' values in various rammed earth mixes

While the sample representing a very clayey blend exhibited the most propensity for absorption by having the highest sorptivity value, it is discovered to have the second highest 'S' values. This confirms that the sorptivity value as measured experimentally includes other elements such as diffusivity (even though this does not dominate the initial part of moisture intake).

8.2 Prediction by PKS Content

The amount of Palm Kernel Shell contained in a sample appeared to affect sorptivity.

Table 8.2 Predictive values for rammed earth containing PKS using the capillary-diffusive model

Sample	soil type	Additions	N	S	Co	D	R2
622-OKS0CE	622	Nil	9.994451	1.571418	4.904603	0.208824	0.991767
622-10KS0CE	622	10% PKS	0.008843	6.814881	22.81192	0.000121	0.997583
622-50KS0CE	622	50% PKS	0.011819	2.495739	13.92493	0.000063	0.997412
622-90KS0CE	622	90% PKS	0.05	0.953	79.58704	0.001141	0.980656
622-100KS0CE	622	100% PKS	1.989889	0.864449	80.05997	0.00066	0.928852

Table 8.2 provides values for parameters needed in the Capillary-Diffusive models for samples containing Palm Kernel Shell. Predictive patterns for the 'S' value is much closer to experimental curves as a 10% PKS content acts to increase Sorptivity and is immediately followed by a fall in Sorptivity on further addition of PKS as observed. The total value of sorbed water is highest in the sample containing 10% PKS as compared with available values.

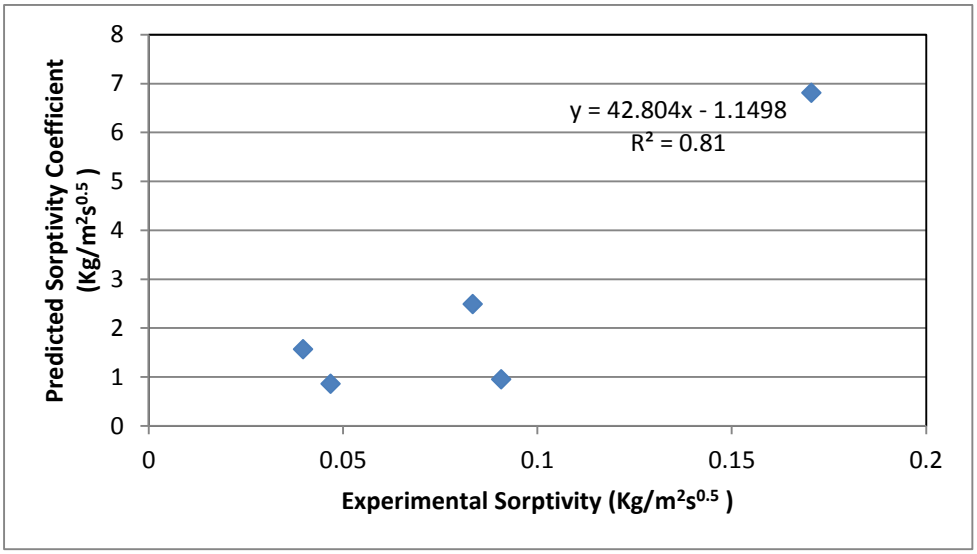

Figure 8.7 Comparison between experimental Sorptivity and 's' values for samples containing PKS

Figures 8.8 to 8.12 show how close the experiments fit to the experimental model. Samples containing 50% and 90% PKS show absorption characteristics that conforms most to the capillary-Diffusive formula. Figure 8.7 shows a strong positive correlation between experimental Sorptivity and theoretical values.

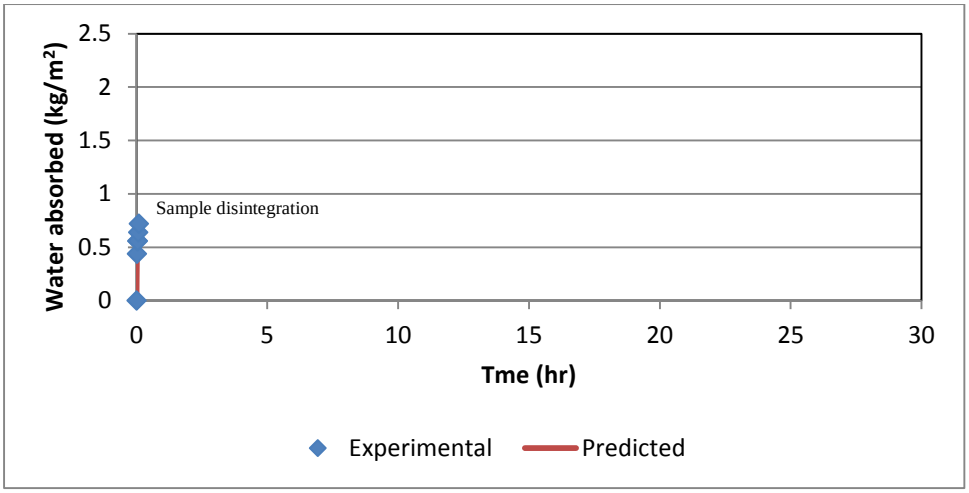

Figure 8.8 Sample 622-OKS0CE time dependent water absorption. Theoretical and experimental

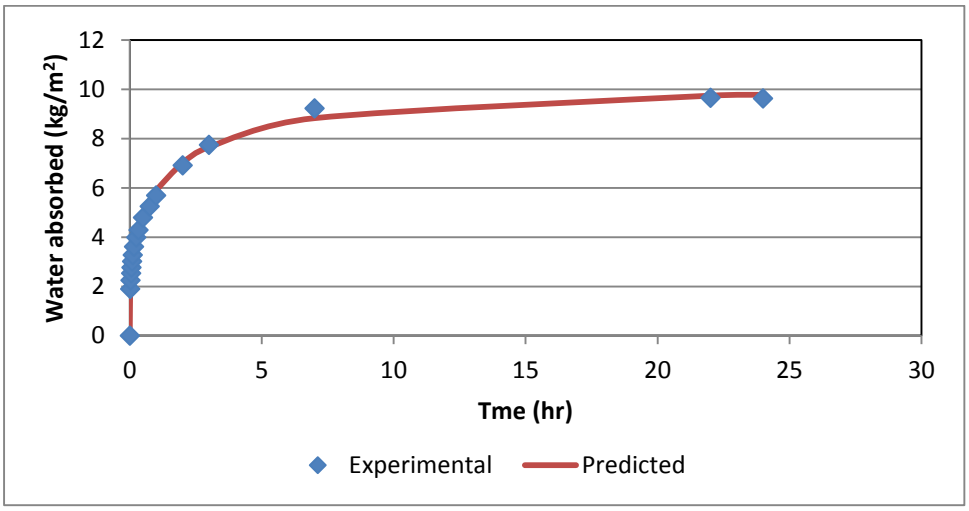

Figure 8.9 Sample 622-10KS0CE time dependent water absorption. Theoretical and experimental

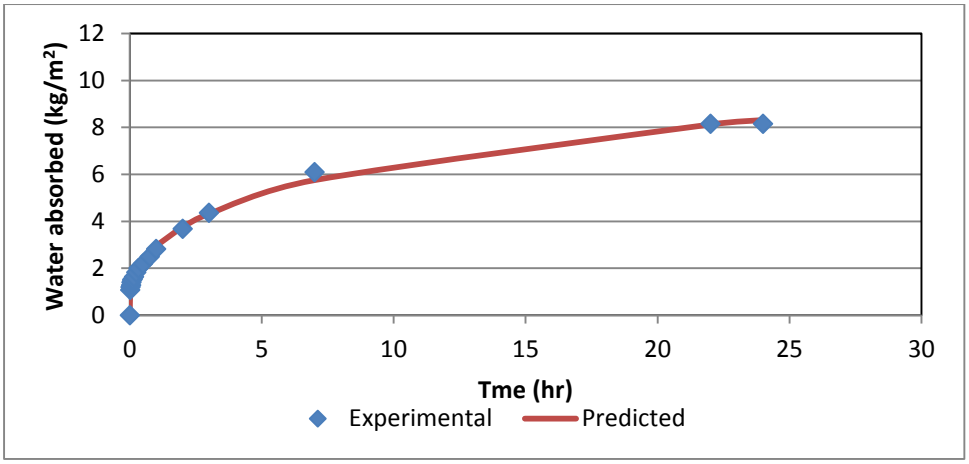

Figure 8.10 Sample 622-50KS0CE time dependent water absorption. Theoretical and experimental

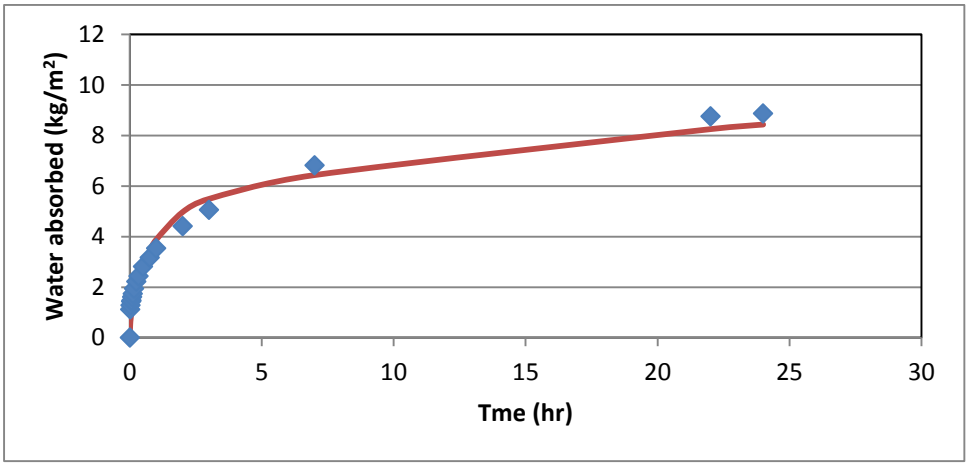

Figure 8.11 Sample 622-90KS0CE time dependent water absorption. Theoretical and experimental

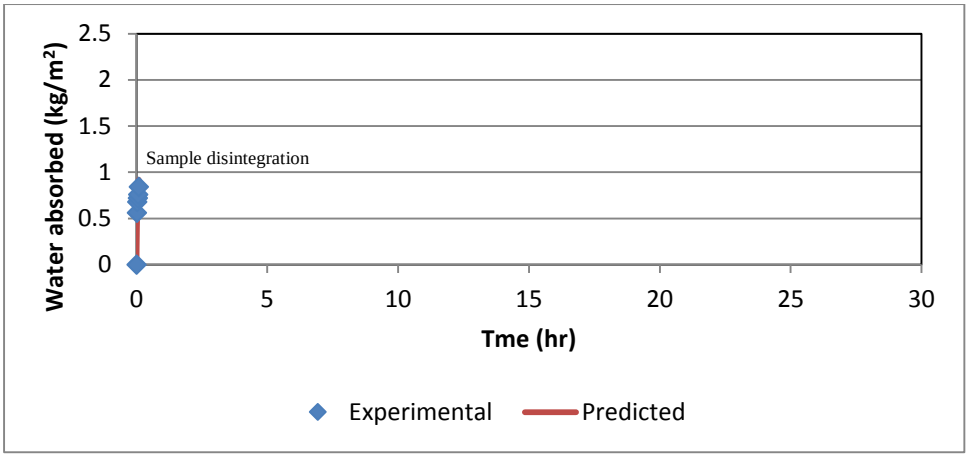

Figure 8.12 Sample 622-100KS0CE time dependent water absorption. theoretical and experimental

8.3 Prediction by Cement Content

Table 8.3 shows the predicted parameters for the Capillarity-Diffusivity model. It would appear that the value of 'S' rises with increase in cement content. Figure 8.13 shows how experimental sorptivity values differ from the predicted values for 'S' the coefficient or the extent to which similarities exist. Addition of cement is seen to create a weak negative correlation between the samples.

Table 8.3 Predictive values for cement stabilised rammed earth using the capillary-diffusive model

Sample	soil type	Additions	N	S	Co	D	R2
451-0FA0CE	451	Nil	49.99915	1.660599	29.85893	3.808802	0.975399
451-0FA2CE	451	2% Cement	54.65907	1.547843	63.84177	0.00253	0.991981
451-0FA4CE	451	4% Cement	149.9991	2.072431	50.99682	16.94918	0.885183
451-0FA9CE	451	9% Cement	123.9984	1.25656	93.79986	1.855504	0.901082

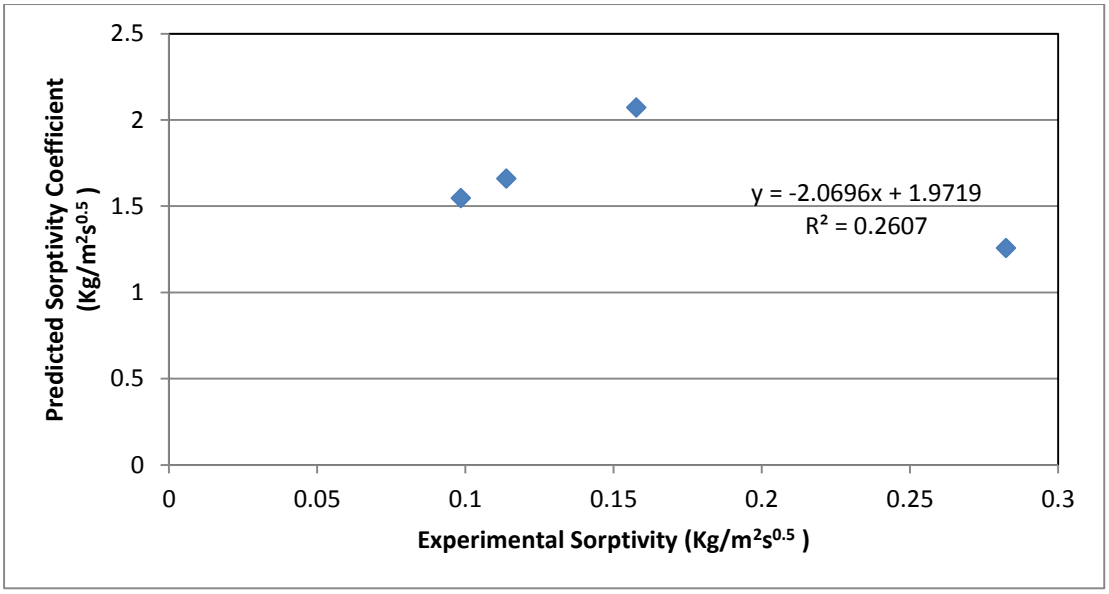

Figure 8.13 Comparison between experimental Sorptivity and 's' values for cement stabilised rammed earth

Figures 8.14 to 8.17 show the curve of water absorption for samples stabilised to various degrees with cement. As this model defines parameters best suited for rammed earth, it appears that increased stabilisation changes the mechanical, material and chemical properties of rammed earth to the extent that experimental results start to deviate significantly from results predicted from the model. This can be observed in the R^2 values in Table 8.3.

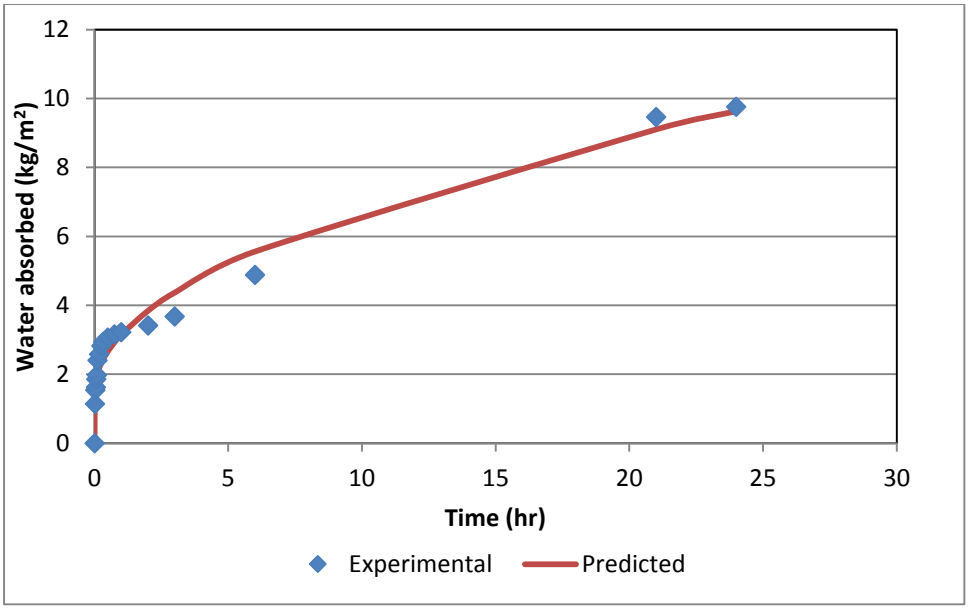

Figure 8.14 Sample 451-0FA0CE time dependent water absorption. Theoretical and experimental

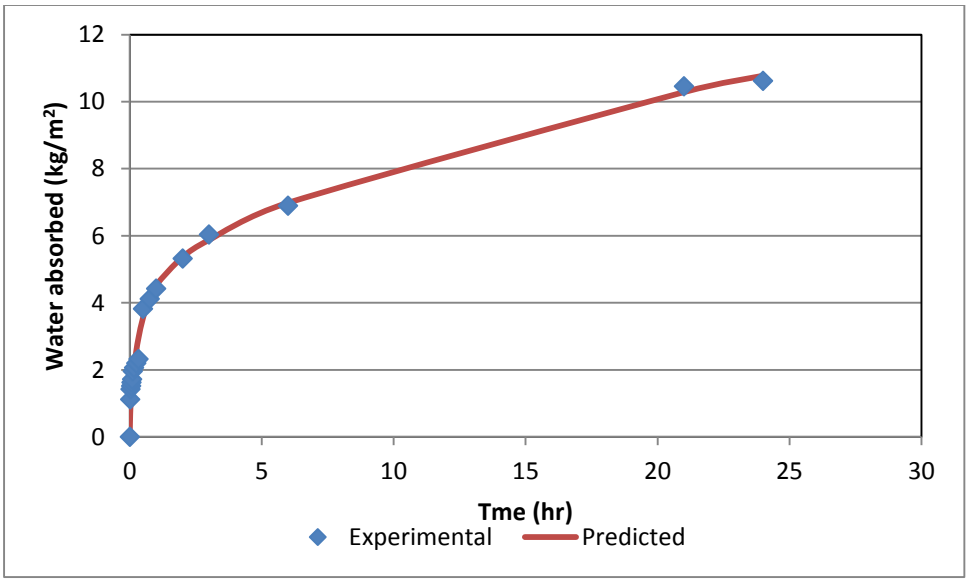

Figure 8.15 Sample 451-0FA2CE time dependent water absorption. Theoretical and experimental

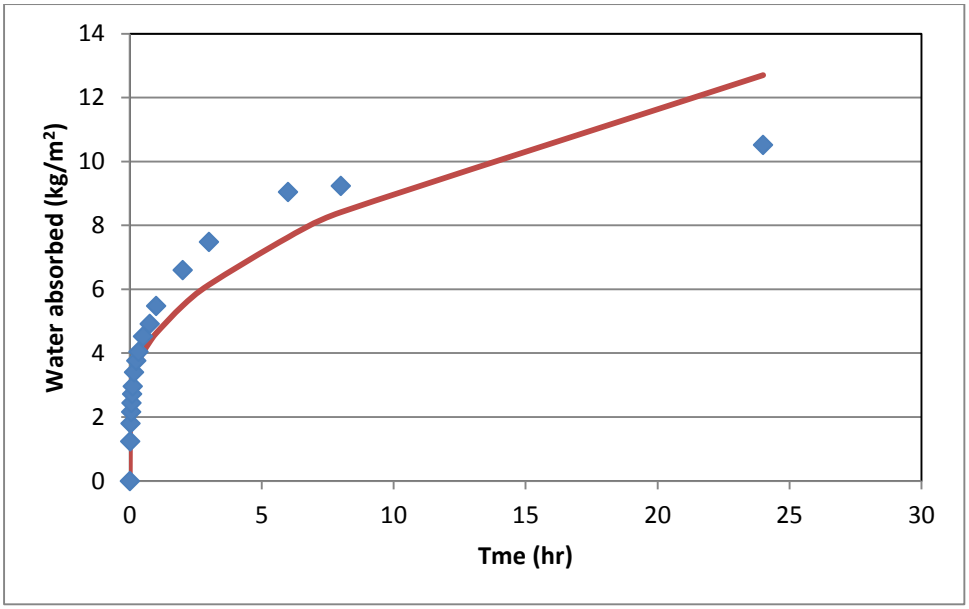

Figure 8.16 Sample 451-0FA4CE time dependent water absorption. theoretical and experimental

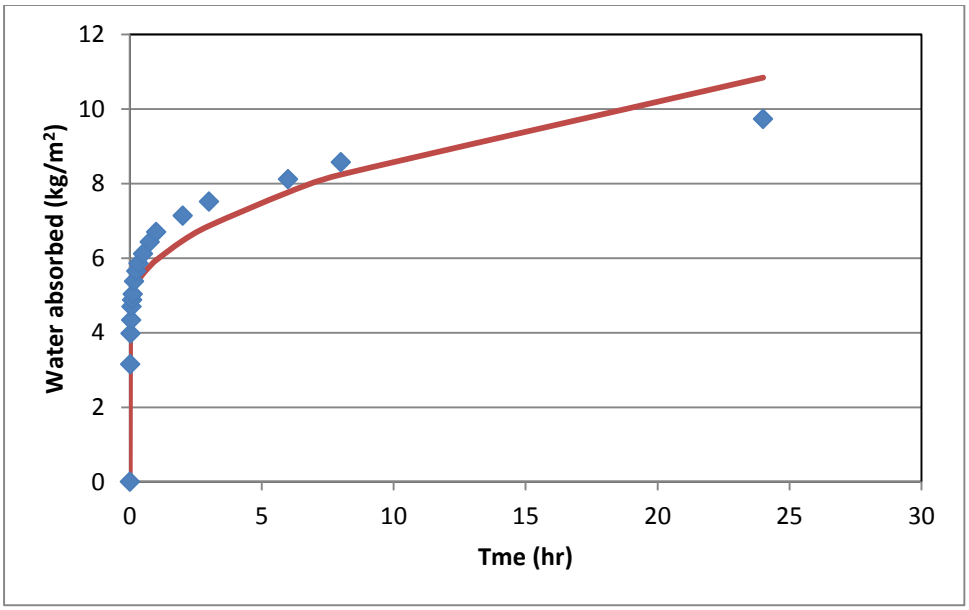

Figure 8.17 Sample 451-0FA9CE time dependent water absorption. Theoretical and experimental

8.4. Prediction by Pulverised Fuel Ash Content

Each soil grade was plotted using the model described above the results obtained at various Pulverised Fuel Ash contents are presented below.

8.4.1 451 Soil Grade

Table 8.4 Predictive values for rammed earth grade 451 containing Pulverised Fuel Ash using the capillary-diffusive model

Sample	soil type	Additions	N	S	Co	D	R2
451-0FA0CE	451	Nil	49.99915	1.660599	29.85893	3.808802	0.975399
451-10FA0CE	451	10% Pulverised Fuel Ash	49.07617	1.347152	14.70599	0.031269	0.96296
451-20FA0CE	451	20% Pulverised Fuel Ash	48.69117	1.382277	132.1171	0.018181	0.975411
451-30FA0CE	451	30% Pulverised Fuel Ash	84.5427	2.001879	186.7456	0.004274	0.971929
451-50FA0CE	451	50% Pulverised Fuel Ash	63.61464	0.355777	412.481	0.001464	0.998923

Figure 8.18 is a chart showing figures extracted from Table 8.4. Predicted values from the model are shown to differ significantly. Although both experimental and predictive values show an initial drop in sorptivity with addition of Pulverised Fuel Ash (Table 8.4), the degree to which it is seen to rise with increased dosage appears to be very different. The correlation, between both sets of value is weak and is observed to be negative.

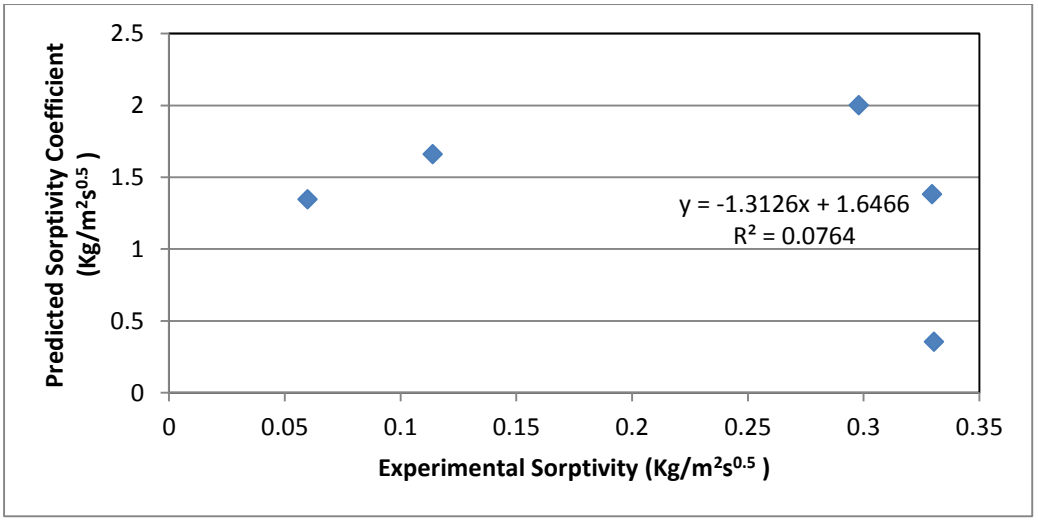

Figure 8.18 Comparison between experimental Sorptivity and 's' values for grade 451 rammed earth containing Pulverised Fuel Ash

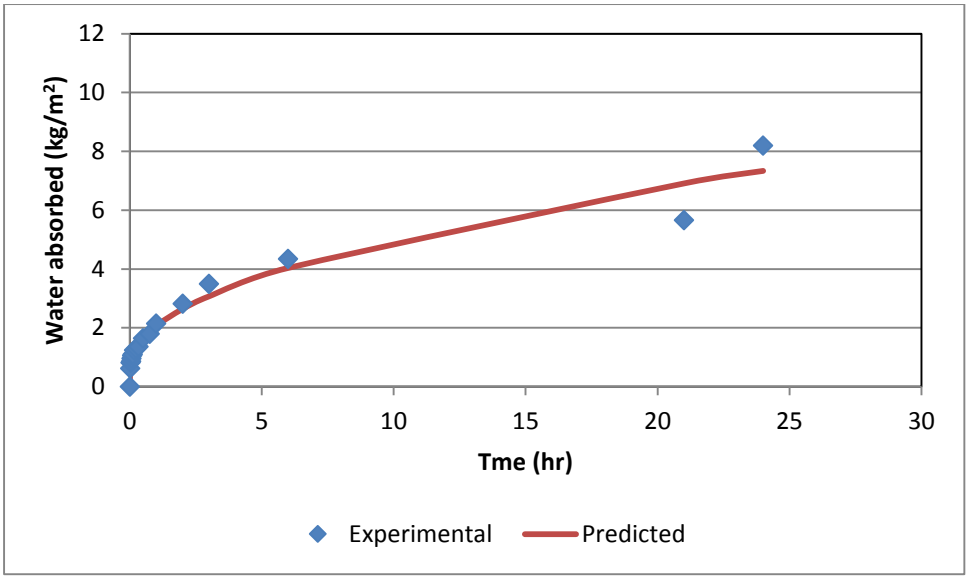

Figure 8.19 Sample 451-10FA0CE time dependent water absorption. Theoretical and experimental

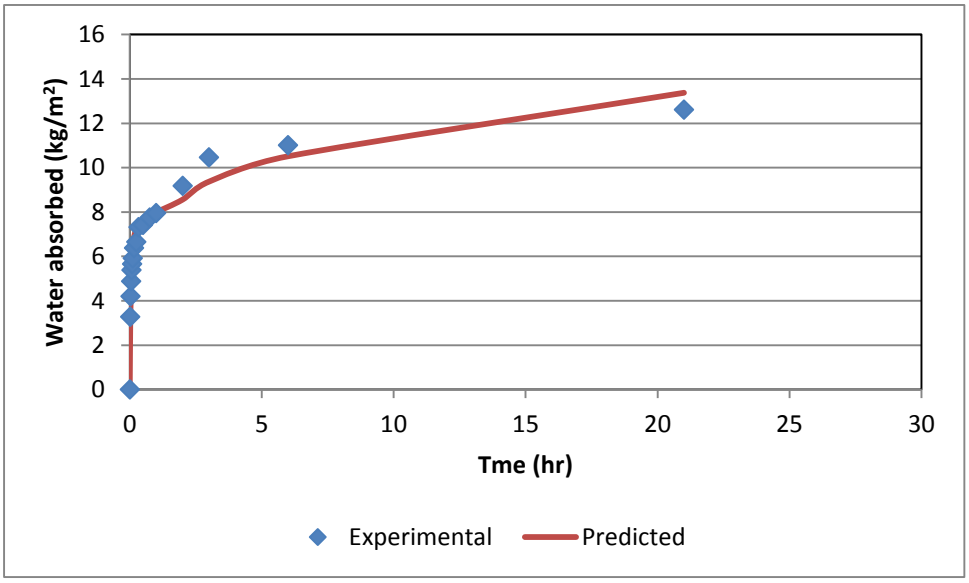

Figure 8.20 Sample 451-20FA0CE time dependent water absorption. Theoretical and experimental

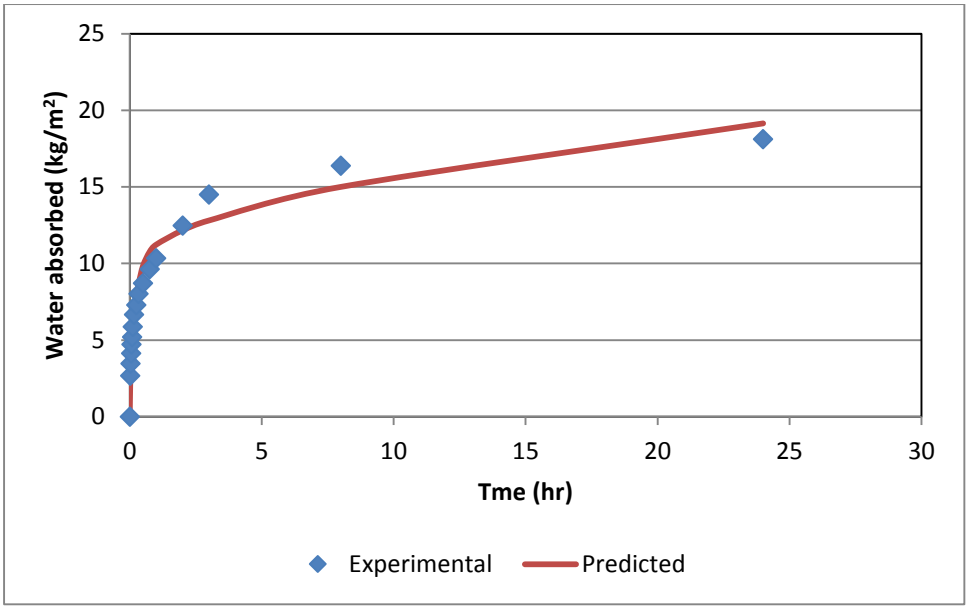

Figure 8.21 Sample 451-30FA0CE time dependent water absorption. Theoretical and experimental

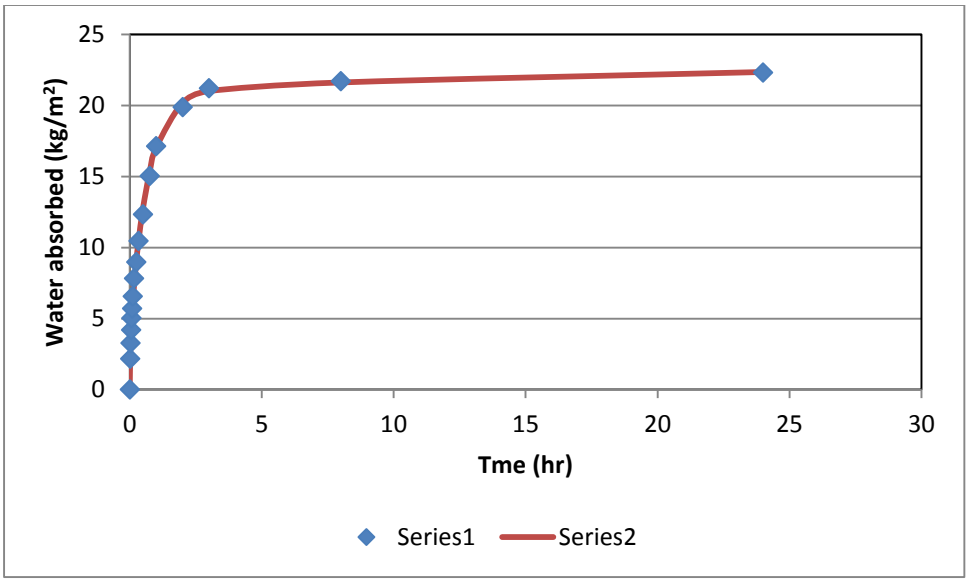

Figure 8.22 Sample 451-50FA0CE time dependent water absorption. Theoretical and experimental

Figures 8.19 to 8.22 show the effect of addition of Pulverised Fuel Ash to rammed earth made from a 451 soil mix. It suggests that the addition of Pulverised Fuel Ash progressively causes the resulting material to deviate from the Capillary-Diffusive model. As can be noted in Table 8.4 the R^2 value gives an indication of how well the equation fits the curve.

8.4.2 532 Soil Grade

While an increase in value is observed in both experimental and predicted values of sorptivity, figure 8.23 shows that the gradient for 'S' values was much more than that obtained for predicted values (Table 8.5). The correlation between both values is positive but rather weak.

Table 8.5 Predictive values for rammed earth grade 532 containing Pulverised Fuel Ash using the capillary-diffusive model

Sample	soil type	Additions	N	S	Co	D	R2
Pulverised Fuel Ash							
532-0FA0CE	532	Nil	1.999762	0.497531	100.0004	0.00475	0.983006
532-10FA0CE	532	10% Pulverised Fuel Ash	47.84854	1.310127	84.21958	0.009969	0.971272
532-20FA0CE	532	20% Pulverised Fuel Ash	46.38306	0.993944	182.7499	0.005061	0.968268
532-50FA0CE	532	50% Pulverised Fuel Ash	48.73957	0.719708	266.2897	0.010248	0.993294

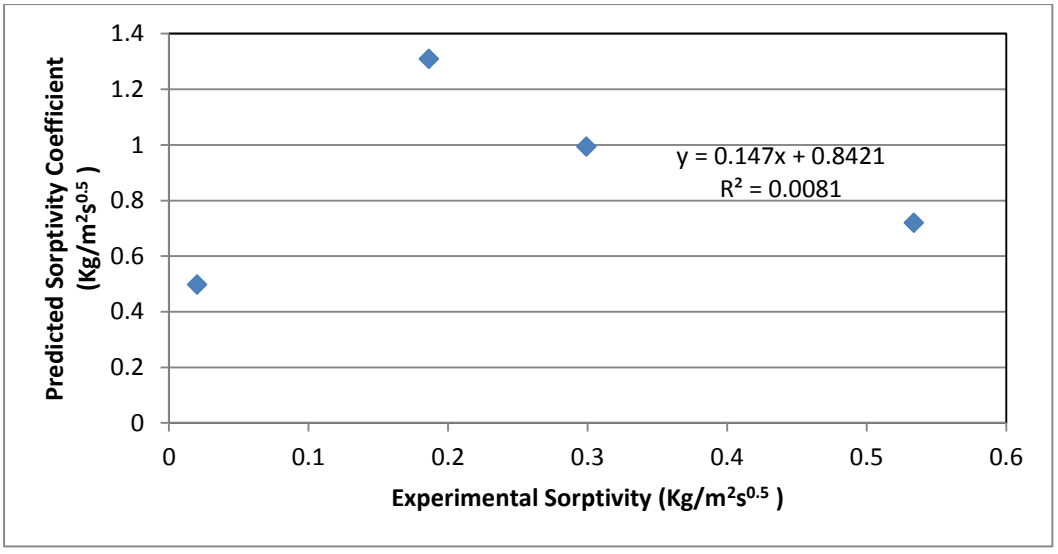

Figure 8.23 Comparison between experimental Sorptivity and 's' values for grade 532 rammed earth containing Pulverised Fuel Ash

When Pulverised Fuel Ash was added to the 451 soil (very clayey) mix, it resulted in distortions in the experimental results as there was an increasing

disproportionate ratio between clay size elements and coarse aggregates in the mix. Adding the same proportion of Pulverised Fuel Ash to the 532 mix (well blended) only served to provide a more densely packed arrangement that provided better capillary channels that encouraged water ingress, thus staying true to the Capillary-Diffusive model. As seen in Table 8.5 and Figures 8.24 to 8.26, the experimental results stayed true to the predicted values derived from the model.

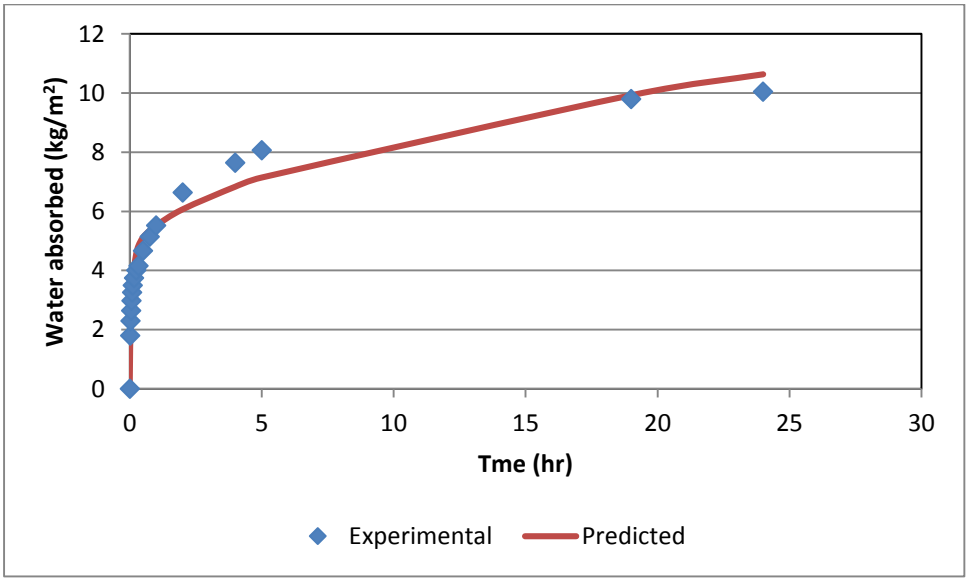

Figure 8.24 Sample 532-10FA0CE time dependent water absorption. Theoretical and experimental

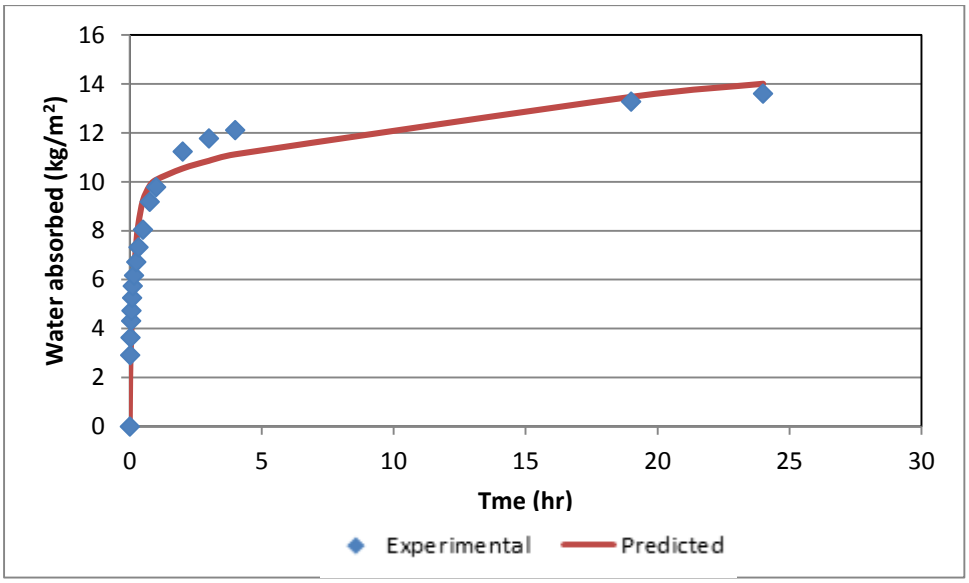

Figure 8.25 Sample 532-20FA0CE time dependent water absorption. Theoretical and experimental

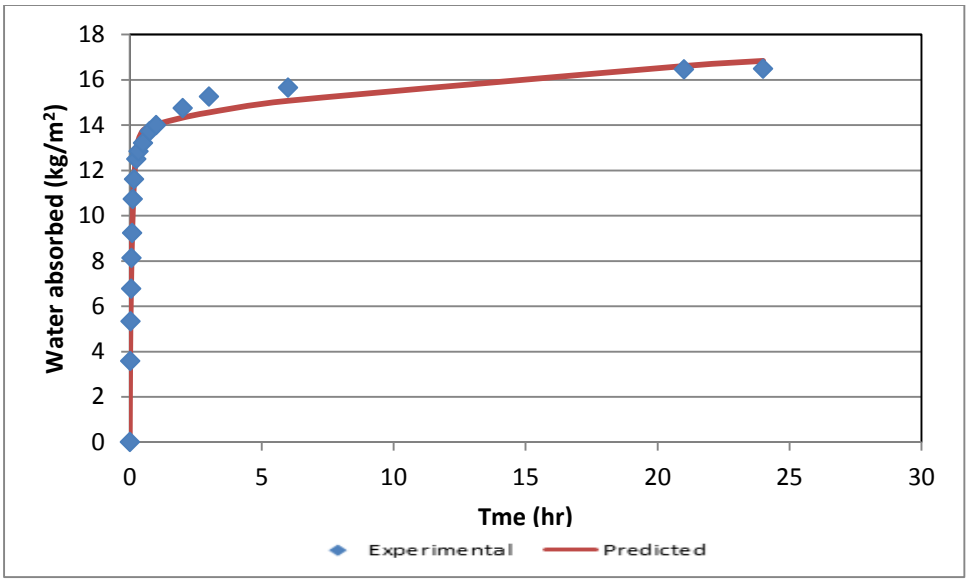

Figure 8.26 Sample 532-50FA0CE time dependent water absorption. Theoretical and experimental

8.4.3 721 Soil Grade

Sorptivity values derived experimentally rose and fell with predictive 'S' values derived from the Capillary-Diffusive models. As shown in Figure 9.27, the positive correlation didn't hold strongly however as the R^2 value came to less than 0.01. Table 9.6 showed that the constant representing diffusivity (D) appeared to increase with the addition of Pulverised Fuel Ash to the mix.

Table 8.6 Predictive values for rammed earth grade 721 containing Pulverised Fuel Ash using the capillary-diffusive model

Sample	soil type	Additions	N	S	Co	D	R2
721-0FA0CE	721	Nill	49.19337	2.909074	23.19685	0.292386	0.999977
721-10FA0CE	721	10% Pulverised Fuel Ash	99.99975	2.016374	29.86458	1.274331	0.981739
721-20FA0CE	721	20% Pulverised Fuel Ash	159.998	4.37929	77.96815	1.525681	0.777819
721-50FA0CE	721	50% Pulverised Fuel Ash	99.99983	3.189615	12.96091	1.274331	0.988085

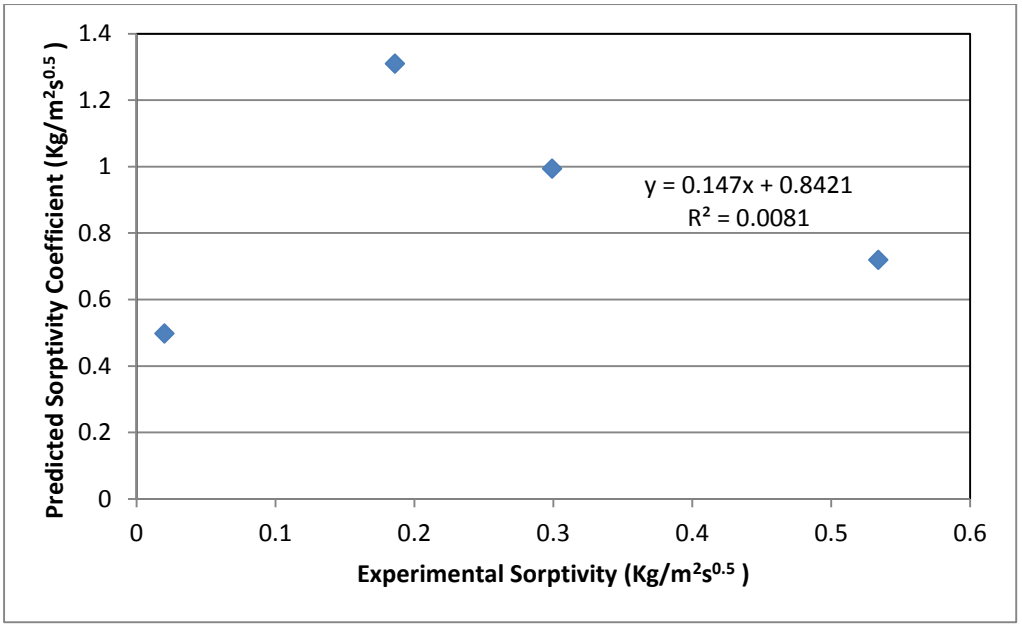

Figure 8.27 Comparison between experimental Sorptivity and 's' values for grade 721 rammed earth containing Pulverised Fuel Ash

721 mix containing Pulverised Fuel Ash showed very similar 'D' values to rammed earth containing no Pulverised Fuel Ash. The 'D' value relates to the constant that refers to the coefficient of Diffusivity. This is seen in Table 8.7. It would appear that the influence of diffusion does not change for rammed earth made from a 721 mix regardless of the amount of Pulverised Fuel Ash contained within. Figure 8.28 to 8.30 also show that experimental values follow closely to values obtained from the Capillary-Diffusive model.

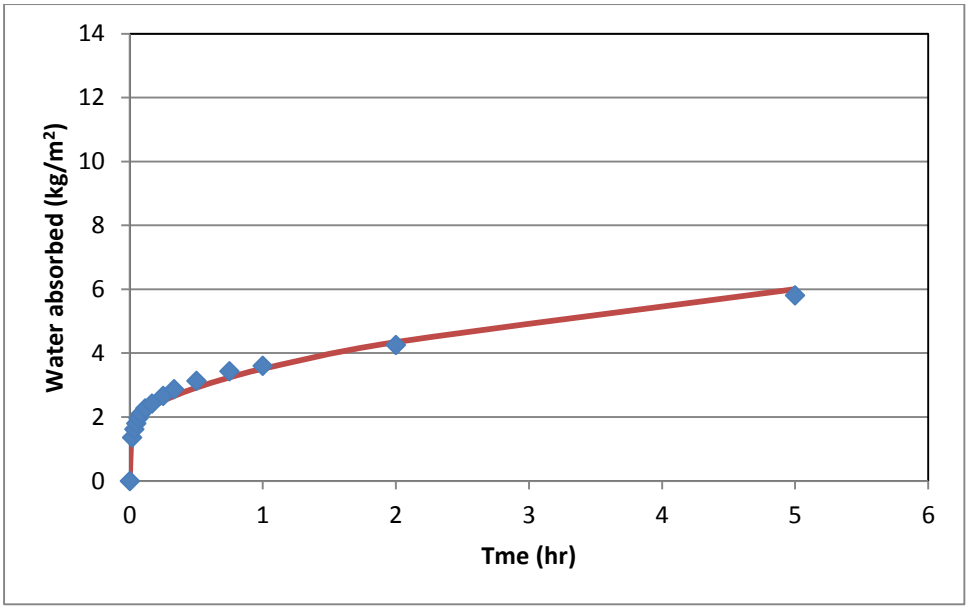

Figure 8.28 Sample 721-10FA0CE time dependent water absorption. Theoretical and experimental

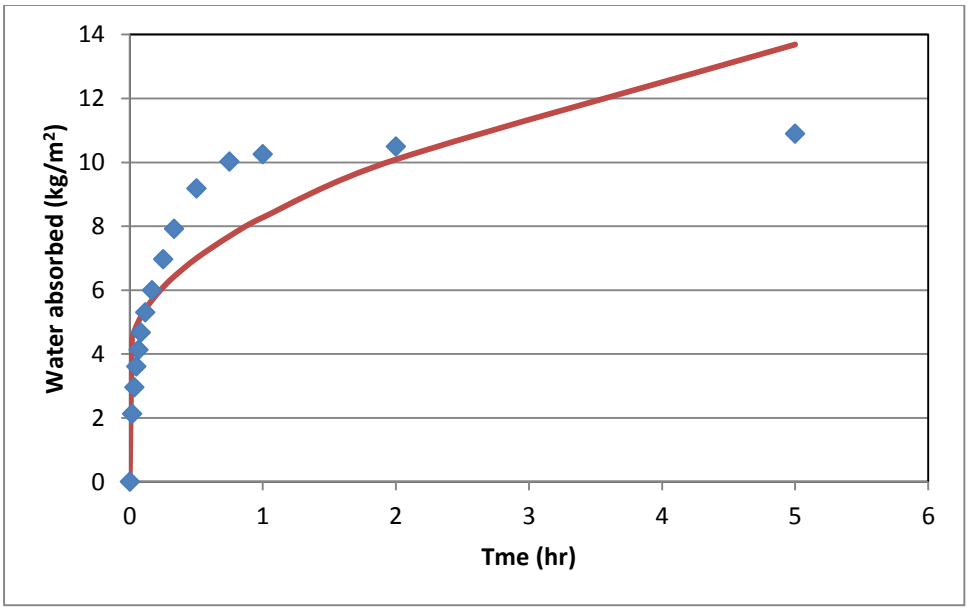

Figure 8.29 Sample 721-20FA0CE time dependent water absorption. Theoretical and experimental

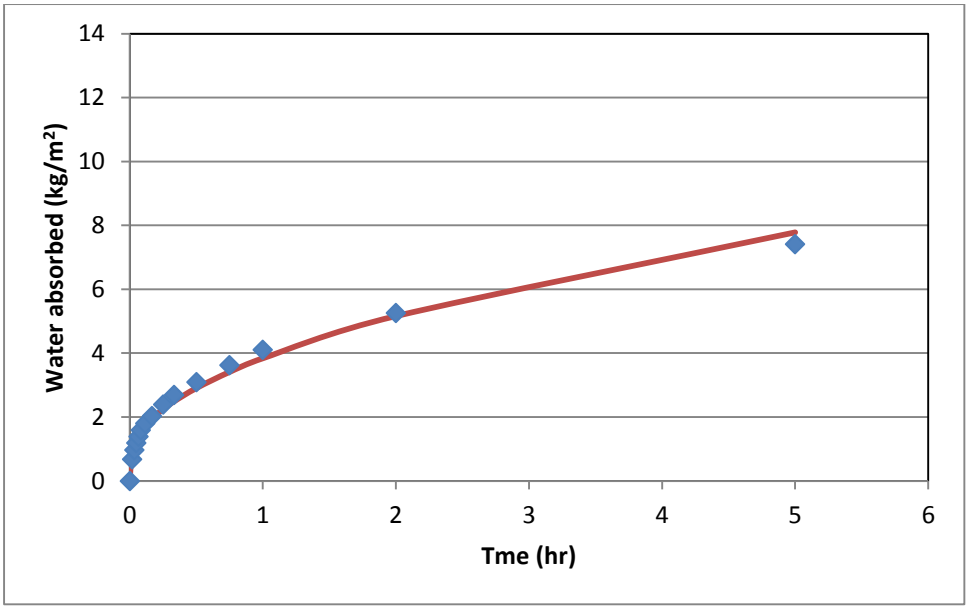

Figure 8.30 Sample 721-50FA0CE time dependent water absorption. Theoretical and experimental

These Models are similar to models used in literature (Table 8.7 and Figure 8.31) for the moisture ingress of water in mortar.

Table 8.7 Extract of values used in predicting moisture ingress in slag cement mortar (villar-cocina et al. 2002)

Mixture	Sorptivity coefficient S $(kg/m^2 s^{\frac{1}{2}})$	Diffusion coefficient D (m^2/s)	Co (kg/m^3)	N (m)
S80W100	$3,16.10^{-2} \pm 0,25.10^{-2}$	$1,38.10^{-8} \pm 0,08.10^{-8}$	$140,52 \pm 5,42$	$1,51.10^{-3} \pm 0,14.10^{-3}$
S70W100	$2,75.10^{-2} \pm 0,24.10^{-2}$	$2,50.10^{-8} \pm 0,23.10^{-8}$	$137,34 \pm 8,32$	$1,52.10^{-3} \pm 0,15.10^{-3}$
S60W100	$2,81.10^{-2} \pm 0,15.10^{-2}$	$6,10.10^{-8} \pm 0,27.10^{-8}$	$94,62 \pm 3,86$	$4,02.10^{-3} \pm 0,20.10^{-3}$
S80W50	$4,80.10^{-3} \pm 0,45.10^{-3}$	$2,83.10^{-8} \pm 0,14.10^{-8}$	$63,75 \pm 3,70$	$2,17.10^{-3} \pm 0,17.10^{-3}$
S80A100	$21,31.10^{-2} \pm 2,1.10^{-2}$	$1,28.10^{-7} \pm 0,08.10^{-7}$	$121,52 \pm 6,29$	$2,75.10^{-3} \pm 0,26.10^{-3}$

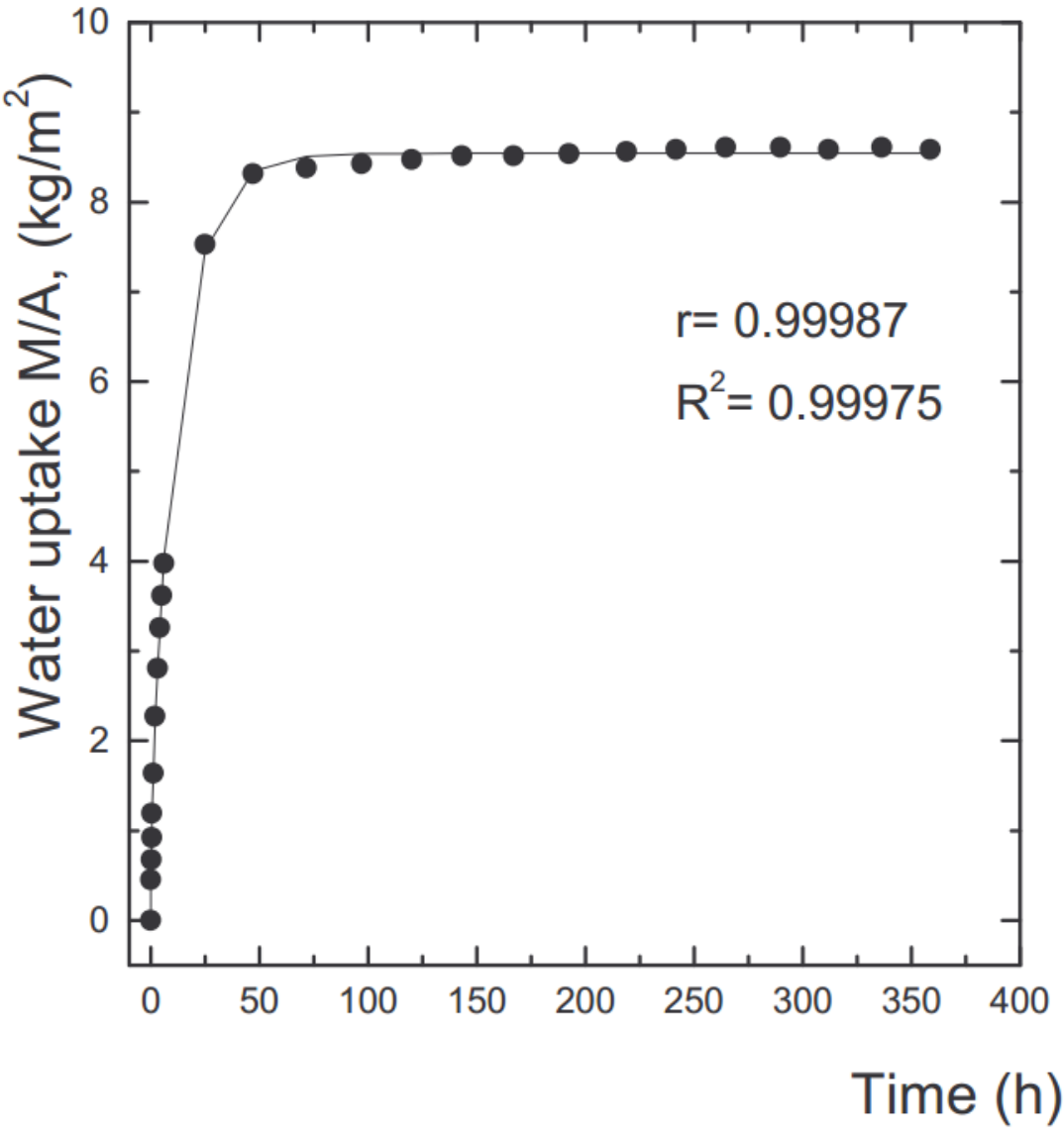

Figure 8.31 Experimental vs theoretical result for moisture ingress in slag cement mortar (villar-cocina et al. 2002)

Rammed earth, to an extent follows the theory and model of most building materials and until adequate testing methods are developed for the unique traits of rammed earth (like slaking when immersed in water), then various tests for concrete and mortar can be adapted for use in testing rammed earth materials.

Chapter Nine

Drying Shrinkage of Rammed Earth

This chapter investigates the changes in length that occur when rammed earth is cured in air. Rammed earth is subject to changes in volume. There are various reasons for this. Plastic shrinkage would usually occur due to evaporation of moisture at the surface or by moisture absorption by aggregates while the material is still placed in the formwork. Autogeneous shrinkage usually occurs when no moisture movement is allowed in or out of the system and is more usually found in concrete. There has been no investigation into Autogeneous shrinkage of rammed earth. Cement stabilised rammed earth sometimes undergoes carbonation shrinkage where carbon dioxide in the atmosphere reacts with hydrated cement in the presence of water.

Drying shrinkage arises in rammed earth as the material dries out unevenly. Where cracks may not develop, dimension change is usually observed. While ASTM C 157 requires testing to be carried out over 6 months in the lab or 12 to 18 months in the field, data has been collected over 90 days. While it can be expected that accuracy of predicting drying shrinkage improves with later age test data, ACI 209 and BS ISO 1920-8: 2009 allows for data collection from early age data in predicting potential mixtures.

9.1 Drying shrinkage in Rammed Earth containing PKS

Figures 9.1 and 9.2 show the shrinkage and expansion that occur in rammed earth over 90 days. Figure 9.4 shows rammed earth of 532 grade containing 100% aggregate and that containing 100% PKS. Rammed earth containing the same proportion of coarse aggregates but of 622 grade is shown in Figure 9.2.

Comparing both soil grades, it was noted that barring the initial steep increase in size, 532 soil grade containing granite followed a close expansion pattern as rammed earth grade 622 containing only PKS. This is seen in figure 9.3.

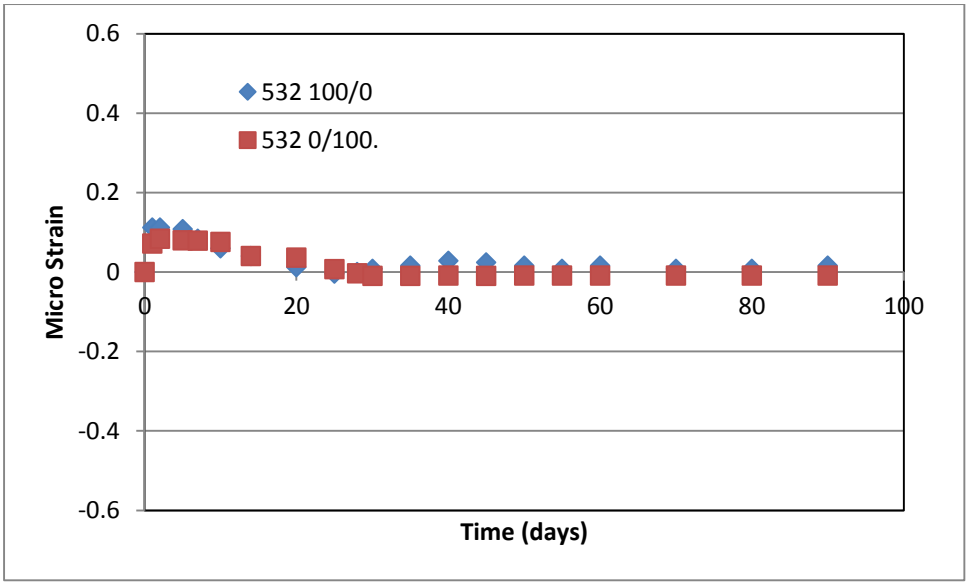

Figure 9.1 Length change in 532 soil grade.

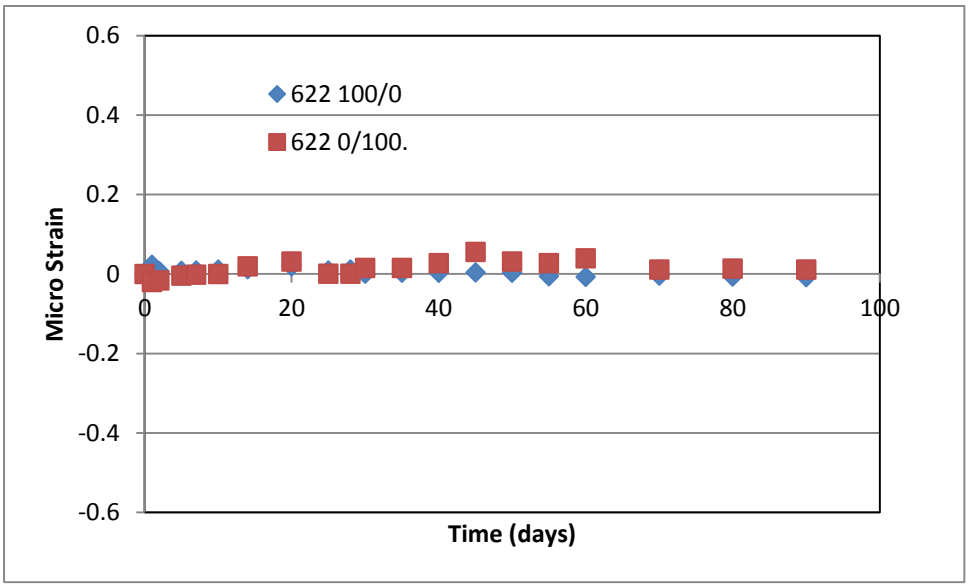

Figure 9.2 Length change in 622 grade soil.

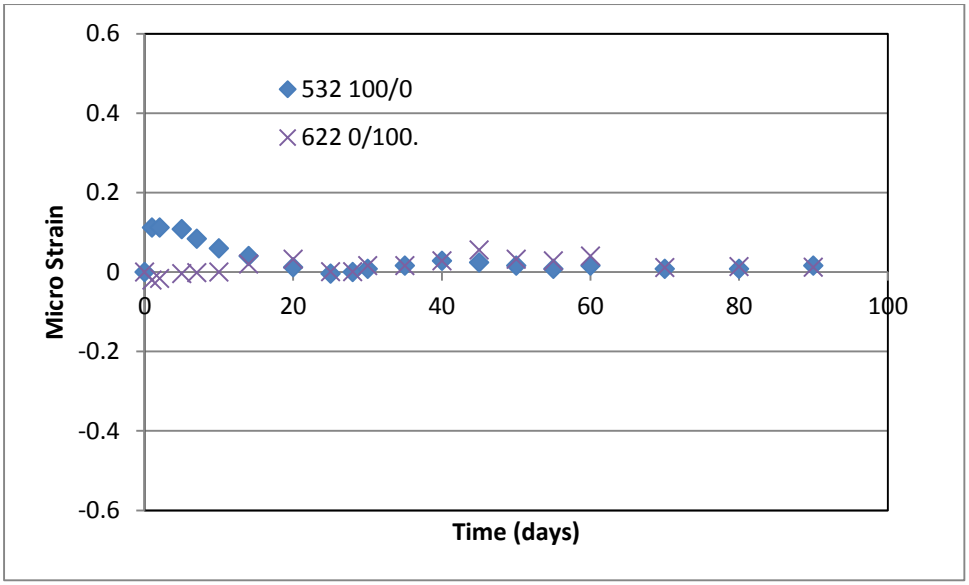

Figure 9.3 Expansion in rammed earth samples

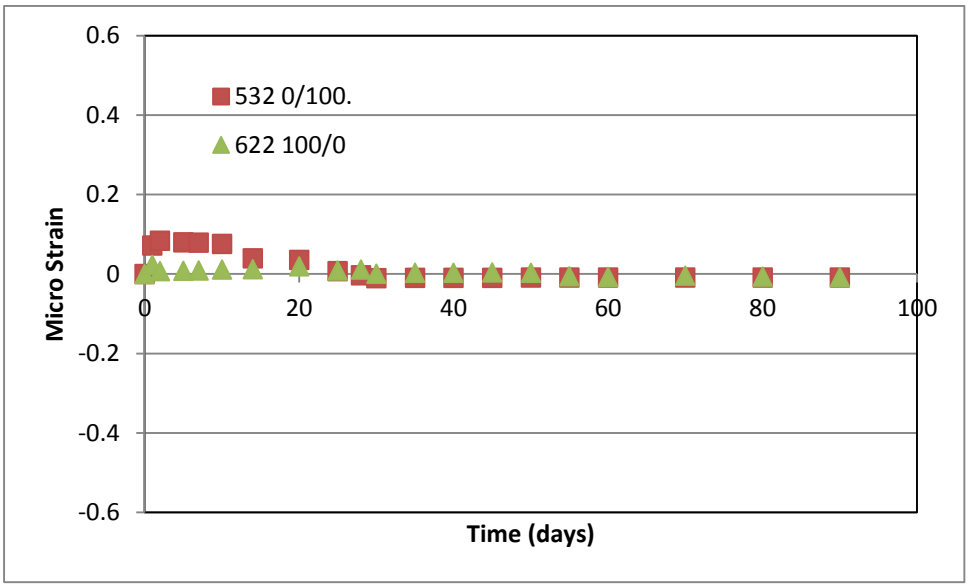

Figure 9.4 Shrinkage and expansion circle in rammed earth samples

Figure 9.4 shows that rammed earth grade 532 containing only PKS and grade 622 containing granite show a similar trend of going from a state of expansion to shrinkage. When shrinkage is the factor in consideration, these mixes can be used interchangeably to achieve the same long term results.

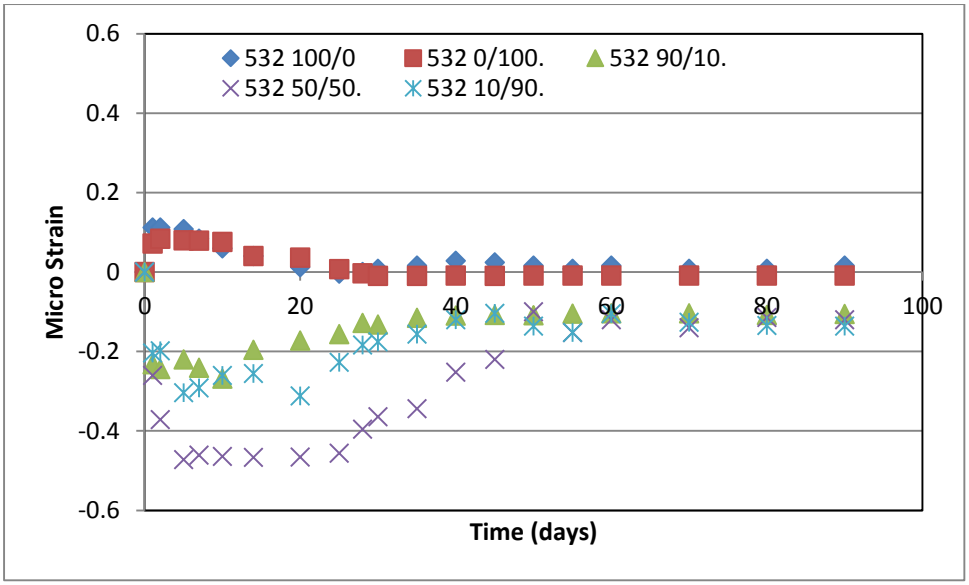

Figure 9.5 Length change in 532 soil grade containing different proportion of PKS.

When the PKS content is increased from 10% to 90% in the 532 grade soil, shrinkage can be seen in Figure 9.5 to increase for the first few days. This trend does changes with age with contraction setting in. Between the 30th and 50th day, all samples were seen to return close to their original length. Expansion is observed to take over after about the 20th day. Shrinkage is not readily observed in the 622 sample. While samples containing 10% to 100% PKS experienced marginal initial shrinkage before expanding as seen in Figure 9.6, sample containing 50% PKS was an exception as it witnessed massive expansion and no shrinkage all through the 90 days of testing.

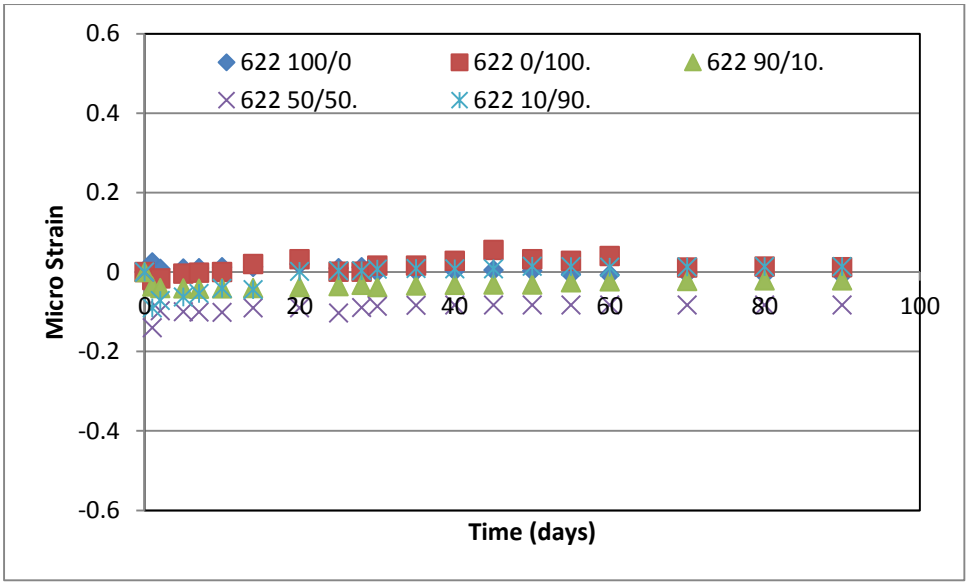

Figure 9.6 Length change in 622 soil grade containing different proportion of PKS.

9.2 Drying shrinkage in Rammed Earth Containing Cement

Stabilising with cement at small quantities appeared to impact greatly on initial shrinkage. As seen in Figure 9.7, 2% cement increased the shrinkage amplitude and the circle length. Adding more cement appeared to stabilise the sample further as 9% cement content reduced the amount of initial shrinkage and appeared to stabilise the length of the sample after only 7 days. This cannot readily be explained by Yoo et al (2014) who insists that initial shrinkage in samples containing cement could be due to differences in ambient temperature and hydration heat. It would have been expected that higher cement content would produce more heat during hydration and thus lead to increased shrinkage as the material cooled to ambient temperature.

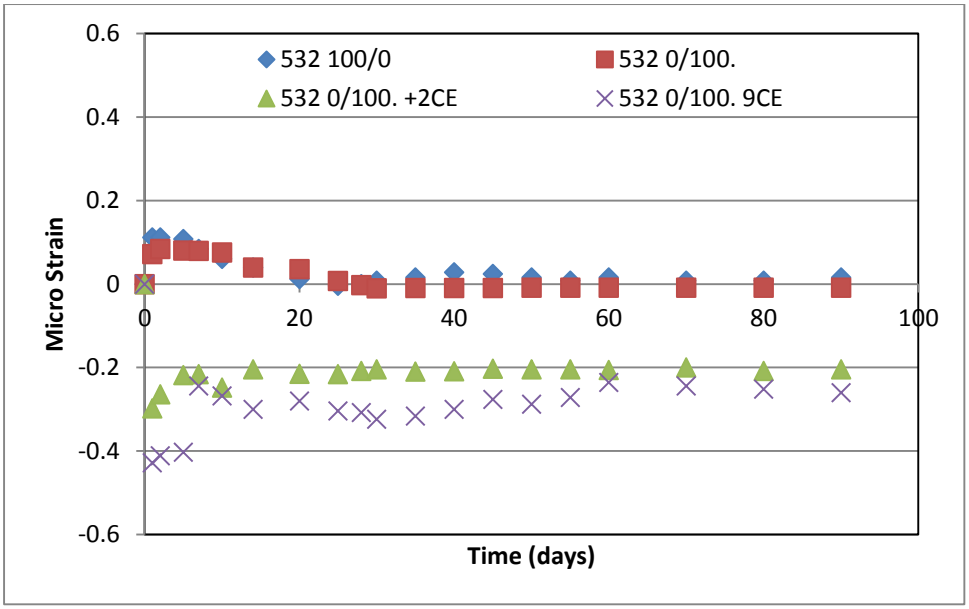

Figure 9.7 Length change in 532 soil grade containing different proportion of cement.

Adding Cement to 622 mix also resulted in increased shrinkage. However the PKS content accounted for a difference in reaction. While rammed earth containing only coarse aggregate experienced very high shrinkage from day 1, expansion started to set in on day 30. When testing was carried out on the 90th day, the length of the sample had very nearly returned to its original length. However, for rammed earth samples containing only PKS as coarse aggregate, day 1 shrinkage was less sever and while expansion set in on day 20, the dimensions remained relatively unchanged by day 90. This is observed in Figure 9.8 and could be , as a result of the self-restraint of the chemical shrinkage and the volume contraction from the negative pressure in the internal voids from the hydration of cement (Yoo et al. 2014).

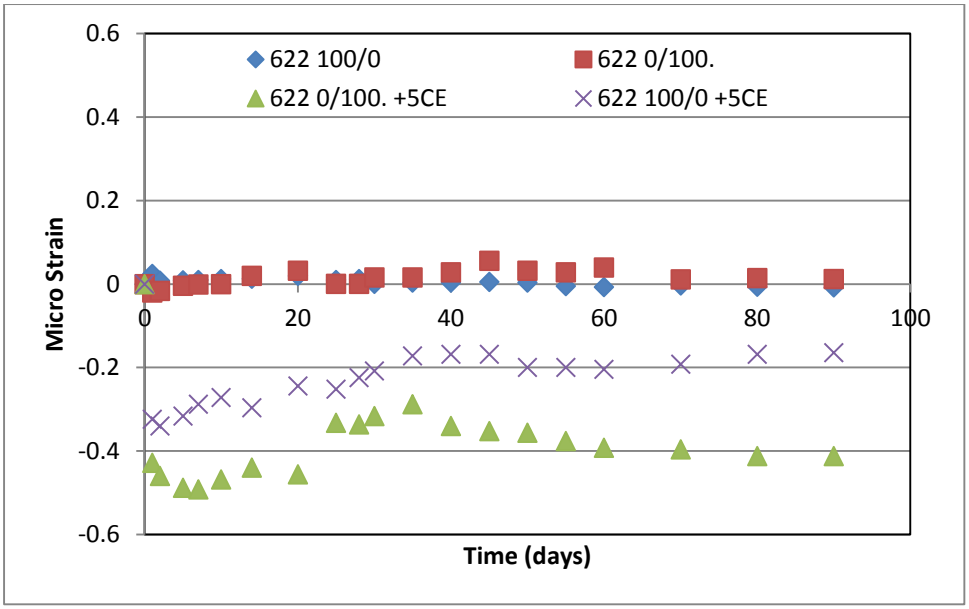

Figure 9.8 Length change in 622 soil grade containing cement.

9.3 Drying Shrinkage in Rammed Earth Containing Pulverised Fuel Ash

When Rammed Earth samples made from blending various proportions of soil types was tested for shrinkage, the following result was obtained. It can be observed from Figure 9.9 that all soil types tested experienced shrinkage. It should be noted that Figure 9.9 shows shrinkage for unstabilised Rammed Earth without any additions.

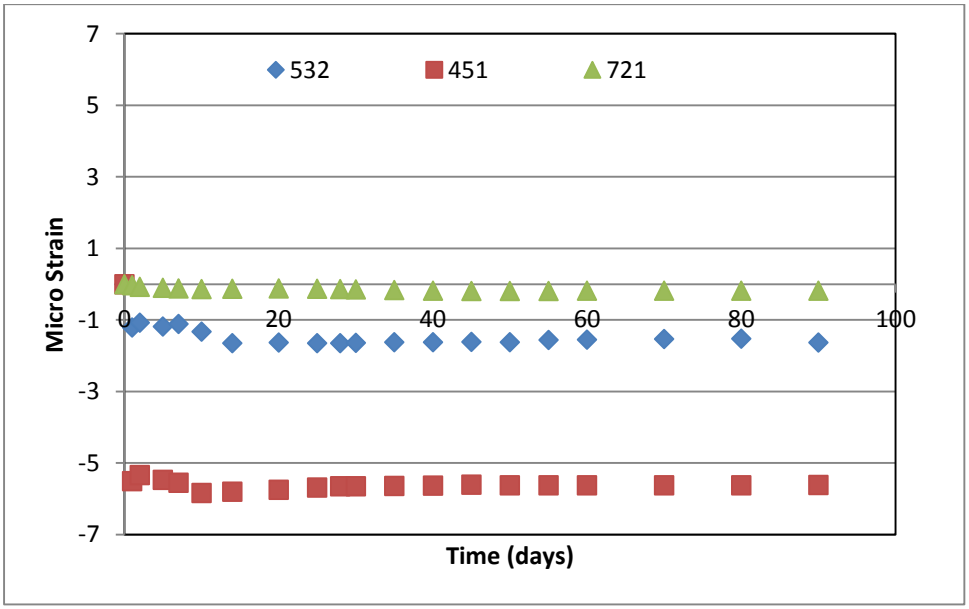

Figure 9.9 Shrinkage in rammed earth made from soil mix 532, 451 and 721.

Sample that recorded highest level of shrinkage was the very clayey mix 451. This mix has 4 parts sand, 5 parts clay and 1 part coarse aggregate. This sample recorded a negative micro strain of 5.512 one day after demoulding. Further shrinkage was noted over the next 10days however, by day 30, after very minor expansion, the sample was seen to retain a near stable structural dimension.

721 which is a very sandy soil type experienced very little shrinkage in the first day after demoulding. However, the sample continued to record micro strain in little amounts up to the last day of testing.

The 532 soil grade which is a medium blend soil mix exhibited similar characteristics in the early days of testing as the 721 even though shrinkage was observed to be 5 times less. First day testing showed a negative micro strain 1.216. This was followed by a brief period of cycling between dimension gain and shrinkage as internal moisture moved particles around within the structure. The sample's dimension saw very little change after the 14th day.

9.3.1 451 Soil Mix

The 451 soil mix which is described as clayey was mixed with varying proportions of Pulverised Fuel Ash. Some of these samples were further stabilised with cement. A summary can be seen in Figure 9.10. Figure 9.11 shows that when Pulverised Fuel Ash is added to the mix, the material is better held together and drying shrinkage is reduced. A 10% addition of Pulverised Fuel Ash easily results in a 70% reduction in strain.

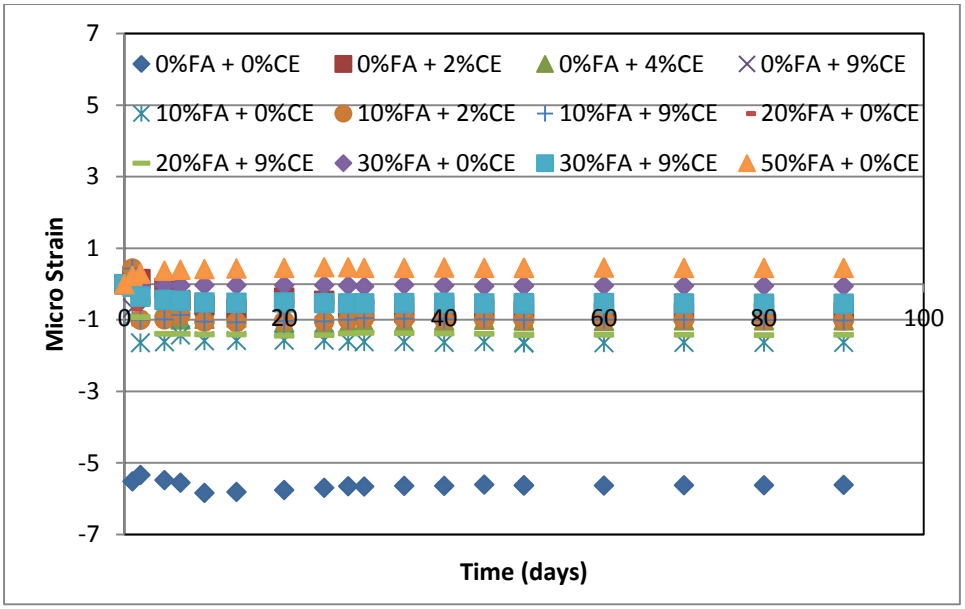

Figure 9.10 summary of shrinkage in rammed earth 451 mix containing various additives

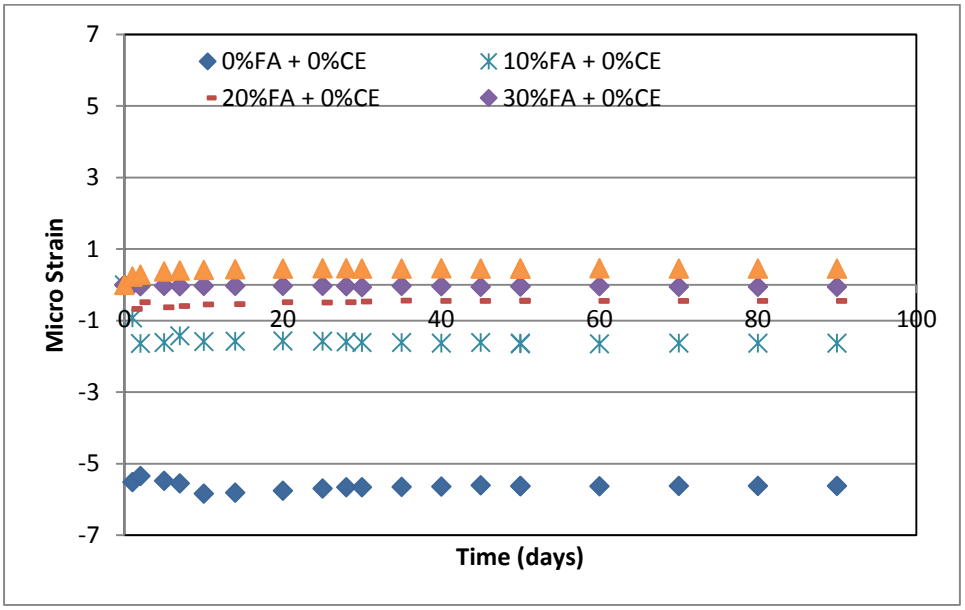

Figure 9.11 Effect of Pulverised Fuel Ash on shrinkage in rammed earth 451 mix

Increasing this to 20% Pulverised Fuel Ash content further reduces shrinkage strain by 58%. At 30% Pulverised Fuel Ash content, there is very little observable shrinkage. However, further addition of Pulverised Fuel Ash resulted in an expansion of the material.

When the 451 rammed earth mix is cement stabilised, shrinkage is also seen to reduce. However, figure 9.12 shows that a 2% stabilisation is more beneficial than a 4% cement stabilisation, especially at very early ages. The best shrinkage result for stabilised rammed earth containing no further additives appeared to be obtained by a 9% cement stabilisation. However, it can be noted that the gain from a 9% stabilisation was not noted immediately but rather after about 30 days of testing. Figure 9.13 shows results obtained when Pulverised Fuel Ash is blended in with Cement Stabilised Rammed Earth.

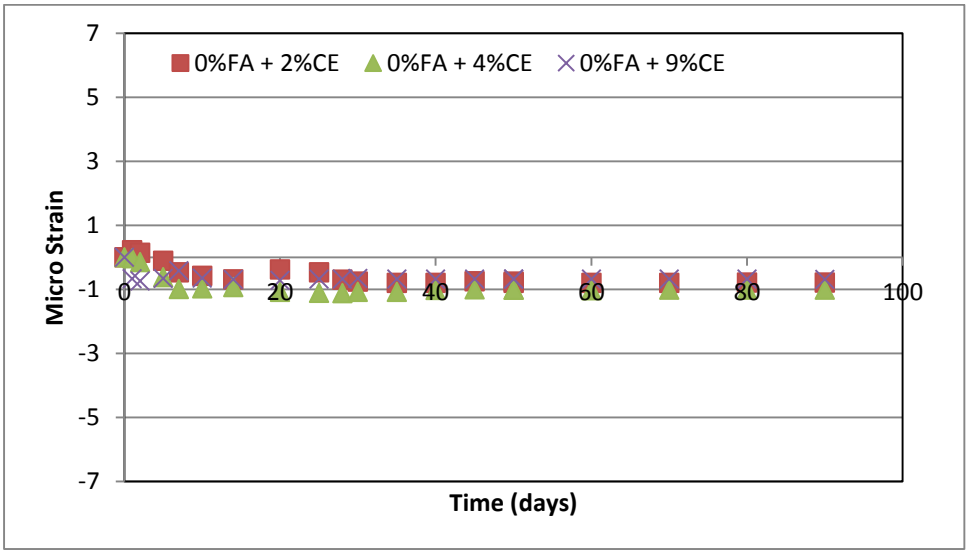

Figure 9.12 Effect of cement stabilisation on shrinkage in rammed earth 451 mix

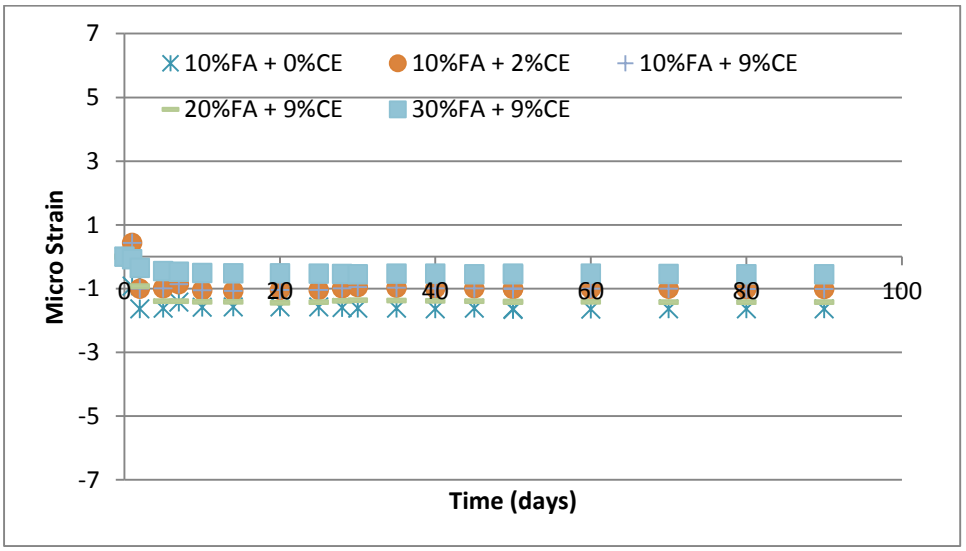

Figure 9.13 Effects on shrinkage of adding Pulverised Fuel Ash to cement stabilised 451 rammed earth

9.3.2 532 Soil Mix

Figure 9.14 shows a summary of shrinkage strain obtainable at various levels of stabilisation and Pulverised Fuel Ash contents.

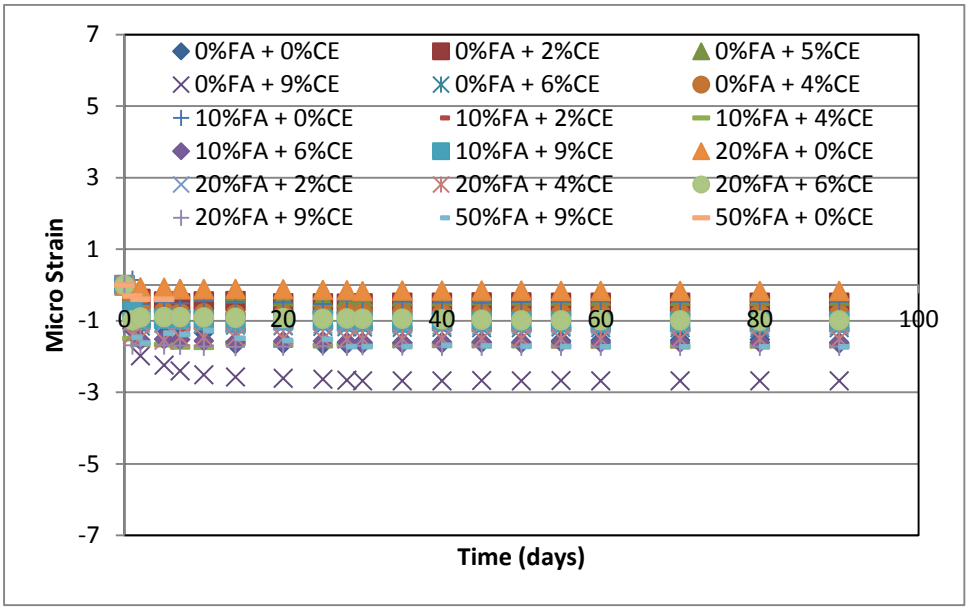

Figure 9.14 Summary of shrinkage in rammed earth 532 mix containing various additives

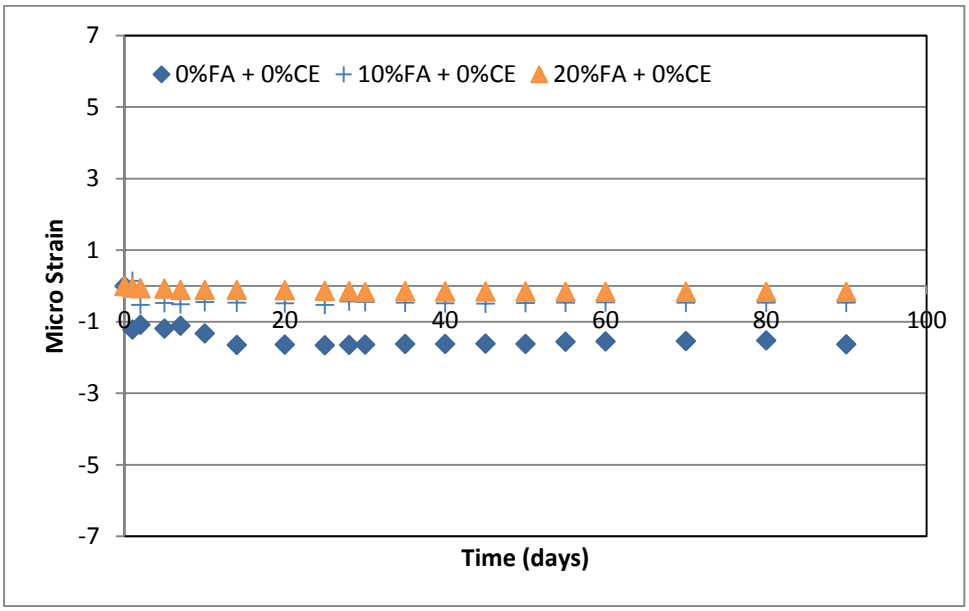

Figure 9.15 Effect of Pulverised Fuel Ash on shrinkage in rammed earth 532 mix

As was observed for the 451 Rammed Earth mix, increased Pulverised Fuel Ash content impacts positively on shrinkage. Introducing 10% Pulverised Fuel

Ash into the mix reduced shrinkage by at least 55% when testing was carried out one day after demoulding (Figure 9.15). Increasing the Pulverised Fuel Ash content serves to further decrease the level of shrinkage observed in the mix.

When cement was used in stabilisation, Figure 9.16 shows that shrinkage was also reduced up to a point where diminishing returns set in. at 2% cement stabilisation, shrinkage is at its lowest. Further increase in cement stabilisation did not have the desired effect of further reducing shrinkage. 4 % and 6% stabilisation resulted in a progressively worse shrinkage performance but stayed at a level better than an unstabilised position. 9% cement stabilisation however resulted in the very worst performance as day 1 shrinkage strain was 72% worse than unstabilised rammed earth.

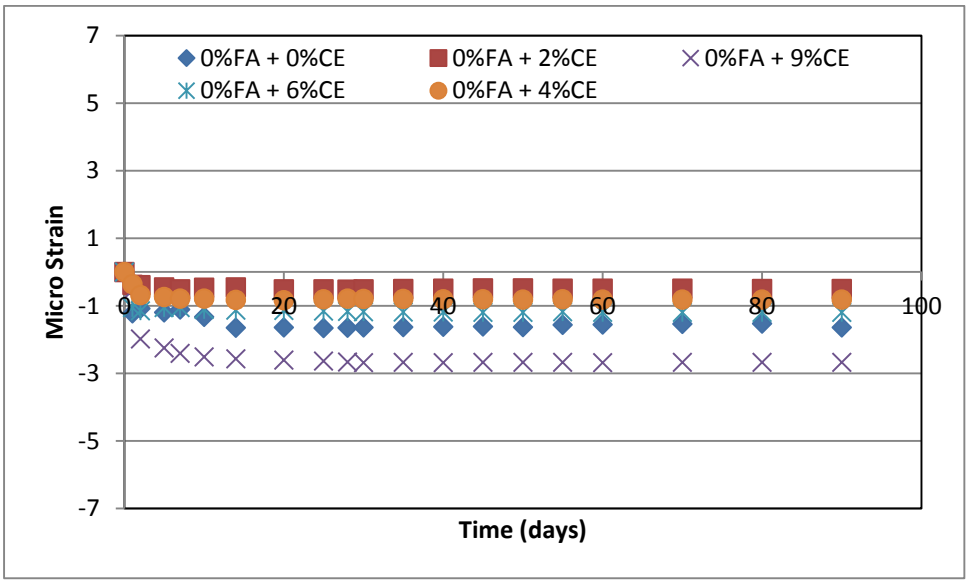

Figure 9.16 Effect of cement stabilisation on shrinkage in rammed earth 451 mix

9.3.3 721 Soil Mix

721 mix of rammed earth produced the best results for shrinkage among the samples tested. However addition of Pulverised Fuel Ash to the mix did not produce the same result as witnessed in the other 2 soil mixes. Figure 9.17 show that addition of Pulverised Fuel Ash had a progressively worse effect on shrinkage. A 10% Pulverised Fuel Ash content resulted in micro strain increasing by over 8 times as compared to shrinkage observed in the

unstabilised rammed earth on day one tests. Further Pulverised Fuel Ash content (up to 20%) resulted in even more shrinkage strain (over 9 times expected shrinkage on day 2 of testing). A 30% Pulverised Fuel Ash content resulted in shrinkage that was observed to be worse than all other combinations by day 90 tests.

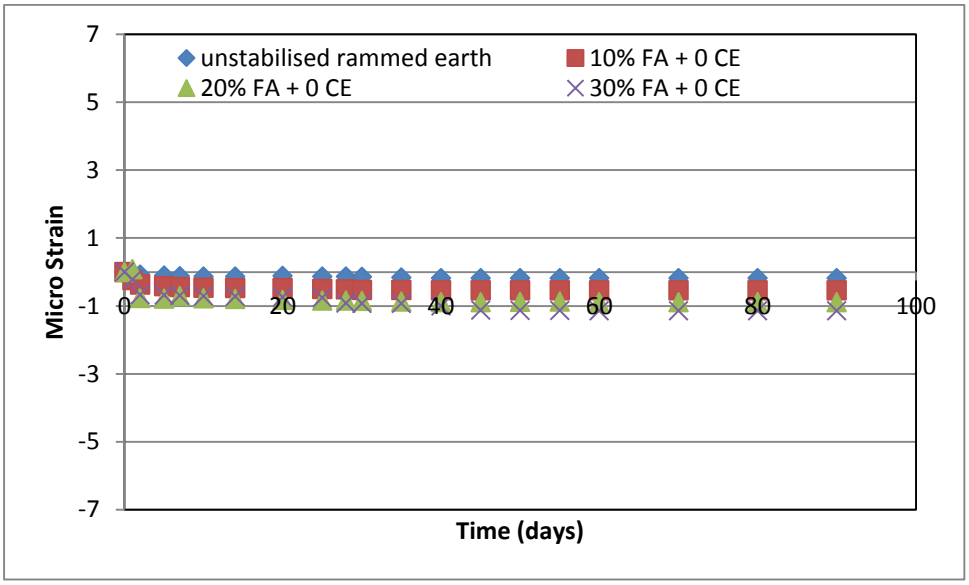

Figure 9.17 Effect of Pulverised Fuel Ash on shrinkage in rammed earth 721 mix

Chapter Ten

Thermal Conductivity and Numerical Simulations

The increase in the surface temperature of rammed earth causes heat to flow to the interior of the material. This could lead to physical and chemical changes in the material. The rate of flow of heat through the material is essential knowledge for safety and comfort reasons. When such material is used as a construction material there is a need to characterise the quality of the material in deciding comfort factors of users of such structures. This chapter looks at the experimental determination of thermal conductivity in rammed earth and compares that with figures obtained through finite element simulation.

10.1 Thermal Conductivity

Results from the experiment described in chapter 3.11 yielded values for thermal conductivity and thermal diffusivity for different soil types. Each sample tested was dried in the oven at about 75^0C until constant mass was achieved and it was then allowed to cool to room temperature before testing commenced. This was to ensure that water content did not play an active role in the determination of thermal conductivity. Figure 10.1 describes the thermal conductivity of rammed earth made from 7 different blends.

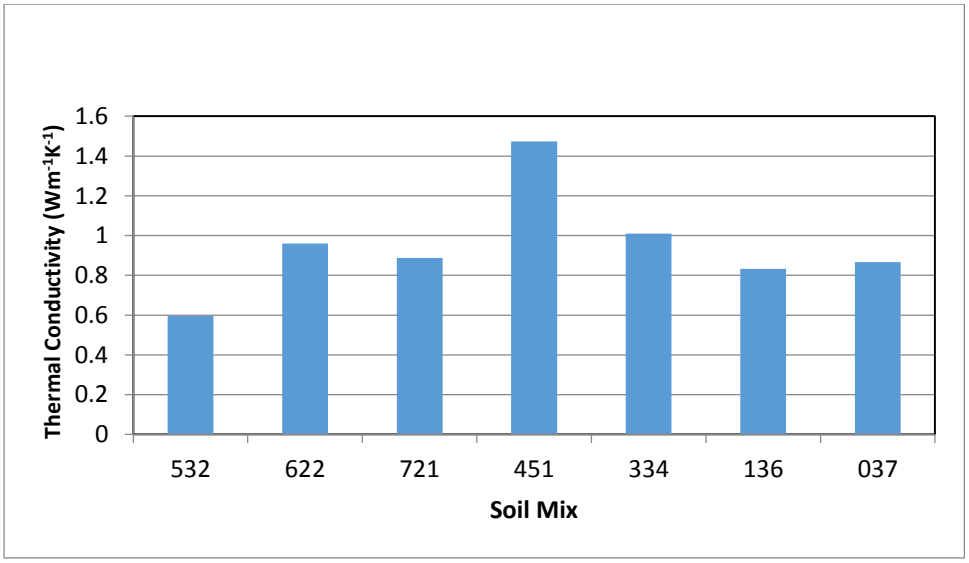

Figure 10.1 Thermal conductivity values for rammed earth mixes

Thermal conductivity values for the first 4 blends (532, 622,721,451) was obtained by the author through experimentation. The values from the last 3

blends(334, 136,037) was obtained from literature and constituting materials are described in Table 10.1. With regards to the blends prepared and tested by the author, it is noted that the mix that resulted in the lowest thermal conductivity was the 532 mix. This mix has previously been described as a well blended mix. The 721 mix had the next best result with thermal conductivity increasing by 80%. The 451 soil blend produced rammed earth with the highest thermal conductivity constant. These values come close to results described in the works of Hall and Allinson (2009) as shown in Table 10.1 and 10.2. The sample labels have been rewritten in figure 10.1 to provide emphasis on the soil composition proportion. Mix 433 was rewritten as 334, 613 as 136 and 703 as 073.

The effect of adding Palm kernel shell (PKS) to rammed earth was investigated. It can be observed in figure 10.2 that thermal conductivity rises as palm kernel shell is mixed with granite. When the 622 grade sample contained only coarse aggregate or palm kernel shells, thermal conductivity was below 1 $Wm^{-1}K^{-1}$. The 532 grade rammed earth sample exhibited higher thermal conductivity with the mix of PKS and coarse aggregate. When the sample contained only PKS, however, thermal conductivity was observed to be just under 2 $Wm^{-1}K^{-1}$.

Table 10.1 Definition of rammed earth mixes used in Hall & Allinson (2009)

Mix type	Soil component proportions (kg/kg × 10)			
	14–6.3 mm rounded pea gravel	⩽5 mm medium grit sand	Silty clay	OMC (%)
433	4	3	3	8
613	6	1	3	8
703	7	0	3	8

Table 10.2 Thermal conductivity of similar rammed earth samples (hall & allinson 2009).

Mix type	Dry density (kg/m^3)	Void ratio, e	Porosity, f	Dry-state thermal conductivity, λ (W/mK)[a]
433	2120	0.313	0.239	1.010
613	2020	0.376	0.273	0.833
703	1980	0.432	0.302	0.866

When Pulverised Fuel Ash was added to the rammed earth however, the result varied depending on the soil mix. Figure10.3 shows that soil sample made from grade 532 soil blend showed an increase in thermal conductivity as 10% and 20% Pulverised Fuel Ash was added to the mix. Further addition of Pulverised Fuel Ash led to a decrease in thermal conductivity.

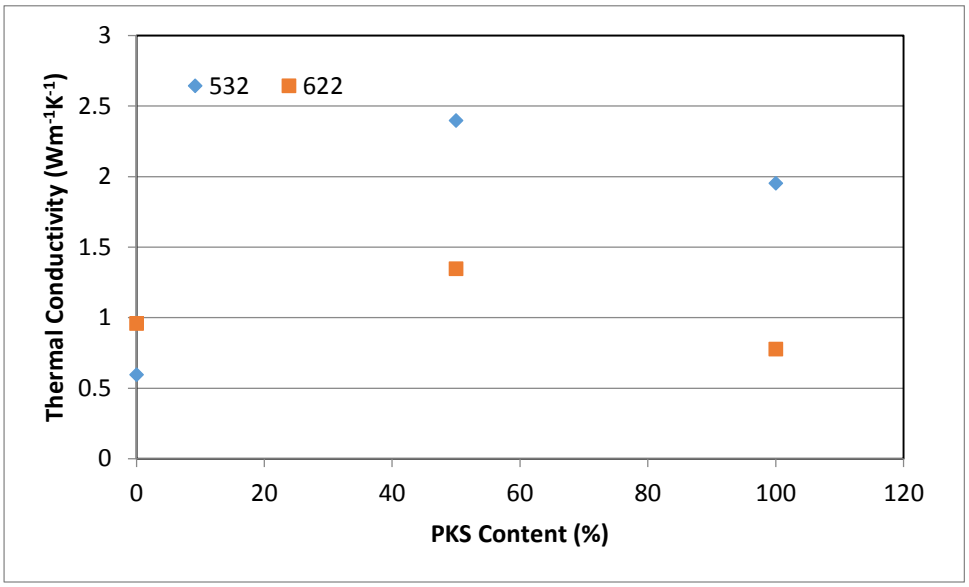

Figure 10.2 Thermal conductivity of samples containing palm kernel shell.

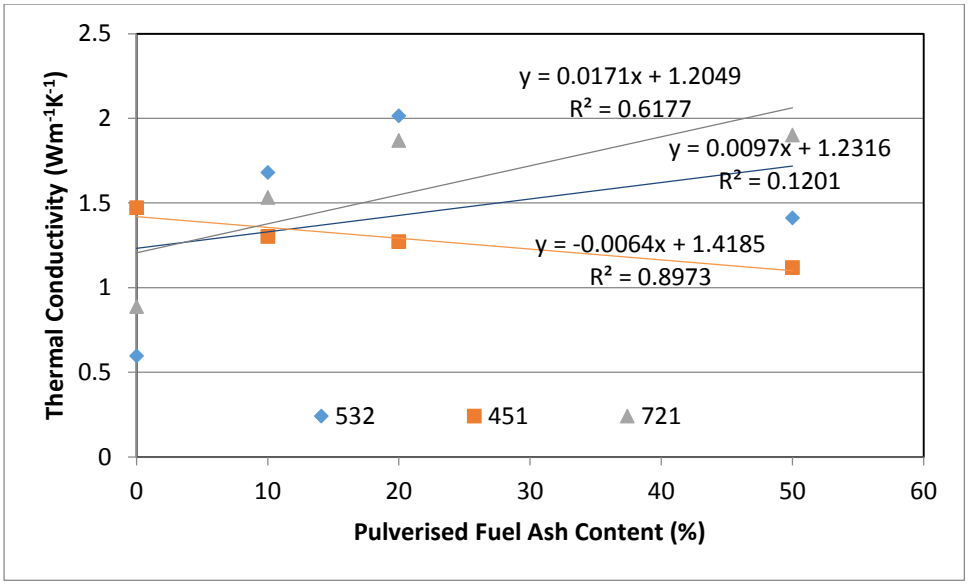

Figure 10.3 Thermal conductivity of samples containing Pulverised Fuel Ash.

A similar positive trend was observed for rammed earth made from 721 soil grade except for the fact that thermal conductivity was seen to continue rising past day 28. It should be noted that these two samples both contain a higher proportion of sand to clay. For rammed earth mix 451, adding Pulverised Fuel Ash serves to lower thermal conductivity. In this case, adding 10% Pulverised Fuel Ash lowered thermal conductivity by 11.6%. Adding a further 10% resulted in further decrease of 2%. At 50% Pulverised Fuel Ash content, total thermal conductivity had fallen by almost 24%. Adding cement also resulted in thermal conductivity loss as shown in figure 10.4. Sample containing only cement as additive showed a decrease in thermal conductivity value.

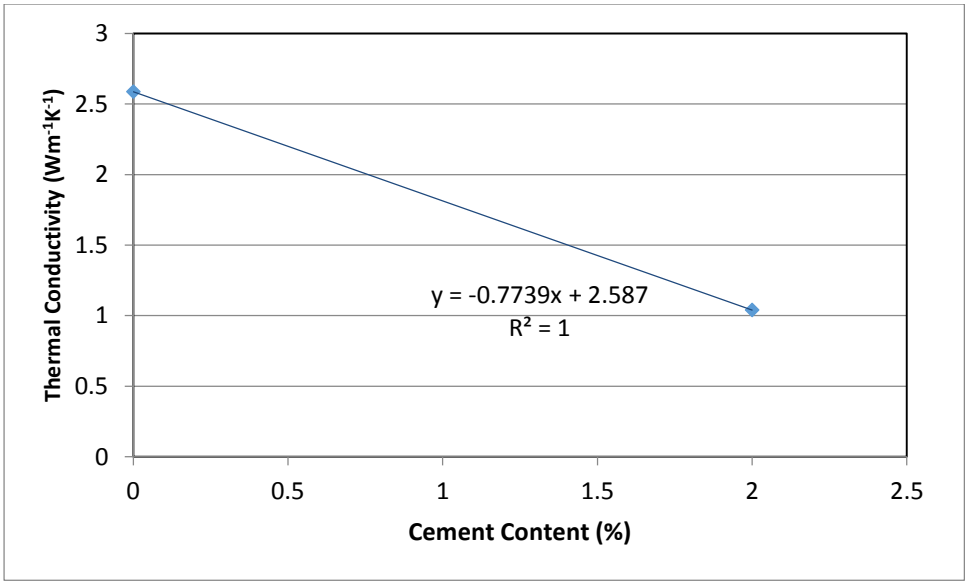

Figure 10.4 Thermal conductivity of 721 samples containing cement.

10.2 Finite Element (FE) Simulation

This chapter concerns the development of simulation models for representation of experimental tests carried out to determine the thermal properties rammed earth constituted by Pulverised Fuel Ash or PKS in varying proportions. A heat source was applied at one face of 50mm cubes and the extent of thermal propagation determined by taking readings at the surface over 2 hours.

FE simulations were created using the dynamic thermal energy model of the Mentat pre and post processing software and solved on the Marc software. The dynamic thermal model used, as opposed to the steady state analysis uses an automatic time stepping scheme to adjust the time step for each increment. This is based on a maximum allowable temperature change per step allowing the program to obtain a solution for a step and calculate the maximum temperature change in the step and checks this value against the specified control value. If the actual maximum change exceeds the specified value, the program repeats the step with a smaller time step and continues repeating the step until the maximum temperature change is smaller than the specified value of until the maximum number of recycles given on the control option is reached. This results in longer run time but more reliable output.

10.2.1 Governing Classical Heat transfer equation used in Marc Software

The Marc software uses an equation (as obtained from the user guide) very similar to the heat equation described in section 2. When T(x) is the temperature within an element, it can be interpolated from the nodal values T of the element through the interpolation functions N(x) so that

$$T(x) = N(x)T \qquad 10.1$$

The governing equation of the heat transfer problem is

$$C(T)\dot{T} + K(T)T = Q \qquad 10.2$$

In equation 10.2, C(T) and K(T) are the temperature-dependent heat capacity and thermal conductivity matrices, respectively, T is the nodal temperature vector, $\dot{T}$ is the time derivative of the temperature vector, and Q is the heat flux vector. The selection of the backward difference scheme for the discretization of the time variable in equation 10.2 yields the following expression:

$$\left[\frac{1}{\Delta t}C(T)+K(T)\right]T_n = Q_n + \frac{1}{\Delta t}C(T)T_{n-1} \qquad 10.3$$

Equation 10.3 computes nodal temperatures for each time increment ∆(t). For the evaluation of temperature-dependent matrices, the temperatures at two previous steps provide a linear (extrapolated) temperature description over the desired interval

$$T(\tau) = T(t-\Delta t) + \frac{\tau}{\Delta t}(T(t-\Delta t) - T9t - 2\Delta t)) \qquad 10.4$$

This temperature is then used to obtain an average property of the material f over the interval to be used in equation 10.3, such that

$$f = \frac{1}{\Delta t}\int_{t-\Delta t}^{t} f[T(\tau)]d\tau \qquad 10.5$$

During iteration, the average property is obtained based on the result of the previous iteration

$$T(\tau) = T(t-\Delta t) + \frac{\tau}{\Delta t}(T*(t) - T(t-\Delta t)) \qquad 10.6$$

Where T(τ) is the result of the previous iteration.

The expression of convective boundary condition is

$$q = H(T_s - T_\infty) \qquad 10.7$$

Here, q,H, T_s and T_∞ are heat flux, film coefficient, unknown surface temperature and ambient temperature respectively.

The radiative boundary condition can be expressed as

$$q = \sigma\varepsilon(T_s^4 - T_\infty^4) \qquad 10.8$$

Where q is the heat flux, σ is the Stefan-Boltzmann coefficient, ε is the emissivity and Ts and T∞ are unknown surface and ambient temperatures respectively. The radiative boundary conditions can be rewritten as

$$q = \sigma\varepsilon(T_s^3 + T_s^2 T_\infty + T_s T_\infty^2 + T_\infty^3)(T_s - T_\infty) \qquad 10.9$$

$$q = H(\sigma, \varepsilon, T_s, T_\infty)(T_s - T_\infty) \qquad 10.10$$

This shows that the radiative boundary condition is equivalent to a nonlinear convective boundary condition, in which the equivalent film coefficient $H(\sigma, \varepsilon, T_s, T_\infty)$ depends on the unknown surface temperature T_s.

10.2.1 Simulation Methodology

The methodology described below explains the steps that were taken to create the model.

1. Creation of geometry data for representing specimen
2. Creation of mesh and node count.
3. Quality check of the mesh.
4. Material properties assigned
5. Physical properties assigned
6. Boundary conditions applied
7. Load conditions applied
8. Run simulation
9. Analyse results

10.2.2 Creation of geometry data.

Geometry Points were created by defining dimension similar to material tested in the lab (Figure 10.5). The software used was Marc Mentat (Msc Software, 2013). As the geometry was a simple one this was completed efficiently. More complicated models can be completed and imported from AutoCAD

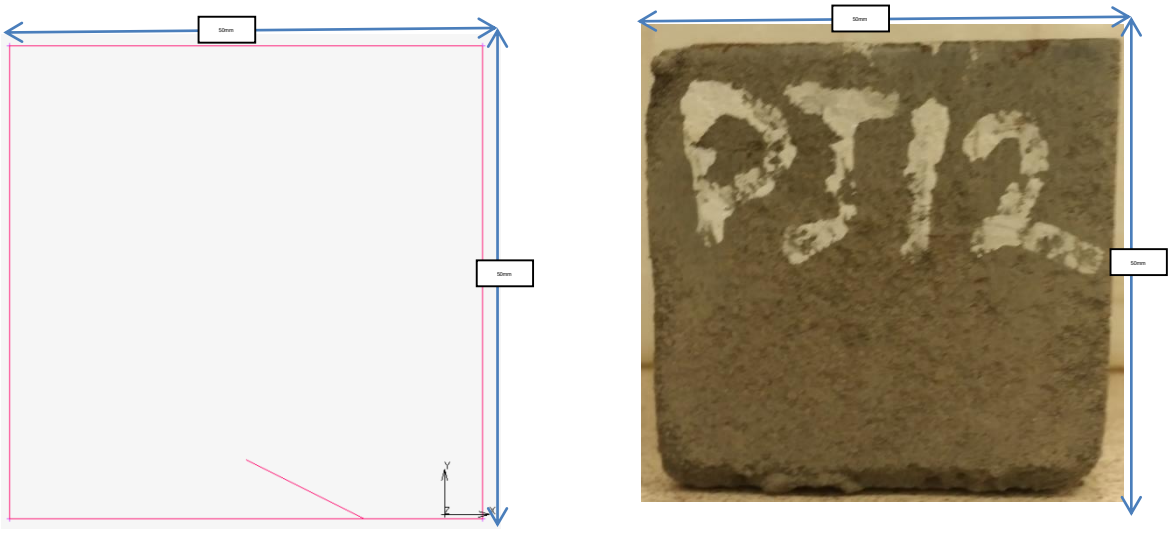

Figure 10.5 Geometric representation of rammed earth sample.

10.2.3 Creation of Mesh and Quality Check.

Meshing was carried out automatically within defined parameters. The density of mesh was determined after several trials with consideration to the time taken for the solver to complete each solution. More refined meshing did not result in significantly different results. The mesh was swept and meshes that were duplicated were deleted. Elements were also checked for distortion and nodes were checked to ensure that they were all referenced.

10.2.4 Material and Physical Property Definition

A planar element was used with a standard material property. As rammed earth is a combination of different soil types, the material type was distinguished by properties such as density, thermal conductivity and specific heat. Specific heat values was obtained from literature (Soebarto 2009; Allinson & Hall 2010; Taylor & Luther 2004; Hall & Allinson 2009; Taylor et al. 2008).

Initial conditions were set for each sample. The initial temperature of the sample before any heat was introduced was input into the pre-processor. This formed the boundary conditions for the faces that was not subject to a heat source (Figure 10.5). The ambient temperature was the room temperature

observed on the day of taking experimental readings. This was noted to be 24ºC. Boundary conditions were set to be constant throughout the test. Thermal transmission by convection was allowed. Loading was achieved by introducing 60ºC temperature source on one of the faces of the model (Figure 10.7). The simulation was run and results recorded (Figure 10.8).

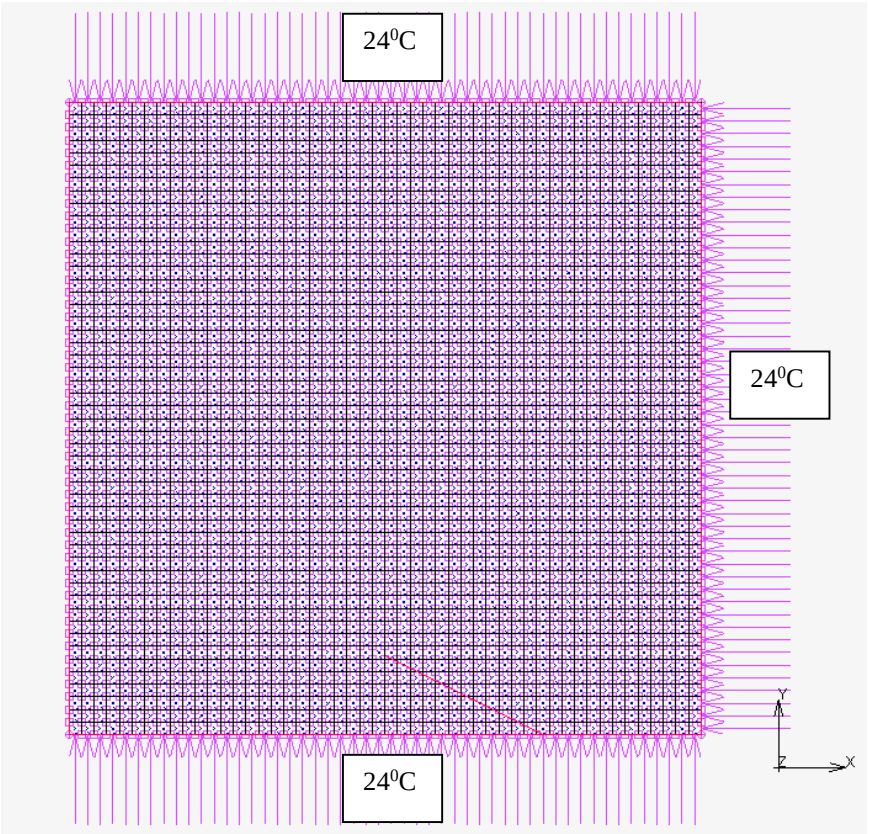

Figure 10.6 Boundary condition specification

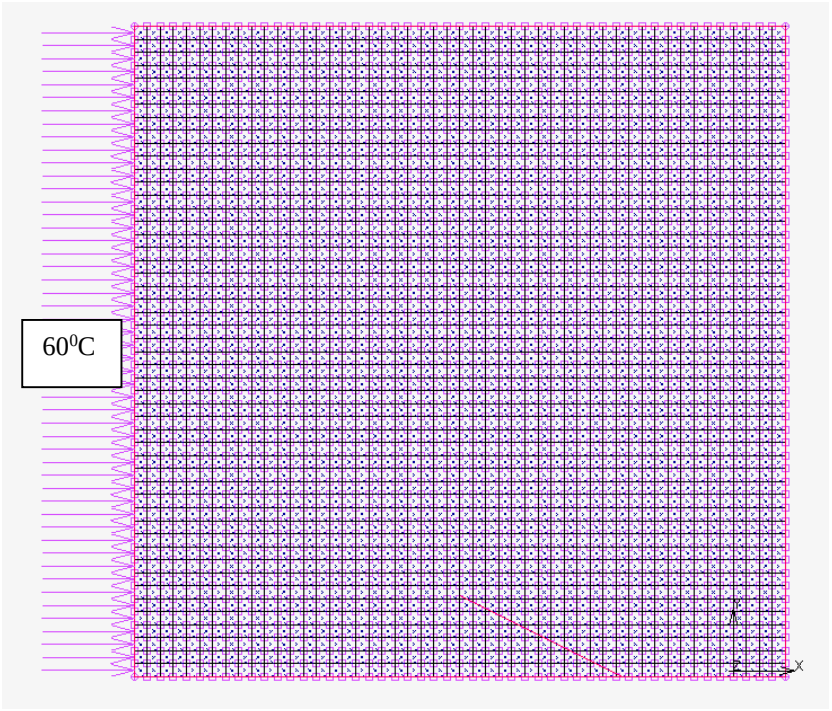

Figure 10.7 Heat source (load) specification

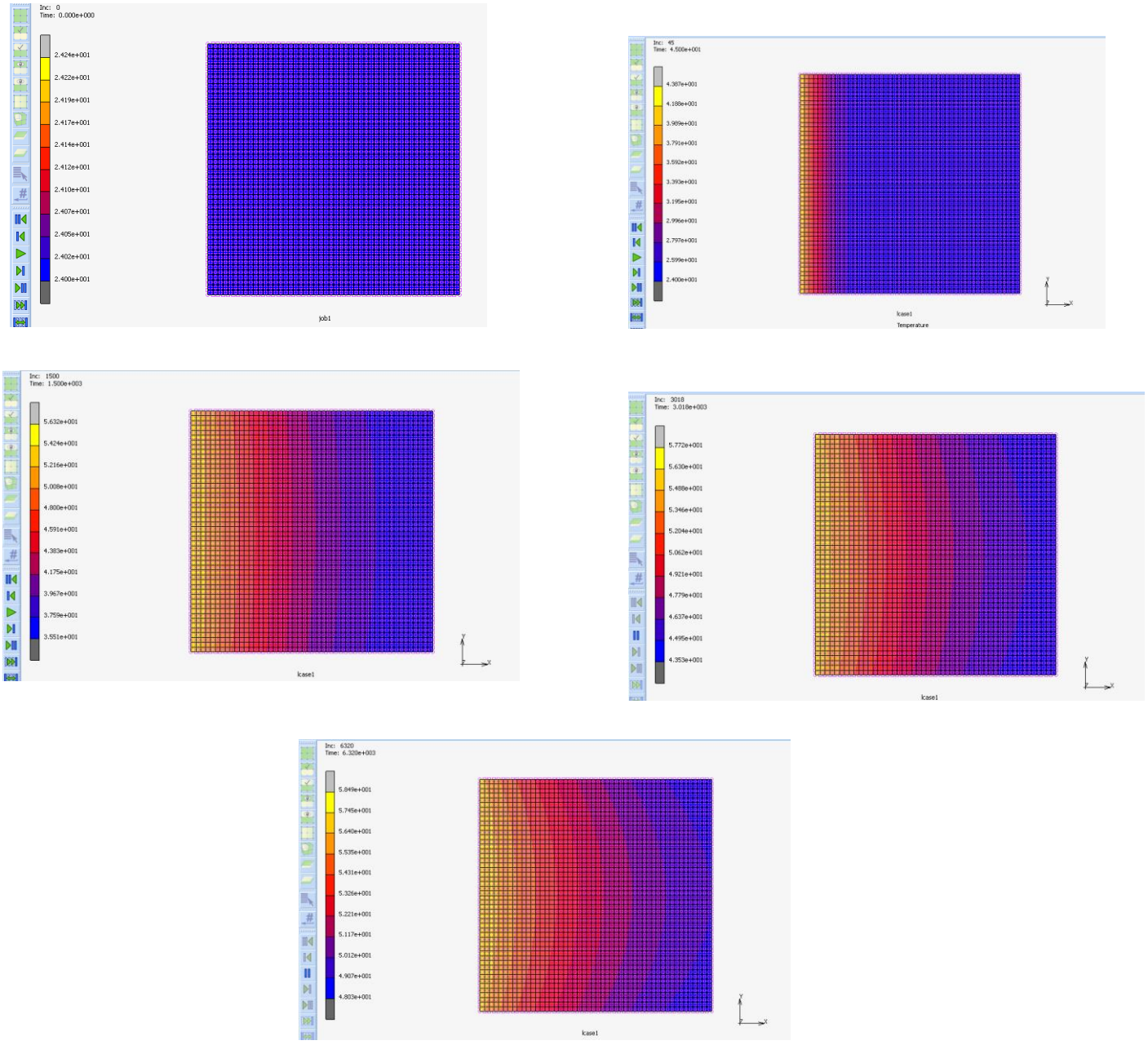

Figure 10.8 Temperature propagation at various time steps

10.2.5 Comparison with experimental data

The accuracy of the solver has been validated with experimental data to simulate the combined mode of heat transfer by conduction, convection and radiation. All the simulations have been tested experimentally.

It was necessary to validate the finite element model created based on the material properties and geometry information used in designing the model. Rammed earth samples measuring 50x50x50mm and having similar material properties was used in the validation. The effect of different mesh densities and total computation time was examined. This is because a poor mesh may result in a larger element aspect ratio than is desirable. In the long term this could lead to inaccurate prediction or convergence problem. No appreciable difference was however observed when different mesh densities were used as the model was relatively uncomplicated (Figure 10.9).

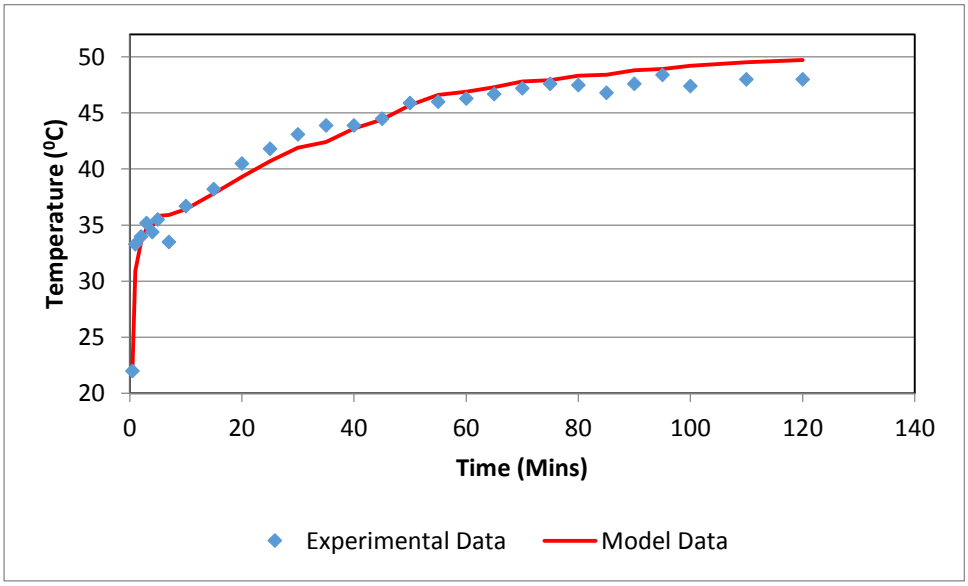

Figure 10.9 Comparison of experimental and model data for 721 grade rammed earth

The finite element model reproduces quite accurately the heat transfer mechanism in walls made from rammed earth. Further work will have to be carried out in choosing or developing appropriate mathematical models depending on what phenomena is to be predicted. The thermal qualities of

rammed earth is a key selling point in regions that have low sociocultural tolerance for rammed earth buildings.

Chapter Eleven

Conclusion and Future work

The selection of earth to be constituted into rammed earth is sometimes not determined by the builder. Best practice in the use of rammed earth as a building material is to use whatever materials are available locally. While it is possible to import different grades of soil components to mix into available earth to produce a different grade (for example, adding granite or clayey soil to very sandy soil to produce an evenly blended mix), it is important for a builder to know how to improve each soil type to ensure the best attribute is obtained from available soils. The addition of waste material that can be obtained cheaper than other soil types can provide properties that are desirable without increasing cost astronomically (for example obtaining palm kernel shells for free rather than paying for granite chippings to increase the amount of coarse aggregate in a mix).

While various earth mixes would perform adequately as a structural material, choosing an acceptable mix depends on what property is most desirable to the builder. While a rammed earth mix would perform poorly as a thermal buffer and have a high thermal diffusivity constant, it might have a low density and perform better as a light weight material. Each material tested will be summarised in terms of material property.

11.1 Rammed earth made from 532 Soil grade

At 90 days of testing, rammed earth samples grade 532 containing the most Pulverised Fuel Ash had the lowest density at 1656 Kg/m^3. Density stood at 1925 Kg/m^3 for sample containing no additives except Palm kernel shell. Unstabilised rammed earth of this grade having granite as its coarse aggregate had a density of 2289Kg/m^3. Using 100% PKS as coarse aggregate or adding 50% Pulverised Fuel Ash to the mix served to reduce density by 16% and 28% respectively.

Compressive strength results did not follow the same trend as density. The highest Pulverised Fuel Ash content did not provide the highest compressive strength even when mixed with the highest cement content. However, sample containing 20% Pulverised Fuel Ash and 9% cement showed the highest compressive strength of samples tested. Of samples containing PKS, rammed

earth containing a mix of PKS and coarse aggregate in the ratio 10/90 produced the highest compressive strength recorded.

Thermal conductivity appeared to be lowest in unstabilised rammed earth. Increasing the PKS and Pulverised Fuel Ash content served to increase thermal conductivity. At 50% Pulverised Fuel Ash content, thermal conductivity had started to decrease. Further Pulverised Fuel Ash content could serve to lower thermal conductivity but this could be at a cost to compressive strength. This matter needs to be further investigated.

Sorptivity was lowest for unstabilised rammed earth. While increasing the level of stabilisation served to increase sorptivity, this increase was marginal compared to the effect of adding Pulverised Fuel Ash. While sorptivity increased with increase in proportion of PKS, the effect was marginal. Adding cement to stabilise however raised sorptivity further.

11.2 Rammed Earth Made from 451 Soil Grade

The sample having the lowest density on the 90th day of testing was the sample containing 50% Pulverised Fuel Ash at 1738Kg/m^3. Although unstabilised 451 grade rammed earth was consistently lower than unstabilised 532 soil grade samples at all ages, adding 50% Pulverised Fuel Ash served to lower density in 532 grade rammed earth much more than the 451 grade rammed earth. There was only a 12% decrease in the density of the 451 grade sample as opposed to the 28% decrease in density observed in the 532 grade rammed earth. Palm Kernel shell was not added to the 451 grade so there is no data to determine the effect of PKS on 451 grade rammed earth.

Compressive strength values for 451 soil grade rammed earth were the worst at all ages when compared to all other grades tested. When Pulverised Fuel Ash was added to the mix, compressive strength was improved. This improvement was most important in day 1 values as it would mean the difference between accepting the mix for weight bearing purposes or rejecting it as it moves day 1 strengths above the minimum accepted compressive strength of 1.3MPa as specified in the New Zealand building code. This

improvement however didn't last beyond 20% Pulverised Fuel Ash content as diminishing return set in for each increase in the proportion of Pulverised Fuel Ash above 20%. When tested at 90 days, sample containing 10% Pulverised Fuel Ash and 9% cement exhibited the highest compressive strength in this soil grade.

The 451 rammed earth grade was the only soil mix tested that showed a decrease in thermal conductivity when Pulverised Fuel Ash was added. Thermal conductivity had fallen by 24% at 50%. At 50% Pulverised Fuel Ash content, 451 had the lowest thermal conductivity constant as compared to other soil grades tested. However without the Pulverised Fuel Ash, unstabilised rammed earth made from 415 soil mix had the highest thermal conductivity value.

Unlike the 532 sample, sorptivity was not at its lowest for unstabilised samples. Rather, sorptivity was lowest for the 2% cement stabilised sample containing no Pulverised Fuel Ash. The highest levels of sorptivity were noticed in samples that had a combination of cement and Pulverised Fuel Ash.

11.3 Rammed earth made from 622 Soil Grade

No tests were carried out for 622 soil grade samples containing Pulverised Fuel Ash. However properties of the same grade containing PKS in various proportions were investigated.

Density was observed to be at its lowest after 90 days in samples containing the highest quantity of PKS. Density was lowered by 12% when 100% of the coarse aggregate was replaced by PKS. It was also observed that stabilising this soil grade with 5% cement led to an increase in density.

Unlike the 532 sample where 10% PKS content produced the highest Compressive strength, compressive strength was highest at 50% PKS content for the 622 soil grade. Compressive strength started falling at higher PKS content. At 5% cement stabilisation, compressive strength was higher for

samples containing only granite chippings by 29% when compared to samples containing only PKS.

Thermal conductivity was higher in 622 grade soil than in 532 grade soil when both samples contained only crushed granite as coarse aggregate. However, at 50% PKS content, thermal conductivity started to fall. At 100% PKS content thermal conductivity value for 622 soil grade was the lowest recorded for every sample tested.

While sorptivity in 622 soil grade was 97% more than that observed in 532 soil mix, sorptivity was lowest in unstabilised 622 soil grade samples when compared to values obtained from various combinations of PKS and crushed granite.

11.4 Rammed Earth Made from 721 Soil Grade

Density was lowest at 90 days for sample containing 50% Pulverised Fuel Ash and 2% cement. This was only marginally lower (0.5%) than values obtained in samples containing 20% Pulverised Fuel Ash and 0% cement. Adding cement appeared to increase density values.

In unstabilised rammed earth made from 721 grade soil, compressive strength was highest at the highest level of Pulverised Fuel Ash content. When cement was used as a stabiliser, compressive strength rose significantly. The sample that had the highest compressive strength after 90 days of testing for all 721 mix samples was the sample containing 20% Pulverised Fuel Ash and 9% cement.

Thermal conductivity in the 721 blend started to rise as Pulverised Fuel Ash was added to the mix. Values were still on the increase at 50% Pulverised Fuel Ash content.

Sorptivity was lowest for sample containing 20% Pulverised Fuel Ash and 9% cement. Sorptivity appeared to be high when cement was used as a stabiliser and no Pulverised Fuel Ash was added. A combination of cement and Pulverised Fuel Ash produced lower values of sorptivity.

This research has shown that materials that would otherwise have made it to landfill and other waste dump sites have been put to use in ensuring that most soils can be utilised in producing rammed earth walls.

11.5 Recommendation

As the trend in rammed earth building continues to grow, there is a need for the development of proper codes that guides and streamlines the building, testing and utilization of rammed earth structures.

More tests have to be carried out to determine the effect of other additives like oil and how it influences the mechanical and physical attributes of rammed earth. The use of glass fibre should also be investigated against its potentials to offer additional reinforcement in rammed earth. And lastly, the introduction of steel reinforcement could widen the application for rammed earth. This requires investigation.

11.6 Summary

This research effort was aimed at finding ways to dispose waste material safely in rammed earth. It was a plus to discover that there was added benefits in incorporating fuel ash and palm kernel shell in rammed earth. This has direct consequence on potential users of rammed earth. One direct utilization is the addition of palm kernel shell to rammed earth in regions that have predominantly sandy soils and coarse aggregate is not found locally.

Where most power stations have found application for low LOI fuel ash, high LOI fuel ash continue to be a problem as environmental laws get tougher. The ability to use this material in rammed earth provides a solution that is economical providing building sites are close to power plants.

The physical and material properties outlined for various soil grades would serve as a guide for local soil found at any building site.

References

Abd Rashid, R.Z. et al. (2014) Reduction of low grade iron ore pellet using palm kernel shell. *Renewable Energy,* **63**, pp.617–623.

Abd. Rashid, N. et al. (2012) Crystallisation kinetics of palm stearin, palm kernel olein and their blends. *LWT - Food Science and Technology*, **46**(2), pp.571–573

Abdelatif, A.O., Owen, J.S., & Hussein, M.F.M. (2015) Modelling the prestress transfer in pre-tensioned concrete elements. *Finite Elements in Analysis and Design,* **94**, pp.47–63.

Abdelmalik, A.A. (2014) Chemically modified palm kernel oil ester: A possible sustainable alternative insulating fluid. *Sustainable Materials and Technologies,* 1-2, pp.42–51.

Abdullah, M.S. (2006) *Determination of optimum concentration of lime slurry for soil stabilisation.* Universiti Teknologi Malaysia, Faculty of Civil Engineering.

Abechi, E.S. et al. (2011) Kinetics of adsorption of methylene blue onto activated carbon prepared from palm kernel shell. *Arch Appl Sci Res*, **3**(1), pp.154–164.

Acker, P. & Ulm, F.-J. (2001) Creep and shrinkage of concrete: physical origins and practical measurements. *Nuclear Engineering and Design,* **203**(2–3), pp.143–158

Ahn, H.K., Richard, T.L. & Glanville, T.D. (2008) Optimum moisture levels for biodegradation of mortality composting envelope materials. *Waste Management,* **28**(8), pp.1411–1416.

Aimin, Y., Yuli, D., & Litang, G. (2013) Behavior of unbonded prestressed continuous concrete slabs with the middle and edge span subjected to fire in sequence. *Fire Safety Journal,* **56**, pp.20–29.

Aïtcin, P.C. (2003) The durability characteristics of high performance concrete: a review. *Cement and Concrete Composites*, **25**(4–5), pp.409–420.

Alengaram, U. J., Jumaat, M. Z., & Mahmud, H. (2008) Influence of cementitious materials and aggregates content on compressive strength of palm kernel shell concrete. *Journal of Applied Sciences*, **8**(18), pp.3207–3213.

Alengaram, U. J., Jumaat, M. Z., & Mahmud, H. (2008) Influence of sand content and silica fume on mechanical properties of palm kernel shell

concrete. *In International conference on construction and building technology ICCBT*. pp. 251–262.

Alengaram, U. J., Jumaat, M. Z., & Mahmud, H. (2008) Ductility behaviour of reinforced palm kernel shell concrete beams. *European Journal of Scientific Research*, **23**(3), pp.406–420.

Allinson, D., & Hall, M. (2010) Hygrothermal analysis of a stabilised rammed earth test building in the UK. *Energy and Buildings*, **42**(6), 845-852.

Angulo-IbÃ¡Ã±ez, Q., Mas-TomÃ¡s, Ã., GalvaÃ±-LLopis, V., & SÃ¡ntolaria-Montesinos, J. L. (2012) Traditional braces of earth constructions. *Construction and Building Materials*, **30**(0), 389.

Anon, (1986) Fourth international symposium on creep and shrinkage of concrete: Mathematical modelling. *Computers & Structures*, **22**(6), p.109 – 118.

Anon, (1996) Ultimate strength of rammed earth walls with openings : D. M. Lilley & J. Robinson, Proceedings — ICE: Structures & Buildings, 110(3), 1995, pp 278–287. *International Journal of Rock Mechanics and Mining Sciences & Geomechanics* **33**(2), p.A84.

Anon, (2006) A comparative study of concrete properties using coconut shell and palm kernel shell as coarse aggregates: Building and Environment, 2006, 41, (3), 297–301.

Aripin, N.F.K., Park, J.W. & Park, H.J. (2012) Preparation of vesicle drug carrier from palm oil- and palm kernel oil-based glycosides. Colloids and surfaces. B, Biointerfaces, 95, pp.144–53.

Asadullah, M. et al. (2014) Optimization of palm kernel shell torrefaction to produce energy densified bio-coal. *Energy Conversion and Management*, **88**, pp.1086–1093.

Asif, M., Muneer, T. & Kelley, R. (2007) Life cycle assessment: A case study of a dwelling home in Scotland. *Building and Environment,* **42**(3), pp.1391–1394.

Bai, J., Wild, S. & Sabir, B.B. (2002) Sorptivity and strength of air-cured and water-cured PC–PFA–MK concrete and the influence of binder composition on carbonation depth. *Cement and Concrete Research*, **32**(11), pp.1813–1821.

Bažant, Z.P. (1983) Mathematical model for creep and thermal shrinkage of concrete at high temperature. *Nuclear Engineering and Design*, **76**(2), pp.183–191.

Bažant, Z.P. (2001) Prediction of concrete creep and shrinkage: past, present and future. *Nuclear Engineering and Design*, **203**(1), pp.27–38.

Bazargan, A., Rough, S.L. & McKay, G. (2014) Compaction of palm kernel shell biochars for application as solid fuel. *Biomass and Bioenergy*, **70**, pp.489–497.

Beckett, C. & Augarde, C. (2012) The Effect of Relative Humidity and Temperature on the Unconfined Compressive Strength of Rammed Earth. *In Unsaturated Soils: Research and Applications*. Springer, pp. 287–292.

Benboudjema, F., Meftah, F. & Torrenti, J.M. (2005) Interaction between drying, shrinkage, creep and cracking phenomena in concrete. *Engineering Structures,* **27**(2), pp.239–250.

Bergaya, F., Theng, B.K.G. & Lagaly, G. (2011) Handbook of clay science, Elsevier.

Berger, K.G. (2003) Encyclopaedia of Food Sciences and Nutrition, Elsevier.

Beygi, M.H.A. et al. (2014) The influence of coarse aggregate size and volume on the fracture behaviour and brittleness of self-compacting concrete. *Cement and Concrete Research*, **66**, pp.75–90.

Bijen, J., (2005) Other uses of Pulverised Fuel Ash. Pulverised Fuel Ash in concrete, pp.173–179.

Bodman, G.B., & Edlefsen, N.E. (1934) The soil-moisture system. *Soil Science,* **38**(6), pp.425–444.

Bravo-Osuna, I., Ferrero, C. & Jiménez-Castellanos, M.R. (2007) Influence of moisture content on the mechanical properties of methyl methacrylate–starch copolymers. *European Journal of Pharmaceutics and Biopharmaceutics,* **66**(1), pp.63–72.

British Standard Institution, (2004) *Wood-based panels for use in construction - Characteristics, evaluation of conformity and marking*. BS EN 13986:2004.

British Standard Institution, (2008) *Metallic Materials. Sheet and strip. Determination of forming-limit curves. Part 1: Measurement and application of forming-limit diagrams in the press shop* B. S. Institution, ed. BS EN ISO 12004-1:2008.

British Standard Institution, (2009) *Quantities and units*. General. BS-ISO 80000-1:2009. Available at: http://www.mendeley.com/c/5208617444/p/18992101/british-standard-institution-2009-quantities-and-units-general/.

Brooks, J.J. (2015) *Concrete and Masonry Movements*, Elsevier.

Brown, C. (2010) Cicely in Nigeria.

Brown, R. (2009) Bradessono: Napa Valley's Eco Resort.

Bui, Q. -., Hans, S., Morel, J. -., & Do, A. -. (2011) First exploratory study on dynamic characteristics of rammed earth buildings. *Engineering Structures*, **33**(12), 3690-3695.

Bui, Q. B., Morel, J. C., Venkatarama Reddy, B. V., & Ghayad, W. (2009) Durability of rammed earth walls exposed for 20 years to natural weathering. *Building and Environment*, **44**(5), 912-919.

Bui, Q., & Morel, J. (2009) Assessing the anisotropy of rammed earth. *Construction and Building Materials,* **23**(9), 3005-3011.

Bui, Q.-B. et al., (2009) Compression behaviour of non-industrial materials in civil engineering by three scale experiments: the case of rammed earth. *Materials and structures*, **42**(8), pp.1101–1116.

Bui, Q.B. et al., (2009) Durability of rammed earth walls exposed for 20 years to natural weathering. *Building and Environment*, **44**(5), pp.912–919.

Bui, Q.-B. et al., (2011) First exploratory study on dynamic characteristics of rammed earth buildings. *Engineering Structures,* **33**(12), pp.3690–3695.

Burroughs, S., (2008) Soil property criteria for rammed earth stabilization. *Journal of Materials in Civil Engineering,* **20**(3), pp.264–273.

Burroughs, S., (2009) Relationships between the density and strength of rammed earth. *Proceedings of the ICE-Construction Materials*, **162**(3), pp.113–120.

Cardoso, F.A. et al., (2009) Carbide lime and industrial hydrated lime characterization. *Powder Technology*, **195**(2), pp.143–149.

Carew, A. L., & Mitchell, C. A. (2008) Teaching sustainability as a contested concept: Capitalizing on variation in engineering educators' conceptions of environmental, social and economic sustainability. *Journal of Cleaner Production,* **16**(1), 105.

Carrick, S. et al., (2011) Atypical early-time infiltration into a structured soil near field capacity: The dynamic interplay between sorptivity, hydrophobicity, and air encapsulation. *Geoderma*, **160**(3–4), pp.579–589.

Carvers, (2011) *Carvers Building Suppliers*. Available at: http://www.carvers.co.uk/ [Accessed September 9, 2011].

Castro-Lacouture, D. et al., (2009) Optimization model for the selection of materials using a LEED-based green building rating system in Colombia. *Building and Environment,* **44**(6), pp.1162–1170.

Chan, S.Y.N. & Ji, X., (1998) Water sorptivity and chloride diffusivity of oil shale ash concrete. *Construction and Building Materials*, **12**(4), pp.177–183.

Chang, S.K. et al., (2014) Biochemical characterisation of the soluble proteins, protein isolates and hydrolysates from oil palm (Elaeis guineensis) kernel. *Food Bioscience*, **7,** pp.1–10.

Che, A., Ge, X. & Li, Y., Use of non-destructive techniques in Chinese traditional timber structures.

Cheerarot, R. & Jaturapitakkul, C., (2004) A study of disposed Pulverised Fuel Ash from landfill to replace Portland cement. *Waste Management,* **24**(7), pp.701–709.

Chen, H. et al., (2000) Oxygen sorptivity of mesoporous aluminosilicate modified by Co-salen complex. *Microporous and Mesoporous Materials,* **40**(1–3), pp.289–298.

Chen, J., Han, J., Oztoprak, S., & Yang, X. (2009). Behavior of single rammed aggregate piers considering installation effects. *Computers and Geotechnics,* **36**(7), 1191-1199.

Chen, J.-F. et al., (2009) Behavior of single rammed aggregate piers considering installation effects. *Computers and Geotechnics*, **36**(7), pp.1191–1199.

Chen, W. et al., (2012) Water retention and gas relative permeability of two industrial concretes. *Cement and Concrete Research*, **42**(7), pp.1001–1013.

Chen, W., Gast, K.L.B. & Smithey, S., (2000) The effects of different freeze-drying processes on the moisture content, color, and physical strength of roses and carnations. *Scientia Horticulturae,* **84**(3–4), pp.321–332.

Chindaprasirt, P. & Pimraksa, K., (2008) A study of Pulverised Fuel Ash–lime granule unfired brick. *Powder Technology,* **182**(1), pp.33–41.

Choi, W.-C., Khil, B.-S. & Yun, H.-D., (2015) Characteristics of structural concrete containing fluorosilicate-based admixture (FBA) for improving water-tightness. *Construction and Building Materials,* **74**, pp.241–248.

Choong, C.G. & McKay, A., (2014) Sustainability in the Malaysian palm oil industry. *Journal of Cleaner Production,* **85**, pp.258–264.

Choong, T.S.Y. et al., (2006) Film-pore-concentration-dependent surface diffusion model for the adsorption of dye onto palm kernel shell activated carbon. *Journal of Colloid and Interface Science*, **301**(2), pp.436–440.

Christen, A., Navarro, C. M., & MÃ¤usezahl, D. (2009). Safe drinking water and clean air: An experimental study evaluating the concept of combining household water treatment and indoor air improvement using the water disinfection stove (WADIS). *International Journal of Hygiene and Environmental Health,* **212**(5), 562.

Ciancio, D. & Gibbings, J., (2012) Experimental investigation on the compressive strength of cored and molded cement-stabilized rammed earth samples. *Construction and Building Materials*, **28**(1), pp.294–304.

Cid-Falceto, J., MazarrÃ³n, F. R., & CaÃ±as, I. (2012) Assessment of compressed earth blocks made in Spain: International durability tests. *Construction and Building Materials,* **37**(0), 738.

Cluley, N.C. & Shepherd, R., (1996) Analysis of concrete cable-stayed bridges for creep, shrinkage and relaxation effects. *Computers & Structures*, **58**(2), pp.337–350.

Çokça, E. & Tilgen, H.P., (2010) Shear strength-suction relationship of compacted Ankara clay. *Applied Clay Science*, **49**(4), pp.400–404.

Coleman, J.S., (1960) Nigeria: Background to Nationalism, University of California Pr.

Comley, P.N., (2007) The ASTM International Standard Test Method for Determining the Superplastic Properties of Metallic *Materials. Materials Science Forum,* 551-552 (Superplasticity in Advanced Materials - ICSAM 2006), pp.105–110.

Conciatori, D., Sadouki, H. & Brühwiler, E., (2008) Capillary suction and diffusion model for chloride ingress into concrete. *Cement and Concrete Research,* **38**(12), pp.1401–1408.

Cowles, L.A., (2012) Social work in the health field: A care perspective, Routledge.

Cremonesi, M., Frangi, A. & Perego, U., (2011) A Lagrangian finite element approach for the simulation of water-waves induced by landslides. *Computers & Structures,* **89**(11), pp.1086–1093.

Culligan, P.J., Ivanov, V. & Germaine, J.T., (2005) Sorptivity and liquid infiltration into dry soil. *Advances in Water Resources*, **28**(10), pp.1010–1020.

Dakwale, V. A., Ralegaonkar, R. V., & Mandavgane, S. (2011) Improving environmental performance of building through increased energy efficiency: A review. *Sustainable Cities and Society,* **1**(4), 211.

Dawood, N.N., (1995) Scheduling in the precast concrete industry using the simulation modelling approach. *Building and Environment*, **30**(2), pp.197–207.

De Wilde, P. et al., (2009) Progress in simulation of a thermal probe: modelling the probe to sample conductance.

Dellinghausen, L.M. et al., (2012) Total shrinkage, oxygen permeability, and chloride ion penetration in concrete made with white Portland cement and blast-furnace slag. *Construction and Building Materials*, **37**(0), pp.652–659.

Den Heede, P. Van, Gruyaert, E. & Belie, N. De, (2010) Transport properties of high-volume Pulverised Fuel Ash concrete: Capillary water sorption, water sorption under vacuum and gas permeability. *Cement and Concrete Composites*, *32*(10), pp.749–756.

Dias, W.P.S., (2000) Reduction of concrete sorptivity with age through carbonation. *Cement and Concrete Research,* **30**(8), pp.1255–1261.

Dickinson, R.E., (1984) Modelling evapotranspiration for three-dimensional global climate models. Climate processes and climate sensitivity, pp.58–72.

Dimoudi, A. & Tompa, C., (2008) Energy and environmental indicators related to construction of office buildings. *Resources, Conservation and Recycling,* **53**(1–2), pp.86–95

Dixit, M.K. et al., (2012) Need for an embodied energy measurement protocol for buildings: A review paper. *Renewable and Sustainable Energy Reviews*, **16**(6), pp.3730–3743.

Djongyang, N., Tchinda, R. & Njomo, D. (2010) Thermal comfort: A review paper. *Renewable and Sustainable Energy Reviews*, **14**(9), p.2626.

Dmochowski, Z.R. (1990) An introduction to Nigeria traditional architecture. Vol. 1: Northern Nigeria. Vol. 2: South west and central Nigeria.

Dong, N. (2010) Reducing Carbon-in-ash

Durá, A.A., Boquera, A.M. & Pulido, V.L., (2012) Analysis and characterization of earthen architecture as a structural material: The corbelled course domes in Syria. *In Rammed Earth Conservation: Proceedings of the First Internatonal Conference on Rammed Earth Conservation*, Restapia 2012, Valencia, Spain, 21-23 June 2012. p. 445.

Easton, D., (2007) The rammed earth house, *Chelsea Green Publishing*.

Ecke, H., (2003) Sequestration of metals in carbonated municipal solid waste incineration (MSWI) Pulverised Fuel Ash. *Waste Management*, **23**(7), pp.631–640.

Edwards, B., (2007) Rough guide to sustainability second edi., *RIBA Enterprises Ltd.*

El-Sayed, G.O., (2011) Removal of methylene blue and crystal violet from aqueous solutions by palm kernel fibre. *Desalination*, **272**(1–3), pp.225–232.

Emmanuel, R., (2004) Estimating the environmental suitability of wall materials: preliminary results from Sri Lanka. *Building and Environment,* **39**(10), pp.1253–1261.

Erkal, A., Dâ€TMAyala, D. & Sequeira, L. (2012) Assessment of wind-driven rain impact, related surface erosion and surface strength reduction of historic building materials. *Building and Environment,* **57**(0), p.336.

Erkmen, R.E. & Bradford, M.A. (2011) Time-dependent creep and shrinkage analysis of composite beams curved in-plan. *Computers & Structures*, **89**(1–2), pp.67–77.

Esin, T. (2007) A study regarding the environmental impact analysis of the building materials production process (in Turkey). *Building and Environment,* **42**(11), pp.3860–3871.

Esping, O. (2008) Effect of limestone filler BET(H2O)-area on the fresh and hardened properties of self-compacting concrete. *Cement and Concrete Research,* **38**(7), pp.938–944.

Faria, P., Henriques, F. & Rato, V. (2008) Comparative evaluation of lime mortars for architectural conservation. *Journal of Cultural Heritage*, **9**(3), pp.338–346.

Febriansyah, H. et al., (2014) Gama Stove: Biomass Stove for Palm Kernel Shells in Indonesia. *Energy Procedia*, **47**, pp.123–132.

Florez, L. & Castro-Lacouture, D. (2013) Optimization model for sustainable materials selection using objective and subjective factors. *Materials & Design,* **46**(0), pp.310–321.

Franzoni, E. (2011) Materials Selection for Green Buildings: which Tools for Engineers and Architects? *Procedia Engineering*, **21**(0), pp.883–890.

Galán-Marín, C., Rivera-Gómez, C., & Petric, J. (2010). Clay-based composite stabilized with natural polymer and fibre. *Construction and Building Materials,* **24**(8), 1462-1468.

Gasparatos, A., El-Haram, M. & Horner, M. (2008) A critical review of reductionist approaches for assessing the progress towards sustainability.

Godwin, P. J. (2011) Building conservation and sustainability in the United Kingdom. *Procedia Engineering*, **20**(0), 12.

Gomes, M. I., Lopes, M., & Brito, J. D. (2011) Seismic resistance of earth construction in Portugal. *Engineering Structures*, **33**(3), 932.

Gonen, T. & Yazicioglu, S. (2007) The influence of compaction pores on sorptivity and carbonation of concrete. *Construction and Building Materials,* **21**(5), pp.1040–1045.

Gonen, T. & Yazicioglu, S. (2007) The influence of mineral admixtures on the short and long-term performance of concrete. *Building and Environment,* **42**(8), pp.3080–3085.

Gopalan, M.K. (1996) Sorptivity of Pulverised Fuel Ash concretes. *Cement and Concrete Research,* **26**(8), pp.1189–1197.

Gospodinov, P.N. (2005) Numerical simulation of 3D sulphate ion diffusion and liquid push out of the material capillaries in cement composites. *Cement and Concrete Research,* **35**(3), pp.520–526.

Goual, M.S. et al., (2000) Estimation of the capillary transport coefficient of Clayey Aerated Concrete using a gravimetric technique. *Cement and Concrete Research,* **30**(10), pp.1559–1563.

Graymore, M. L. M., Sipe, N. G., & Rickson, R. E. (2008) Regional sustainability: How useful are current tools of sustainability assessment at the regional scale? *Ecological Economics,* **67**(3), 362.

Greaves, H.M. (1996) An introduction to lime stabilisation. *In Proceedings of Seminar on Lime Stabilisation at Loughborough University* (Rogers CD, Glendinning S and Dixon N (eds)). Thomas Telford, London. pp. 5–12.

Guerra, M. et al., (2014) Anchorage of steel rebars to recycled aggregates concrete. *Construction and Building Materials*, **72**, pp.113–123.

Gummerson, R.J., Hall, C. & Hoff, W.D. (1980) Water movement in porous building materials—II. Hydraulic suction and sorptivity of brick and other masonry materials. *Building and Environment*, **15**(2), pp.101–108.

Gummerson, R.J., Hall, C. & Hoff, W.D. (1981) Water movement in porous building materials—III. A sorptivity test procedure for chemical injection damp proofing. *Building and Environment,* **16**(3), pp.193–199.

Gungat, L., Putri, E.E. & Makinda, J. (2013) Effects of Oil Palm Shell and Curing Time to the Load-Bearing Capacity of Clay Subgrade. *Procedia Engineering,* **54**(0), pp.690–697.

Gustavsson, L. & Joelsson, A. (2010) Life cycle primary energy analysis of residential buildings. *Energy and Buildings*, **42**(2), pp.210–220.

Haapio, A. & Viitaniemi, P. (2008) Environmental effect of structural solutions and building materials to a building. *Environmental Impact Assessment Review,* **28**(8), pp.587–600.

Habert, G. et al. (2012) Power: A new paradigm for energy use in sustainable construction. *Ecological Indicators,* **23**(0), p.109.

Habert, G., Castillo, E., Vincens, E., & Morel, J. C. (2012) Power: A new paradigm for energy use in sustainable construction. *Ecological Indicators,* **23**(0), 109.

Hall, C. & Tse, T.K.-M. (1986) Water movement in porous building materials—VII. The sorptivity of mortars. *Building and Environment*, **21**(2), pp.113–118.

Hall, C. & Yau, M.H.R., (1987) Water movement in porous building materials—IX. The water absorption and sorptivity of concretes. *Building and Environment,* **22**(1), pp.77–82.

Hall, C. (1981) Water movement in porous building materials—IV. The initial surface absorption and the sorptivity. *Building and Environment*, **16**(3), pp.201–207.

Hall, M. & Allinson, D. (2008) Assessing the moisture-content-dependent parameters of stabilised earth materials using the cyclic-response admittance method. *Energy and Buildings*, **40**(11), pp.2044–2051.

Hall, M. & Allinson, D. (2009) Assessing the effects of soil grading on the moisture content-dependent thermal conductivity of stabilised rammed earth materials. *Applied Thermal Engineering*, **29**(4), pp.740–747.

Hall, M. & Allinson, D. (2009) Analysis of the hygrothermal functional properties of stabilised rammed earth materials. *Building and Environment*, **44**(9), pp.1935–1942.

Hall, M. & Allinson, D. (2009) Assessing the effects of soil grading on the moisture content-dependent thermal conductivity of stabilised rammed earth materials. *Applied Thermal Engineering*, **29**(4), pp.740–747.

Hall, M. & Djerbib, Y. (2004) Moisture ingress in rammed earth: Part 1—the effect of soil particle-size distribution on the rate of capillary suction. *Construction and Building Materials*, **18**(4), pp.269–280.

Hall, M. & Djerbib, Y. (2004) Rammed earth sample production: context, recommendations and consistency. *Construction and Building Materials,* **18**(4), p.281.

Hall, M. & Djerbib, Y. (2006) Moisture ingress in rammed earth: Part 3 – Sorptivity, surface receptiveness and surface inflow velocity. *Construction and Building Materials,* **20**(6), pp.384–395.

Hall, M. & Djerbib, Y. (2006) Moisture ingress in rammed earth: Part 2 – The effect of soil particle-size distribution on the absorption of static pressure-driven water. *Construction and Building Materials,* **20**(6), pp.374–383.

Hall, M. R., & Allinson, D. (2010) Transient numerical and physical modelling of temperature profile evolution in stabilised rammed earth walls. *Applied Thermal Engineering,* **30**(5), 433-441.

Hamed, E. & Bradford, M. A. (2010) Creep in concrete beams strengthened with composite materials. *European Journal of Mechanics - A/Solids*, **29**(6), pp.951–965.

Hanžič, L. & Ilić, R. (2003) Relationship between liquid sorptivity and capillarity in concrete. *Cement and Concrete Research*, **33**(9), pp.1385–1388.

Hanžič, L., Kosec, L. & Anžel, I. (2010) Capillary absorption in concrete and the Lucas–Washburn equation. *Cement and Concrete Composites*, **32**(1), pp.84–91.

Harakuwe, A.H., Haddad, P.R. & Thomas, R. (1998) Analysis of difficult samples by capillary zone electrophoresis: I. Simultaneous separation of detrimental anions in concrete digested with concentrated nitric acid. *Journal of Chromatography A,* **793**(1), pp.187–192.

Hardwick, J. & Little, J. (2010) Seismic Performance of Mud Brick Structures. In EWB-UK National Research Conference 2010 'From Small Steps to Giant Leaps... putting research into practice.

He, G.-P. & Wong, W.-G. (2008) Effects of moisture on strength and permanent deformation of foamed asphalt mix incorporating RAP materials. *Construction and Building Materials*, **22**(1), pp.30–40.

Heathcote, K.A. (1995) Durability of earthwall buildings. *Construction and Building Materials,* **9**(3), pp.185–189.

Ho, Y.-S. & Ofomaja, A.E. (2005) Kinetics and thermodynamics of lead ion sorption on palm kernel fibre from aqueous solution. *Process Biochemistry*, **40**(11), pp.3455–3461.

Ho, Y.-S. & Ofomaja, A.E. (2006) Kinetic studies of copper ion adsorption on palm kernel fibre. *Journal of Hazardous Materials*, **137**(3), pp.1796–1802.

Huberman, N. & Pearlmutter, D. (2008) A life-cycle energy analysis of building materials in the Negev desert. *Energy and Buildings,* **40**(5), pp.837–848.

Ibell, T. (2010) Learning structural engineering. *The Structural Engineer*, **88**(8), pp.17–19.

Ibhadode, A.O.A. & Dagwa, I.M. (2008) Development of asbestos-free friction lining material from palm kernel shell. *Journal of the Brazilian Society of Mechanical Sciences and Engineering,* **30**(2), pp.166–173.

Ichikawa, Y. & England, G.L. (2004) Prediction of moisture migration and pore pressure build-up in concrete at high temperatures. *Nuclear Engineering and Design*, **228**(1–3), pp.245–259.

Idiart, A. et al., (2012) A numerical and experimental study of aggregate-induced shrinkage cracking in cementitious composites. *Cement and Concrete Research,* **42**(2), pp.272–281.

Igarashi, S., Watanabe, A. & Kawamura, M. (2005) Evaluation of capillary pore size characteristics in high-strength concrete at early ages. *Cement and Concrete Research,* **35**(3), pp.513–519.

Ikpambese, K.K., Gundu, D.T. & Tuleun, L.T. (2014) Evaluation of palm kernel fibres (PKFs) for production of asbestos-free automotive brake pads. *Journal of King Saud University - Engineering Sciences.*

Infonet-Biovision, (2014) *Soil Monitoring*. Available at: http://www.google.co.uk/url?sa=i&source=images&cd=&cad=rja&uact=8&ved=0CAYQjhw4qgI&url=http://www.infonet-biovision.org/default/ct/263/soilManagement&ei=UxtEVPyIEorC7Aag0oC4Cw&psig=AFQjCNH8nyqIYjnFySvecdAQpasSb2VyGA&ust=1413835987407143 [Accessed August 20, 2014].

Ioannou, I., Hamilton, A. & Hall, C. (2008) Capillary absorption of water and n-decane by autoclaved aerated concrete. *Cement and Concrete Research,* **38**(6), pp.766–771.

Ioannou, I., Hoff, W.D. & Hall, C. (2004) On the role of organic adlayers in the anomalous water sorptivity of Lépine limestone. *Journal of Colloid and Interface Science,* **279**(1), pp.228–234.

Ip, K. & Miller, A., (2009) Thermal behaviour of an earth-sheltered autonomous building- The Brighton Earthship. *Renewable Energy*, **34**(9), p.2037.

Isik, B. & Tulbentci, T. (2008) Sustainable housing in island conditions using Alker-gypsum-stabilized earth: A case study from northern Cyprus. *Building and Environment,* **43**(9), p.1426.

Jaafar, A. & Ahmad, M. (2011) Torrefaction of Malaysian Palm Kernel Shell into Value-Added Solid Fuels. *World Acad. Sci. Eng. Technol*, pp.554–557.

Jafarifar, N., Pilakoutas, K. & Bennett, T. (2014) Moisture transport and drying shrinkage properties of steel–fibre-reinforced-concrete. *Construction and Building Materials*, **73**, pp.41–50.

Jamaluddin, M. 'Azim et al. (2013) Microwave-assisted pyrolysis of palm kernel shell: Optimization using response surface methodology (RSM). *Renewable Energy,* **55**(0), pp.357–365.

Jaquin, P.A. et al. (2009) The strength of unstabilised rammed earth materials. *Geotechnique*, **59**(5), pp.487–490.

Jaquin, P.A., Augarde, C.E. & Gerrard, C.M. (2004) Analysis of Tapial structures for modern use and conservation. *Structural Analysis of Historical Constructions*, pp.1315–1321.

Jayasinghe, C. & Kamaladasa, N. (2007) Compressive strength characteristics of cement stabilized rammed earth walls. *Construction and Building Materials,* **21**(11), pp.1971–1976.

Jendele, L. & Phillips, D. V, (1992) Finite element software for creep and shrinkage in concrete. *Computers & Structures,* **45**(1), pp.113–126. Available at: http://www.sciencedirect.com/science/article/pii/0045794992903495.

Johnson Alengaram, U. et al. (2011) Shear behaviour of reinforced palm kernel shell concrete beams. *Construction and Building Materials*, **25**(6), pp.2918–2927.

Jr., J.E.B. & Berton, S. (2004) Simulation of shrinkage induced cracking in cement composite overlays. *Cement and Concrete Composites*, **26**(7), pp.861–871.

Jumaat, Z. (2010) Effect of aggregate size and proportion on strength properties of palm kernel shell concrete. *International Journal of the Physical Sciences,* **5**(12), pp.1848–1856.

Jumasiah, A. et al. (2005) Adsorption of basic dye onto palm kernel shell activated carbon: sorption equilibrium and kinetics studies. *Desalination*, **186**(1–3), pp.57–64.

Kaniraj, S.R. & Havanagi, V.G. (1999) Compressive strength of cement stabilized Pulverised Fuel Ash-soil mixtures. *Cement and Concrete Research,* **29**(5), pp.673–677.

Keating, J., Hannant, D.J. & Hibbert, A.P. (1989) Correlation between cube strength, ultrasonic pulse velocity and volume change for oil well cement slurries. *Cement and Concrete Research,* **19**(5), pp.715–726.

Keefe, L. (2005) *Earth building: methods and materials, repair and conservation,* Taylor & Francis.

Keefe, L. (2012) *Earth building: methods and materials, repair and conservation*, Routledge.

Kewalramani, M. A., & Gupta, R. (2006) Concrete compressive strength prediction using ultrasonic pulse velocity through artificial neural networks. *Automation in Construction,* **15**(3), pp.374–379.

Khan, Z., Yusup, S., Ahmad, M.M. & Chin, B.L.F. (2014) Hydrogen production from palm kernel shell via integrated catalytic adsorption (ICA) steam gasification. *Energy Conversion and Management,* **87**, pp.1224–1230.

Khan, Z., Yusup, S., Ahmad, M.M. & Rashidi, N.A. (2014) Integrated catalytic adsorption (ICA) steam gasification system for enhanced hydrogen production using palm kernel shell. *International Journal of Hydrogen Energy*, **39**(7), pp.3286–3293.

Khatib, J.M. & Clay, R.M. (2004) Absorption characteristics of metakaolin concrete. *Cement and Concrete Research*, **34**(1), pp.19–29.

Khatib, J.M., Halliday, C., et al., 2014. Activation of fly ash-metakaolin paste using lime. Engineering (ICITE 2014), **1**, p.18.

Khatib, J.M., Onaidhe, E., et al., 2014. Fly ash paste activated with lime incorporating metakaolin. Engineering (ICITE 2014), **1**, p.13.

Khatib, J.M. et al., 2014. Lime Activated Fly Ash Paste in the Presence of Metakaolin. Procedia Engineering, **95**, pp.415–418.

Khatib, J.M., 2008. Performance of self-compacting concrete containing fly ash. Construction and Building Materials, **22**(9), pp.1963–1971.

Khatib, J.M., 2009. Sustainability of construction materials, Woodhead Publishing, CRC Press.

Khatib, J.M. et al., 2011. Water Absorption by Capillary Action of Self-Compacting Concrete containing Fly Ash. In INVACO2: International Seminar:

Innovation & Valorization in Civil Engineering & Construction Materials, Morocco. p. No–10.

Khatib, J.M., Kayali, O. & Siddique, R., 2009. Dimensional change and strength of mortars containing fly ash and metakaolin. Journal of Materials in Civil Engineering, ASCE, **21**(9), pp.523–528.

Khatib, J.M., Menadi, B. & Kenai, S., 2008. Effect of cement type on strength development of mortars containing limestone fines. Excellence in Concrete Construction through Innovation: Proceedings of the conference held at the Kingston University, United Kingdom, 9-10 September 2008, p.227.

Khatib, J.M. et al. (2010) Foundry sand utilisation in concrete production. In 2nd International conference on sustainable construction materials and technologies. pp. 28–30.

Khatib, J.M. (2005) Properties of concrete incorporating fine recycled aggregate. *Cement and Concrete Research*, **35**(4), pp.763–769.

Khatib, J.M. (2008) Metakaolin concrete at a low water to binder ratio. Construction and Building Materials, **22**(8), pp.1691–1700.

Khatib, J.M., Mangat, P.S. & Wright, L. (2013) Early age porosity and pore size distribution of cement paste with flue gas desulphurisation (FGD) waste. *Journal of Civil Engineering and Management,* **19**(5), pp.622–627.

Kim, H.-S. & Cho, S.-H. (2004) Shrinkage stress analysis of concrete slabs with shrinkage strips in a multistory building. *Computers & Structures*, **82**(15–16), pp.1143–1152.

Kim, S.-J., Jung, S.-H. & Kim, J.-S. (2010) Fast pyrolysis of palm kernel shells: Influence of operation parameters on the bio-oil yield and the yield of phenol and phenolic compounds. *Bio-resource Technology*, **101**(23), pp.9294–9300.

Kim, S.W., Koo, B.S. & Lee, D.H. (2014) Catalytic pyrolysis of palm kernel shell waste in a fluidized bed. *Bio-resource Technology*, **167**, pp.425–32.

Koh, C.G., Ang, K.K. & Zhang, L. (1997) Effects of repeated loading on creep deflection of reinforced concrete beams. *Engineering Structures,* **19**(1), pp.2–18.

Kolias, S. & Georgiou, C. (2005) The effect of paste volume and of water content on the strength and water absorption of concrete. *Cement and Concrete Composites,* **27**(2), pp.211–216.

Komlos, K. et al. (1996) Ultrasonic pulse velocity test of concrete properties as specified in various standards. *Cement and Concrete Composites*, **18**(5), pp.357–364.

Kouakou, C.H. & Morel, J.C. (2009) Strength and elasto-plastic properties of non-industrial building materials manufactured with clay as a natural binder. *Applied Clay Science,* **44**(1), pp.27–34.

Koya, O.A. & Faborode, M.O. (2006) Separation Theory for Palm Kernel and Shell Mixture on a Spinning Disc. *Biosystems Engineering*, **95**(3), pp.405–412.

Kubissa, W. & Jaskulski, R. (2013) Measuring and Time Variability of The Sorptivity of Concrete. *Procedia Engineering*, **57**(0), pp.634–641.

Kuo, W.-T., Wang, H.-Y. & Shu, C.-Y. (2014) Engineering properties of cementless concrete produced from GGBFS and recycled desulfurization slag. *Construction and Building Materials,* **63**, pp.189–196.

Kupaei, R.H. et al. (2013) Mix design for Pulverised Fuel Ash based oil palm shell geopolymer lightweight concrete. *Construction and Building Materials*, **43**(0), pp.490–496.

Labuschagne, C., Brent, A. C., & Erck, R. P. G. (2005) Assessing the sustainability performances of industries. *Journal of Cleaner Production,* **13**(4), 373.

Lamberton, G. (2005) Sustainability accounting - A brief history and conceptual framework. *Accounting Forum,* **29**(1), 7.

Lanbo, l. (2007) *Soil Consistency*, Atterberg Limits, CE 240 Soil Mechanics & Foundations Lecture 3.1. University of Connecticut, unpublished.

Larsson, S., Rothhämel, M. & Jacks, G. (2009) A laboratory study on strength loss in kaolin surrounding lime--cement columns. *Applied Clay Science*, **44**(1), pp.116–126.

Lee, K., & Saen, R. F. (2012) Measuring corporate sustainability management: A data envelopment analysis approach. *International Journal of Production Economics,* **140**(1), 219.

Lee, S. et al., (1999) Measuring thermal conductivity of fluids containing oxide nanoparticles. *Journal of Heat Transfer*, **121**(2), pp.280–289.

Lenci, S. et al., A mechanical characterization of unfired dry earth: ultimate strength, damage and fracture parameters. In Proceedings of XIX Aimeta Conference. pp. 14–17.

Lertpanyapornchai, B. & Ngamcharussrivichai, C. (2015) Mesostructured Sr and Ti mixed oxides as heterogeneous base catalysts for transesterification of palm kernel oil with methanol. *Chemical Engineering Journal*, **264**, pp.789–796.

Li, N. et al., (2000) The coupled heat-moisture-mechanic model of the frozen soil. *Cold Regions Science and Technology*, **31**(3), pp.199–205.

Lin, M.W. et al., (2006) Modelling of moisture migration in an {FRP} reinforced masonry structure. *Building and Environment*, **41**(5), pp.646–656.

Ling, N.P., (2005) *Determination of optimum concentration of lime solution for soil stabilization*. Universiti Teknologi Malaysia.

Little, D.N. (1987) *Evaluation of structural properties of lime stabilized soils and aggregates,* National Lime Association.

Little, D.N., Epps, J.A. & Sebaaly, P.E. (2001) *The benefits of hydrated lime in hot mix asphalt.* National Lime Association.

Luzio, G. Di & Cusatis, G. (2013) Solidification–microprestress–microplane (SMM) theory for concrete at early age: Theory, validation and application. *International Journal of Solids and Structures*, **50**(6), pp.957–975.

Ma, Z. et al. (2015) Determination of pyrolysis characteristics and kinetics of palm kernel shell using TGA–FTIR and model-free integral methods. *Energy Conversion and Management,* **89**, pp.251–259.

Mabrouk, R., Ishida, T. & Maekawa, K. (2004) A unified solidification model of hardening concrete composite for predicting the young age behavior of concrete. *Cement and Concrete Composites,* **26**(5), pp.453–461.

Macorini, L. et al., (2006) Long-term analysis of steel–concrete composite beams: {FE} modelling for effective width evaluation. *Engineering Structures*, **28**(8), pp.1110–1121.

Maes, M. & De Belie, N. (2014) Resistance of concrete and mortar against combined attack of chloride and sodium sulphate. *Cement and Concrete Composites,* **53**, pp.59–72.

Mahmud, H. et al., (2009) Influence of sand/cement ratio on mechanical properties of palm kernel shell concrete. *Journal of Applied Sciences,* **9**(9), pp.1764–1769.

Mallela, J. et al., (2004) *Consideration of lime-stabilized layers in mechanistic-empirical pavement design.* The National Lime Association.

Maniatidis, V. & Walker, P. (2003) *A review of rammed earth construction.* University of Bath.

Mannan, M.A. & Ganapathy, C. (2001) Long-term strengths of concrete with oil palm shell as coarse aggregate. *Cement and Concrete Research*, **31**(9), pp.1319–1321.

Mannan, M.A. & Ganapathy, C. (2004) Concrete from an agricultural waste-oil palm shell (OPS). *Building and Environment*, **39**(4), pp.441–448.

Manzini, F., Islas, J. & MacÃ¬as, P., (2011) Model for evaluating the environmental sustainability of energy projects. *Technological Forecasting and Social Change,* **78**(6), p.931.

Martys, N.S. & Ferraris, C.F. (1997) Capillary transport in mortars and concrete. *Cement and Concrete Research*, **27**(5), pp.747–760.

Maskell, D., Heath, A. & Walker, P. (2013) Laboratory scale testing of extruded earth masonry units. *Materials & Design*, **45**(0), p.359.

Matthew R., H. (2007) Assessing the environmental performance of stabilised rammed earth walls using a climatic simulation chamber. *Building and Environment,* **42**(1), 139-145.

McCarthy, M.J. & Giannakou, A. (2002) In-situ performance of CPF concrete in a coastal environment. *Cement and Concrete Research*, **32**(3), pp.451–457.

McDowell, C., (1959) *Stabilization of Soils with Lime, Lime-Pulverised Fuel Ash, and Other Lime Reactive Materials*. Highway Research Board Bulletin.

McGlinn, P.J. et al., (2010) Appraisal of a cementitious material for waste disposal: Neutron imaging studies of pore structure and sorptivity. *Cement and Concrete Research*, **40**(8), pp.1320–1326.

Menoufi, K. et al., (2012) Evaluation of the environmental impact of experimental cubicles using Life Cycle Assessment: A highlight on the manufacturing phase. *Applied Energy*, **92**(0), p.534.

Mequignon, M. et al., (2013) Impact of the lifespan of building external walls on greenhouse gas index. *Building and Environment*, **59**(0), pp.654–661.

Mermerdaş, K. et al., (2013) Experimental evaluation and modelling of drying shrinkage behavior of metakaolin and calcined kaolin blended concretes. *Construction and Building Materials*, **43**(0), pp.337–347.

Mikeska, T. & Svendsen, S. (2013) Study of thermal performance of capillary micro tubes integrated into the building sandwich element made of high performance concrete. *Applied Thermal Engineering,* **52**(2), pp.576–584.

Minasny, B. & McBratney, A.B. (2000) Estimation of sorptivity from disc-permeameter measurements. *Geoderma*, **95**(3–4), pp.305–324.

Mironova, M.K., Gospodinov, P.N. & Kazandjiev, R.F., (2002) The effect of liquid push out of the material capillaries under sulphate ion diffusion in cement composites. *Cement and Concrete Research,* **32**(1), pp.9–15.

Mora-Ruacho, J., Gettu, R. & Aguado, A. (2009) Influence of shrinkage-reducing admixtures on the reduction of plastic shrinkage cracking in concrete. *Cement and Concrete Research,* **39**(3), pp.141–146.

Morin, V. et al., (2002) Evolution of the capillary network in a reactive powder concrete during hydration process. *Cement and Concrete Research*, **32**(12), pp.1907–1914.

Mouterde, R., Morel, J. C., Martinet, V., & Sallet, F. (2011) The mechanical performance of cordwood. *Biosystems Engineering*, **108**(3), 237.

MSC Software, (2013). Marc Mentat (2013.1.0 Student Edition). [computer program] [Accessed 30 August 2013].

Muntohar, A.S. & Rahman, M.E., (2014) Lightweight masonry block from oil palm kernel shell. *Construction and Building Materials*, **54**, pp.477–484.

Murray-White, J., (2013) *Sustainable Build. Using Lime in Building Techniques*. Available at: http://www.sustainablebuild.co.uk/usinglime.html [Accessed February 7, 2013].

Mymrin, V. & Corrêa, S.M., (2007) New construction material from concrete production and demolition wastes and lime production waste. *Construction and Building Materials,* **21**(3), pp.578–582.

Nalbantoglu, Z. & Gucbilmez, E., (2001) Improvement of calcareous expansive soils in semi-arid environments. *Journal of Arid Environments,* **47**(4), pp.453–463.

Narasimha Rao, S. & Rajasekaran, G., (1994) Lime injection technique to improve the behaviour of soft marine clays. *Ocean engineering*, **21**(1), pp.29–43.

Narayanan, N. & Ramamurthy, K. (2000) Microstructural investigations on aerated concrete. *Cement and Concrete Research*, **30**(3), pp.457–464.

Ndoke, P.N. (2006) Performance of palm kernel shells as a partial replacement for coarse aggregate in asphalt concrete. *Leonardo Electronic Journal of Practices and Technologies,* **5**(9), pp.145–152.

Ninduangdee, P. & Kuprianov, V.I. (2013) Study on burning oil palm kernel shell in a conical fluidized-bed combustor using alumina as the bed material. *Journal of the Taiwan Institute of Chemical Engineers*

Niroumand, H., Zain, M.F.M. & Jamil, M. (2012) Modern rammed earth in earth architecture. *Advanced Materials Research,* **457**, pp.399–402.

Nourouzi, M.M., Chuah, T.G. & Choong, T.S.Y., (2009) Equilibrium and kinetic study on reactive dyes adsorption by palm kernel shell-based activated carbon: in single and binary systems. *Journal of Environmental Engineering,* **135**(12), pp.1393–1398.

Nowamooz, H. & Chazallon, C., (2011) Finite element modelling of a rammed earth wall. *Construction and Building Materials*, **25**(4), pp.2112–2121.

Nwaubani, S.O. (2013) Fineness of Waste Glass Powder and the Influence on Properties of Cement Mortars. *IJCEBM*, p.106.

Obeng, K., Ocran, K.A.G. & Anaba, D., (1997) Palm kernel shell as fuel for burning bricks. *Building Research & Information,* **25**(3), pp.131–136.

Ochoa George, P.A. et al., (2010) Cleaner production in a small lime factory by means of process control. *Journal of Cleaner Production*, **18**(12), pp.1171–1176.

Ogedengbe, O., Oriaje, A.T. & Tella, A. (1985) Carbonisation and activation of palm kernel shells for household water filters. *Water International*, **10**(3), pp.132–138.

Okafor, F.O. (1988) Palm kernel shell as a lightweight aggregate for concrete. *Cement and Concrete Research*, **18**(6), pp.901–910.

Okafor, F.O., (1991) An investigation on the use of superplasticizer in palm kernel shell aggregate concrete. *Cement and Concrete Research*, **21**(4), pp.551–557.

Okpala, D.C. (1990) Palm kernel shell as a lightweight aggregate in concrete. *Building and Environment*, **25**(4), pp.291–296.

Oladoja, N.A. & Akinlabi, A.K. (2009) Congo red biosorption on palm kernel seed coat. *Industrial & Engineering Chemistry Research*, **48**(13), pp.6188–6196.

Olanipekun, E.A., Olusola, K.O. & Ata, O. (2006) A comparative study of concrete properties using coconut shell and palm kernel shell as coarse aggregates. *Building and Environment,* **41**(3), pp.297–301.

Oliveira, D. V et al., (2006) Experimental investigation on the structural behaviour and strengthening of three-leaf stone masonry walls.

Olorede, B.R., Longe, O.G. & others, (2000) Effect of replacing palm kernel cake with sheabutter cake on egg quality characteristics, haematology and serum chemistry of laying hens. *Nigerian Journal of Animal production*, **27**, pp.19–23.

Olotuah, A.O., (2002) Recourse to earth for low-cost housing in Nigeria. *Building and environment*, **37**(1), pp.123–129.

Olutoge, F.A., (2010) Investigations on sawdust and palm kernel shells as aggregate replacement. *ARPN Journal of Engineering and Applied Sciences*, **5**(4), pp.7–13.

Ooteghem, K. Van & Xu, L., (2012) The life-cycle assessment of a single-storey retail building in Canada. *Building and Environment*, **49**(0), pp.212–226.

Open sustainability, 2013. . . Available at: http://open-sustainability.org/wiki/Sustainable_Development.

Orchard, V.A. & Cook, F.J., (1983) Relationship between soil respiration and soil moisture. *Soil Biology and Biochemistry*, **15**(4), pp.447–453.

Ortiz, O., Castells, F. & Sonnemann, G., (2010) Operational energy in the life cycle of residential dwellings: The experience of Spain and Colombia. *Applied Energy*, **87**(2), pp.673–680.

Osei, D.Y. & Jackson, E.N. (2012) Experimental Study on Palm Kernel Shells as Coarse Aggregates in Concrete. *International Journal of Scientific and Engineering Research*, **3**(8).

Østergaard, L. et al., (2001) Tensile basic creep of early-age concrete under constant load. *Cement and Concrete Research*, **31**(12), pp.1895–1899.

Oti, J. E., & Kinuthia, J. M. (2012) Stabilised unfired clay bricks for environmental and sustainable use. *Applied Clay Science*, **58**(0), 52.

Pacheco-Torgal, F. & Jalali, S., (2012) Earth construction: Lessons from the past for future eco-efficient construction. *Construction and Building Materials,* **29**(0), pp.512–519.

Pan, H.-L. & Mahrt, L., (1987) Interaction between soil hydrology and boundary-layer development. *Boundary-Layer Meteorology*, **38**(1-2), pp.185–202.

Pane, I. & Hansen, W., (2008) Investigation on key properties controlling early-age stress development of blended cement concrete. *Cement and Concrete Research,* **38**(11), pp.1325–1335.

Panesar, D.K. & Chidiac, S.E., (2009) Capillary suction model for characterizing salt scaling resistance of concrete containing GGBFS. *Cement and Concrete Composites*, **31**(8), pp.570–576.

Park, Y.J. & Heo, J., (2002) Vitrification of Pulverised Fuel Ash from municipal solid waste incinerator. *Journal of Hazardous Materials*, **91**(1), pp.83–93.

Peltier, L.C., (1950) The geographic cycle in periglacial regions as it is related to climatic geomorphology. *Annals of the Association of American Geographers,* **40**(3), pp.214–236.

Pereira, T. (2009) Sustainability: An integral engineering design approach. *Renewable and Sustainable Energy Reviews,* **13**(5), 1133.

Peters, L. & Sellick, K. (2006) Quality of life of cancer patients receiving inpatient and home-based palliative care. *Journal of advanced nursing*, **53**(5), pp.524–533.

Philip, J.R. & Knight, J.H. (1974) On solving the unsaturated flow equation: 3. New quasi-analytical technique. *Soil science*, **117**(1), pp.1–13.

Popovics, S., (2001) Analysis of the concrete strength versus ultrasonic pulse velocity relationship. *Materials Evaluation,* **59**(2), pp.123–130.

Prasertsan, S. & Prasertsan, P. (1996) Biomass residues from palm oil mills in Thailand: an overview on quantity and potential usage. *Biomass and Bioenergy,* **11**(5), pp.387–395.

Pullen, S., (1996) *Data quality of embodied energy methods*. Embodied Energy the Current State of Play.

Rael, R., (2009) *Earth architecture*, Princeton Architectural Press.

Rahman, M.K., Baluch, M.H. & Al-Gadhib, A.H., (2000) Simulation of shrinkage distress and creep relief in concrete repair. *Composites Part B: Engineering*, **31**(6–7), pp.541–553.

Rajasekaran, G. & Narasimha Rao, S., (2002) Compressibility behaviour of lime-treated marine clay. *Ocean engineering*, **29**(5), pp.545–559.

Rao, S.M. & Shivananda, P., (2005) Role of curing temperature in progress of lime-soil reactions. *Geotechnical & Geological Engineering*, **23**(1), pp.79–85.

Razuan, R. et al., (2010) Pyrolysis and combustion of oil palm stone and palm kernel cake in fixed-bed reactors. *Bioresource Technology,* **101**(12), pp.4622–4629.

Razuan, R. et al., (2011) Pelletised fuel production from palm kernel cake. *Fuel Processing Technology*, **92**(3), pp.609–615.

Río Suárez, O., Mateo, J. & Theodossopoulos, D. (2010) Assessment and Evaluation of the Repair Options for the *Torroja Institute Winter Garden*.

Roos, J. et al., *Dynamic in-situ determination of thermal diffusivity of soil cement pressed earth blocks.*

Russell, S. L., & Thomson, I. (2009) Analysing the role of sustainable development indicators in accounting for and constructing a sustainable scotland. *Accounting Forum*, **33**(3), 225-244.

Sabil, K.M. et al., (2013) Effects of torrefaction on the physiochemical properties of oil palm empty fruit bunches, mesocarp fiber and kernel shell. *Biomass and Bioenergy*, **56**(0), pp.351–360.

Saghafi, M.D. & Teshnizi, Z.S.H., (2011) Recycling value of building materials in building assessment systems. *Energy and Buildings*, **43**(11), pp.3181–3188. Available at: http://www.sciencedirect.com/science/article/pii/S0378778811003501.

Sakulich, A.R., (2011) Reinforced geopolymer composites for enhanced material greenness and durability. *Sustainable Cities and Society,* **1**(4), p.195.

Salehi, M. & Salem, A. (2008) Effect of moisture content on extrusion process of kaolinitic–illitic clay in manufacturing of ceramic Raschig ring. *Journal of Materials Processing Technology*, **200**(1–3), pp.232–237.

Samuelsson, R. et al., (2012) Moisture content and storage time influence the binding mechanisms in biofuel wood pellets. *Applied Energy*, **99**(0), pp.109–115.

Saw, H.Y., Janaun, J. & Subbarao, D., (2008) Hydration properties of palm kernel cake. *Journal of Food Engineering,* **89**(2), pp.227–231.

Sepaskhah, A.R., Ahmadi, S.H. & Shahbazi, A.R.N., (2005) Geostatistical analysis of sorptivity for a soil under tilled and no-tilled conditions. *Soil and Tillage Research,* **83**(2), pp.237–245.

Serrano, C. et al., (2011) Effect of moisture content, particle size and pine addition on quality parameters of barley straw pellets. *Fuel Processing Technology,* **92**(3), pp.699–706.

Shafigh, P. et al., (2012) Lightweight concrete made from crushed oil palm shell: Tensile strength and effect of initial curing on compressive strength. *Construction and Building Materials*, **27**(1), pp.252–258..

Shafigh, P., Jumaat, M.Z. & Mahmud, H. (2011) Oil palm shell as a lightweight aggregate for production high strength lightweight concrete. *Construction and Building Materials,* **25**(4), pp.1848–1853.

Shaughnessy, P.W. & Kramer, A.M., (1990) The increased needs of patients in nursing homes and patients receiving home health care. *New England Journal of Medicine*, **322**(1), pp.21–27.

Shaver, T.M. et al., (2013) Soil sorptivity enhancement with crop residue accumulation in semiarid dryland no-till agroecosystems. *Geoderma*, **192**(0), pp.254–258.

Shenley, M., (2011) *Nigerian People and Culture*. Available at: http://images.markshenley.co.uk/v/stock/78603602/7928284602/kano-city-cities-northern-travel [Accessed July 23, 2013].

Sherwood, P., (1993) *Soil stabilization with cement and lime*

Sheweka, S., (2011) Using Mud Bricks as a Temporary Solution for Gaza Reconstruction. *Energy Procedia*, **6**(0), p.236.

Shoop, S.A. & Bigl, S.R., (1997) Moisture migration during freeze and thaw of unsaturated soils: modelling and large scale experiments. *Cold Regions Science and Technology,* **25**(1), pp.33–45.

Shuit, S.H. et al., (2009) Oil palm biomass as a sustainable energy source: a Malaysian case study. *Energy Journal*, **34**(9), pp.1225–1235.

Siddique, R., (2013) Compressive strength, water absorption, sorptivity, abrasion resistance and permeability of self-compacting concrete containing coal bottom ash. *Construction and Building Materials*, **47**(0), pp.1444–1450.

Siddique, R., Khatib, J. & Kaur, I., (2008) Use of recycled plastic in concrete: a review. *Waste management,* **28**(10), pp.1835–1852.

Slowik, V., Schmidt, M. & Fritzsch, R., (2008) Capillary pressure in fresh cement-based materials and identification of the air entry value. *Cement and Concrete Composites,* **30**(7), pp.557–565.

Soebarto, V., (2009) Analysis of indoor performance of houses using rammed earth walls. *Building Simulation* 2009.

Song, H.-W. & Kwon, S.-J., (2007) Permeability characteristics of carbonated concrete considering capillary pore structure. *Cement and Concrete Research*, **37**(6), pp.909–915.

Spengler, C. et al., (2014) Transposition of 2D Molten Corium–Concrete Interactions (MCCI) from experiment to reactor. *Annals of Nuclear Energy*, **74**, pp.89–99.

Standards New Zealand, (1998) *Materials and Workmanship for Earth Buildings*, Wellington, New Zealand.

Stewart, S., Pearson, S. & Horowitz, J.D., (1998) Effects of a home-based intervention among patients with congestive heart failure discharged from acute hospital care. *Archives of Internal Medicine,* **158**(10), pp.1067–1072.

Stratton, M., (1997) *Structure and style: conserving twentieth century buildings,* Taylor & Francis.

Stroh, J. et al., (2014) Applying high resolution SyXRD analysis on sulfate attacked concrete field samples. *Cement and Concrete Research*, **66**, pp.19–26.

Sugumaran, K.R. et al., (2014) Statistical optimization of pullulan production from Asian palm kernel and evaluation of its properties. *International journal of biological macromolecules*, **66**, pp.229–35.

Sumathi, S., Chai, S.P. & Mohamed, A.R., (2008) Utilization of oil palm as a source of renewable energy in Malaysia. *Renewable and Sustainable Energy Reviews,* **12**(9), pp.2404–2421.

Sundu, B., Kumar, A. & Dingle, J., (2006) Palm kernel meal in broiler diets: effect on chicken performance and health. *World's Poultry Science Journal,* **62**(2), pp.316–325.

Swanepoel, J.C. & Strydom, C.A., (2002) Utilisation of Pulverised Fuel Ash in a geopolymeric material. *Applied Geochemistry,* **17**(8), pp.1143–1148.

Tarantini, M., Loprieno, A.D. & Porta, P.L., (2011) A life cycle approach to Green Public Procurement of building materials and elements: A case study on windows. *Energy Journal*, **36**(5), pp.2473–2482.

Tarque, N. et al., (2010) *Structural properties of adobe dwellings in Cusco for seismic risk assessment*.

Tasdemir, C., (2003) Combined effects of mineral admixtures and curing conditions on the sorptivity coefficient of concrete. *Cement and Concrete Research,* **33**(10), pp.1637–1642.

Taylor, P. & Luther, M.B., (2004) Evaluating rammed earth walls: a case study. *Solar World Congress 2001,* **76**(1-3), pp.79–84.

Taylor, P., Fuller, R.J. & Luther, M.B., (2008) Energy use and thermal comfort in a rammed earth office building. *Energy and Buildings,* **40**(5), pp.793–800.

Thormark, C., (2006) The effect of material choice on the total energy need and recycling potential of a building. *Building and Environment,* **41**(8), pp.1019–1026.

Tritthart, J., (2003) Transport of a surface-applied corrosion inhibitor in cement paste and concrete. *Cement and Concrete Research,* **33**(6), pp.829–834.

Trtnik, G., Kavčič, F. & Turk, G., (2009) Prediction of concrete strength using ultrasonic pulse velocity and artificial neural networks. *Ultrasonics*, **49**(1), pp.53–60.

U. Johnson Alengaram, Hilmi Mahmud, M.Z.J., (2010) Comparison of mechanical and bond properties of oil palm kernel shell concrete with normal weight concrete. *International Journal of the Physical Sciences*, **5**(8), pp.1231–1239.

U. Johnson Alengaram, Hilmi Mahmud, Mohd Zamin Jumaat, S.M.S., (2010) Effect of aggregate size and proportion on strength properties of palm kernel shell concrete. *International Journal of the Physical Sciences*, **5**(12), pp.1848–1856.

ulilley D. M. & J. robinson (1996) Ultimate strength of rammed earth walls with openings :, proceedings — ICE: Structures & buildings, **110**(3), 1995, pp 278–287. *International Journal of Rock Mechanics and Mining Sciences & Geomechanics Abstracts*, **33**(2), A84.

Valentine, (2011) Valentine Clays LTD. Available at: http://www.valentineclays.co.uk/ [Accessed September 9, 2011].

Valiantzas, J.D., (2010) New linearized two-parameter infiltration equation for direct determination of conductivity and sorptivity. *Journal of Hydrology*, **384**(1–2), pp.1–13.

Van Wyngaard, J.D.V., Meeske, R. & Erasmus, L.J., (2015) Effect of palm kernel expeller as supplementation on production performance of Jersey cows grazing kikuyu-ryegrass pasture. *Animal Feed Science and Technology,* **199**, pp.29–40.

Vasconcelos, G. & Lourenço, P.B., (2006) Assessment of the in-plane shear strength of stone masonry walls by simplified models.

Venkatarama Reddy, B. V., & Prasanna Kumar, P. (2010) Embodied energy in cement stabilised rammed earth walls. *Energy and Buildings*, **42**(3), 380-385.

Verkoeijen, D. et al., (2002) Determining granule strength as a function of moisture content. *Powder Technology*, **124**(3), pp.195–200.

Vilane, B.R.T., (2010) Assessment of stabilisation of adobes by confined compression tests. *Biosystems Engineering*, **106**(4), p.551.

Villar-Cocina, E. et al., (2002) Kinetics of the water absorption in slag cement mortars. arXiv preprint cond-mat/0210138.

Vinai, R., Lawane, A., Minane, J. R., & Amadou, A. (2013) Coal combustion residues valorisation: Research and development on compressed brick production. *Construction and Building Materials*, **40**(0), 1088.

Vinhal, J.O., Lima, C.F. & Barbosa, L.C.A., (2014) Analytical pyrolysis of the kernel and oil of babassu palm (Orbignya phalerata). *Journal of Analytical and Applied Pyrolysis*, **107**, pp.73–81.

Walker, P. & Britain, G., (2005) *Rammed earth: design and construction guidelines,* BRE Bookshop Watford.

Wan Ab Karim Ghani, W.A. et al., (2009) Air gasification of agricultural waste in a fluidized bed gasifier: hydrogen production performance. *Energies*, **2**(2), pp.258–268.

Wang, L. & Ueda, T., (2011) Mesoscale modeling of water penetration into concrete by capillary absorption. *Ocean Engineering,* **38**(4), pp.519–528.

WANG, Q.-J., ZHANG, J.-H. & FAN, J., (2006) An Analytical Method for Relationship Between Hydraulic Diffusivity and Soil Sorptivity. *Pedosphere*, **16**(4), pp.444–450.

Wekesa, B.W., Steyn, G.S. & Otieno, F.A.O., (2010) The response of common building construction technologies to the urban poor and their environment. *Building and Environment*, **45**(10), p.2327.

Wild, S., Hadi, M., & Khatib, J. (1995) The influence of gypsum content on the porosity and pore-size distribution of cured PFA-lime mixes. *Advances in Cement Research,* **7**(26), 47-56.

Winfield, M., Gibson, R. B., Markvart, T., Gaudreau, K., & Taylor, J. (2010) Implications of sustainability assessment for electricity system design: The

case of the ontario power Authority integrated power system plan. *Energy Policy,* **38**(8), 4115.

Wong, W.H. et al., (2015) Two level half factorial design for the extraction of phenolics, flavonoids and antioxidants recovery from palm kernel by-product. *Industrial Crops and Products*, **63**, pp.238–248.

Yang, I.H., (2007) Uncertainty and sensitivity analysis of time-dependent effects in concrete structures. *Engineering Structures*, **29**(7), pp.1366–1374.

Yoo, D.-Y. et al., (2014) Shrinkage and cracking of restrained ultra-high-performance fiber-reinforced concrete slabs at early age. *Construction and Building Materials*, **73**, pp.357–365. Available at: http://www.sciencedirect.com/science/article/pii/S0950061814011131 [Accessed December 20, 2014].

Yuan, X. et al., (2014) Shrinkage compensation of alkali-activated slag concrete and microstructural analysis. *Construction and Building Materials*, **66**, pp.422–428.

Yuan, Y. & Wan, Z.L., (2002) Prediction of cracking within early-age concrete due to thermal, drying and creep behavior. *Cement and Concrete Research,* **32**(7), pp.1053–1059.

Yuan, Y., Li, G. & Cai, Y., (2003) Modelling for prediction of restrained shrinkage effect in concrete repair. *Cement and Concrete Research*, **33**(3), pp.347–352.

Yung, P., Lam, K.C. & Yu, C., (2013) An audit of life cycle energy analyses of buildings. *Habitat International*, **39**(0), pp.43–54.

Zaidul, I.S.M. et al., (2007) Separation of palm kernel oil from palm kernel with supercritical carbon dioxide using pressure swing technique. *Journal of Food Engineering,* **81**(2), pp.419–428.

Zarei, M. et al., (2014) Identification and characterization of papain-generated antioxidant peptides from palm kernel cake proteins. *Food Research International,* **62**, pp.726–734.

Zhai, Z.J. & Previtali, J.M., (2010) Ancient vernacular architecture: characteristics categorization and energy performance evaluation. *Energy and Buildings,* **42**(3), pp.357–365.

List of conference papers

Okoronkwo, D. C., Khatib, J., Emekwuru, N., & Hall, R. F. (2014). The Rammed Earth Building In Nigeria. In *Construcción con tierra, patrimonio y vivienda: Congreso de Arquitectura de Tierra en Cuenca de Campos 2013* (p. 27). ETS de Arquitectura de Valladolid.

Okoronkwo, D. C., Emekwuru, N., Khatib, J., & Hall, R. F. (2014). Accessing the Initial rate of sorption for rammed earth made with palm kernel shell. In *Construcción con tierra, patrimonio y vivienda: Congreso de Arquitectura de Tierra en Cuenca de Campos 2013* (p. 267). ETS de Arquitectura de Valladolid.

Okoronkwo, D. C., Khatib, J., Emekwuru, N., & Hall, R. F. (2014). sustainability elements of rammed earth, Kazakhstan.

Okoronkwo, D. C., Khatib, J., Emekwuru, N., & Hall, R. F. (2012). Gains of Fly-Ash in Rammed-Earth. *AES-ATEMA' 2012 Eleventh International Conference on Advances and Trends in Engineering Materials and their Applications. Toronto, Canada.*

Okoronkwo, D. C., Khatib, J., Emekwuru, N., & Hall, R. F. (2013). Use of modified aggregate in rammed earth. earth usa 2013, the seventh international earthbuilding conference, santa fe, new mexico - usa.

Okoronkwo, D. C., Khatib, J., Emekwuru, N., & Hall, R. F. (2013). The optimum moisture content of rammed earth. Earth Building UK (EBUK), 3rd Annual Conference, Devon, UK.